Kinematic And Electromyographic Analysis Of The Legs, Torso, And Arms During An Exhaustive Run

by

James Michael Smoliga

Doctor of Veterinary Medicine, Cornell University, 2003

Submitted to the Graduate Faculty of

School of Health and Rehabilitation Science in partial fulfillment

of the requirements for the degree of

Doctor of Philosophy

University of Pittsburgh

2007

UNIVERSITY OF PITTSBURGH

SCHOOL OF HEALTH AND REHABILITATION SCIENCE

This dissertation was presented

by

James Michael Smoliga DVM

It was defended on September 21st, 2007

and approved by

Joseph B. Myers, PhD, ATC, Assistant Professr
Department of Exercise and Sports Science, University of North Carolina

Mark A. Redfern, PhD, Professor
Department of Bioengineering, University of Pittsburgh

Elaine Rubinstein PhD, Research Specialist
Department of Measurement and Evaluation, University of Pittsburgh

Dissertation Advisor: Scott M. Lephart, PhD, ATC
Associate Professor and Chair, Department of Sports Medicine and Nutrition

Kinematic And Electromyographic Analysis Of The Legs, Torso, And Arms During An Exhaustive Run

James Smoliga, DVM, PhD

University of Pittsburgh, 2007

Distance running performance is dependent on the integration of the complex mechanisms of neuromuscular control, central and peripheral cardiovascular performance, and fatigue resistance. The end result of these interactions is movement, as defined by running mechanics. During high-intensity running, specific muscles may demonstrate signs of neuromuscular fatigue, which may alter running local and whole-body running mechanics. There are few published studies specific to running which describe neuromuscular fatigue of torso and arm muscles, how fatigue affects the kinematics of the upper body, and how neuromuscular fatigue relates to kinematic changes.

Fifteen trained male distance runners were recruited to participate in this study. Each subject performed an exhaustive run at an intensity approximating 95% of maximal oxygen consumption. Electromyographic data were collected from thirteen muscles unilaterally and kinematic data were collected from key joints of the upper and lower body during the exhaustive run.

Increased motor unit recruitment was observed in nearly all muscles studied, many demonstrating statistically significant linear trends. Torso muscles demonstrated similar levels of recruitment to the leg muscles. Statistically significant models of neuromuscular fatigue were observed during the exhaustive run for two leg muscles and one torso muscle. None of the arm muscles demonstrated statistically significant changes indicative of fatigue. A number of statistically significant kinematic changes were observed throughout the run for all regions of the body. Some kinematic changes were significantly correlated to changes in motor unit recruitment patterns or neuromuscular fatigue.

These results confirm that runners develop neuromuscular fatigue during high intensity running and this may limit performance. Based on these results, general recommendations for muscle-specific training programs may be made for groups of athletes similar to the population studied. However, there are many individual differences within this population and therefore personalized training recommendations require a thorough neuromuscular and kinematic evaluation. Groups of runners with different demographics may also show different trends in fatigue patterns. Therefore, further research is needed to investigate the effect of exhaustive running on various populations. Additionally, research is needed to validate training programs which aim to delay or prevent neuromuscular fatigue as a means of enhancing running performance.

TABLE OF CONTENTS

LIST OF TABLES

LIST OF FIGURES

LIST OF EQUATIONS

PREFACE

This dissertation is dedicated to a good friend, colleague, and fellow athlete, the late David Hutton. Dave shared my passion for running research and helped me develop this project and assisted throughout much of its early phases. Dave will forever be missed, but never forgotten.

I would like to acknowledge all that have helped me along the way on this journey. To start, I would like to thank my advisor, Dr. Scott Lephart, for his support in this project. The science of distance running is truly a passion of mine, and I am thankful I was able to perform research in this area in the Neuromuscular Research Laboratory under Dr. Lephart's guidance. Additionally, I would like to acknowledge the rest of my committee members for each of their unique contributions. I would like to thank Dr. Joseph Myers for helping me learn the essential skills to develop as a researcher. I would also like to thank Dr. Mark Redfern for his contributions to key engineering principles of this project. I would like to thank Dr. Elaine Rubinstein for all of her guidance with the methodology behind this study. Though he was not a member of my committee, I would like to give a special thank you to my external statistical consultant, Li-Wu Hsu, for his tireless efforts to help me transform a complex data set into meaningful results.

I would also like to thank all of the many members of the Neuromuscular Research Laboratory who were present throughout my graduate assistanceship. From summer internships through full-time faculty, each of you contributed to the learning process and the development of this project in your own unique ways which I will always remember. To Dr. John Abt and Dr. Timothy Sell, thank you for teaching me how to operate all the many pieces of equipment that this project depended on. To John Jolly, thank you for helping me better understand the concepts of programming and technical aspects of research. To Dr. Criag Wassinger and Takashi Nagai, thank you for all of your help throughout the data collection process. To all, thank you for your help in making me the best researcher I can be.

Each of my subjects deserve special thanks for their time commitment to the study, enthusiastic attitudes, aid in recruiting additional subjects, and becoming friends in the process. None of this would have been possible if you didn't share the same passion for running that I did. I wish all of you the most success in your continued running careers.

Of course, none of this would have been possible without the loving support of all of my family and friends. Mom and Dad, you are the best. Thank you for always trusting me and being there – I will always do my best to make you proud. To Andrea, thank you for your help and support the past few years. And to all my friends who were there for me at any point during my experience in Pittsburgh, thanks for being there and making life a lot of fun and providing some great memories.

And to the reader, whoever you may be, thanks for your interest in reading this long document! I truly put my best effort into it and sincerely hope it is valuable to you!

I. INTRODUCTION

In the past century, extensive research has been devoted to improving running performance. This wealth of discovered knowledge has been utilized by coaches and athletes to reach levels of performance that were once thought unattainable[171, 186]. A significant portion of this research has been dedicated to determining biomechanical contributors to running[6, 22, 36, 116, 227, 263], the physiological variables which limit performance[19, 20, 53, 63, 195] and methods of improving these limitations[28, 120, 141]. Additionally, interest in running biomechanics has led researchers to examine the neuromuscular system's role in running performance[29, 110, 111, 177, 197, 240]. Researchers have examined the relationship between various physiological variables and neuromuscular variables in an attempt to further understand the association between central and peripheral factors[21, 29, 31, 110, 133, 134]. However, research examining potentially modifiable performance limitations, such as running-induced neuromuscular fatigue, is limited[111, 115, 177]. Furthermore, the vast majority of running research has overlooked the concept that running is a whole-body activity whereby the arms and torso have significant influence on the legs[57, 90, 123]. Thus, there is a great need to ascertain the role of neuromuscular fatigue in all major muscle groups which are active during running. This data could then be used to construct running-specific neuromuscular training programs to improve fatigue resistance, thus performance, in competitive runners.

A. BIOMECHANICS OF RUNNING

A significant amount of research has been performed to determine the role of the legs during running. Electromyographic (EMG) studies have brought insight into which muscles are the most active during running[183], as well as which muscles are most susceptible to fatigue[111]. Leg movement has been viewed as the chief contributor to mechanical work which creates horizontal drive and vertical lift to propel the body forward[45, 116, 194]. Drive and lift are often represented by changes in the vertical and horizontal displacement and velocity body's center of mass (COM)[44].

While it may be intuitively obvious to coaches and athletes that the upper body is active during running[1, 24, 39], there is very little scientific research to quantitatively describe this activity. The relationship between neuromuscular characteristics of the upper body and physiological variables has not been reported in the literature. Likewise, the effect of running-induced neuromuscular fatigue in the upper body has received little attention in the literature[190]. General locomotion studies have revealed that arm muscles are active during gait and do not simply swing reactively[135]. Likewise, torso muscles are active and serve to stabilize the torso in the sagittal plane during running[190, 244]. Kinematic and kinetic data indicate the arms contribute to the vertical lift component of the body during running, but not to the horizontal drive component[125]. As running speed increases, the arms contribute to a greater percentage of lift, which emphasizes the importance of the arms during intense running[125]. Additionally, the actions of the upper body provide the majority of the angular impulse about the body's long axis to counteract the momentum of the legs, which allows for the running cycle to occur[124]. Furthermore, the temporal coordination between movements of the legs, torso, and arms serves to reduce energy cost through minimization of jerky movements[122, 125, 135].

B. INTENSITY-DURATION RELATIONSHIP

The most functionally relevant measure of distance running performance is actual race performance, defined by the total time it takes to cover a set distance[28]. Distance running events are generally defined as races of 3000m or greater[186]. This is determined by an individual's maximal sustained ability to efficiently convert a finite source of biochemical energy into effective mechanical work to propel the body forward[46]. Thus, there is a balance between maximizing mechanical work output and minimizing metabolic energy expenditure, which is reflected by the intensity-duration relationship (Figure 1) [256].

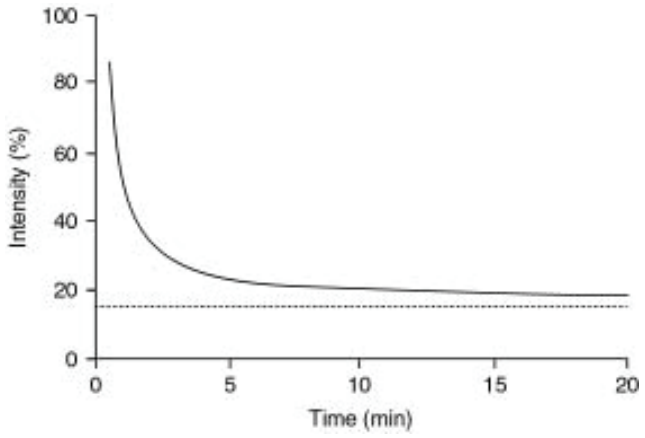

Figure 1 – The Intensity-Duration Relationship (from Walsh[256])

Mechanical work is limited by the force, velocity, and patterns of muscle contraction and biomechanical tissue properties[47]. This is regulated through the complex interactions of central and peripheral components of the cardiovascular and neuromuscular systems[195]. Likewise, duration of intense running is limited by the integrated capability of these systems to supply and

drive the mechanical machinery of the muscles to maintain the given power output. Therefore, one specific system or factor alone cannot be considered the most critical limitation to distance running performance[129, 212]. Thus, fatigue at any level of any one component may limit performance of the whole system.

1. Aerobic Metabolism

The cardiovascular system has traditionally been viewed as the primary limitation to distance running performance[121], thus is often considered the principal cause for fatigue during distance racing events[19, 20, 212]. During long distance races, aerobic metabolism, or oxidative phosphorylation, is the primary energy source for adenosine triphosphate (ATP) generation[76, 259]. Oxidative phosphorylation fuels muscle contraction and is quantified in the laboratory as volume of oxygen uptake (VO_2). Running economy, also known as submaximal oxygen consumption, represents the metabolic cost of running at a given velocity relative to maximal oxygen consumption (VO_{2max})[53, 63]. Thus, running economy represents the overall metabolic efficiency of the system to perform work and is an excellent predictor of performance in a group of homogenous athletes[63]. Running economy is dependent on a variety of factors, including peripheral metabolic adaptation and mechanical efficiency[53, 63]. A high rate of oxidative phosphorylation may alter the metabolic status of the active muscle cells and cause a greater contribution of metabolic energy to be derived from anaerobic glycolysis[128, 176, 208]. The degree to which this happens is dependent on motor unit recruitment, as different muscle fiber types vary in their metabolic optimization. During intense exercise, fast-twitch motor units are progressively recruited[29, 117, 118, 201]. This results in a gradual and progressive increase in VO_2, and this has been labeled the VO_2 slow component (SC)[29, 99, 201].

Anaerobic glycolysis is associated with further cellular changes, such as accumulation of hydrogen ions (H^+), inorganic phosphate (P_i), and other metabolites[54, 92]. Because anaerobic glycolysis does not produce ATP as efficiently as oxidative phosphorylation, mechanical work rate cannot be maintained when the metabolic demands exceed the capability of the system. Furthermore, metabolic by-products formed during glycolysis, including lactate and H^+, are ultimately linked to neuromuscular fatigue and performance limitations[92].

2. Relationship Between Mechanical and Metabolic Variables

The relationship between mechanical factors and performance-related variables has been explored. It is theorized that experienced runners naturally optimize their kinematics to minimize metabolic costs[6, 263], and deviation from an individual's normal kinematics, including fatigue-induced changes, decreases running efficiency[40]. While regression analysis has revealed a considerable amount of the variation in running economy to be attributable to mechanical factors, the relationship between biomechanics and running economy is complex and not clearly established[263]. The relationship between running biomechanics and metabolic factors is best exemplified through studying variations in stride rate and stride length. Running at the naturally developed stride length is more economical than intentionally running with longer or shorter strides[172]. In addition to stride parameters, biomechanical variables related to running economy include vertical COM displacement[116, 226], vertical ground reaction force[263], and plantarflexion angle at impact[263]. Thus, mechanical inefficiency is a contributor to poor running economy. There has been little research published to describe the relationship between upper body mechanics and metabolic variables[113, 263].

3. Relationship between Metabolic and Neuromuscular Systems

There is considerable evidence that the metabolic and neuromuscular systems are interdependent. For instance, the SC has been linked to an increase in EMG activity of the leg muscles[21, 29, 213]. This may be a result of increased recruitment of fast twitch muscle fibers to maintain power output. Similarly, the greater VO_2 required for uphill running relative to horizontal running is attributable to increased muscle activation[228]. There is evidence that muscle contraction makes significant contributions to venous return during exercise and may actually limit cardiac output and therefore aerobic performance[210]. Thus, appropriate muscle activation patterns and sufficient levels of muscular contraction have the potential to affect VO_2, and therefore aerobic performance[29, 99, 152].

C. NEUROMUSCULAR FATIGUE

1. Science Basis for Neuromuscular Fatigue

There is evidence that the neuromuscular system is susceptible to fatigue during intense exercise which may reduce performance. The neuromuscular model defines central fatigue as a decreased neural drive from the brain[148] and peripheral fatigue a result of impaired electrical transmission at the level of the muscle[107]. Glycolytic metabolites from the muscles may feed back into the central nervous system to cause central neuromuscular fatigue[160], though this is likely not a factor in exercise of relatively short duration[192, 235]. Alterations in intracellular electrolyte concentrations[107] and accumulation of glycolytic metabolites, such as lactate and H^+, have been implicated in uncoupling muscle excitation and contraction to result in neuromuscular

fatigue[31, 89, 92, 107, 221]. Neuromuscular fatigue, as measured by MdPF during intense exercise is related to aerobic performance variables, including blood lactate and ventilatory thresholds[134], and oxygenated hemoglobin and myolglobin concentrations[181]. Furthermore, neuromuscular fatigue has been demonstrated to occur parallel to decreases in power output in endurance activity[235]. However, the exact metabolic cause of neuromuscular fatigue is controversial and evidence suggests it is not any one metabolite which alters EMG, but rather a complex interaction of metabolites combined with other factors[31, 140, 221].

2. Quantification of Neuromuscular Fatigue

Neuromuscular fatigue can be quantified in a laboratory setting using EMG. Integrated EMG (iEMG) can be used to determine patterns of muscle recruitment. Fatigue of active motor units during intense exercise results in increased motor unit recruitment, namely fast-twitch motor units. This results in increased iEMG. Changes in mean power frequency (MnPF) or median power frequency (MdPF), also known as a phase shift, also provide insight to the status of the neuromuscular system. Because MnPF and MdPF are similar calculations and both valid measures of myoelectric power spectrum[67], they will be generalized to spectral power frequency (SPF) in this manuscript where applicable. The duration and intensity of the exercise protocol determine the nature of the neuromuscular fatigue, and variations in methodologies have resulted in increased SPF[29, 213], decreased SPF[114, 134], or a patterned combination of the two[182, 240]. Median power frequency increases are thought to result from fast-twitch muscle fibers recruitment to maintain work rate as other active muscle fibers become fatigued[179, 252, 255]. Median power frequency decreases may be due to local metabolic changes affiliated with decreased mean fiber conduction velocity (MFCV)[10, 165]. The balance between these factors are

thought to ultimately determine whether SPF rises or falls with continuous exercise (Figure 2)[94]. It has been suggested that training may attenuate accumulation of metabolites. Thus, during intense exercise the SPF of highly trained muscles will increase due to increased motor unit recruitment in the absence of metabolic byproduct accumulation[29, 94]. Conversely, untrained muscles may experience significant metabolic disturbance, resulting in decreased MFCV, thus decreased SPF[94].

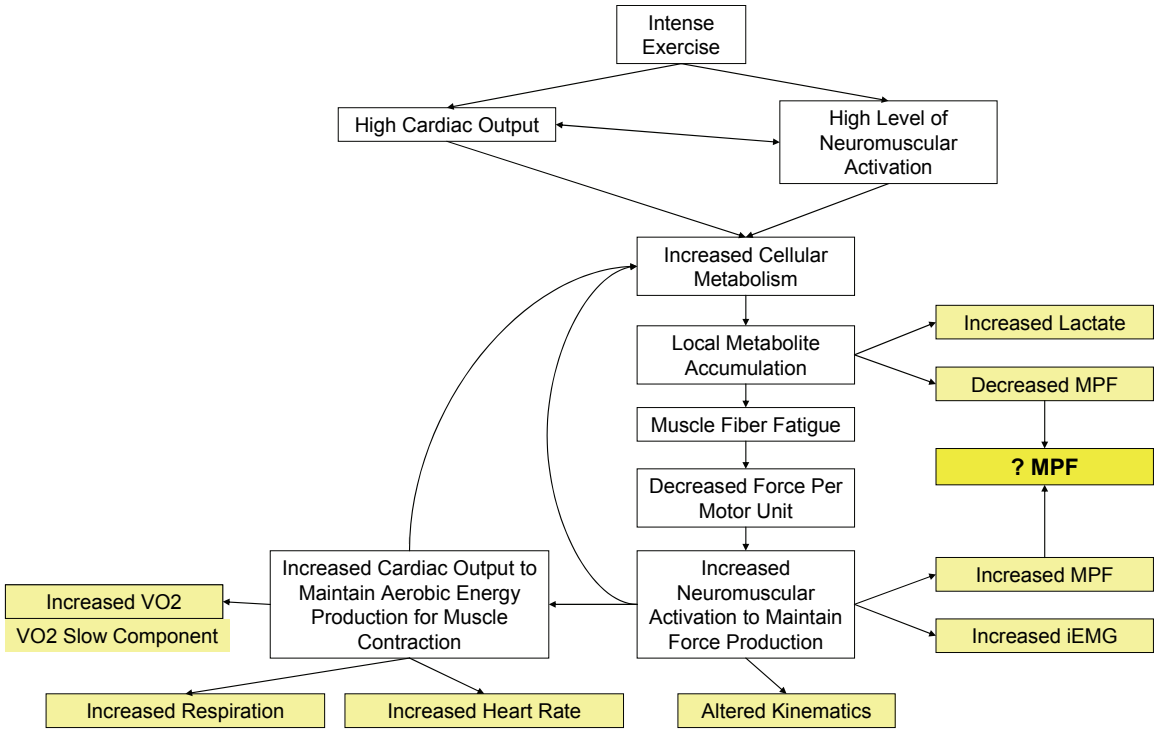

Figure 2 – Paradigm of the potential for neuromuscular fatigue to affect multiple factors related to running performance.

Though researchers have attempted to relate neuromuscular fatigue to physiological variables, many of these studies are limited by collecting EMG from a single muscle[114, 173, 213] or a few selected leg muscles[29, 110] and therefore it is necessary to develop a more specific model of

neuromuscular fatigue[110, 173]. Furthermore, neuromuscular fatigue exhibits varying patterns between muscles of the legs due to different patterns of muscle recruitment, with biarticular muscles fatiguing earlier than monoarticular muscles[111]. Because running is a whole body activity, neuromuscular fatigue analysis should not be limited to the legs, let alone a single muscle within the legs. For instance, the erector spinae muscle group exhibits decreased MnPF during running[190], and it is possible that other muscle groups of the upper body may exhibit fatigue as well.

D. IMPACT OF FATIGUE ON RUNNING KINEMATICS

1. Legs and Whole Body

Running kinematics are altered with fatigue[84], and these changes may be a result of neuromuscular fatigue[115]. Researchers have found fatigue to alter stride parameters, including decreased[111, 113] or increased stride length[102, 264], decreased[15, 102] or increased stride rate[36, 111, 266], and increased variability in these parameters[40]. In fatiguing five kilometer (5K) runs, fatigue-induced changes in stride length, knee flexion, and hip flexion have been observed[264]. Protocol-induced localized muscle fatigue has been demonstrated to affect stride length[115]. During a 42.2km marathon race, hip range of motion in female runners increases as pace decreases, with changes being possible compensatory attempts to maintain horizontal velocity while fatigued[36]. Furthermore, vertical displacement of the body's COM has been shown to decrease during a laboratory fatigue protocol[15] and after the first quarter of a marathon race[36]. Alterations in kinematics may represent decreased mechanical efficiency, thus decreased running economy and performance. There have been attempts to relate changes in whole-body mechanical work to the

SC, but no significant relationships have been found[15]. However, techniques relying on COM to calculate work are not as accurate as those which utilize sum of segmental work[268], because they do not take into consideration movement of all segments and how the net work was produced[6].

2. Upper Body

Despite visible changes to upper body running mechanics during fatigued running, no scientific literature has described the effect of fatigue on running mechanics of the arms and few have examined the torso[83]. While research examining neuromuscular fatigue of the upper body in running is very limited, there is evidence that torso muscles are susceptible to neuromuscular fatigue during running[190]. Because movements of the upper body influence the whole body[122, 124, 125], it is possible that neuromuscular fatigue of the upper body may change the kinematics of the entire body and limit running performance (Figure 3). Furthermore, the upper body musculature of runners may be less fatigue resistant than the lower body, as running performance researchers and coaches have focused on improving the strength and endurance of the leg muscles while largely ignoring the upper body[120, 166, 167, 196, 233]. Therefore, it is reasonable to hypothesize that muscles of the upper body in runners are less fatigue resistant than the legs, and neuromuscular fatigue of the upper body may alter running kinematics and reduce performance during intense running. Upper body weight training has been suggested as a means of delaying or preventing fatigue-induced kinematic changes during running[1, 39], however there is no scientific research to support this. To maximize the specificity of any training program for runners to delay or prevent neuromuscular fatigue, it is first necessary to determine which muscle groups are most susceptible to neuromuscular fatigue.

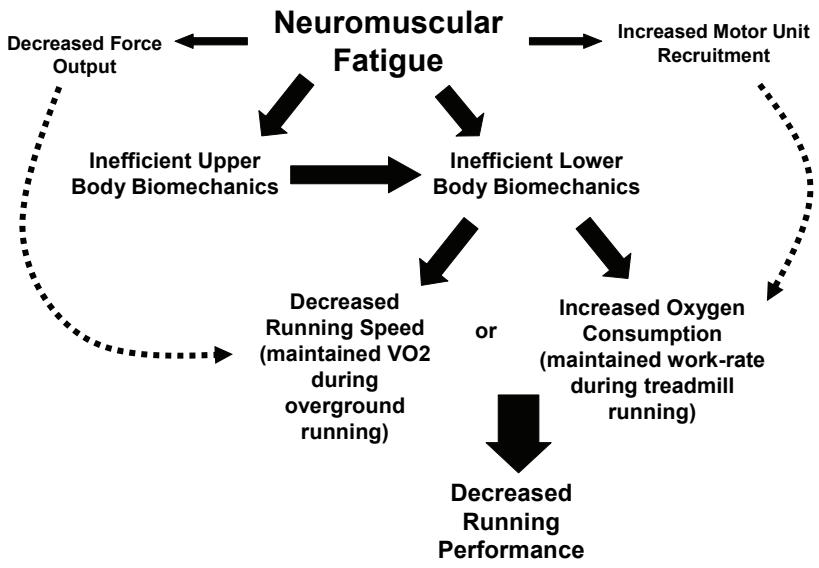

Figure 3 – Potential consequences of upper body fatigue on racing performance.

E. PARADIGM OF WHOLE BODY NEUROMUSCULAR FATIGUE DURING RUNNING

During a 5K race, the arms and torso serve to stabilize the lower body during each stride and make significant contributions to vertical lift. Neuromuscular fatigue in the arms and torso may result in respective kinematic changes, which may decrease their contribution to vertical lift. This may impose a greater load on the legs, which may then exhibit neuromuscular fatigue and consequent kinematic changes shortly before volitional fatigue occurs. If neuromuscular fatigue is found to cause kinematic changes during intense running, then fatigue-resistance training programs may be implemented to improve running performance. Training programs aiming to delay or prevent neuromuscular fatigue should be designed to specifically target the muscle

groups most susceptible to fatigue. Thus, it is necessary to determine the patterns of neuromuscular fatigue during intense running.

F. SPECIFIC AIMS/HYPOTHESES

Specific Aim 1 – To determine alterations in neuromuscular activation patterns of the major prime mover and stability muscle groups of elite runners while running at an intensity of 95% of VO_{2max}. Specifically, the iEMG of selected leg muscles (vastus lateralis, semimembranosus, gluteus maximus, rectus femoris), torso muscles (erector spinae, latissimus dorsi, rectus abdominus, external oblique), and arm muscles (anterior deltoid, middle deltoid, posterior deltoid, upper trapezius, and brachioradialis) will be evaluated unilaterally while running at 95% of VO_{2max} on a treadmill.

Hypothesis 1 – Integrated EMG of all muscles measured will increase relative to initial baselines during the run.

Specific Aim 2 – To determine if neuromuscular fatigue occurs in the major prime mover and stability muscle groups of elite runners while running at an intensity of 95% of VO_{2max}. Specifically, median power frequency of selected leg muscles (vastus lateralis, semimembranosus, gluteus maximus, rectus femoris), torso muscles (erector spinae, latissimus dorsi, rectus abdominus, external oblique), and arm muscles (anterior deltoid, middle deltoid, posterior deltoid, upper trapezius, and brachioradialis) will be evaluated unilaterally while running at 95% of VO_{2max} on a treadmill.

Hypothesis 2a – The MdPF of the leg muscles will increase relative to initial baselines during the run.

Hypothesis 2b – The MdPF of the torso muscles will decrease relative to initial baselines during the run.

Hypothesis 2c – The MdPF of the arm muscles will decrease relative to initial baselines during the run.

Specific Aim 3 – To determine if neuromuscular activation and neuromuscular fatigue are associated with kinematic changes.

Hypothesis 3a – Neuromuscular activation, as measured by normalized iEMG, in any muscle will be associated with altered kinematics at the respective joint. Additionally, these changes will be associated with altered whole-body running kinematics.

Hypothesis 3b – Neuromuscular fatigue, as measured by MdPF, in any muscle will be associated with altered kinematics at the respective joint. Additionally, these changes will be associated with altered whole-body running kinematics.

II. REVIEW OF LITERATURE

Running performance is dependent on maximizing the speed that can be maintained over a given distance[256]. Current models of running performance suggest the integration of mechanical, physiological, biochemical, and neuromuscular factors make significant contributions to running performance[46, 186, 195, 256]. Ultimately, performance is dependent on these factors optimizing the balance between maximizing power output and duration of exercise[256] (Figure 4). During intense running, fatigue may develop and limit maximal performance. Improving limitations within any of these systems will theoretically increase running performance, likely though delaying or preventing fatigue if all other factors are held equal[195]. To understand the basis for performance optimization, it is necessary to understand the components of running performance, how they relate to one another, and how they are affected by fatigue. These factors will be reviewed and specific emphasis will be placed on how these factors relate to neuromuscular fatigue. Furthermore, the potential for neuromuscular fatigue to affect the upper body and limit performance will be considered.

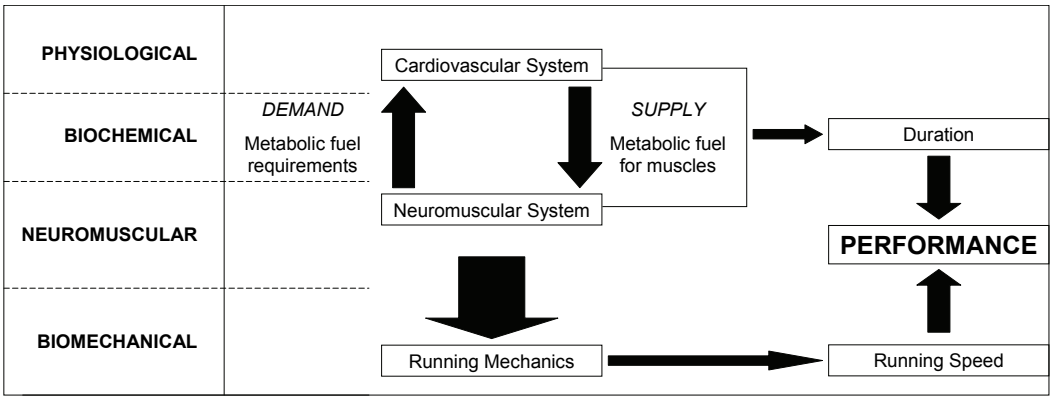

Figure 4 – The interdependent nature of multiple systems contributing to performance.

A. GENERAL RUNNING MECHANICS

Running mechanics represent the end product of the coordinated integration of the physiological, biochemical, and neuromuscular components mentioned above. The hierarchy of movement is seen in Figure 5 [204].

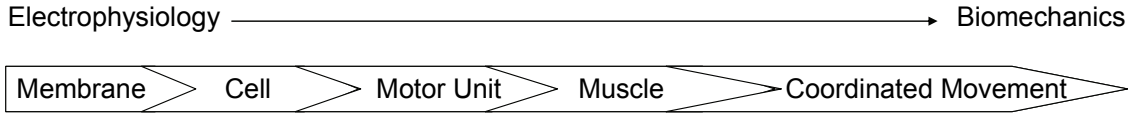

Figure 5 - The sequence of factors leading to movement (from Rau[204]).

1. The Running Stride

The stride is the most fundamental mechanical component of running mechanics and a number of specific events are defined within it. The terminology of Slocum and James[227] is widely used in the literature in describing the running gait cycle and will be employed for this research project. The time the foot is in contact with the ground is defined as the *support* phase and the remainder of the stride is the *swing* phase. Support is divided into foot *contact, midsupport,* and *toe-off*. Foot contact is defined as the initial contact with the ground until full weight acceptance. Midsupport represents the time of full weight acceptance until ankle plantar flexion begins. Toe-off is defined as initiation of ankle plantar flexion until the foot is no longer in contact with the ground. The swing phase is divided into *follow-through, forward swing*, and *foot descent*. Follow-through occurs from toe-off until maximal hip extension. Forward swing is the time period from maximal hip extension through maximal hip flexion. Foot descent takes place from maximal hip flexion until foot contact. During follow-through and foot descent, neither foot is on the ground and this is referred to as the *float* phase. There is considerable variation in the literature in defining specific events of running, including inconsistent use of additional terms such as footstrike (contact), impact (contact), stance (support), takeoff (toe-off), and flight (float),. For the purposes of this review, the original terminology of the respective authors will be used at all times.

The net result of the stride cycle is horizontal and vertical motion, respectively known as drive and lift. Drive is quantified as stride length. Lift is quantified by the vertical displacement of the body's center of gravity (COG) or COM. The COG is at its minimum during midstance as

it passes over the foot, and reaches its maximum immediately after takeoff[36, 136]. The total displacement of the COG is typically between 5 and 10cm[36].

2. Leg Muscle Activation Patterns of the Stride

Stance

The three vastus lateralis, vastus medialis, vastus intermedius, and rectus femoris muscles all exhibit an EMG peak as they contract to support the knee joint as it accepts much of the body weight[8, 183]. This is the only time the vastus lateralis and vastus medialis exhibit an EMG peak during the running cycle[183]. The normalized iEMG of the vastus lateralis and vastus medialis are greater than those of the vastus intermedius and rectus femoris during stance[183]. This is likely due to the oblique pull of the vastus lateralis and vastus medialis muscles contributing more to patellar stabilization than the more direct pull of the vastus intermedius[183].

During early stance, the gluteus maximus and hamstring muscle groups contract concentrically, which creates a hip extensor moment which drives the body over the foot[157]. The adductor magnus, gluteus medius, and tensor fascia lata also have a peak in EMG during stance, as these muscles stabilize the hip medially and laterally[170, 183]. The semimembranosus and long head of the biceps femoris each have a peak in EMG during stance[183]. The biceps femoris contracts to initiate knee flexion and the gastrocnemius contracts to plantar flex the ankle[157]. The long head of the biceps femoris initiates hip extension as the COG moves anterior to the knee[183]. Shortly thereafter, the short head of the biceps femoris is activated to eccentrically control knee extension during late stance, and initiate knee flexion as the swing phase beings[183]. This contraction continues through the mid-swing.

The tibialis anterior muscle displays EMG through the first half of stance to stabilize the ankle joint[86, 170]. Additionally, tibialis anterior activity may be responsible for accelerating the tibia over the support foot[170]. The gastrocnemius and other posterior calf muscles are active during stance, displaying their greatest EMG peak as they eccentrically contract to stabilize the ankle joint as the tibia moves over the foot[170, 205]. The gastrocnemius then displays its greatest EMG peak during midstance, as it concentrically contracts to initiate plantar flexion to begin the toe-off phase[170]. Though plantar flexion does occur during late stance, the activity of the gastrocnemius is not active through most of this movement, indicating it does not actually cause a "push off" from the ground[170, 205].

Swing

During middle swing, the semimembransosus and long head of the biceps contract eccentrically to control hip flexion[183]. At running pace increases, the gluteus maximus contributes to this[183].

The rectus femoris, psoas major, and iliacus contribute to initiation of hip flexion during early and middle swing, displaying peaks of EMG activity during this phase[8, 170, 183]. The tensor fascia lata and adductor magnus contribute to this movement, with both muscles having peaks in early and middle swing[170, 183].

The rectus femoris and vastus intermedius contract eccentrically during swing to eccentrically control knee flexion during middle swing[183]. During late swing, the vasti initiate knee extension and the rectus femoris does not contribute to this[183]. The short head of the biceps femoris eccentrically contracts to control knee extension. The semimembranosus, long head of the biceps, and gluteus maximus are active to extend the hip. During the follow through, the

rectus femoris activates to initiate hip flexion. The hamstrings and gluteals then eccentrically contract during foot descent to allow for a controlled descent[157].

Prior to ground contact, there is considerable pre-activation of the hip and knee extensor muscle groups, which increases tendomuscular stiffness to enhance force production during the stride[157, 170]. This is seen as an EMG peak in the semimembranosus and long head of the biceps femoris[183]. During late swing, the short head of the biceps is active to eccentrically control knee extension.

The tibialis anterior displays EMG activity after toe-off and this continues through the entire swing phase to dorsiflex the ankle joint[170]. The gastrocnemius is active during foot descent to stabilize the foot as it prepares for impact[170].

3. Upper Body Running Mechanics

The majority of running biomechanics research has focused on the legs, though the arms and torso have been examined sporadically. Despite the lack of research, the torso and arms have been considered important components of running performance by athletes and coaches alike. The role of the arms was first recorded by the ancient Greek philosopher Aristotle, who wrote that "runners run faster if they swing their arms; for in extension of the arms there is a kind of leaning upon the hands and wrists.[12]" Numerous elite running coaches have suggested the upper body plays an important role in running performance and anecdotal claims of improved running through changes in the upper body are plentiful. It has been argued that a runner with "serious form faults, such as excessive upper-body rotation, is inefficient because he or she is wasting energy on movements that impede forward progress [24]." It has been anecdotally suggested that arm and torso movement serve to drive the legs and entire body forward, keep the

trunk in a neutral position, and maintain the runner's balance[125]. Such coaching may or may not be effective for improving running performance, as there is very little published research relating these movements to performance. The following section will provide a comprehensive review of literature describing the role of the upper body during running.

Neural Connection Between the Legs and Arms

The interactions between the arms and legs are rooted in the nervous system, as rhythmic activities of the legs are associated with rhythmic arm movements. Functional MRI imaging has revealed coordination between the upper and lower body to be a complex task controlled by multiple areas of a motor network, distributed across cortical and subcortical regions of the brain[61]. Coordination of the arms and legs is task-specific, with a reflex pathway active during locomotion[73, 112], but not during tasks performed while standing or seated[73]. This may be due to nervous system coordination between the arms and legs to aid in balance[180]. Arm movement may increase the neuromuscular activation patterns of the legs during certain activities, such as recumbent stepping[132]. Together, these data suggest that neuromuscular activation patterns of the upper limb may affect the neuromuscular activation patterns of the lower limbs during cycling movements and *vice versa*.

Role of the Arms During Running

General locomotion studies have revealed that arm muscles are electrically active during gait and do not simply swing reactively[135]. Mathematical modeling demonstrates that locomotion would be jerky without active muscular contribution from the arms[135]. This is consistent with the observations of Fenn[90], Hinrichs[125], and Cromwell[57]. The arms appear to contribute to the stability of the body during running by reducing displacement of the body's

COM in the mediolateral and anterioposterior directions. By reducing mediolateral movement, the arms serve to maximize running efficiency by keeping the body moving in straight line. Reduction of anterioposterior movement results in a smoother motion in this plane.

Hinrichs[123] studied the kinematics and EMG of selected upper body muscles bilaterally in a group of ten recreational runners at three running speeds on a treadmill. He found these data to be similar for the right and left side, which suggests that it is valid to study arm data unilaterally. Arm motion is divided into forward and backward swing phases, quantified by shoulder flexion and extension, respectively. The forward swing occurrs shortly after ipsilateral toe-off and the backward swing occurs after contralateral toe-off. The shoulder is abducted 10 to 25 degrees throughout the running cycle. The shoulder does not cross the vertical of the coordinate system, and therefore always remained extended in this respect. The elbow generally shows two peaks of flexion and extension, with the primary peak occurring at contralateral foot strike, and the secondary peak at ipsilateral foot strike[123].

The EMG activity of the anterior deltoid and clavicular portion of the pectoralis major is correlated with the net flexor moment of the shoulder joint. Electromyographic activity of the middle and posterior deltoid and latissimus dorsi is correlated to the net extensor moment of the shoulder. The EMG of the biceps brachii and brachioradialis muscles are correlated to the elbow flexion moments to stop elbow extension. Elbow extension is correlated with triceps activity for the primary extensor moment, though not consistently for the secondary extensor moment. The EMG activity of each of these muscles, net joint moments, and ROM of each of these joint increase with running speed[123].

Hinrichs[125] found movement of the arms increased vertical displacement of the body's COM. With increases in running speed, the vertical displacement of the body's COM decreases,

which is consistent with Buckalew et al's observations in female marathon runners[36]. Although the arms move in opposite directions to one another, their vertical momentum are synched, with negative momentum present in the first half of stance, and positive momentum developing by mid-stance (Figure 6)[125]. Overall, synchronization of arm vertical momentum contributes to approximately 5% of the body's vertical lift, and this contribution increases with increasing speed. The momentum of the trunk negates about half of the arms' contribution to lift. While lift itself decreases with increased running speed, the arms play a relatively greater role in generating lift with increased speed. In mid-stance the arms accelerate upward as a result of an upward force from the rest of the body. The arms react by producing a downward force on the whole body, which creates greater ground reaction forces and results in increases in vertical impulse from the ground. Therefore, it is not necessary for the feet to apply as much torque to the ground to generate the magnitude of ground reaction force that could be attained without arm movement.

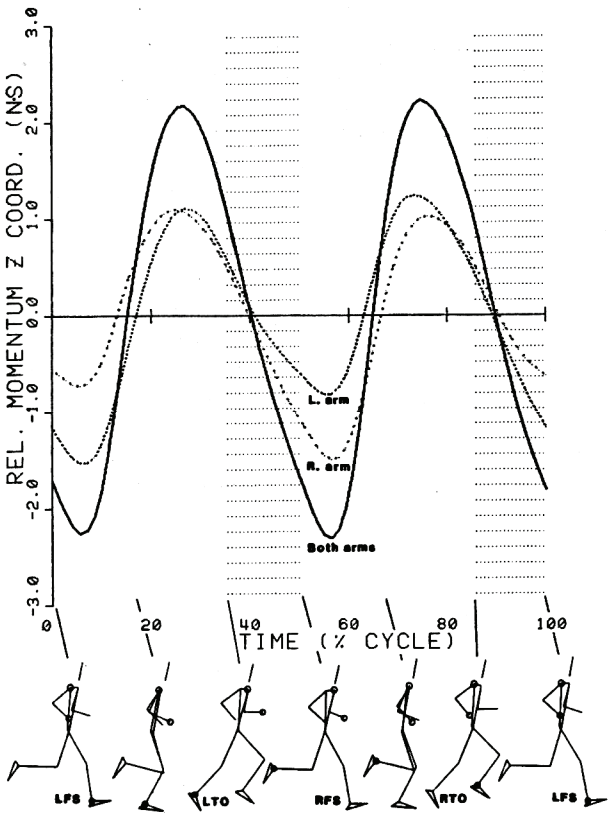

Figure 6 – Vertical Momentum of the Arms During Running (from Hinrichs[125])

Though the arms to have some role in generating lift, they contribute very little to drive in most individuals. In the horizontal plane, the momenta of the arms cancel each other out (Figure 7). While the average individual in Hinrichs' study was not able to generate drive with his arms, some runners were able to generate drive during the contact phase[125]. Thus, individual variation in arm kinematics may determine whether or not the arms contribute to drive. Though the arms do not directly contribute to drive, their contribution to lift allows the legs to do less work propelling the body upward in exchange for greater propulsion forward.

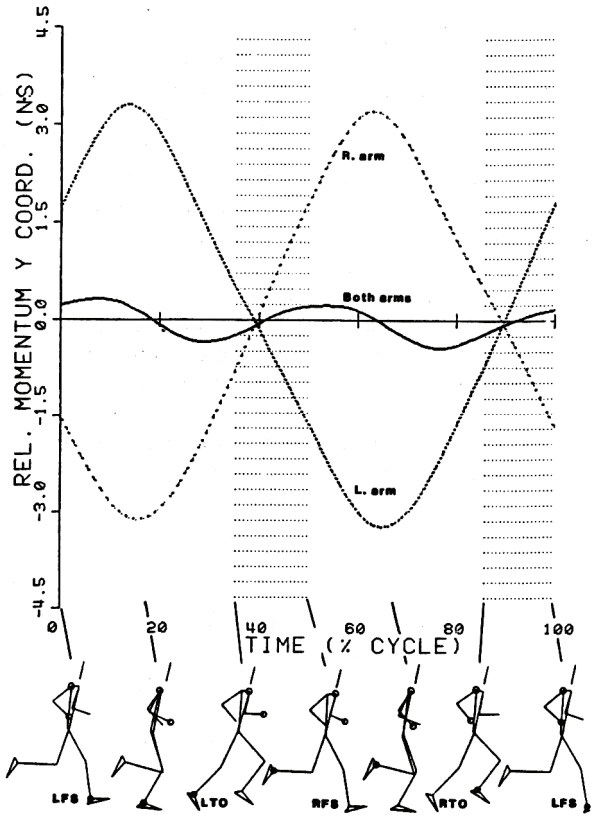

Figure 7 – Horizontal Momentum of the Arms During Running (from Hinrichs[125])

The arms play a significant role in generating angular momentum about the vertical axis of the body. Axial momentum is generated by the legs with each stride, and an equal and opposite magnitude of axial momentum is needed to complete the stride cycle. While the legs possess considerably greater mass than the arms, the arms are still able to generate a large amount of momentum about the transverse plane due to their greater distance from this axis compared to the legs. Abduction of the shoulder joint increases this distance. When axial momenta of the upper trunk, arms, and head are combined, they generally balance out the axial momenta of the lower trunk and legs (Figure 8)[124]. Any differences in axial momentum between the upper and lower body decrease with increases in running speed. In Cappozzo's model[42], the

arms provided the only significant contribution to torques in the transverse plane, and this was attributable to the synchronous action of the arms.

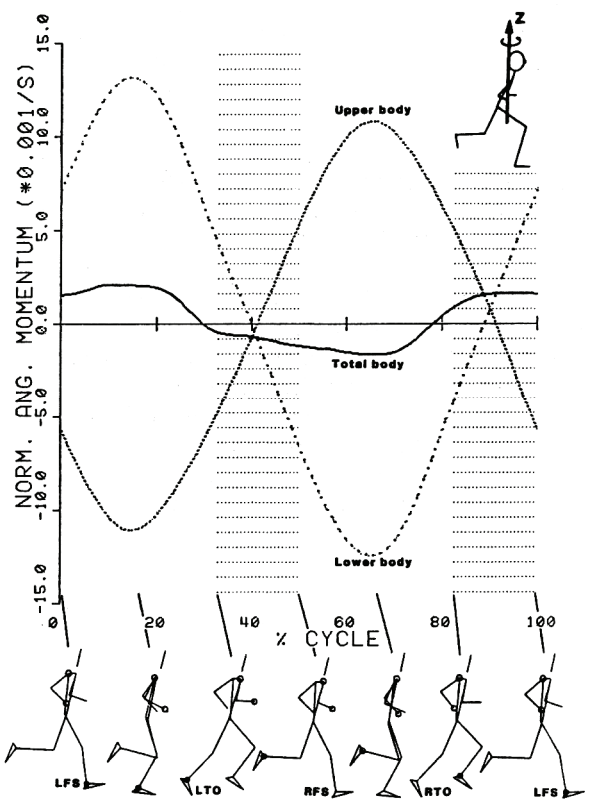

Figure 8 – Angular Momentum of the Legs and Arms About the Vertical Axis (from Hinrichs[124])

Role of the Torso in Running

Like the arms, the torso's role during running has received limited attention by researchers. There is a transfer or momentum between the trunk and the arms, and this results in fluctuations in trunk flexion and extension. As the arms drive upward, the trunk is pushed downward to some degree. The trunk contributes to drive, having positive momentum in before

landing lasting into early stance, and negative momentum later in stance. However, the negative momentum which occurs during stance is great enough to make the overall momentum of the trunk negative. Changes in the trunk momentum oppose that of the whole body, serving to decrease the net change in whole body momentum during braking and propulsion, allowing for smoother movement over the entire stance phase[125]. In the antero-posterior axis, the major contributors of force are inertia and gravity, and these are in counterphase to forces acting on the arms[42]. Lateral forces acting upon the torso during running are significantly influenced by the arm during ipsilateral support[42]. The torso experiences contralateral lateral flexion torque during the support phase of the running cycle which is greatest through the first half of the support phase of the gait cycle[42].

The trunk experiences some angular momentum about the transverse plane, and this momentum is primarily in the upper part of the trunk. The upper trunk displays a similar pattern of momentum about the transverse plane as the arms do throughout the running cycle. The lower trunk has nearly no momentum about the transverse plane[124]. During walking[261] and running[215], the lumbar spine rotates before the pelvis. This has been attributed to be a mechanism for conserving angular momentum[261] and reducing energy expenditure[215]. This is consistent with Hinrichs'[124] concept that upper body rotation is necessary to rotate the lower body for the running stride to occur.

The largest changes in axial momentum occur during the airborne phase of running. Because a change in angular momentum requires application of external force, the only way axial momentum can change while airborne is through the force of the upper body. In order to receive angular impulse from the upper body, the lower body must provide angular momentum in an equal and opposite direction (Figure 9). Thus, the upper body pushes the legs through their

alternating strides[124, 215]. The lower body receives most of its axial torque from the upper body, even during stance[124]. This enables the foot to apply force downward and backward, allowing for efficient forward movement. Additionally, this limits the amount of torsion experienced by the legs. However, because the feet do not pass directly beneath the body's center of mass, a small amount of angular momentum about the body's longitudinal axis is generated during stance.

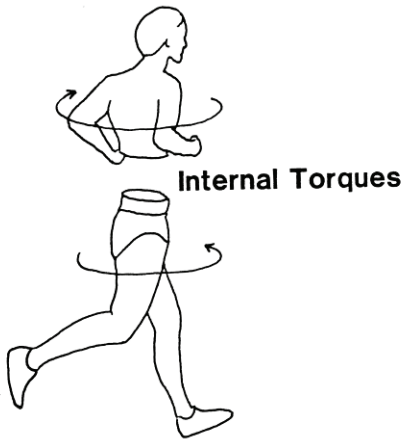

Figure 9 – Opposing Angular Momentum of the Upper and Lower Body About the Vertical Axis (From Hinrichs[124])

The muscle activity of the trunk during running has been described as quasi-isometric, as these muscles serve to stabilize the body and produce little mechanical work[42]. Trunk flexion torque[42] is controlled by erector spinae activation[42, 244]. During running, the same pattern of activity is observed for the multifidus and longissimus bilaterally[244]. Two EMG bursts in the erector spinae are observed per gait cycle; one just prior to ground contact of the ipsilateral limb, and the other just prior to ground contact of the contralateral limb (though slightly after the

ipsilateral activation)[244]. The lateral flexion torque is associated with a contralateral burst of erector spinae activity[42]. Activity of the erector spinae during ground contact corresponds to the activity of the ipsilateral vastus lateralis[244]. The rectus abdominis shows peaks of EMG activity that are not correlated to the running cycle. The external abdominal obliques may serve to stabilize the torso, restrict the abdominal viscera, and assist with breathing during running, and this makes their data difficult to interpret[42]. Irregular muscle activation patterns of the trunk during locomotion may be related to the concept that the muscles are used for subtle movements to maintain balance[57].

Clearly, the arms and torso make significant contributions to moving and stabilizing the body during running. As such, the upper body has been described as "a stable system in a dynamic equilibrium" which can "produce oscillations about a mean position to maintain this stable state.[57]" Thus, it can be hypothesized that deviations from normal motion will affect performance. Such kinematic deviations are likely to occur with fatigue. Though anecdotal claims of runners "losing form" are common and often obvious to novice spectators, fatigue-induced neuromuscular and kinematic changes of the torso and upper body have not been adequately quantified. To optimally train runners, it is essential to further investigate the effects of fatigue on the upper body during running so that training programs may be developed which delay or prevent neuromuscular fatigue.

B. GENERAL PHYSIOLOGY OF RUNNING PERFORMANCE

Broadly speaking, performance is dependent upon the duration an individual can perform at a given work rate or intensity[256]. Physiological mechanisms have traditionally been viewed as

the chief limitation of distance running performance[19, 20]. In distance racing, the vast majority of biochemical energy is supplied via aerobic metabolism, or oxidative phosphorylation[76, 259]. The duration of intense running is ultimately dependent on the body's ability utilize atmospheric oxygen deliver to the mitochondria of muscle cells[260]. This is quantified as VO_2. The integration of a number of systems contributes to the balance between energy supply and demand (Figure 10)[20, 126]. Ultimately, the rate of oxidative phosphorylation, thus VO_2, is dependent on the demand for mechanical power output via muscle contraction[128] and the efficiency of cellular metabolism[126, 265].

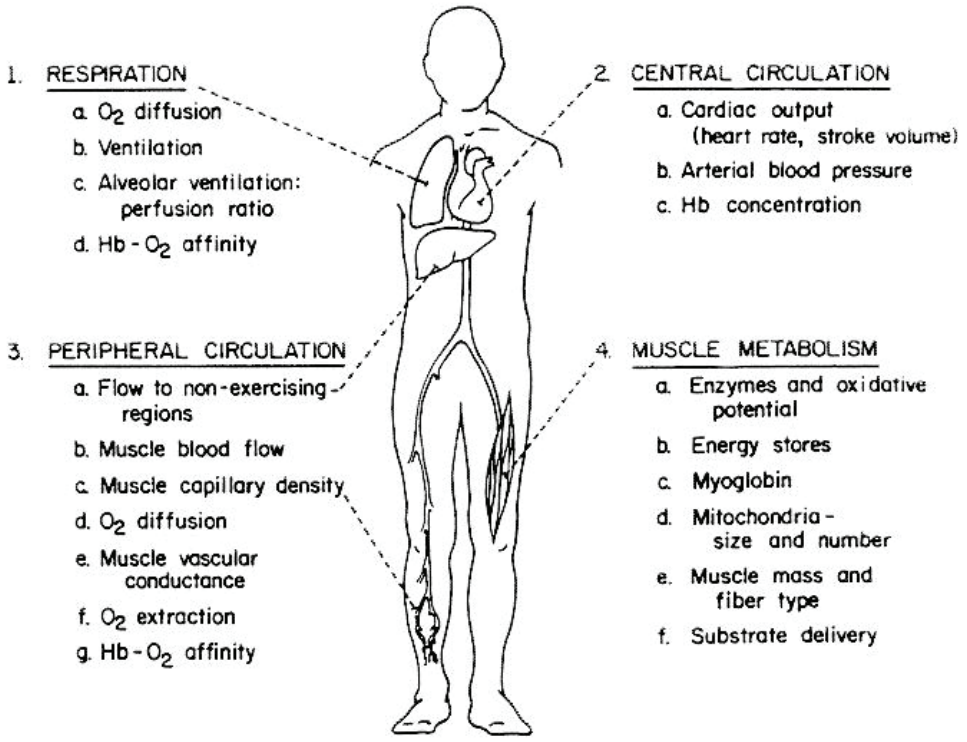

Figure 10 – Integration of Systems Contributing to Oxidative Phosphorylation (from Bassett[20]).

1. Metabolic Pathways

Adenosine triphosphate is the chief biochemical fuel utilized by muscle cells for contractile mechanisms and maintaining ion balance within the cell (Figure 11)[92, 103].

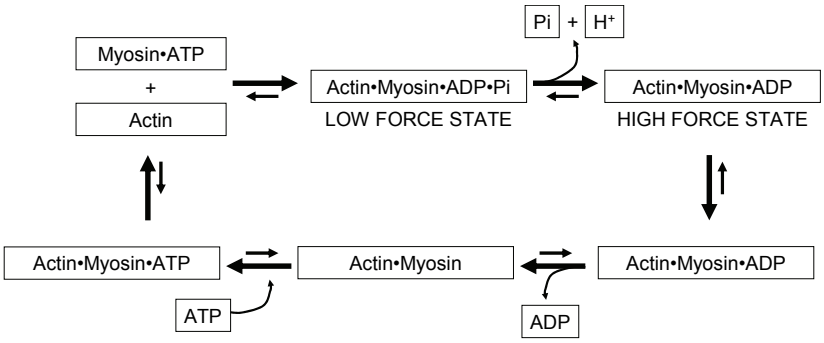

Figure 11 – Mechanism of muscle contraction (From Fitts[92])

The majority of ATP is utilized for actomyosin interaction and calcium ion (Ca^{2+}) release and uptake from the sarcoplasmic reticulum[239]. Oxidative phosphorylation occurs within the mitochondria and is the most efficient metabolic process for generating ATP, resulting in approximately 39 ATP molecules per glucose molecule[232]. The process begins with glycolysis, where glucose or glycogen is converted to pyruvate in the cytosol. Each pyruvate molecule may be transported into the mitochondria and converted to acetyl coenzyme-A. This reduces nicotinamide adenine dinucleotide (NAD) to NADH in a reaction catalyzed by pyruvate dehydrogenase[232]. Acetyl coenzyme-A can then enter the citric acid cycle where reducing equivalents are produced to be used in the electron transport chain for ATP generation[232]. This pathway produces approximately 15 more ATP molecules per pyruvate. The net result of glycolysis and the citric acid cycle is generation of the equivalent of approximately 39 molecules of ATP[232]. Alternatively, pyruvate may be anaerobically fermented into lactate in the cytoplasm. Fermentation results in a net of 2 ATP per molecule per pyruvate when exogenous glucose is used, or 3 ATP per molecule when muscle glycogen is used[232]**.** This is energetically inefficient compared to oxidative phosphorylation. Other metabolic reactions, such as the phosphocreatine

pathway, are minimally used as a source of ATP production during distance running following the onset of exercise and will not be discussed in this review.

On the cellular level, aerobic metabolism is driven by adenosine diphosphate concentration ([ADP]), so that increased [ADP] increases oxidative phosphorylation[128, 245]. During exercise, the chief source of ADP, as well as P_i, and H^+, is ATP hydrolysis used to drive muscle contraction[208]. ADP and P_i can be transported into the mitochondria to undergo oxidative phosphorylation to replenish ATP supply. Additionally, H^+ and electrons produced in the cytosol can be transported into the mitochondria to be used in the electron transport chain of oxidative phosphorylation. When the work rate is below the cell's aerobic capacity, oxidative phosphorylation and ATP hydrolysis are balanced and [ADP] reaches a steady state, which results in a steady state of oxidative phosphorylation[128]. In this steady state, P_i, and H^+ do not accumulate within the muscle cell (Figure 12).

If the work rate is greater than the cell's capacity for oxidative phosphorylation, a steady [ADP] is not reached, and a relatively high [ADP] is required to drive oxidative phosphorylation for sufficient ATP production. This results in significant nonmitochondrial ATP production occurs[208]. With high [ADP], there are also high concentrations of P_i, and H^+. These metabolites have been implicated in fatigue at multiple levels[54]. During intense exercise, the ATP requirement of the cell is greater than mitochondirial oxidative phosphorylation can supply and cytosolic (anaerobic) ATP production is increased. At these high work rates, cytosolic P_i is produced at a faster rate than it can be transported into the mitochondria to undergo oxidative phosphorylation. This results in cytoplasmic pyruvate, NADH, and H^+ accumulation (Figure 13). This drives the lactate dehydrogenase reaction, which results in increases in lactate production[20, 208]. The lactate dehydrogenase reaction produces NAD^+, which maintains cytosolic

redox potential. Maintained redox potential allows for continued cytosolic glycolysis to supply pyruvate for continued ATP production[208]. When muscle glycogen is the original source of pyruvate, lactate formation consumes one H^+ for every pyruvate and therefore serves as a buffer to cellular acidosis[208]. The conversion of pyruvate to lactate results in no net H^+ formation when the process starts with glucose[208]. Lactate is transported out of the cell with H^+, which further limits intramuscular pH changes[208]. However, with intense exercise, the cell may reach its limit in transporting lactate from the cell, and this results in intracellular lactate and H^+ accumulation.

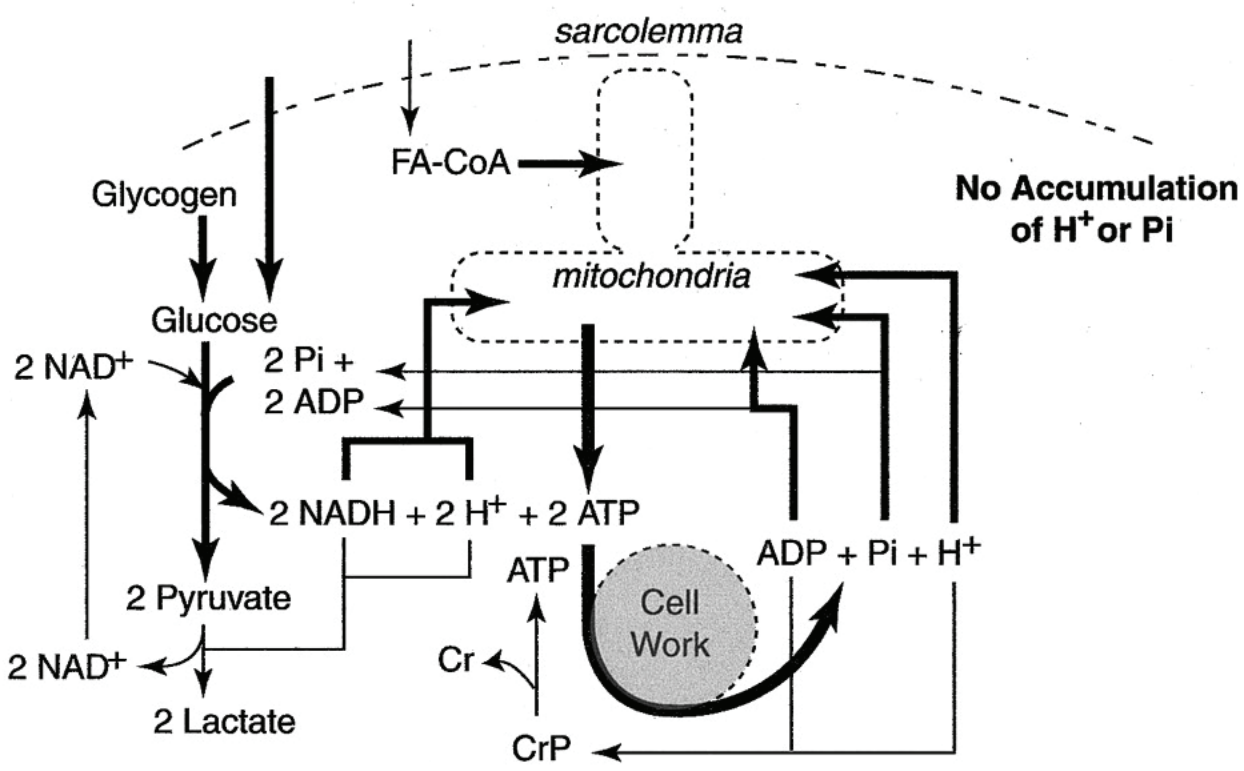

Figure 12 – Metabolic Steady State During Submaximal Exercise (from Robergs[208])

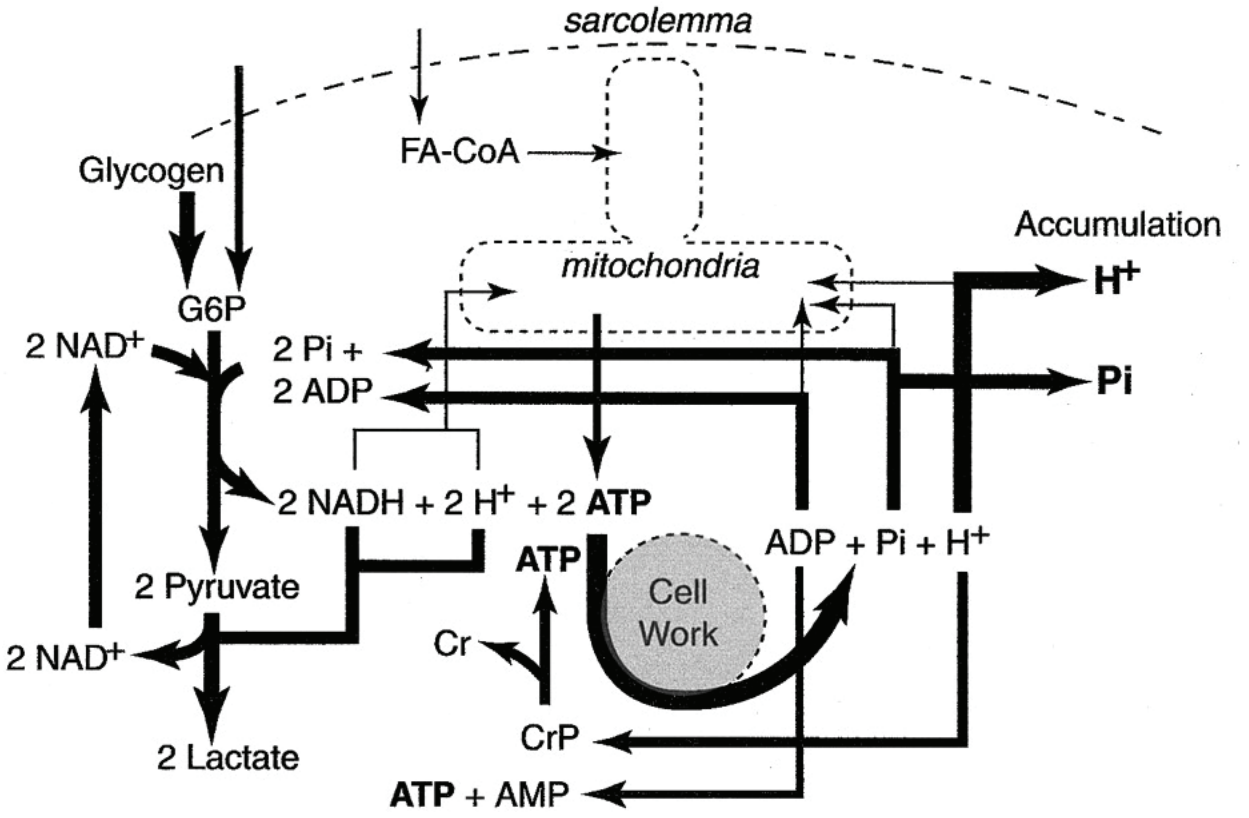

Figure 13 – Metabolic Non-steady State During Intense Exercise (from Robergs[208])

Mitochondrial capacity ultimately determines the extent to which the cytosolic glycolytic pathways are required to assist in meeting the ATP demand[208, 232]. Thus, pyruvate fermentation to lactate is not a result of insufficient oxygen supply *per se*, but rather insufficient cellular adaptation for sufficient rates of ATP production through oxidative phosphorylation. At any given work rate, a greater number of mitochondria reduces the oxidative stress per mitochondria[245]. If cellular mitochondria are not sufficient, higher [ADP] is needed for oxidative phosphorylation.

C. NEUROMUSCULAR COMPONENTS OF RUNNING

The metabolic status of the system is dependent upon the number and type of motor units activated. The motor unit itself is defined as the alpha motoneuron and all the muscle fibers innervated by it[220]. Motor units are divided into slow-twitch or fast-twitch, with the latter divisible into fast-twitch fatigue-resistant, fast-twitch fatigue-intermediate, and fast-twitch fatigable[37]. These classifications are based on the contractile and fatigue characteristics of the muscle fibers they innervate, with all fibers of a motor unit having similar histochemical profiles[37]. Larger, fast twitch motor units have higher propagation velocities than smaller slow twitch motor units[9, 97, 131].

1. Motor Unit Classification

Metabolic classification allows muscle fibers to be divided into three general fiber types: slow-twitch oxidative, fast-twitch oxidative, and fast-twitch glycolytic fiber types[17]. Histochemical myosin ATPase staining techniques have allowed muscle fibers to be divided into multiple fiber types, with type I, IIa, and IIb being the most widely described, with hybrid fiber types also being described in the literature. The correlation between fiber types classified by different systems is somewhat controversial. Slow-twitch oxidative fibers are correlated to type I fibers. Generally, type IIa are considered synonymous with fast-twitch oxidative fibers and type IIb with fast-twitch glycolytic fibers. However, this relationship is somewhat variable, and it has been recommended that the terms not be used interchangeably[220]. For the purposes of this review, the terminology used will be consistent with that of the original publication.

There are inherent differences between the principle fiber types. Type II fibers can generate greater force than Type I fibers[158], in-part due to their considerably greater content of actomyosin and Ca2+ ATPase[239]. Type IIb has the fastest unloaded shortening velocity, and type I the slowest[30]. Type I muscle fibers have greater aerobic capacity and fatigue resistance than type II fibers. This is attributable to greater mitochondria, therefore aerobic enzyme concentration, in type I fibers. Succinate dehydrogenase (SDH) is found in the mitochondria and has been used as a marker of aerobic capacity, and is found in significantly higher concentrations in slow twitch muscle fibers. Lactate dehydrogenase (LDH) has been used as a marker for anaerobic capacity and found in higher concentrations in type II fibers. As a result, Type II fibers are better equipped to convert pyruvate into lactate and therefore activation of Type II fibers will result in a greater percentage of cytosolic ATP production, thus metabolite accumulation[158]. Taken together, this indicates Type I fibers have greater oxidative capacity and metabolic efficiency than Type II fibers[156]. Therefore, type I fibers are best suited for repetitive tasks requiring low force output, type IIa fibers for tasks of intermediate duration requiring intermediate force output, and type IIb fibers for tasks of short duration requiring high force output.

Training has been shown to be related to muscle fiber composition and the relationship between muscle fiber composition and performance has been studied. Endurance athletes have greater SDH in fast twitch fibers of their primarily trained muscle groups compared to the fast twitch fibers of untrained subjects[105]. Elite long distance runners have significantly greater percentage of slow twitch muscle fibers in the gastrocnemius[55, 56] and vastus lateralis[105, 242] compared to trained mid-distance runners and untrained men[55, 56]. Muscle fiber SDH of the gastrocnemius is highly correlated with distance running performance (0.79)[55] with distance

runners having significantly greater SDH than other athletic populations[55, 56, 105]. Furthermore, there is a moderate correlation between distance running 6-mile run time and percentage of slow twitch fibers in the gastrocnemius[56]. Lactate dehydrogenase activity is significantly lower in athletes with greater slow twitch fiber composition, with a significant correlation (-0.70)[55] and athletes with greater fast twitch fiber distribution have significantly more LDH[55]. The significant degree of metabolic adaptation in the primary mover muscles of elite distance runners suggests local metabolic adaptations contribute to distance running performance. Because metabolic adaptations allow for decreased P_i and H^+ accumulation, endurance trained muscles are more fatigue-resistant than muscles which are not as highly trained.

2. Motor Unit Recruitment

Maximal performance is attained through optimizing the balance of motor unit recruitment specific to the task, so that too few active fast twitch motor units limiting power and too many active fast twitch motor units limiting duration. During exercise, the balance between power and duration is governed through orderly recruitment of motor units, with slow-twitch units being recruited before fast-twitch units[72, 117, 231, 251]. Power output may be increased through increasing the number of motor units recruited, increasing the firing frequency, or a combination of the two[107]. Large muscles, such as those of the legs and arms, utilize a recruitment strategy to increase their force, with recruitment occurring at least through 88% of maximal voluntary contraction (MVC) in the biceps brachii[154]. Smaller muscles tend to rely on increases in firing rate rather than recruitment, with the brachialis increasing its firing rate above 70% MVC[146], and the first dorsal interosseous muscle above 50% MVC[69, 154]. This recruitment pattern is also observed in dynamic exercise where all of the type I fibers are recruited by 43% of

VO_{2max}, and all of the type IIa fibers are activated by 75% VO_{2max} in healthy individuals. Beyond 75% VO_{2max}, type IIab and type IIb fibers are recruited. Approximately 80-85% of the motor unit pool recruited during cycling at 75% VO_{2max} in physically active individuals[251, 252].

Serial muscle biopsy studies have revealed that type I and type II muscle fibers are recruited and metabolically active during submaximal intense exercise[152]. During moderate exercise, only type I fibers were recruited and metabolically active, as evidenced through decreased serial [glycogen] in type I fibers and unchanged [glycogen] in type II fibers.

3. Relationship Between Metabolic and Neuromuscular Variables

There exists a definite relationship between muscle activation and metabolic requirement. This is best demonstrated through the gradual and progressive rise in VO_2 during constant pace exercise, referred to as the VO_2 slow component (SC). Oxygen consumption reaches a steady state after about 3 minutes of intense sub-maximal exercise, and later begins to progressively rise further[16]**.** During constant pace[14, 133, 137] and progressive[26, 138] exercise protocols, RMS values increase proportionately with VO_2. Essentially, this means that running economy progressively decreases during intense exercise and appears to be related to increased motor unit recruitment, principally the less metabolically efficient type II fibers[16, 152] which require greater metabolic energy[156]. Thus, with high intensity exercise, progressive recruitment of type II fibers increases the VO_2, and in theory should increase the MnPF in trained athletes[29]. During cycling, 86% of the SC can be attributed to the oxygen consumption of leg muscles[201]. Wavelet analysis of EMG from the rectus femoris, biceps femoris, tibialis anterior, and gastrocnemius muscles revealed that the high-frequency components of the M-wave increase with concurrent decreases in the

low-frequency components during 30 minutes of running in proficient runners[255]. Increased frequency of EMG is consistent with additional type II fiber recruitment[131].

4. Relationship Between Mechanical Variables and Metabolic Variables

Hill's concept of oxygen requirement represents the link between metabolic requirements and net mechanical work. This can be quantified by VO_2 at a given velocity, known as running economy [53]. Running economy can be defined at any velocity, though VO2 at race pace is the most functionally relevant value to obtain when evaluating performance[63]. In a homogenous group of athletes, running economy is a better predictor of performance than VO_{2max}. A multitude of factors, intrinsic and extrinsic to the athlete, influence to running economy. Extrinsic factors include ambient temperature, running surface, and wind velocity. Intrinsic factors include cellular adaptation and running mechanics. By traditional models of performance, running economy and anaerobic threshold interact to theoretically set the duration of performance, as a greater VO_2 at a given pace represents greater metabolic stress, therefore increased lactate production.

Relationship Between Lower Body Mechanics and Running Performance Variables

In attempts to optimize performance, researchers have examined the relationship between running mechanics with metabolic performance variables to determine which are the most important for minimizing energy expenditure during running. It is thought that runners naturally reduce their energy expenditure, thus maximize running economy, through developing neuromuscular activation and movement patterns that are optimal for their individual anatomic and physiological traits[6]. Perhaps the most commonly cited example of a self-optimized

neuromuscular activation pattern which influences running economy is stride length. Increasing or decreasing stride length and/or stride rate from naturally developed preferred stride characteristics has been shown to decrease running economy. Excessively long strides increase the demand for propulsive power and increase breaking forces. Conversely, strides shorter than naturally developed require a higher stride rate to maintain the same speed, which increases work. Therefore any factors which influence stride rate or stride length have potential to influence running performance.

A number of other mechanical variables have been found to be related to running economy. A smaller maximal plantar flexion angle at toe off, a greater angle of the shank with respect to the vertical at foot strike, and a smaller minimum knee velocity during contact are characteristics of more economical runners[263]. Economical runners exhibit a lower first peak of the vertical ground reaction force curve[263]. Non-significant trends have been observed for more economical runners to have greater knee flexion angles during support and lower vertical oscillation[263].

Relationship Between Upper Body Mechanics and Running Performance Variables

The relationship between upper body mechanics and running economy has been largely overlooked in the literature. In comparing runners with low, medium, and high VO_2 at submaximal paces, the total distance of the wrist excursion path was greater in runners with poor running economy than those with good running economy, though the differences were non-significant[263]. In this same study, trunk angle with respect to the vertical showed a significant trend to be greater in the more economical runners[263]. Running with the arms behind the back has been shown to significantly increase VO_2 in trained female subjects at 75% of 5K race pace[80]. Beyond these observations, the relationship between running performance and the upper

body has not been reported in the literature. Likewise, the effect of fatigue on the upper body has received little attention in the literature.

Relationship Between Whole Body Mechanics and Running Performance Variables

Running economy has been found to be related to whole body vertical stiffness, though not leg stiffness[116]. National caliber runners tend to run with less vertical displacement of the center of mass compared to other runners and non-runners[226]. Likewise, more economical runners tend to run with less vertical oscillation of the center of mass than less economical runners[263]. This may be related to leg stiffness[78], as well as other lower body mechanical variables described above. There exists an inverse relationship between vertical stiffness and running economy[116]. Thus, runners who have a more compliant running style may require greater extensor muscle force generation and therefore increased aerobic demand[116].

D. FATIGUE AND EXHAUSTION

Fatigue must be defined within the context of the research issue to be explored. In the case of dynamic exercise, such as running, fatigue can be described as a "reduction of force or power output of the working muscle(s) over time[38]." This definition can be expanded upon to define fatigue as "an acute impairment of exercise performance that includes both an increase in the perceived effort necessary to exert a desired force or power output and the eventual inability to produce that force or power output[65]." This impairment of performance can be regarded as a complex set of task-dependent factors which impair motor performance, rather than a single mechanism[89]. This task-dependency is related to the intensity and duration of the activity contributing to the mechanism(s) of fatigue[89, 256]. Thus, sprinters and distance runners

experience different mechanisms of fatigue. Fatigue may lead to exhaustion, which may be defined as "the voluntary inability to generate the required demand for the physical task"[256]. One major goal of training is to enhance performance by improving fatigue-resistance[84, 195]. To optimize training, it is necessary to understand key contributors to fatigue during running.

In vitro studies have revealed the power output of each muscle fiber is reduced during sustained exercise due to neuromuscular fatigue[93]. This is reflected *in vivo* by a decrease in knee flexion strength[106], vertical jump[106], and maximal sprint speed[91] following sustained running. During fatiguing submaximal contractions, type I motor units are not able to maintain the work rate from the beginning of the exercise period[252]. Therefore, to maintain the mechanical power output to maintain a given running pace, it is necessary to increase force output to the active muscle groups[255]. During running, this is accomplished through increases in motor unit recruitment moreso than increases in firing rate. When muscles are already maximally activated, fatigue-related decreases in force production cannot be balanced through compensatory increases in muscle activation[179, 252]. This ultimately results in decreases in running speed[229]. To develop training programs which limit neuromuscular fatigue, it is imperative to understand which muscle groups are most susceptible to neuromuscular fatigue during running.

1. Types of Neuromuscular Fatigue

Neuromuscular fatigue can be a result of a fatiguing mechanism at any point between the brain and the muscle contractile machinery[65]. Fatigue of the central nervous system may occur and is defined as "failure to maintain the required or expected force or power output, associated with specific alterations in CNS function that cannot reasonably be explained by dysfunction within the muscle itself[65]." This definition includes conscious psychomotor components, such as

motivation and perceived exertion. Central fatigue may be the result of reduced corticospinal input to motoneurons or due to motorneuron inhibition through afferent feedback from the muscle[65]. Accumulation of metabolic byproducts may feedback on mechanoreceptors and type III and IV free nerve endings to contribute to central motor neuron inhibition at the level of the spinal cord[65]. However, most of the literature regarding central fatigue has been conducted using isometric exercise, and these protocols may not be applicable to intense running protocols. Central fatigue is considered to play a role during prolonged running events[200], though appears to make minimal contributions to races of shorter duration in trained athletes. Because the limited available research indicates that central fatigue is not a significant contributor to performance in short intense running events, it will not be discussed further in this review.

Peripheral mechanisms of fatigue have been implicated as limitations to running performance. Excitation-contraction coupling failure is regarded as a chief mechanism of peripheral fatigue. Excitation-contraction encompasses the sequence of events from action potential generation through mechanical muscle contraction[103]. This includes decreased Ca^{2+} release and reuptake by the sarcoplasmic reticulum, decreased myofibrillar sensitivity to Ca^{2+}, and reduced cross-bridge for production[103, 149, 250, 258]. Additionally $[K^+]$ balance, P_i accumulation, $[H^+]$ accumulation, and increased [BLa] have been implicated in fatigue, amongst other hypotheses[149, 250, 258].

2. Quantification of Neuromuscular Fatigue

Neuromuscular fatigue can be quantified through analysis of muscle activity via EMG. Electromyographic signals are recorded using monopolar or bipolar electrodes and represent the summation of motor unit action potentials (MUAP) at a specific site, as well as system noise

(Figure 14)[67]. This signal is commonly referred to as the M-wave[23]. Each individual MUAP represents muscle fiber depolarization and repolarization and this action potential propagates along the muscle fiber[273].

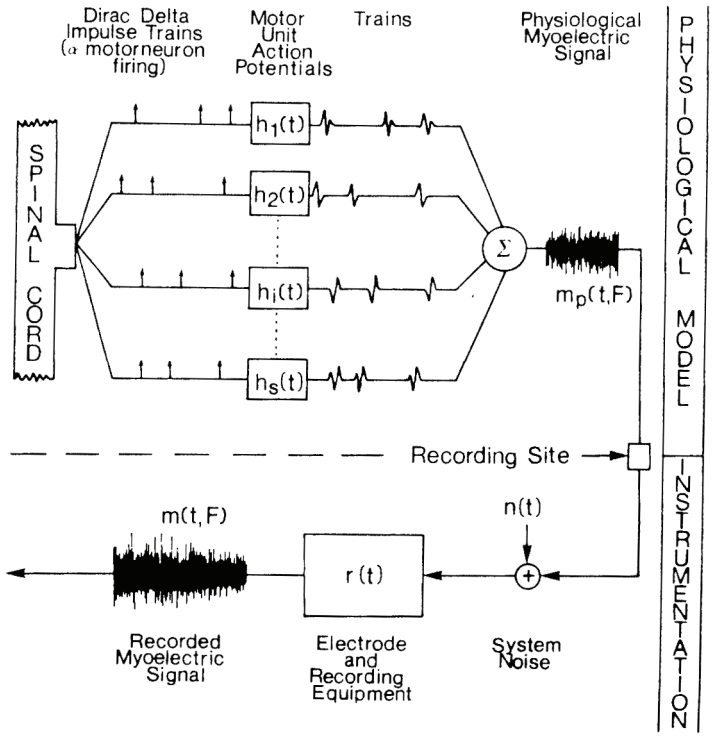

Figure 14 – Contributors to the EMG Signal (from De Luca[67])

Spectral analysis of the mean power frequency and median power frequency are used to determine the nature of motor unit recruitment patterns. Mean power frequency and MdPF are commonly used to examine patterns of fatigue through frequency shifts in the myoelectirc power spectrum[67]. Spectral power frequency is proportional to MFCV of the motor units being measured[79, 164, 189, 274]. Mean fiber conduction velocity represents the propagation of MUAP's

from the muscle fibers of multiple motoneurons[273]. This is dependent on muscle fiber type, with type II motor units having greater MFCV than type I motor units[118, 231]. The MCFV is also dependent upon temperature. Muscle temperature increases with exercise[151, 198, 211], and this increases MFCV[236, 246], which may increase SPF substantially[25, 199].

The SPF kinetics provide a window into the physiological events within the cell[95]. During exercise, SPF may increase or decrease, and the change is dependent on the balance of multiple factors. During exercise, increases in SPF have been regarded as a sign of increased fast twitch motor unit recruitment., due to their greater MFCV. Median power frequency increases with increases in torque[222]. This is related to the low-pass filter effect of muscle tissue on the EMG signal due to the spatial distribution of muscle fiber types. Type II muscle fibers are located more superficially than type I fibers[109, 222] and increases in torque require activation of these fibers. With high levels of type II fiber activation, low-pass filtering is reduced due to shorter average distance between the active muscle fibers and the electrodes[222]. This helps to suggest that increases in torque are due to increased motor unit recruitment, rather than increased firing, as previously discussed. Conversely, SPF is not affected by changes in muscle contraction velocity, and this indicates that contraction speed is more likely due to increased firing rate[222, 231]. Likewise, SPF is lower when type I muscles are the predominantly active fiber type due to their lower MFCV combined with their central distribution and the related low-pass filtering effect[222].

Metabolic changes are associated with decreases in MFCV and SPF. *In vitro* studies have demonstrated decreases in muscle pH cause decreases in MFCV and SPF. This may be due decreases in pH altering the activity of Ca^{2+} channels[269], and thereby altering excitation-contraction coupling. Additionally, lactate accumulation has been viewed as a potential

contributor to frequency shifts with fatigue[130, 243]. This is due to the concept that lactate accumulation can decrease MFCV[185]. However, evidence points to the relationship between lactate and MFCV being associative rather than causative[31, 140, 173]. For instance, M-wave amplitude decreases while duration increases during incremental cycling exercise, and these alterations are correlated to changes in pH, but not [BLa][138]. An example of metabolic influence on SPF kinetics is seen in Scheuermann's[218] work, where healthy subjects completed a fast-ramp and slow-ramp protocol on a cycle ergometer while EMG of the vastus lateralis and vastus medialis was recorded. During the fast-ramp protocol, MdPF decreased, whereas MdPF remained relatively constant during the slow-ramp protocol. This suggests the possibility that accumulation of fatigue-related metabolic factors which should have decreased MdPF were balanced out by increased type II motor unit recruitment during the slow-ramp protocol, and therefore MdPF remained steady[218]. However it is likely that other factors also influence this and this is task-dependent[33].

With fatigue, the M-wave may be widened and this can lower SPF without a decrease in MFCV[33]. The EMG waveform is dependent on the rate of depolarization and repolarization of the sarcolemma[33], chiefly in Na+ and K+[143]. With fatigue, the repolarization phase of the M-wave is increased, while depolarization remains the same, thereby increasing the duration independently of MFCV[33]. Potassium ions have been implicated in altering excitation-contraction coupling. With exercise, K^+ is lost from the muscle into the intracellular space and this affects the membrane potential. This is consistent with the concept that excitation-contraction coupling is a key player in fatigue. Central factors such as motor unit firing rate and synchrony have been considered potential contributors to frequency shifts[150], though synchronization is relatively uncommon[70, 150].

The overall balance between motor unit activity, local metabolic conditions, temperature, and other described factors described above determines SPF. The variation in SPF kinetics is likely related to training status, as training may delay the metabolic alterations which potentially lower SPF[94]. This is consistent with studies which demonstrate training induced cellular alterations, such as increases in mitochondrial density. Thus, type II motor unit recruitment may occur during sustained exercise in untrained individuals, but lack of metabolic adaptation may significantly affect the local metabolic status to shift the balance of factors towards a decrease in SPF. During progressive[138] and constant-load[133] exercise at the ventilatory threshold, untrained subjects exhibited an increase in M-wave duration and decrease in M-wave amplitude, whereas the amplitude and duration of trained cyclists remained unchanged. Gamet[94] found subjects demonstrated four varied patterns of MnPF kinetics with fatigue during one incremental exercise protocol: continuous increase, continuous decrease, increase followed by decrease, decrease followed by increase. Thus, increases in SPF occur when increased fast twitch recruitment and muscle temperature exceed the accumulation of metabolic by-products. Decreases in SPF are a result of metabolic changes in the muscles, which reflect insufficient cellular adaptation for the work performed[94].

The task-dependent complex nature of neuromuscular fatigue makes it difficult to establish an accurate paradigm of general neuromuscular fatigue. The existing knowledge based is based on a wide variety of conflicting *in vitro* and *in vivo* research in human and animal muscle exposed to a variety of fatiguing conditions[92]. This makes it quite difficult to establish a general fatigue paradigm during running, especially for a given intensity or duration.

E. NEUROMUSCULAR FATIGUE DURING RUNNING

Research methodologies investigating neuromuscular fatigue during running have been inconsistent. Determination of neuromuscular fatigue has been varied, with some researchers reporting mean or median power frequency while others reporting iEMG or RMS EMG, and others analyzing combination of the two. Fatigue protocols have employed continuous and intermittent exercise protocols and have analyzed different muscles. Continuous running protocols have considerable variation, including steady paces at slow or fast speeds, and incremental tests where either belt speed or treadmill incline is increased at various points. Previous research has examined individuals ranging from world class runners to healthy individuals unaccustomed to running, and it is expected that there are inherent differences between these groups. These inconsistencies make it difficult to compare results between studies and extrapolate the results to race performance. Therefore, the following section will review the pertinent literature regarding neuromuscular fatigue during running and the information will be used collectively to justify the hypotheses of this project.

1. Neuromuscular Fatigue of the Lower Body

There is limited research on neuromuscular fatigue during continuous running, with very little research specific to 5K performance. Borrani[29] examined the EMG activity of the vastus lateralis, gastrocnemius, and soleus bilaterally while regionally competitive runners ran at 95% VO_2 max until exhaustion. This intensity may be regarded as 5K-specific[28]. During the run, MnPF significantly increased in the vastus lateralis and gastrocnemius and remained unchanged in the soleus. The increases in MnPF were correlated to the SC, which is likely attributable to

recruitment of type II muscle fibers[29, 252]. The lack of change in the soleus is likely attributed to the type I fiber composition of the muscle providing fatigue resistance[29, 89]. It is noteworthy that Borrani's subjects were well trained runners and their results are consistent with Gamet's[94] findings of increased MnPF in trained athletes.

Mizrahi explored the neuromuscular effects of 30 minutes of continuous intense running in recreational runners[182]. Integrated EMG of the gastrocnemius was found to be unchanged with fatigue, while iEMG of the tibialis anterior was increased significantly. The MnPF of the gastronemius significantly increased with fatigue, while that MnPF of the tibialis anterior were significantly decreased. The authors interpreted this to mean that the activity of the gastrocnemius was maintained (unchanged iEMG), with a possible enhancement of motor unit firing (increased MnPF), while the soleus had a reduced number of active motor units (decreased iEMG) and decreased firing rate (decreased MnPF).

Taylor and Bronks[240] found trained runners who ran on a treadmill with progressively increasing speed exhibited an increase in iEMG of the vastus lateralis and gastrocnemius[240]. Following the onset of exercise, MnPF of these muscles progressively increased before showing a gradual decrease. The maximal MnPF (76.4% VO_{2max}) occurred after the lactate threshold (72.1% VO_{2max}) and before ventilatory threshold (79.1% VO_{2max}), while iEMG increased throughout the protocol. These findings indicated that progressive type II motor unit recruitment occurred, as indicated by progressive increases in iEMG and initial increases in MnPF. Following the maximal MnPF, the decreases in MnPF may be attributable to metabolic alterations, as indicated by the temporal relationship to lactate and ventilatory thresholds[240]. This is consistent with Gamet's[94] description of the balance between factors which influence SPF,

with initial increases in SPF resulting from increases in motor unit recruitment, and subsequent decreases in SPF resulting from metabolic alterations.

Hanon studied the EMG of the vastus lateralis, biceps femoris, rectus femoris, tibialis anterior, and gastrocnemius in well-trained runners during an incremental running fatigue protocol[111]. The authors found the iEMG of the rectus femoris and biceps femoris to progressively increase, whereas the other muscles did not demonstrate these changes. This is attributed to the biphasic muscle activation patterns of these muscles. Biphasic muscle activation decreases relaxation time between activations, and this increases metabolic requirements, muscle tension development is more energetically costly than tension maintenance[75]. This is a result of the Ca^{2+} ATPase repeatedly needing to reestablish the ionic gradients between contractions. The recorded increases in stride frequency may also have contributed to fatigue by decreasing the duration of relaxation between muscle contractions[159]. This may reduce the blood flow to these muscles for oxygen delivery and metabolite removal. The results of this study emphasize that neuromuscular fatigue varies between muscle groups, which furthers the need to study more muscles during running.

2. Neuromuscular Fatigue of the Upper Body

To date, only one study has examined the role of neuromuscular fatigue in the upper body during running. Nagamachi studied the EMG activity of the erector spinae in healthy individuals during running and found steady decreases in MnPF after the point they defined as anaerobic threshold[190]. It should be noted that the erector spinae are stabilizer muscles and therefore have a high percentage of type I muscle fibers, and are therefore relatively fatigue resistant. Thus, if there are alterations in this relatively fatigue resistant muscle group, it is likely that other muscle

groups may also be subject to neuromuscular fatigue during running. While the aim of the authors was not specifically to relate trunk muscle fatigue to running performance, this study provides evidence that trunk muscles are susceptible to fatigue during running, and this fatigue can be quantified using EMG.

The diversity of results due to methodological inconsistencies demonstrate the need to justify the proposed methodology for each study so that results are functionally relevant. Because 5K represents a commonly raced distance for elite, scholastic, and recreational runners, a running protocol which simulate the intensity and duration of a 5K race is the most functionally-specific protocol for this study. This protocol is most similar to Borrani[29], who used a velocity associated with 95% of VO_{2max}; an intensity at which trained subjects ran about 15 minutes before exhaustion. It should be noted that this methodology may be ideal for investigating NM fatigue for a 5K race, but due to the task dependent nature of fatigue, the results may not be applicable to significantly shorter or longer racing distances. This study does not aim to produce results general to the concepts of neuromuscular fatigue, but rather specific to neuromuscular fatigue during a 5K race in elite-level runners. The results may or may not be generalized to cycling and other forms of exercises, or to exercise of different intensities or durations.

F. MECHANICAL CHANGES WITH FATIGUE

1. Relationship Between Neuromuscular Fatigue and Mechanical Changes

Fatigue-related changes in neuromuscular activation are at the root of kinematic changes[115]. Hayes et al[115] examined the endurance of the hip and knee flexors and extensors

using an isokinetic protocol in subelite runners and related these measures to kinematic changes during an exhaustive run. Eccentric knee flexion, eccentric hip extension, and concentric hip extension endurance were significantly correlated to changes in stride length. Thus, subjects with the greatest local muscular endurance displayed the smallest alterations in stride length. However, there were no significant changes in the group for stride rate, stride length, or hip and knee joint angles during running. The lack of differences in these variables within the group may be attributed to the inter-individual variability of kinematic changes with fatigue.

2. Mechanical Changes of the Lower Body

With fatigue, muscle co-activation patterns may be altered, thereby decreasing leg stiffness and whole body vertical stiffness. Overall vertical and leg stiffness of trained runners have been demonstrated to decrease during a run to exhaustion. However, it should be noted that this reflected the majority of subjects, though three of the fifteen subjects exhibited an increase in vertical stiffness. Decreased stiffness is associated with decreased stride rate. Changes in vertical stiffness are thought to reflect the dynamics of the physiological state of working muscles as they fatigue[78].

Neuromuscular fatigue induced alterations in running mechanics may affect running economy, and ultimately performance. Changes in stride parameters with fatigue have been extensively studied. Stride rate has been observed to increase[84], decrease[102], or remain the same[83] during fatigue. Likewise, stride length has been observed to increase[71, 102], decrease[83, 84], or remain the same during fatigue. In some studies, changes in stride rate[78] or stride length[115] have exhibited great variation between subjects with some increasing and others decreasing. Contradictory results may be related to the fatigue protocol used or the training status of the

subjects. Changes in stride length with fatigue are varied between individuals, and this is likely a result of inter-individual variation in joint angles of the legs in response to fatigue[264].

Fatigue-related changes in stride parameters are likely the product of other kinematic changes. Hip flexion angular velocity is not increased with fatigue during intense running at competition paces in collegiate runners[264]. Maximal hip flexion angle increases significantly during a competitive run and shows a non-significant trend to increase during noncompetitive and treadmill runs. During a 10K race, running velocity, stride length, and foot velocity at contact decrease and the angle of the lower leg with the vertical increases[83]. During a marathon, hip range of motion in female runners increases during the race as pace decreases. It is theorized that early in the marathon, the unfatigued leg extensor muscles did not need a full range of motion to generate race pace velocity. Buckalew suggested this increased range may be a strategy to maintain horizontal velocity[36].

During fatiguing overground and treadmill runs, knee flexion angle slightly (two degrees) but significantly increases in collegiate runners[264]. Increases in knee flexion angle decreases the moment of the inertia of the leg about the hip joint, which may reduce the requirement of hip flexor torque. Marathon running has been found to decrease stride length, increase knee extension angle at foot strike, and increase maximal knee flexion angle during the non-support phase[113]. During a run at 3000m race pace, recreational runners exhibited a decrease in peak impact acceleration, knee flexion at heel contact, maximum knee flexion, maximum knee flexion velocity, subtalar inversion at contact, maximum rearfoot angle, and maximum rearfoot velocity[71].

The angle of the shank with respect to the vertical increased with fatigue during 3000m of intense overground running in elite track athletes[84]. Because mechanical efficiency is

optimized by positioning the foot as near as possible under the body's COM[90, 227], increases in angular position at contact theoretically decreases mechanical efficiency[84]. While running efficiency decreases following a marathon run, no specific kinematic variables have been reported to be related to the change, suggesting that a multitude of factors are responsible for the change[113].

3. Mechanical Changes of the Upper Body

There has been very little published research to describe the impact of fatigue on the upper body. Forward trunk tilt does not appear to change with fatigue in highly trained mid-dstance runners[84] or marathoners[13] during races of their respective distances. However, during a simulated triathlon run, trained triathletes exhibited a significant increase in trunk flexion angle at foot strike compared to an isolated training run and simulated marathon run[113]. Alterations in trunk flexion angle may potentially increase metabolic costs, as the weight of the upper body needs to be balanced by activation of anti-gravity muscles rather than just supported[227]. During repeated mile runs during a 24-hour relay, elite runners demonstrated increases, decreases, and no changes in shoulder axial rotation and torso lateral bending[3].

4. Mechanical Changes of the Whole Body

The height of the COM has been demonstrated to decrease during exhaustive treadmill running in healthy subjects and this is correlated to the increase in the metabolic cost of running[40]. During a marathon, national class male distance runners exhibited no changes in vertical displacement, while female runners exhibited non-significantl decreases in vertical displacement[13]. Trained triathletes also exhibit a decrease in vertical COM during a 3,000m

race-pace run[40]. There are multiple factors that can account for this, including decreased leg stiffness due to neuromuscular fatigue[78]. However, it must be considered that the arms can contribute COM changes, considering their contribution to vertical lift[90, 125]. Therefore, it is possible that fatigue of the active muscles of the arms decreases vertical lift.

G. METHODOLOGICAL CONSIDERATIONS

1. Motion Analysis

Two-dimensional and three-dimensional optical motion analysis systems have been frequently used for evaluating running kinematics. Skin movement may affect marker positions during running and serve as a source of error in this type of kinematic analysis[207]. For instance, the root mean square error in knee flexion/extension during running has been reported at 5.3^{o} relative to bone-pin markers using a 200Hz three cine camera system[207]. While skin movement introduces error to the system, they have been used for a considerable number of running studies, as they are considerably less invasive than markers attached to cortical bone pins. Additionally, the within-day reliability of skin markers is very good during human locomotion[144]. Intra- and inter-day reliability in lower body kinematics of subjects walking at their natural speed is very high within day for motions in the sagittal plane, and less reliable in the transverse plane[144]. Specifically, the reliability of hip, knee, and ankle joint kinematics during running is high (R >0.93) when an optical motion analysis system and skin markers are used for data collection[74]. Intra-day reliability in the angular kinematics of the lumbo-pelvic-hip complex during running is high using skin markers[217]. While the reliability of three-dimensional arm kinematics have not been measured in running, reliability results of functional arm movement tasks have been high

(coefficient of multiple correlation >0.85) and these values are consistent with the reliability of lower extremity kinematics[169]. Because skin markers are considerably less invasive than cortical bone pins, commonly used in published running studies, and demonstrated to be reliable in studying running kinematics, skin markers will be used for this study.

2. Treadmill

Fatigue-related biomechanical changes may be dependent on whether treadmill or overground running is utilized. During treadmill running, subjects are constrained to a particular speed and must stop when they can no longer maintain that speed. However, overground running allows runners to slow down as fatigue develops, and kinematic changes may be different[78].

A number of studies have compared overground running to treadmill running. It has been suggested that individual differences in running style, shoe characteristics, and treadmill running experience may result in differences between overground and treadmill running[257]. It should be noted that the variability between treadmill and overground running varies between subjects, as well as within a subject running at different speeds[193]. Furthermore, air resistance and mechanical differences between running surfaces may explain differences[216]. Lastly, conflicting results between different studies may be due to differences between treadmills[216]. While treadmill running during a laboratory test is not a perfect representation of actual running during competition, a number of researchers have concluded the treadmill is an acceptable tool for studying running[58, 85, 153, 174, 216].

Kinematics

In joggers who were not competitive runners, stride characteristics were not significantly different between overground and treadmill running between 3.33 and 4.80 $m \cdot s^{-1}$ [85]. However, at higher speeds, treadmill running was characterized by increased stride rate, decreased stride length, and decreased non-support phase[85]. Healthy individuals have significantly greater stride frequency, and significantly shorter stride length, contact time, vertical variance of speed, and horizontal variance of speed while running on a treadmill compared to overground running at 4.0 and 6.0 $m \cdot s^{-1}$ [257]. However, other studies have found stride frequency to be lower and stride length to be longer in treadmill running compared to overground running[216]. Furthermore, knee joint angle at impact and stance, as well as vertical center of gravity displacement, were significantly lower in treadmill running[257]. Additionally, the hip joint range of motion during treadmill running has been found to be significantly lower[257] or greater[216] than overground running. However, these subjects were not trained runners, and may have exhibited these differences because they were not accustomed to treadmill running[257]. It has also been suggested that these differences may be reduced by using a treadmill with a sufficiently powerful motor which drives the belt at a constant speed[247].

The trunk angle with respect to the vertical has been observed to be significantly greater in healthy individuals during treadmill running compared to overground running[257]. Schache[216] examined 25 variables related to lumbo-pelvic-hip complex kinematics bilaterally, and found lumbar extension and anterior pelvic tilt at initial contact, and the first maximum anterior pelvic tilt to be the only variables significantly different between treadmill and overground running[216]. Comparisons between overground and treadmill running for upper extremity variables have not been published.

Metabolic Variables

In collegiate distance runners, VO_{2max}, maximum heart rate, oxygen pulse, and peak ventilation were not significantly different during intense track running than during a ramped treadmill protocol[58]. The same holds true for trained endurance athletes during incremental speed tests[174]. However, in collegiate runners blood lactate concentration was significantly greater during track running[58]. In well trained runners, maximal lactate steady state was not significantly different between a 5K track run and three different methods of incremental treadmill tests[153]. It has been suggested that a 1% treadmill incline results in a VO2 most consistent with that of level outdoor running at velocities of 2.92 to 5.0 $m \cdot s^{-1}$ in trained runners[142]. While this may be useful for training purposes, this gradient will not be employed in this research project, as level running is most consistently used in the literature.

Neuromuscular Variables

There is very little reported in the literature regarding the relationship between treadmill and overground running on the neuromuscular system. In healthy individuals, the biceps femoris displayed a greater magnitude and longer duration of activity during the contact and early swing phase of treadmill running compared to oveground running[257]. Conversely, the rectus femoris displayed lower activity during treadmill running compared to overground running[257]. These results were exaggerated with increasing treadmill speed[257]. However, the soleus, gastrocnemius, and gluteus maximus did not display significant differences between treadmill running and overground running[257]. These EMG differences are likely related to the slight kinematic differences between the two types of running[257].

3. Metabolic Analysis

VO_{2max}

The classic scientific model of aerobic performance was first described by A.V. Hill in 1924. Hill stated, "A man may fail to be a good runner by reason of a low oxygen uptake, a low maximal oxygen debt, or a high oxygen requirement.[121]" By current terminology, Hill was referring to VO_{2max}, anaerobic threshold, and running economy, respectively[19]. While decades of research have expanded upon Hill's concepts, these three classical variables are central tenets of running performance physiology.

Maximal oxygen consumption represents an individual's ability to deliver oxygen from atmospheric air to the working muscles and has traditionally been viewed as the limitation to performance in endurance sports. This was initially based on Hill's observations that superior runners have higher VO_{2max} values. Later research supported this, showing that VO_{2max} is an excellent predictor of performance in a group of heterogeneous individuals. Highly trained athletes can run at 100% of VO_{2max} for approximately 10 minutes, 95% for 15 minutes, 90% for 30 minutes, and 75-85% for over 2 hours[28]. Though VO_{2max} is a good predictor of running performance in a heterogeneous group of athletes, it is not a good predictor of performance in a group of distance runners with similar racing performance. This is due to the fact that VO_{2max} solely reflects metabolic work and does take mechanical work into consideration. Thus, it is possible for two athletes to have equal VO_{2max} values but very different racing performances. The cardiovascular system has classically been considered to be the chief limitation to VO_{2max}, with cardiac output (CO) considered the principal limitation to the system. However, there has been considerable debate whether other factors, such as pulmonary gas exchange or cellular metabolism, limit VO_{2max}[253, 254]. A thorough discussion of VO_{2max} models is beyond the scope of

this paper, as VO_{2max} is only one component of running performance and will only serve as a descriptive variable in this study.

The Astrand protocol has been validated as an appropriate test for determining VO2max in trained men[145]. Maximal oxygen consumption in runners is typically measured using the Astrand protocol, though the Bruce and Costill/Fox protocols are also used[139]. While all three protocols result in statistically similar VO_{2max} values in untrained adults, the Bruce protocol has been demonstrated to produce significantly lower results in trained men[139]. Statistically similar values have been attained in VO_{2max} values in collegiate runners performing incremental treadmill tests and intense track running[58]. Incremental speed treadmill tests have also been used to test VO_{2max}, and it has been demonstrated that 1, 3, and 6 minute stages elicit VO_{2max} and maximal heart rate values which are not significantly different[153]. However, maximal velocity attained during incremental speed tests is lower with longer protocols[153].

The Cosmed $K4b^2$ has been compared to traditional metabolic carts. The $K4b^2$ system has been demonstrated to measure a consistently slightly higher (0.5-1.0 ml/kg/min higher)[77, 81] VO_2 than a metabolic cart during running . The ICC for repeated measurements on the system has been measured from 0.7-0.9 during running[77].

VO_2 Estimation

It has been recommended that running studies be performed at intensities which reflect actual race paces[63]. A 5K race is run at an intensity approximately 95% of VO_{2max}[28], and this intensity has been used to study running performance in trained runners[29]. This intensity may be estimated during running using heart rate parameters[237]. Percentage of maximum heart rate (HR_{max}) may be used to estimate $\%VO_{2max}$, however this generally overestimates the corresponding percentage VO_{2max}[64]. Using the percentage of heart rate reserve (HRR), rather

than $\%HR_{max}$ allows for a better estimation of $\%VO_{2max}$[237]. The HRR is the difference between maximal heart rate and resting heart rate[209]. In healthy adults, the relationship between %HRR and $\%VO_{2max}$ during running can be expressed as a linear regression model (Equation 1)[237]:

Equation 1 – Relationship Between %HRR and $\%VO2_{max}$

$$\%HRR = 1.10 \times \%VO_{2max} - 6.1, \quad r=0.990$$

While this represents a good estimation of $\%VO_{2max}$, the relationship between %HRR and percent VO2 (VO_{2res}) reserve is a slightly better estimate[237]. The VO_2 reserve (VO_{2res}) is defined as the difference between VO_{2max} and resting VO_2[209]. This relationship during running can also be expressed as a linear regression model (Equation 2)[237]:

Equation 2 – Relationship between %HRR and $\%VO_{2res}$

$$\%HRR = 1.03 \times \%VO_{2res} + 1.5, \quad r=0.990$$

While %HRR predicts VO_{2res} better than VO_{2max}[237], this difference is more exaggerated in subjects who do not have high levels of fitness during running[237] and cycling[238]. Because the runners in this study will be well-trained, the VO_{2max} estimate will be sufficient, as $\%VO_{2max}$ is also a more standard measurement of exercise intensity than $\%VO_{2res}$. The use of %HRR to estimate $\%VO_{2max}$ allows for an objective measure of exercise intensity during the exhaustive run.

4. Electromyography

Electromyographic signals are recorded using monopolar or bipolar electrodes and represent the summation of MUAP's at a specific site, as well as system noise[67]. This signal is commonly referred to as the M-wave[23], and is a result of the electrical signal from the flux of Na^+ and K^+ across the sarcolemma[34] as it is transmitted through electrically conductive tissue[87]. Each individual MUAP represents muscle fiber depolarization and repolarization and this action potential propagates along the muscle fiber[273]. As the firing rates of already recruited motor units increase, or more motor units are recruited, more MUAPs occur and this increases the amplitude of EMG signals[34]. Surface bipolar electrode placements in surface EMG can detect MUAPs within 1 to 2 cm of the electrodes[87]. Because surface EMG records the M-wave of many superimposed MUAPs representing positive and negative phases fluctuating about the isoelectric line, the signal is irregular in appearance and referred to as an interference EMG[87].

Movement of the electrodes and the leads, electromagnetic radiation, and cross-talk between muscles represent sources of noise which may contaminate the EMG signal[87]. Common mode rejection is often used to eliminate noise by subtracting signals which are common to both electrodes in a bipolar arrangement[87]. Signal filtering is used to modify the frequency content of a signal to further reduce noise. A band-stop filter may be used to reduce the 60Hz electromagnetic radiation noise of the signal. A band-pass filter may be used to eliminate frequencies above and below a specified range[87]. Setting a range of 15Hz through 500Hz retains the physiologic frequencies of motor activation[18].

The EMG can be interpreted in the time-domain, most often processed by calculating the absolute value of the M-wave, also known as rectifying[87]. The rectified signal is smoothed by integration[87]. The integral of the signal can then be calculated to quantify the amplitude of

muscle activity over a given time period, quantified as iEMG. Another means of quantifying muscle activation is by calculating the root-mean-square of the signal. This yields information regarding the mean power of the signal[87]. These are dependent on the numbers, firing rates, and areas of MUAPs[18]. The iEMG is affected by cancellation which occurs with superimposition of MUAPs, while RMS is not susceptible to this[18]. Fatigue studies have revealed RMS is not a sensitive measurement for muscle fatigue. Normalization is used to standardize the value of iEMG and RMS. Typically, this is done by dividing the amplitude of the signal of interest by the amplitude of the signal from a MVC of that muscle during a reference task or electrical stimulation[87].

EMG can be evaluated in the frequency domain. When conduction velocity decreases, the time from the signal to pass between two electrodes is increased, so that recorded MUAPs have longer durations[18]. This increases the low frequency components of the signal while decreasing the high frequency components[18]. Because MUAP duration increases, the EMG amplitude also increases[18].

Electromyographic spectral frequency parameters have been studied and deemed reliable. The reproducibility of MnPF over several weeks of quadriceps muscles during incremental exercise is good, with ICC's greater than 0.80 in five of seven subjects tested, with the remaining two subjects' lower ICC's attributable to methodological shortcomings[95]. This emphasizes the need for proper subject preparation[95]. The MnPF and RMS of the vastus lateralis, vastus medialis, and rectus femoris were studied during isokinetic knee extensions and it was found that these parameters were highly reproducible between three tests of ten repetitions[161]. The reproducibility of MnPF for the biceps brachii muscle has been demonstrated to have a high ICC

(0.93 to 0.99)[60]. Additionally, the phase shift in MnPF of the erector spinae during running has been demonstrated to be reliable[190].

The magnitude and shape of total EMG power spectrum have been shown to be reproducible over the course of multiple weeks in the vastus lateralis[95]. Integrated EMG is reproducible during incremental dynamic exercise, with sessions 24 to 72 hours apart[241]. The phasic muscle activity of leg muscles was repeatable within and between tests while subjects walked at their natural speed[144].

III. METHODOLOGY

A. EXPERIMENTAL DESIGN

The purpose of this study was to evaluate EMG and kinematic changes during an exhaustive 5K run. A within-subject repeated measures design was be used for this study.

B. SUBJECTS

A group of 15 male competitive distance runners was recruited to participate in this study. Subjects were recruited from local intercollegiate track teams and running clubs. Subjects provided written informed consent prior to participation in research in accordance with the University of Pittsburgh Institutional Review Board. Eligibility was determined by the following inclusion and exclusion criteria:

1. Inclusion criteria

- Males with a history of running of at least three years
- Performing his normal training routine for at least 3 months
- Competitive runner in intercollegiate or open track, road, or cross country races of 1500m to 10,000m

- Participation in at least 3 races per year
- Successful completion of medical questionnaire

2. Exclusion criteria

- History of neurologic or metabolic disease
- History of cardiovascular or pulmonary disease
- History of musculoskeletal injury within the previous 3 months
- History of allergy to adhesives used for data collection

C. POWER ANALYSIS

Only one study has examined the changes in MnPF of the upper body during running. During an incremental treadmill running protocol, Nagamachi found the mean power frequency of the erector spinae to fall from 74.2 ± 7.2 Hz to 59.4 ± 12.4 Hz on one test, and 74.7 ± 8.3 Hz to 55.0 ± 11.2Hz in 13 healthy subjects. For a conservative estimate of power, the mean decrease of the former (14.8 Hz) and the standard deviation of the former (12.4 Hz) will be used. This yields an effect size of 1.19. Using a power of 0.90, and an alpha of 0.05, this yields an *n* of 8 subjects for a one-tailed test.

There is no available data regarding kinematic changes of the upper body during running. Pilot data has revealed that the total range of upper torso axial rotation increases from 25.2 ± 1.8^{o} to 35.4 ± 1.4^{o} during a 15 minute fatiguing run. Conversely, the total range of pelvis axial

rotation decreases from 15.0 ± 1.5^{o} to 11.7 ± 0.8^{o}, with fatigue. Using an alpha = 0.05 and power = 0.90 for a 2-sided test, these data yield a n = 3 and n = 5, respectively.

While there are no kinetic dependent variables in this study, previous literature may be used to aid in the power analysis. Hinrichs has computed the contribution of the arms to vertical lift, and found the difference between medium (5.2 ± 1.5%) and fast speeds (7.1 ± 2.8%). Using an alpha = 0.05 and power =0.80 for a 1-sided test, this yields an n = 15.

Together, these data indicate that a sample size of 15 subjects should provide sufficient power to reveal statistically significant differences in the non-fatigued and fatigued states, should differences exist.

D. INSTRUMENTATION

Laboratory instrumentation used included a body composition analysis system (BodPod, Life Measurement Instruments, Concord, CA), telemetric metabolic system (K4b^{2}, COSMED USA Inc, Chicago, IL), finger-prick based blood lactate system (Lactate-Pro, KDK Corporation, Kyoto, Japan), an accelerometer module (model 2422-025, Silicon Designs, Inc., Issaquah, WA), telemetric electromyography EMG system (Noraxon Telemyo System, Noraxon USA Inc., Scottsdale, AZ), an 8-camera optical capture motion analysis system (Peak Motus System, Peak Performance Technologies, Inc., Englewood, CO), and two treadmills (Wooday ELG, Woodway, Waukesha, WI and Evo Fitness 3i, Smooth Fitness, Mount Laurel, NJ). Data processing software used included Microsoft Excel (Microsoft Corp., Redmond, WA), Matlab 7.0 R14 (Mathworks Inc., Natick, MA), MyoResearch XP (Noraxon USA Inc., Scottsdale, AZ), SAS 9.0 (SAS Institute Inc., Cary, NC), SPSS 14.0 (SPSS Inc., Chicago, IL), Peak Motus 8.4

(Peak Performance Technologies, Inc., Englewood, CO), and Peak Motus 3D Gait Analysis Module (Peak Performance Technologies, Inc., Englewood, CO).

1. BodPod Body Composition Analysis System

The BodPod Body Composition System is a fiberglass structure which encompasses a 350L reference chamber and 450L testing chamber, a load cell scale, and a personal computer. The subject sat in the testing chamber during body volume measurement. The BodPod was calibrated prior to each use using the supplied 50.683L metal calibration cylinder and two 10kg calibration weights in accordance with the manufacturer's instructions. Calibration of the chambers was considered successful when the average of five volume measurements was within 100mL of the actual volume and the standard deviation of these five measurements is within 75mL. Calibration of the scale was considered successful when the mass of the calibration weights is measured at 20.0kg. Intrasubject reliability within the Neuromuscular Research Laboratory has demonstrated an intraclass correlation coefficient of 0.98 and Standard Error of Measurement of 0.47% body fat. Weight and body composition data were used as descriptive variables.

2. Cosmed K4b^2 Metabolic System

The Cosmed K4b^2 portable metabolic system was used to assess VO_2 during the maximal oxygen uptake test. The K4b^2 is a small rectangular apparatus which contains an indirect calorimetric system that measures oxygen and carbon dioxide concentration and volume on a breath by breath basis. This unit contains individual oxygen and carbon dioxide analyzers. A portable battery was attached to the middle of the subject's back. The system was fitted into an

adjustable harness, which fit around the shoulders and chest of the subjects. A heart rate monitor (Polar USA, Lake Success, NY) was worn by the subject around the chest at the level of the xiphoid process. Electrode gel was placed on the monitor's sensors to maximize signal transmission to the monitor. The system telemetrically transmited data with every breath to a receiver attached to a computer. A high capacity memory within the portable system permitted storage of the data serve as a backup to the telemetrically transmitted data.

This system was be calibrated before each test through a four point calibration. The concentration of oxygen and carbon dioxide of room air was be measured and compared to the expected values. The system then measured a known gas concentration of 16.0% oxygen and 5.0 % carbon dioxide. An oxygen–carbon dioxide delay was calculated to determine the time delay between expired air and system receipt for analysis. A turbine calibration was performed to ensure proper gas flow through the flow meter and turbine with a known air volume.

3. Accelerometer

One triaxial accelerometer module (Model 2422-025, Silicon Designs, Inc., Issaquah, WA) was used to determine the discrete point of impact during the stride cycle. The accelerometer module contains three orthogonal accelerometers within an anodized aluminum case and an integrated circuit sense amplifier. The accelerometer provided analog voltage signals with a full scale acceleration of ±25 G.

4. Noraxon Telemyo Electromyography System

Electromyographic data were recorded using the Noraxon Telemyo Electromyography System. The Noraxon Telemyo system is a frequency modulated (FM) telemetry system.

Electromyographic signals collected from silver-silver chloride surface electrodes passed through a single-ended amplifier with a gain of 500 to an eight channel FM transmitter. The receiver unit obtained the telemetric signals from the transmitter, where they were amplified and filtered using a 15 – 500 Hz band pass Butterworth filter, using a common mode rejection ratio of 130db. Signals from the receiver were converted from analog to digital data via a DT3010/32 (32 channel, 24 bit) analog-to-digital board (Data Translation, Inc., Marlboro, MA) at a rate of 1000Hz. The digital data were collected and stored with Peak Motus 8.4 software.

5. Peak Motus 3D Video Motion Analysis System

Kinematic data of the exhaustive run were collected using the Peak Motus System. Six optical cameras (Pulnix Industrial Product Division, Sunnyvale, CA) was mounted at a distance of approximately 4 m at both sides of the treadmill. A tripod-mounted optical camera was placed approximately 2 m away from each side of the treadmill. All kinematic data were captured at 120 Hz. The capture volume will be 4.5x1.5x2.1 m^3. Calibration was performed using dynamic wand calibration with mean residual errors below 0.0025 m (wand length = 0.914 m). Root mean square errors of 0.002 meters and 0.254 degrees have been established within the Neuromuscular Research Laboratory for determining the measurement accuracy of position and angular data, respectively.

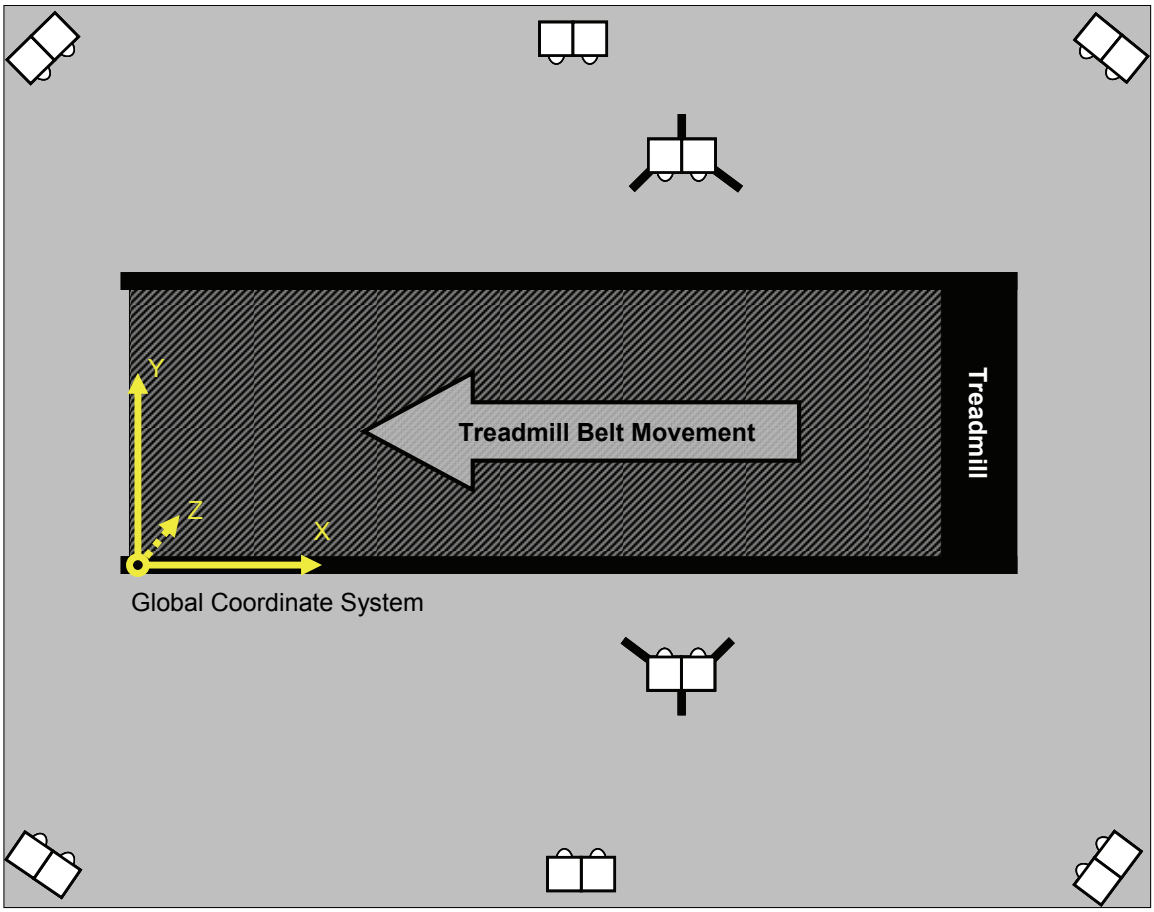

Figure 15 – Schematic of Laboratory Global Coordinate System Setup

6. Treadmills

Subjects ran on a Woodway ELG treadmull during the VO_{2max} test and a Evo Fitness 3i treadmill during exhaustive run. The Evo Fitness treadmill has a speed range of 0 – 5.58 $m \cdot s^{-1}$ with a 0 – 15% incline range. The treadmill belt is 1.58m long and 0.51m wide.

E. TESTING PROCEDURES

1. Subject Preparation

Informed consent was obtained prior to screening subjects. All subjects were required to provide consent prior to participation in accordance with the University's Institutional Review Board. Subjects then filled out a medical questionnaire to determine their eligibility for the study as defined by the inclusion/exclusion criteria. Immediately following this, unqualified subjects were dismissed. Qualified subjects then underwent the first testing session.

2. Order of Testing

Each participant attended two testing sessions within the Neuromuscular Research Laboratory at the University of Pittsburgh. The first testing session lasted for approximately 1 hour. Eligible subjects underwent anthropometric measurement, body composition analysis, and VO_{2max} testing during the initial testing session. One to two weeks after the initial testing session, each participant returned to the laboratory for the second testing session which lasted for approximately 1.5 hours. This second testing session consisted of EMG and kinematic data collection during an exhaustive running protocol.

3. Body Composition Analysis

Subjects were instructed to refrain from eating and exercising for two hours before being tested in the BodPod to obtain a representative resting body volume. Subjects were required to wear a tight fitting bathing suit or spandex outfit with a swim cap covering the hair to minimize

measurement error from external isothermal air volume. Subjects entered the BodPod and were given instructions to breathe normally while sitting motionless with their hands placed on their lap. Subjects sat inside the BodPod for approximately one minute while the system measured body volume. Two body volume measurements were be taken for each test. The Brozek[35] equation (Equation 3) was used to calculate body fat percentage for all subjects.

Equation 3 – Brozek Equation

$$1/D_b = FM/D_{FM} + FFM/D_{FFM}$$

(Where D_b = body density, FM = fat mass, D_{FM} = density of fat mass, FFM = fat-free mass, and D_{FFM} = density of fat-free mass)

4. Maximal Oxygen Consumption Data Acquisition

For the first testing session, subjects wore the K4*b*^{2} portable metabolic system to assess VO_2 during a modified-Astrand incremental running protocol. Total body mass measured by the BodPod was entered into the system to computer VO_{2max} normalized to body weight. Age was entered into the system to determine age predicted maximal heart rate. Prior to warm-up, a resting blood lactate measurement was recorded. Subjects were asked to prepare for the test as they would for a race and will be given the opportunity to perform their personal warm-up routine. The testing pace was determined based on V_{dot} values defined by Daniels[62]**.** Current race performance was used to determine the subject's V_{dot} value, and the corresponding Easy pace from Daniels was the speed used for the VO_{2max} test. Subjects ran at this speed for three minutes at a 0% incline. Following the initial three minute stage, the treadmill incline was increased 2.5 degrees every two minutes. Blood lactate values were collected 30s prior to the

end of each stage. The subjects were instructed to continue running until volitional exhaustion, which took 12-15 minutes using this protocol. Maximal effort was verified by examining the data to determine if 1) a plateau in VO_2 was achieved with increasing intensity, 2) respiratory exchange ratio was > 1.1, or 3) heart rate was within 95% of heart rate max (defined as 220 – age). The VO_{2max} normalized to body mass was used as a descriptive variable. Heart rate at 95% of VO_{2max} was used to determine the initial target heart rate for the start of the exhaustive run.

5. Anthropometric Measurements

Anthropometric measurements were taken using medical calipers and a tape measure. Measurements included body mass and height, hand width, wrist diameter, elbow diameter, hand length, lower and upper arm length, forearm and upper arm circumference, anterior superior iliac spine (ASIS) breadth, thigh length, shank length, foot length, mid-thigh and mid-calf circumference, knee diameter, malleolus height, malleolus width, and foot breadth. These measurements were entered into the Peak Motus system to be used in calculating kinematic measurements during the running fatigue protocol.

6. Accelerometric Data Acquisition During and Exhausive Run

During the exhaustive run, subjects wore the accelerometer module on their right shank. The accelerometer was used to determine impact of the foot with the treadmill. The module was secured to the skin using adhesive spray (Tuf-Skin, Cramer Products, Inc., Gardner, KS) and double-sided adhesive discs (3M Double Stick Disks, 3M Company, St. Paul, MN). The

accelerometer was placed on the medial aspect of the flat surface of the mid-tibia in a level orientation. Athletic wrap and athletic tape were used to secure the module to the shank.

7. Electromyographic Data Acquisition During an Exhaustive Run

Electromyography data were collected with the Noraxon Telemyo System. During the running fatigue protocol, EMG data were collected from thirteen muscles: vastus lateralis, rectus femoris, semimembranosus, gluteus maximus, erector spinae, external oblique, rectus abdominus, latissimus dorsi, anterior deltoid, middle deltoid, posterior deltoid, upper trapezius, and brachioradialis. The proper electrode placement sites were located on the subject based on the methods of De Luca[68] and Zipp[272], whereby the electrodes were placed parallel to the muscle fibers between the myotendinous junction and site of innervation. A surgical pen was used to mark this site on the skin. An electric shaver was used to remove hair from the sites as necessary. Each site was lightly abraded with a callous file and cleaned using isopropyl alcohol to decrease impedance. Silver-silver chloride, pre-gelled, bipolar, self-adhesive surface electrodes (Medicotest, Inc., Rolling Meadows, IL) were placed over the appropriate muscle belly in line with the direction of the fibers with a center to center distance of approximately 20 mm. A single ground electrode from each box was placed over the sternum. Electrodes on the arms were secured using surgical tape, athletic wrap, and athletic tape.

EMG signals from the electrodes were passed to a portable battery-operated FM transmitter worn by the subject and sent to a receiver and personal computer for data storage. EMG data were be sampled at a sample rate of 1000 Hz.

8. Kinematic Data Acquisition During an Exhaustive Run

During the exhaustive run, subjects wore reflective spherical markers, with a diameter of 0.025 m, placed over the heel, lateral malleolus, second metatarsal head, femoral epicondyle, ASIS, sacrum, lateral mid-calf, lateral mid-thigh, acromion, mid-upper arm, elbow joint line (medial and lateral aspects), mid-lower arm, and wrist joint line (medial and lateral aspects) bilaterally. A single marker was placed on the sacrum, C7, the jugular notch, and the xiphoid process. One marker was placed on the front of the mid-thigh on the right side to serve as an asymmetrical marker to aid in digitization. Markers were secured to the skin using adhesive spray and double-sided adhesive discs. The dependent variables were the maximum and minimum angles and maximum angular velocities of shoulder elevation, shoulder plane of elevation, elbow flexion, upper torso rotation, torso flexion, hip flexion, and knee flexion.

9. Exhaustive Run Protocol

Subjects wore the heart rate monitor component of the metabolic system during the run. The telemetric receiver was used to monitor heart rate during the run. Prior to warm-up, a resting blood lactate measurement was taken from the subject's right index finger. Subjects had a 10-minute warm-up period on the treadmill, followed by a period of self-directed stretching during which they were instructed to prepare themselves as if for a 5K race. Estimated 5K race pace was used as a guideline for initially setting the treadmill speed. Treadmill speed was adjusted until the heart rate was equal to the heart rate corresponding to that between 90% and 95% of VO_{2max} as this represents an intensity similar to 5K race pace[28]. Data collection began when heart rate remained steady for 60s. Twenty second trials were recorded every minute using

Peak Motus 8.4 software while the subject continuously ran. Accelerometric, EMG, and kinematic data were recorded simultaneously during each trial. Subjects ran at this pace until volitional exhaustion, at which time the treadmill was stopped. A blood lactate measurement was recorded immediately following termination of the test.

F. DATA REDUCTION

1. BodPod Data Reduction

Total body mass was used to normalize VO_2 data. All other body composition data were used for descriptive purposes. Lean body mass, fat body mass, total mass, and percent body fat data were exported from the BodPod system to be stored in a Microsoft Excel spreadsheet.

2. Maximal Oxygen Consumption Data Reduction

The VO_{2max} data were used to determine the target heart rate for the exhaustive run. A custom made Matlab program was used to calculate metabolic data parameters. Metabolic data were smoothed using a 30 second moving average. The maximal value of the smoothed data was determined and this was the VO_{2max}. The heart rates corresponding to 90% to 95% of VO_{2max} ($HR_{VO2\text{-}95\%}$) were obtained from this data.

3. Accelerometric Data Reduction

Raw voltage from the accelerometer was used to determine the impact time point of each stride. Raw data was exported and Myoresearch XP was used to determine initial contact time.

Impact was defined as the minimum amplitude in raw voltage immediately prior to the peak amplitude in raw voltage. Impact times were exported to a separate file. Stride cycle was defined as the time period from the frame corresponding to impact of the right foot until the frame before the next impact of the right foot. Stride duration was calculated by calculating the time interval between impacts for each cycle. The inverse of the stride duration was the stride rate. Stride length was calculated by multiplying the treadmill speed by stride duration. The mean stride rate for twenty-five stride cycles was calculated for each trial. Mean stride rate served as a dependent variable.

4. Electromyographic Data Reduction

Myoresearch XP (Noraxon) and a customized Matlab program were be used to filter and process the raw EMG signals. Data were smoothed and filtered using a dual-pass 4^{th} order Butterworth bandpass filter with a lower cutoff frequency of 30Hz and an upper cutoff frequency of 500Hz to reduce movement and electrocardiographic artict[206, 267].

A data window of twenty-five complete stride cycles was created using accelerometric data as described above. For each stride cycle, iEMG was calculated for each muscle. To compute iEMG, the absolute value of the previously bandpass filtered EMG signal was calculated and a low-pass Butterworth filter with a frequency cutoff of 20Hz was applied to smooth the rectified data. The area under the curve was then calculated using trapezoidal integration. All iEMG data were normalized to the iEMG from the first data point of the exhaustive run trial. The total iEMG for each stride cycle was divided by the stride length for that cycle to determine the iEMG to travel one meter[111]. For each stride cycle, a fast Fourier transformation was performed to convert each EMG signal to frequency domain to calculate the

MdPF. The mean and standard deviation of MdPF and iEMG were calculated from twenty-five strides per recording. The dependent variables were the mean MdPF and mean iEMG for each trial for the vastus lateralis, semimembranosus, gluteus maximus, erector spinae, external oblique, rectus abdominus, latissimus dorsi, anterior deltoid, middle deltoid, posterior deltoid, upper trapezius, and brachioradialis.

5. Kinematic Data Reduction

Peak Motus Software was used for reduction kinematic data. All markers were digitized to produce 3D coordinate data. This data were filtered using a fourth order zero lag Butterworth digital filter using an optimal cut-off frequency[135]. Anthropometric measurements and raw coordinate data from the camera recordings were used to calculate angles and angular velocities for the knee, hip, torso, shoulder, and elbow joints using the segmentally embedded coordinate systems similar to those described by Vaughan[48, 49, 108, 248], in accordance with the International Society of Biomechanics (ISB) recommendations[270, 271]. Anatomical joint angles, linear kinematic data, and angular kinematic data were calculated based on segmentally embedded local coordinate systems (LCS) to define motion of the distal segment relative to the proximal segment[49, 108] using Peak Motus 3D Gait Analysis Module based on Vaughan[249] and the ISB recommendations[270, 271].

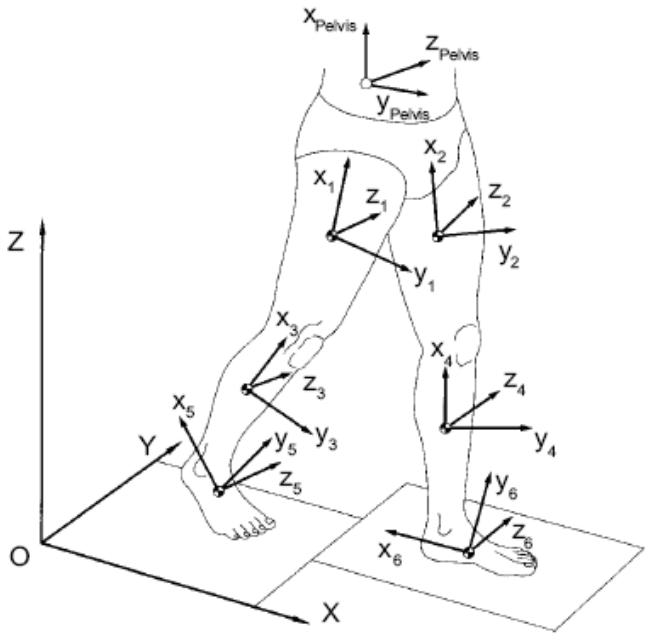

Figure 16 – Example configuration of segmentally embedded coordinate systems (from Vaughan[249])

Joint segments were defined as in Table 1. Joint centers were calculated using the methods described by Chandler[48] and deLeva[66]. The shoulder joint center was calculated as in Equation 4.

Equation 4 – Shoulder Joint Center Calculation

(Marker - 0.0125 x WShoulder) - (0.104 – ArmLength x WShoulder)

where *Marker* is the Shoulder Marker Position, *ArmLength* is the Acromion-Radial Head Antrhopometric Measurement, and *WShoulder* is the cross product between C7 to right shoulder marker vector and C7 to left shoulder marker vector.

Vertical COM was estimated by using the position of the sacral marker, as the waist represents a good estimate of the COM in locomotion studies[32, 40, 188].

Table 1 – Definition of Joint Segments

Segment	Proximal Point	Distal Point
Shank	Knee Joint Center	Ankle Joint Center
Thigh	Hip Joint Center	Knee Joint Center
Pelvis	Plane formed by Right ASIS, Left ASIS, and Sacrum	
Torso	Mid-Shoulders	Mid-Hips
Upper Torso	Right Shoulder Joint Center	Left Shoulder Joint Center
Forearm	Elbow Joint Center	Wrist Joint Line
Upper Arm	Shoulder Joint Center	Elbow Joint Center

Shoulder elevation angle was defined as the angle between the longitudinal axis of the torso LCS and the longitudinal axis upper arm LCS (represented by angle α in Figure 17). Shoulder plane of elevation was defined as the angle between the anterior-posterior vector of the thorax LCS and the projection of vector of the upper arm in the thorax coordinate system onto the transverse plane of the thorax (represented by angle α in Figure 18**)**. Elbow flexion angle was defined as the rotation of the forearm LCS about the medial-lateral axis of the LCS of the upper arm (represented by angle α in Figure 19). Upper torso axial rotation was defined as the rotation of the medial-lateral axis of the upper torso relative to the Y-axis of the global coordinate system (GCS) (represented by angle α in Figure 20). Torso flexion angle was defined as the rotation of the torso LCS about the vertical axis of the GCS (represented by angle α in Figure 21). Hip flexion was defined as the rotation of the thigh LCS about the medial-lateral axis of the pelvis LCS. Knee flexion was defined as the rotation of the shank LCS about the

medial-lateral axis of the thigh LCS. The maximum and minimum values for each angle and velocity during each stride cycle were calculated using a customized Matlab program. The mean of the maximum and minimum angle and angular velocity for each joint motion were calculated for each recording and serve as dependent variables.

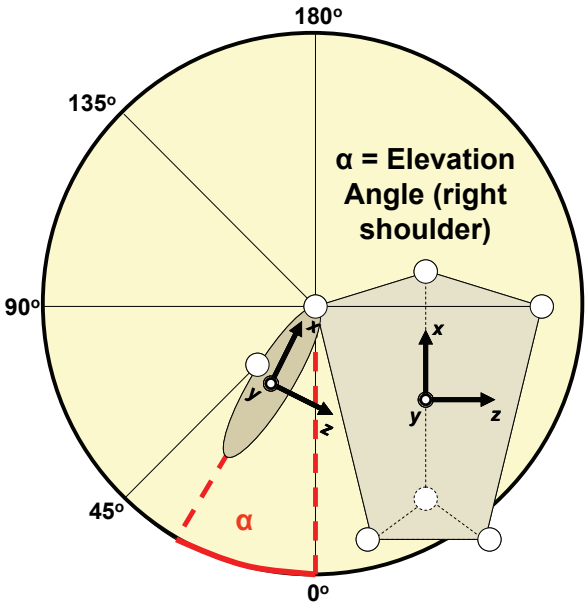

Figure 17 - Shoulder Elevation Angle

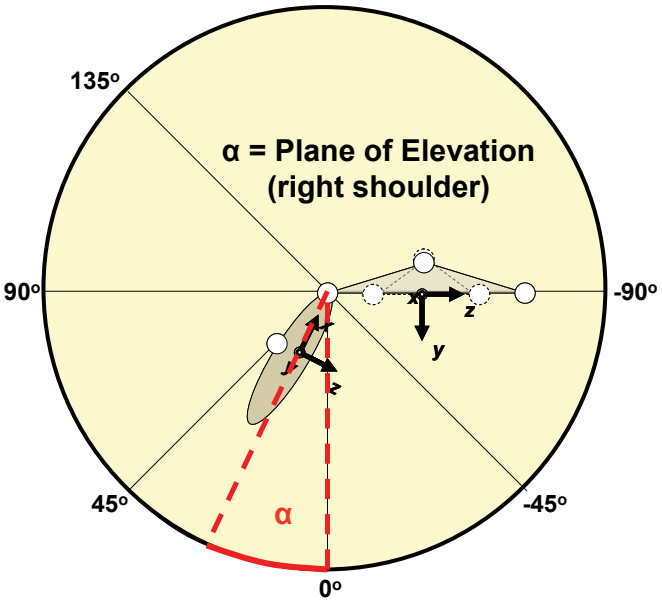

Figure 18 – Shoulder Plane of Elevation

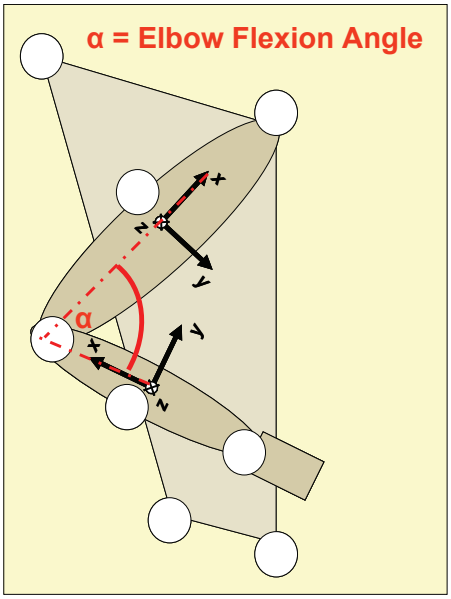

Figure 19 – Elbow Flexion Angle

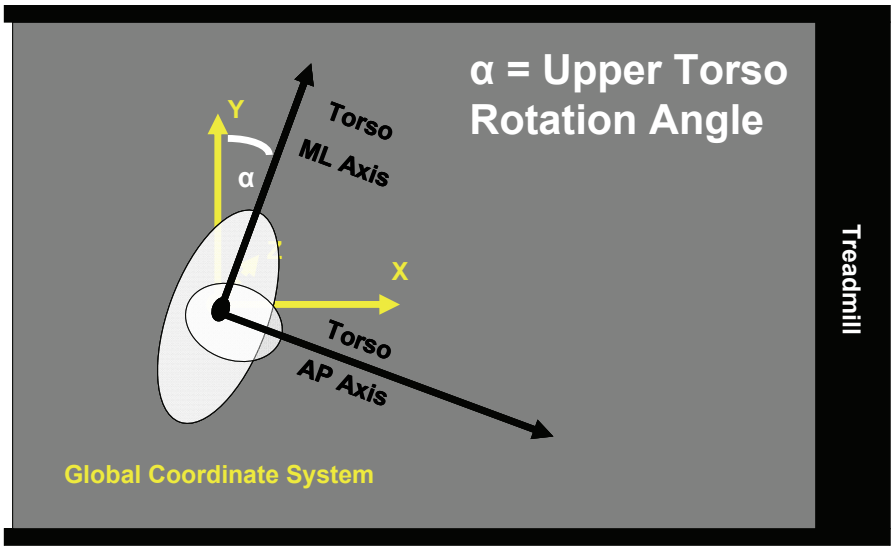

Figure 20 – Upper Torso Rotation Angle

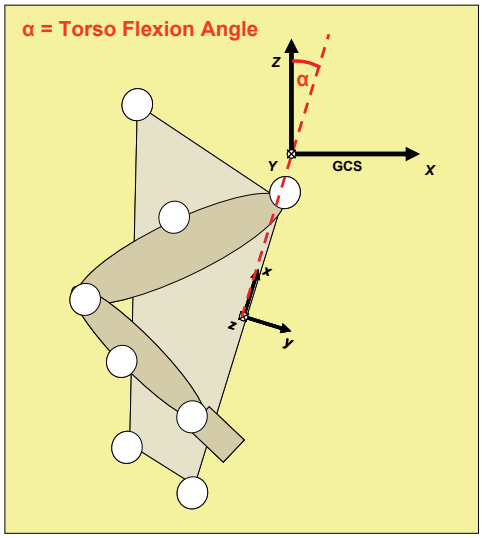

Figure 21 – Torso Flexion Angle

G. TEMPORAL DATA ORGANIZATION

1. Electromyography and Stride Data

The fatigue protocol was of open-loop duration and subjects reached volitional exhaustion at different absolute time points. To account for the between-subject variability in number of time points in EMG and stride data analysis, all time points were normalized to the total duration of the run for each individual. For instance, if a subject ran 18 minutes, the first minute was given a value of 0.056, the 9^{th} minute was given a time value of 0.50 and the 18^{th} minute a value of 1.00. To reduce multicollinearity effects in statistical analysis, time data were centered.

2. Kinematic Data

To account for the between-subject variability in number of time points for kinematic data analysis, only specific time periods were used in kinematic data analysis:

Start of protocol = Data from the first two recordings of data collection (t_{start})

Middle of protocol = Data from the middle two time points of data collection (t_{mid})

End of protocol = Data from the last two recordings of data collection (t_{end})

This allocation of data allowed data from the start, middle, and end of each subject's exhaustive run to be compared regardless of the total duration of running.

H. DATA ANALYSIS

Specific Aims 1 and 2

Analysis of EMG dependent variables was performed using SAS 9.0. A repeated measures analysis using an autoregressive covariance structure was performed to determine MdPF and iEMG kinetics over the course of the exhaustive run. Center measured time was the independent variable. Dependent variables were log transformed to create the normal distribution required for the procedure. Dependent variables were fitted to a quadratic polynomial regression function,as iEMG or MdPF may increase in the initial stages of exercise and decrease with fatigue, thereby forming a parabolic curve rather than a linear trend. Quadratic patterns of EMG changes have been previously reported[173, 240]. The significance of the quadratic effect coefficient and linear effect coefficient was then tested for each dependent variable.

A significant ($p \leq 0.05$) score in the quadratic coefficient of the model was interpreted to mean the dependent variable followed a quadratic pattern. A positive value of the quadratic coefficient indicates the dependent variable falls, then rises. A negative value of the quadratic coefficient indicates the dependent variable rises, then falls.

A significant ($p \leq 0.05$) score in the linear coefficient in the model in the presence of the significant score in the quadratic coefficient indicates the dependent variable follows a time-dependent linear change following the inflection point of the quadratic component. A significant value in the linear component in the model in the absence of a significant quadratic coefficient indicates a linear trend in the data. Non-significant scores with $0.05 \leq p \leq 0.10$ were considered to be non-significant trends. A positive value to the linear coefficient indicates the dependent variable increases in a time-dependent manner. A negative value to the linear coefficient

indicates the dependent variable decreases in a time-dependent fashion. It should be noted that lack of statistical significance in the quadratic or linear coefficients does not necessarily mean lack of change. Rather, it indicates that a quadratic or linear function could not fit the data of the population studied due to a high degree of inter-subject variation. For instance, data may show an overall trend for increasing or decreasing values, but the magnitude or nature of the change may have considerable inter-subject variation which prevents statistical significance of the model coefficients.

The intercept of the model was not considered during analysis, as it reflects the zero time point of the running protocol. All data were normalized to the first recorded time point of the run, which was taken after one minute of running. Changes between the absolute beginning of the running protocol and the first minute of recording may result from subjects adjusting to the treadmill speed. Therefore a recording at the zero time point was not recorded.

Specific Aim 3

Analysis of Kinematic Variables

Differences in kinematic dependent variables were analyzed with SPSS 14.0. A multivariate repeated measures (RM) ANOVA (doubly multivariate) was used to determine if time-dependent differences in kinematic variables existed between the t_{start}, t_{mid}, and t_{end} of exhaustive run protocol. Time category (t_{start}, t_{mid}, and t_{end}) during run served as the within-subject factor. Dependent variables were put into three groups: legs [knee flexion angle (KF), hip flexion angle (HF), and pelvis axial rotation (PAR)], torso [torso flexion (TF) and upper torso axial rotation (UTAR)], and arms [should elevation angle (SE), shoulder plane of elevation angle (SPE), and elbow flexion angle (EF)] (Figure 22). For bilateral movements, only the left side joint angles were used in analysis. A univariate repeated measures ANOVA was used to

analyze time-dependent changes in sacral marker height. For each of these groups, a separate RM ANOVA was used to examine maximal joint angle, minimal joint angle, maximal joint angle velocity, and minimal joint angle velocity (Figure 23).

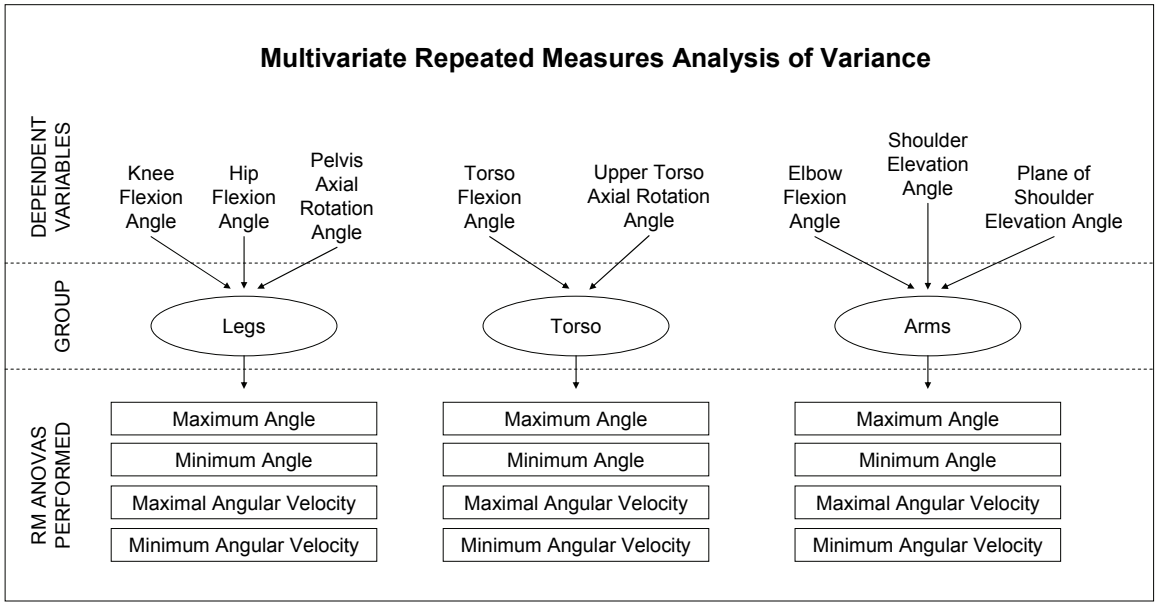

Figure 22 - Multivariate Kinematic Data Groupings

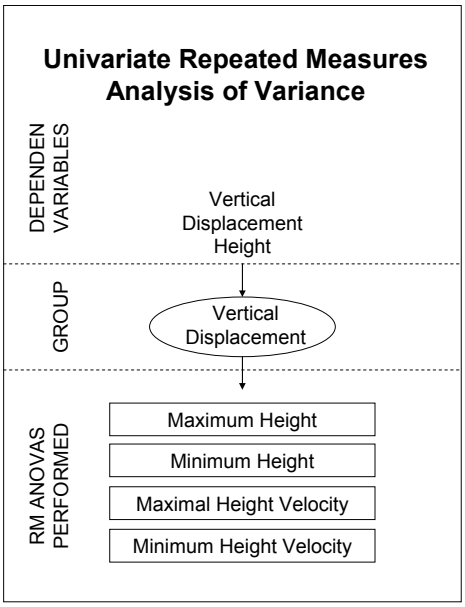

Figure 23 - Univariate Kinematic Data Groupings

For all kinematic data, $p \leq 0.05$ was considered statistically significant and non-significant scores with $0.05 \leq p \leq 0.10$ were considered to be non-significant trends. In the event that Wilks' Lambda was statistically significant in the multivariate RM ANOVA, sphericity was examined using Mauchly's test of sphericity and a univariate RM ANOVA was performed. When the sphericity assumption was met, univariate RM ANOVA was interpreted using sphericity assumed p-values. When the sphericity assumption was not met, univariate RM ANOVA was interpreted using the Huynh-Feltd p-value. In the event that statistically significant findings were observed in univariate analyses, main effect pairwise comparisons were performed using the Bonferroni correction (Figure 24).

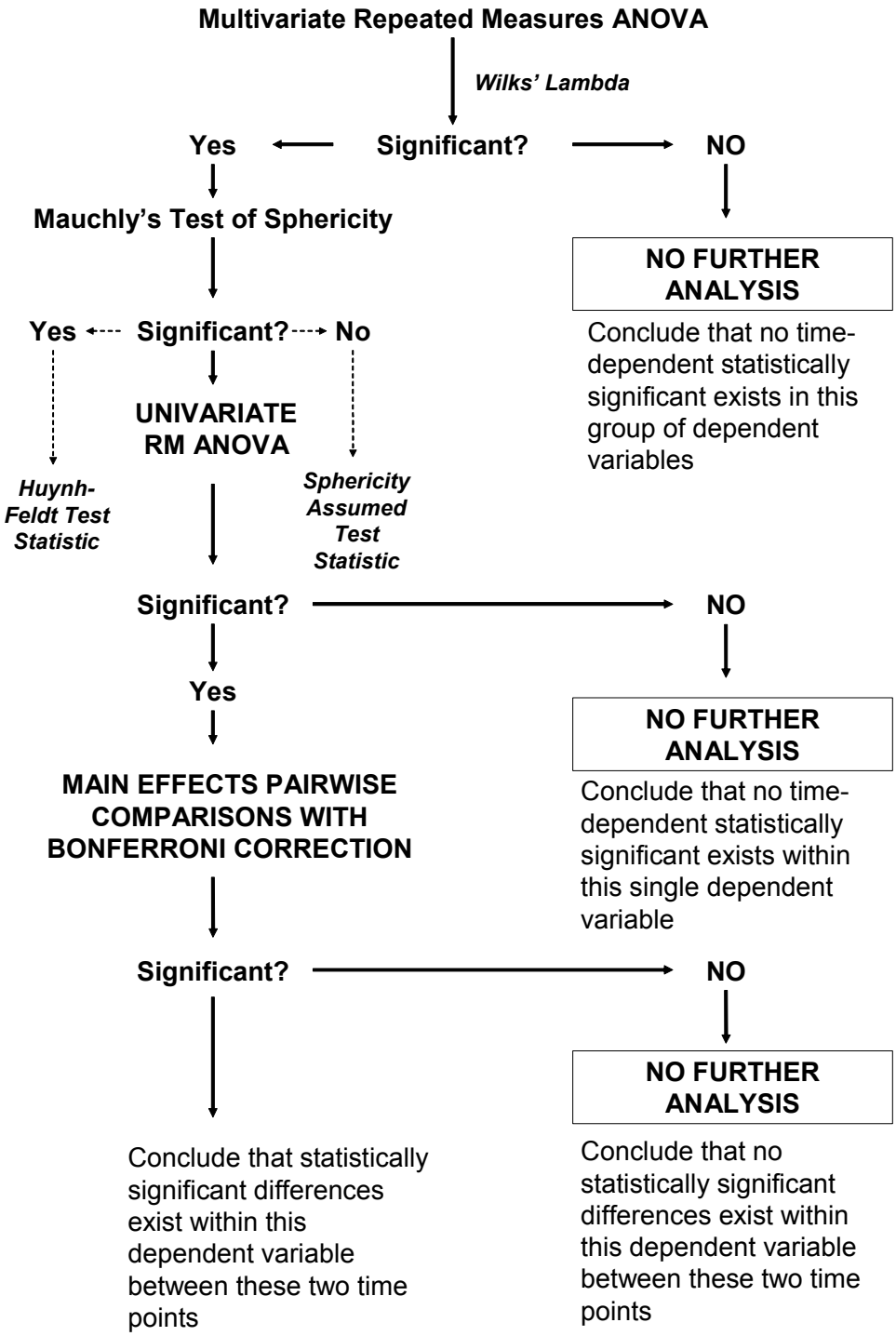

Figure 24 - Kinematic Data Statistical Analysis Paradigm

Relationship Between EMG and Kinematic Variables

The relationships between changes (Δ) in EMG and kinematic variables were analyzed using correlation analysis. The percent change in EMG parameter was compared to the percent change in the relevant kinematic parameters (Table 2). This normalization to initial values has been previously reported for EMG[4, 29] and kinematic[71, 184] analyses. Normalization to baseline values allows comparisons to be made regardless of subjects' initial values, and also allows comparisons between different muscles and different joints. Focus was placed on the specific muscles which exhibited significantly different EMG or MdPF. Pearson's product moment correlations was used. A moderate relationship was defined by an r-value of greater than 0.50 or less than -0.50. A strong relationship was defined by an r-value of greater than 0.80 or less than -0.80. For all correlations, $p \leq 0.05$ were considered statistically significant[51, 187].

Table 2 - Relationship between Kinematic and Neuromuscular Dependent Variables

Kinematic Variables	Corresponding Muscle
Angle, Angular Velocity (% Change)	*MdPF , iEMG* (% Change)
Legs	
Knee Flexion	Vastus Lateralis, Semimembranosus, Rectus Femoris
Hip Flexion	Semimembranosus, Rectus Femoris, Gluteus Maximus
Pelvis Axial Rotation	Erector Spinae, External Oblique
Torso	
Torso Flexion	Erector Spinae, Rectus Abdominus
Upper Torso Axial Rotation	Erector Spinae, External Oblique
Arms	
Elbow Flexion	Brachioradialis
Shoulder Elevation	Latissmus Dorsi, Trapezius, Anterior Deltoid, Middle Deltoid, Posterior Deltoid
Shoulder Plane of Elevation	Latissmus Dorsi, Trapezius, Anterior Deltoid, Middle Deltoid, Posterior Deltoid

IV. RESULTS

A. DEMOGRAPHIC DATA

Demographic data from the 15 subjects who completed both testing sessions are presented in Table 3. All subjects were currently performing their regular training practices and were not injured at the time of both testing sessions. Subjects did not perform intense workouts the day of or one day prior to performing either testing protocol.

Table 3 - Demographic Data

Demographic Data			
	Minimum	Maximum	Mean ± SD
Age (y)	19	35	23.0 ± 4.6
Height (m)	1.71	1.88	1.80 ± 0.05
Mass (kg)	54.7	85.2	67.4 ± 7.9
5K Time (sec)	836	1081	932 ± 74

B. BODY COMPOSITION DATA

Body composition data are presented in Table 4. All data reflect calculations using the Brozek equation and lung volume correction. Subjects did not eat or perform exercise within

two hours of body composition testing. All subjects were tested wearing only a pair of compression shorts and a compression swim cap.

Table 4 - Body Composition Data

Body Composition Data

ABSOLUTE MEASUREMENTS	**Minimum**	**Maximum**	**Mean ± SD**
Lean Body Mass (kg)	48.42	70.31	60.80 ± 6.36
Fat Body Mass (kg)	2.13	14.92	6.64 ± 3.58
RELATIVE MEASUREMENTS			
Lean Body Mass (%)	82.5	96.9	90.35 ± 4.44
Fat Body Mass (%)	3.1	17.5	9.65 ± 4.44

C. MAXIMAL OXYGEN UPTAKE TEST DATA

Data from the VO_{2max} test are presented in Table 5. All subjects gave a maximal effort, as verified by RER > 1.1 and maximal heart rate ≥ 95% of age predicted maximum. All subjects fatigued at either the 10% or 12.5% incline of the test.

Table 5 - Maximal Oxygen Uptake Test Data

Maximal Oxygen Uptake Test Data			
	Minimum	Maximum	Mean ± SD
VO2max (mL $O_2 \cdot min^{-1} \cdot kg^{-1}$)	60.2	84.7	71.5 ± 6.3
HR at 90% VO2max (beats·min^{-1})	153.1	193.1	176.8 ± 12.2
HR at 95% VO2max (beats·min^{-1})	167.0	196.6	183.2 ± 10.4
HR at 100% VO2max (beats·min^{-1})	170.9	200.4	188.2 ± 10.8
Pre-Test Lactate (mmol·L^{-1})	0.9	3.9	2.1 ± 1.0
Post-Test Lactate (mmol·L^{-1})	6.6	22.0	13.8 ± 4.9

D. EXHAUSTIVE RUN DATA

1. Physiologic Data

Data from the exhaustive run are presented in Table 6. Lactate measurements were taken before any running began. All subjects performed a 10-minute warm-up on the treadmill at a subjectively easy pace. The treadmill was then stopped while subjects performed self-directed stretches and other warm-up procedures. The treadmill was then started and gradually increased to approximate 5K race pace speed. Data were recorded during this time. When subjects reached a stable heart rate corresponding to that of 90 to 95% of VO_{2max} for 60s, the test was considered to have begun. All subjects ran for the minimum 12-minute duration of the test. Each subject self-terminated the test by telling the investigator that he could not run for another minute on the treadmill and the treadmill was stopped. Resting lactate samples were recorded immediately thereafter.

Table 6 - Exhaustive Run Test Data

Exhaustive Run Test Data			
	Minimum	**Maximum**	**Mean ± SD**
Treadmill Speed ($m \cdot s^{-1}$)	4.78	5.59	5.18 ± 0.27
Run Duration (min)	12.0	27.0	16.1 ± 4.6
Start HR ($beats \cdot min^{-1}$)	158.5	189.5	172.4 ± 9.5
Middle HR ($beats \cdot min^{-1}$)	163.0	200.0	180.6 ± 12.5
End HR ($beats \cdot min^{-1}$)	169.5	201.5	186.1 ± 11.1
Pre-Test Lactate ($mmol \cdot L^{-1}$)	0.8	2.8	1.7 ± 0.1
Post-Test Lactate ($mmol \cdot L^{-1}$)	6.6	22.3	14.7 ± 4.9

2. Electromyographic Data

Median Power Frequency Data

Legs

Results of quadratic modeling for median power data for the leg muscles are presented in Table 7. Only the semimembranosus displayed a significant (p=.038) quadratic coefficient, positive in magnitude. The inflection point of this muscle was calculated to be 0.72, indicating MdPF decreased for the first 72% of the run and increased thereafter (Figure 25 and Figure 26). The rectus femoris was the only muscle showing a significant (p=0.039) linear coefficient, negative in magnitude. The p-values of linear coefficients for the vastus lateralis (p=0.095) and semimembranosus (p=0.057) were not statistically significant, but suggested linear trends.

Table 7 - Median Power Frequency of the Legs

Median Power Frequency Models

Legs

Muscle	Intercept	SE	p-value	Linear Coefficient	SE	p-value	Quadratic Coefficient	SE	p-value
Vastus Lateralis	-0.0581	0.0308	0.080	-0.0837	0.0499	0.095	0.0654	0.1298	0.615
Semimembranosus	-0.1332	0.0488	0.016 *	-0.1347	0.0703	0.057	0.3531	0.1690	0.038 *
Gluteus Maximus	-0.0378	0.0193	0.070	-0.0157	0.0345	0.650	0.0646	0.0979	0.510
Rectus Femoris	-0.0589	0.0326	0.093	-0.1088	0.0523	0.039 *	0.0446	0.1334	0.738

* indicates statistical significance

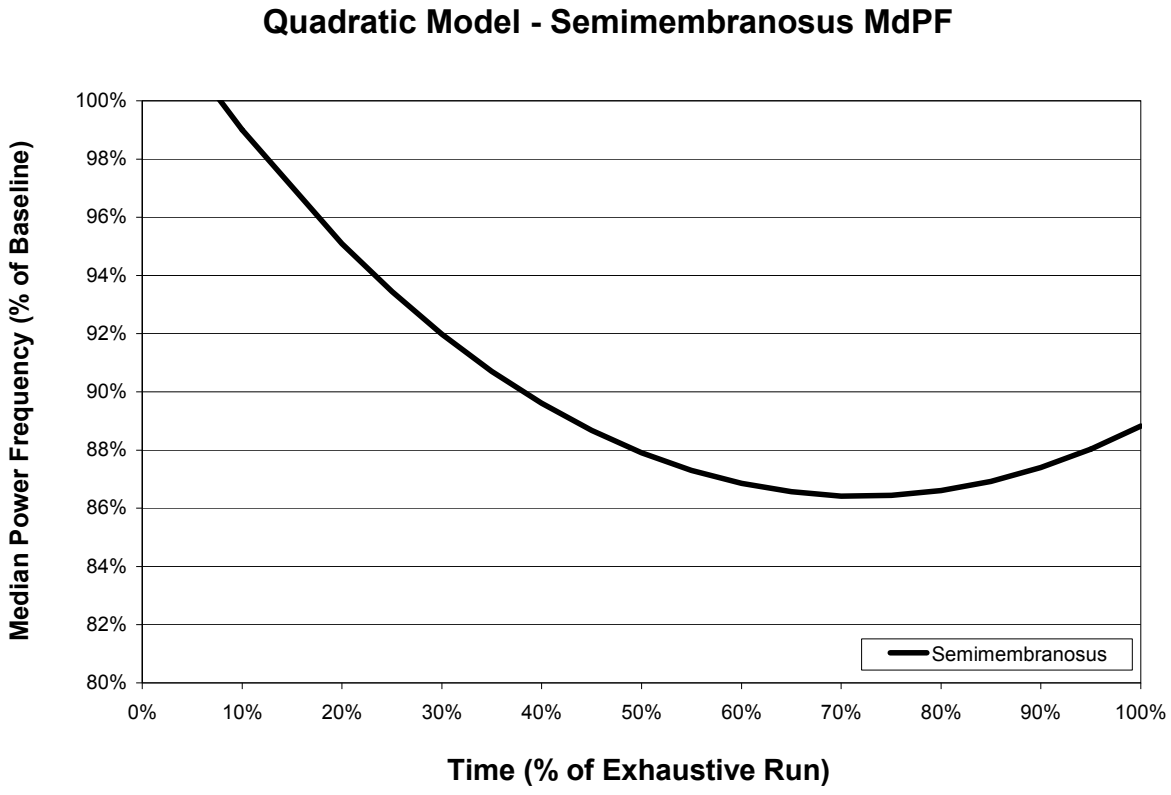

Figure 25 - Quadratic Model of Semimembranosus

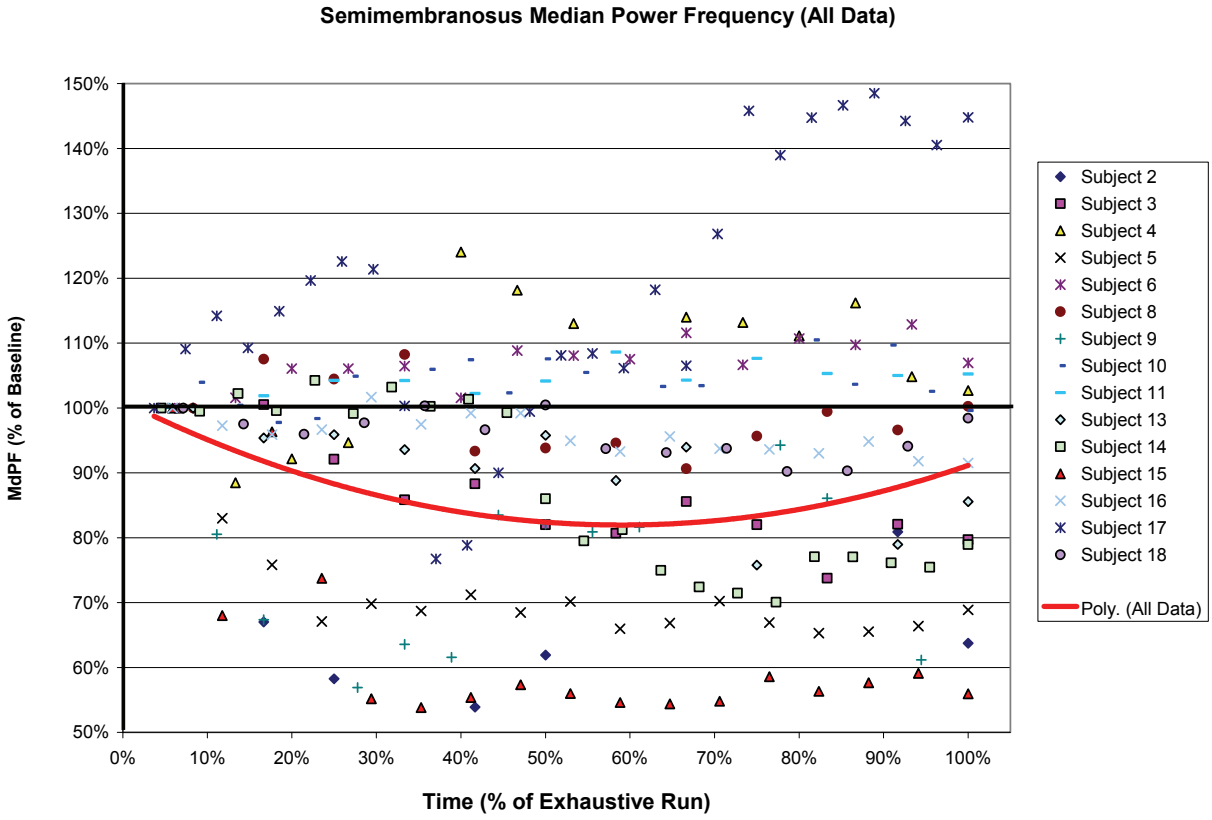

Figure 26 - Median Power Frequency of Semimembranosus

Torso

Results of quadratic modeling for median power data for the torso muscles are presented in Table 8. No muscles had a statistically significant quadratic coefficient. The latissimus dorsi was the only muscle with a significant (p=0.013) linear coefficient, which was negative in magnitude. The p-value of the erector spinae (p=0.074) was not significant, but suggested a linear trend.

Table 8 - Median Power Frequency of the Torso

Median Power Frequency Models									
Torso									
Muscle	**Intercept**	**SE**	**p-value**	**Linear Coefficient**	**SE**	**p-value**	**Quadratic Coefficient**	**SE**	**p-value**
Erector Spinae	-0.1302	0.0435	0.014 *	-0.1319	0.0733	0.074	0.2436	0.1949	0.213
Latissimus Dorsi	-0.0699	0.0491	0.178	-0.1818	0.0727	0.013 *	-0.1385	0.1777	0.437
Rectus Abdominus	-0.0331	0.0233	0.178	-0.0183	0.0413	0.658	0.1028	0.1160	0.377
External Oblique	0.0064	0.0250	0.802	-0.0561	0.0418	0.181	-0.1510	0.1106	0.174

* indicates statistical significance

Arms

Results of quadratic modeling for median power data for the arm muscles are presented in Table 9. No muscles displayed any significant quadratic or linear coefficients.

Table 9 - Median Power Frequency of the Arms

Median Power Frequency Models									
Arms									
Muscle	**Intercept**	**SE**	**p-value**	**Linear Coefficient**	**SE**	**p-value**	**Quadratic Coefficient**	**SE**	**p-value**
Anterior Deltoid	0.0078	0.0206	0.710	-0.0445	0.0377	0.240	-0.1573	0.1095	0.150
Middle Deltoid	-0.0066	0.0322	0.840	0.0005	0.0519	0.992	0.0165	0.1331	0.902
Posterior Deltoid	-0.1453	0.0826	0.100	-0.0416	0.0650	0.522	0.1095	0.1310	0.404
Upper Trapezius	-0.0015	0.0266	0.956	-0.0199	0.0466	0.671	-0.0050	0.1240	0.968
Brachioradialis	0.0019	0.0517	0.971	-0.0164	0.0569	0.774	-0.1048	0.1220	0.392

Integrated EMG data

Legs

Results of quadratic modeling for iEMG data of the leg muscles are presented in Table 10. No muscles displayed a significant quadratic coefficient. The semimembranosus and gluteus maximus displayed significant (p=0.005 and p=0.008, respectively) linear coefficients,

both positive in magnitude. The p-values of linear coefficient for the vastus lateralis (p=0.055) was not statistically significant, but suggested a linear trend.

Table 10 - Integrated EMG of the Legs

Integrated EMG Models

Legs

Muscle	Intercept	SE	p-value	Linear Coefficient	SE	p-value	Quadratic Coefficient	SE	p-value
Vastus Lateralis	0.3160	0.1530	0.058	0.3461	0.1796	0.055	-0.5427	0.3944	0.170
Semimembranosus	0.3287	0.1598	0.059	0.5008	0.1755	0.005 *	-0.5334	0.3774	0.159
Gluteus Maximus	0.3895	0.1345	0.012 *	0.5234	0.1959	0.008 *	-0.5193	0.4729	0.273
Rectus Femoris	0.1957	0.1505	0.214	0.1887	0.1805	0.297	-0.4272	0.3954	0.281

* indicates statistical significance

Torso

Results of quadratic modeling for iEMG data of the torso muscles are presented in Table 11. No muscles displayed a significant quadratic coefficient. All four of these muscles displayed significant positive linear coefficients ($p<0.05$).

Table 11 - Integrated EMG of the Torso

Integrated EMG Models

Torso

Muscle	Intercept	SE	p-value	Linear Coefficient	SE	p-value	Quadratic Coefficient	SE	p-value
Erector Spinae	0.4163	0.1487	0.019	0.5154	0.2075	0.014 *	-0.6079	0.4869	0.214
Latissimus Dorsi	0.1777	0.0921	0.076	0.4497	0.1445	0.002 *	0.2459	0.3669	0.504
Rectus Abdominus	0.2973	0.1648	0.095	1.0798	0.2710	<0.001 *	0.9674	0.7079	0.173
External Oblique	0.2562	0.1535	0.117	0.6142	0.1787	0.001 *	0.1740	0.3921	0.658

* indicates statistical significance

Arms

Results of quadratic modeling for iEMG data for the arm muscles are presented in Table 12. No muscles displayed a significant quadratic coefficient. The brachioradialis displayed a significant (p=0.026) linear coefficient, positive in magnitude.

Table 12 - Integrated EMG of the Arms

Integrated EMG Models

Arms

Muscle	Intercept	SE	p-value	Linear Coefficient	SE	p-value	Quadratic Coefficient	SE	p-value
Anterior Deltoid	0.0583	0.0683	0.410	0.1445	0.1137	0.205	0.0809	0.3005	0.788
Middle Deltoid	-0.0053	0.0684	0.940	-0.1325	0.1172	0.259	-0.1979	0.3133	0.528
Posterior Deltoid	0.2847	0.1770	0.182	0.0119	0.1232	0.923	-0.3709	0.2441	0.130
Upper Trapezius	-0.0618	0.0694	0.400	-0.0117	0.1271	0.927	0.2030	0.3494	0.562
Brachioradialis	0.1117	0.1049	0.308	0.2829	0.1261	0.026 *	0.2167	0.2767	0.435

* indicates statistical significance

Net Change in EMG Parameters

The net change in MdPF and iEMG calculated from the quadratic models are presented in Table 13. All muscles showed a net decrease in MdPF. Only the middle deltoid and trapezius exhibited a net decrease in iEMG, with all other muscles showing a net increase.

Table 13 - Model Predicted Changes in EMG Parameters

Time-Dependent Changes		
	%Initial MdPF	% Initial iEMG
Vastus Lateralis	92.0%	143.2%
Semimembranosus	88.8%	156.2%
Gluteus Maximus	97.0%	168.3%
Rectus Femoris	90.5%	120.9%
Erector Spinae	87.1%	168.9%
Latissimus Dorsi	83.0%	155.8%
Rectus Abdominus	98.1%	276.9%
External Oblique	94.8%	179.2%
Anterior Deltoid	95.3%	115.5%
Middle Deltoid	99.7%	89.5%
Posterior Deltoid	86.9%	123.2%
Upper Trapezius	98.8%	97.8%
Brachioradialis	97.1%	134.0%

3. Kinematic Data

The abbreviation scheme used for defining joint angles was partially defined in the Specific Aims and Hypotheses section of chapter 1. A "v" preceding a joint angle abbreviation indicates angular velocity. A "max" or "min" subscript following the joint angle abbreviation indicates a maximum or minimum parameter of the data. For example, HF_{max} represents maximum hip flexion angle and vHF_{min} represents minimum hip flexion angular velocity.

The nature of the kinematic calculations often produces negative values, which may be somewhat cumbersome to interpret. For instance, the minimum angle is negative in sign and represents the opposing joint movement. For example, HF_{min} may be refered to as "minimum hip flexion angle," though it is more appropriately termed "maximum hip extension angle." To clarify the interpretation of these variables, the magnitude of negative numbers is considered.

For example, if a joint angle changed from -25^{o} to -35^{o} degrees, this could be expressed as a 10^{o} decrease in joint angle, or a 10^{o} increase in the magnitude of the joint angle. The latter description is used throughout the results and discussion section.

Legs

Multivariate Analysis

The results of the multivariate RM ANOVA for the legs are displayed in Table 14. Maximum joint angle was the only multivariate analysis that showed statistical significance (p=0.002, observed power = 0.962) in the leg group and therefore is the only analysis which was further explored statistically. Observed power for minimum joint angle, and maximum and minimum joint angular velocities were 0.613, 0.479, and 0.414, respectively.

Table 14 - Multivariate Analysis of the Legs

Multivariate Tests (Wilks' Lambda)	
Legs	
	p-value
Maximum Joint Angle	0.002 *
Minimum Joint Angle	0.097
MaximumJoint Angular Velocity	0.212
Minimum Joint Angular Velocity	0.289

* indicates statistical significance

Maximum Joint Angles

Data for the maximum joint angle of each movement included in the leg group are shown in Table 15. Mauchly's test of sphericity was not significant for maximum knee flexion (KF_{max}),

hip flexion (HF_{max}), and pelvis axial rotation (PAR_{max}) angles (p-values: 0.701, 0.398, 0.483, respectively). Univariate RM ANOVA revealed significant time-dependent changes for KF_{max} (p=0.030, observed power = 0.675) and HF_{max} (p=0.001, observed power = 0.989), but only a non-signifcant trend was seen for PAR_{max} (p=0.066, observed power = 0.532). Maximum KF showed a non-significant trend for t_{start} vs. t_{end} (p=0.099), and no significant changes between t_{start} vs. t_{mid} (p=0.389) and t_{mid} vs. t_{end} (p=0.481). Maximum HF showed significant changes between t_{start} vs. t_{mid} (p=0.019) and t_{start} vs. t_{end} (p=0.014), but not t_{mid} vs. t_{end} (p=0.253).

Table 15 - Maximum Joint Angles of the Legs

Descriptive Data

Legs - Maximum Joint Angles

	Start		Middle		End	
	Mean	*(C.I.)*	*Mean*	*(C.I.)*	*Mean*	*(C.I.)*
Left Knee Flexion (deg)	109.43	(99.53 , 119.34)	110.59	(100.21 , 120.97)	111.83	(101.82 , 121.85)
Left Hip Flexion (deg)	55.00	(48.85 , 61.14)	56.62	(50.12 , 63.12)	57.46	(50.62 , 64.29)
Pelvis Axial Rotation (deg)	11.75	(6.46 , 17.04)	11.58	(6.42 , 16.75)	12.39	(6.81 , 17.98)

Minimum Joint Angles

Data for the minimum joint angle of each movement included in the leg group are shown in Table 16. Multivariate analysis revealed there was not a significant repeated measures effect in minimum joint angle for this group.

Table 16 - Minimum Joint Angles of the Legs

Descriptive Data

Legs - Minimum Joint Angles

	Start		Middle		End	
	Mean	*(C.I.)*	*Mean*	*(C.I.)*	*Mean*	*(C.I.)*
Left Knee Flexion (deg)	6.28	(1.92 , 10.64)	4.43	(0.34 , 8.53)	5.94	(1.43 , 10.44)
Left Hip Flexion (deg)	-23.03	(-25.55 , -20.51)	-24.05	(-26.77 , -21.33)	-24.19	(-27.28 , -21.11)
Pelvis Axial Rotation (deg)	-5.33	(-9.66 , -1.00)	-5.43	(-9.73 , -1.13)	-5.33	(-9.43 , -1.23)

Maximal Joint Angular Velocities

Data for the maximum joint angular velocities of each movement included in the leg group are shown in Table 17. Multivariate analysis revealed there was not a significant repeated measures effect in maximum joint angular velocity in this group.

Table 17 - Maximum Joint Angular Velocities of the Legs

Descriptive Data

Legs - Maximum Joint Anglular Velocities

	Start		Middle		End	
	Mean	*(C.I.)*	*Mean*	*(C.I.)*	*Mean*	*(C.I.)*
Left Knee Flexion ($deg \cdot s^{-1}$)	853.10	(706.80 , 999.39)	841.88	(775.22 , 908.55)	816.16	(685.37 , 936.95)
Left Hip Flexion ($deg \cdot s^{-1}$)	565.84	(504.91 , 626.76)	578.92	(526.02 , 631.82)	586.40	(516.69 , 656.12)
Pelvis Axial Rotation ($deg \cdot s^{-1}$)	101.84	(75.29 , 128.39)	98.55	(73.98 , 123.13)	108.21	(71.21 , 145.20)

Minimal Joint Angular Velocities

Data for the minimum joint angular velocities of each movement included in the leg group are shown in Table 18. Multivariate analysis revealed there was not a significant repeated measures effect in minimum joint angular velocity for this group.

Table 18 - Minimum Joint Angular Velocities of the Legs

Descriptive Data						
Legs - Minimum Joint Anglular Velocities						
	Start		**Middle**		**End**	
	Mean	*(C.I.)*	*Mean*	*(C.I.)*	*Mean*	*(C.I.)*
Left Knee Flexion ($deg \cdot s^{-1}$)	-848.53	(-945.17 , -751.90)	-847.91	(-910.57 , -785.25)	-813.45	(-922.50 , -704.40)
Left Hip Flexion ($deg \cdot s^{-1}$)	-389.31	(-431.95 , -346.67)	-414.78	(-475.89 , -353.67)	-404.44	(-457.72 , -351.17)
Pelvis Axial Rotation ($deg \cdot s^{-1}$)	-120.93	(-153.06 , -88.80)	-116.23	(-142.12 , -90.34)	-126.67	(-164.61 , -88.73)

Torso

Multivariate Analysis

The results of the multivariate RM ANOVA for the torso group are displayed in Table 19. Maximum angle, minimum angle, and minimum angular velocity all showed statistical significance and were further explored. The observed powers for these analyses were 0.903, 0.941, and 0.750, respectively. Maximum angular velocity was the only component of the multivariate analysis that did not show statistical significance and therefore was not further explored (observed power = 0.492).

Table 19 - Multivariate Analysis of the Torso

Multivariate Tests (Wilks' Lambda)	
Torso	
	p-value
Maximum Joint Angle	0.005 *
Minimum Joint Angle	0.002 *
MaximumJoint Angular Velocity	0.150
Minimum Joint Angular Velocity	0.029 *

* indicates statistical significance

Maximum Joint Angles

Data for the maximum angle of each movement included in the torso group are shown in Table 20. Mauchly's test of sphericity was significant for TF_{max} and $UTAR_{max}$ ($p<0.001$ for each). Univariate RM ANOVA revealed significant time-dependent changes for $UTAR_{max}$ ($p=0.019$, observed power = 0.700), but not for TF_{max} ($p=0.712$, observed power = 0.068). Maximum UTAR showed significant changes between t_{start} vs. t_{mid} ($p<0.001$), a non-significant trend for t_{start} vs. t_{end} ($p=0.063$), and no significance for t_{mid} vs. t_{end} ($p=1.000$).

Table 20 - Maximum Joint Angles of the Torso

Descriptive Data

Torso - Maximum Joint Angles

	Start		Middle		End	
	Mean	*(C.I.)*	*Mean*	*(C.I.)*	*Mean*	*(C.I.)*
Torso Flexion (deg)	-1.07	(-3.36 , 1.21)	-1.37	(-4.09 , 1.35)	-1.51	(-5.35 , 2.33)
Upper Torso Axial Rotation (deg)	20.40	(18.17 , 22.63)	22.12	(19.78 , 24.46)	22.74	(20.16 , 25.32)

Minimum Joint Angles

Data for the minimum angle of each movement included in the torso group are shown in Table 21. Mauchly's test of sphericity was significant for TF_{min} ($p<0.001$), but not for $UTAR_{min}$ ($p=0.275$). Univariate RM ANOVA revealed significant time-dependent changes for $UTAR_{min}$ ($p=0.002$, observed power = 0.939), but not for TF_{min} ($p=0.576$, observed power = 0.087). Minimum UTAR showed significant changes between t_{start} vs. t_{end} ($p=0.024$) and for t_{mid} vs. t_{end} ($p=0.010$), but did not for t_{start} vs. t_{mid} ($p=1.000$).

Table 21 - Minimum Joint Angles of the Torso

Descriptive Data

Torso - Minimum Joint Angles

	Start		Middle		End	
	Mean	*(C.I.)*	*Mean*	*(C.I.)*	*Mean*	*(C.I.)*
Torso Flexion (deg)	-6.11	(-8.27 , -3.95)	-5.97	(-8.40 , -3.54)	-5.82	(-8.56 , -3.09)
Upper Torso Axial Rotation (deg)	-16.33	(-18.89 , -13.76)	-16.86	(-20.01 , -13.70)	-19.35	(-22.54 , -16.16)

Maximum Joint Angular Velocities

Data for the maximum angular velocities of each movement included in the torso group are shown in Table 22. Multivariate analysis revealed there was not a significant repeated measures effect in maximal torso angular velocity.

Table 22 - Maximum Joint Angular Velocities of the Torso

Descriptive Data

Torso - Maximum Joint Angular Velocities

	Start		Middle		End	
	Mean	*(C.I.)*	*Mean*	*(C.I.)*	*Mean*	*(C.I.)*
Torso Flexion ($deg \cdot s^{-1}$)	51.66	(40.66 , 62.66)	49.87	(39.50 , 60.23)	47.92	(36.03 , 59.81)
Upper Torso Axial Rotation ($deg \cdot s^{-1}$)	203.62	(179.32 , 227.92)	215.83	(196.02 , 235.63)	216.38	(199.27 , 233.48)

Minimum Joint Angular Velocities

Data for the minimum angular velocity of each movement included in the torso group are shown in Table 23. Mauchly's test of sphericity was not significant for $vUTAR_{min}$ (p=0.585), or TF_{minV} (p=0.940). Univariate RM ANOVA revealed significant time-dependent changes for $vUTAR_{min}$ (p=0.004, observed power = 0.896), but not for vTF_{min} (p=0.547, observed power = 0.138). Minimum UTAR angular velocity showed significant changes between t_{start} vs. t_{end}

(p=0.031), a non-significant trend for t_{start} vs. t_{mid} (p=0.060), and no significant changes for t_{mid} vs. t_{end} (p=0.691).

Table 23 - Minimum Joint Angular Velocities of the Torso

Descriptive Data						
Torso - Minimum Joint Angular Velocities						
	Start		**Middle**		**End**	
	Mean	*(C.I.)*	*Mean*	*(C.I.)*	*Mean*	*(C.I.)*
Torso Flexion ($deg \cdot s^{-1}$)	-47.25	(-59.08 , -35.43)	-48.87	(-60.08 , -37.65)	-48.75	(-59.54 , -37.96)
Upper Torso Axial Rotation ($deg \cdot s^{-1}$)	-200.82	(-228.78 , -172.86)	-213.84	(-244.11 , -183.56)	-219.51	(-247.64 , -191.38)

Arms

Multivariate Analysis

The results of the multivariate RM ANOVA for the arms group are displayed in Table 24. Maximum angle, minimum angle, maximum joint angular velocity, and minimum joint angular velocity all showed statistical significance and were further explored. The observed powers for these variables were 0.972, 0.755, 0.911, and 0.851, respectively.

Table 24 - Multivariate Analysis of the Arms

Multivariate Tests (Wilks' Lambda)	
Arms	
	p-value
Maximum Joint Angle	0.001 *
Minimum Joint Angle	0.043 *
Maximum Joint Angular Velocity	0.007 *
Minimum Joint Angular Velocity	0.017 *

* indicates statistical significance

Maximum Joint Angles

Data for the maximum joint angle of each movement included in the arm group are shown in Table 25. Mauchly's test of sphericity was not significant for EF_{max}, SE_{max}, or SPE_{max} (p=0.350, 0.281, 0.241, respectively). Univariate RM ANOVA revealed significant time-dependent changes for EF_{max} ($p<0.001$, observed power = 0.998), a non-significant trend for SPE_{max} (p=0.090, observed power = 0.476), and no signifance not for SE_{max} (p=0.102, observed power = 0.453) or Maximum EF showed significant changes between t_{start} vs. t_{mid} (p=0.003), t_{start} vs. t_{end} ($p<0.001$), but not for t_{mid} vs. t_{end} (p=1.000).

Table 25 - Maximum Joint Angles of the Arms

Descriptive Data						
Arms - Maximum Joint Angles						
	Start		**Middle**		**End**	
	Mean	*(C.I.)*	*Mean*	*(C.I.)*	*Mean*	*(C.I.)*
Left Elbow Flexion (deg)	110.95	(104.90 , 117.01)	115.14	(108.76 , 121.52)	116.33	(111.44 , 121.22)
Left Shoulder Elevation (deg)	59.05	(53.17 , 64.93)	60.66	(54.68 , 66.65)	62.17	(56.29 , 68.05)
Left Shoulder Plane of Elevation (deg)	111.39	(95.17 , 127.61)	113.83	(99.17 , 128.50)	118.06	(104.63 , 131.48)

Minimum Joint Angles

Data for the minimum joint angle of each movement included in the arm group are shown in Table 26. Mauchly's test of sphericity was significant for SE_{min} (p=0.010), but not for EF_{min} or SPE_{min} (p=0.989 and 0.141, respectively). Univariate RM ANOVA revealed significant time-dependent changes for SE_{min} (p=0.046, observed power = 0.560), but not for EF_{min} (p=0.452, observed power = 0.171) or SPE_{min} (p=0.106, observed power = 0.445). Minimum SE showed a non-significant trend for and t_{mid} vs. t_{end} (p=0.073), but did not show any significant changes between t_{start} vs. t_{mid} (p=1.00) and t_{start} vs. t_{end} (p=0.178).

Table 26 - Minimum Joint Angles of the Arms

Descriptive Data

Arms - Minimum Joint Angles

	Start		Middle		End	
	Mean	*(C.I.)*	*Mean*	*(C.I.)*	*Mean*	*(C.I.)*
Left Elbow Flexion (deg)	96.38	(89.34 , 103.43)	97.90	(91.00 , 104.80)	98.61	(91.93 , 105.28)
Left Shoulder Elevation (deg)	44.65	(34.53 , 54.77)	41.39	(28.81 , 53.96)	29.10	(8.17 , 50.03)
Left Shoulder Plane of Elevation (deg)	68.89	(59.06 , 78.73)	69.08	(56.59 , 81.58)	58.96	(39.44 , 78.48)

Maximum Joint Angular Velocities

Data for the maximum joint angular velocity of each movement included in the arm group are shown in Table 27. Mauchly's test of sphericity was significant for vSE_{max} (p=0.036) and $vSPE_{max}$ and (p<0.001), but not for vEF_{max} (p=0.320). Univariate RM ANOVA revealed significant time-dependent changes for vSE_{max} (p=0.004, observed power = 0.895) and for $vSPE_{max}$ (p=0.010, observed power = 0.815), but not for maximum vEF_{max} (p=0.131, observed power = 0.404). Maximum SE angular velocity showed significant changes between t_{start} vs. t_{mid} (p=0.020), t_{start} vs. t_{end} (p=0.016), but not for t_{mid} vs. t_{end} (p=0.139). Maximum SPE angular

velocity showed significant changes between t_{start} vs. t_{mid} (p=0.002) and t_{start} vs. t_{end} (p=0.022), and a non-significant trend for t_{mid} vs. t_{end} (p=0.075).

Table 27 - Maximum Joint Angular Velocities of the Arms

Descriptive Data						
Arms - Maximum Joint Angular Velocities						
	Start		**Middle**		**End**	
	Mean	*(C.I.)*	*Mean*	*(C.I.)*	*Mean*	*(C.I.)*
Left Elbow Flexion ($deg \cdot s^{-1}$)	65.89	(50.21 , 81.57)	71.60	(58.10 , 85.10)	75.90	(64.70 , 87.10)
Left Shoulder Elevation ($deg \cdot s^{-1}$)	46.87	(33.93 , 59.80)	52.98	(37.43 , 68.52)	61.10	(42.76 , 79.44)
Left Shoulder Plane of Elevation ($deg \cdot s^{-1}$)	148.24	(107.07 , 189.42)	171.85	(128.47 , 215.23)	230.94	(146.99 , 314.90)

Minimum Joint Angular Velocities

Data for the minimum joint angular velocity of each movement included in the arm group are shown in Table 28 Mauchly's test of sphericity was not significant for vEF_{min}, vSE_{min} or $vSPE_{min}$ (p=0.166, 0.160, and 0.290, respectively). Univariate RM ANOVA revealed significant time-dependent changes for vSE_{min} (p=0.002, observed power = 0.938), but not for vEF_{min} (p=0.473, observed power = 0.165) or $vSPE_{min}$ (p=0.120, observed power = 0.422). Minimum SE angular velocity showed significant changes between t_{start} vs. t_{mid} (p=0.003), t_{start} vs. t_{end} (p=0.019), but not for t_{mid} vs. t_{end} (p=1.000).

Table 28 - Minimum Joint Angular Velocities of the Arms

Descriptive Data						
Arms - Minimum Joint Angular Velocities						
	Start		**Middle**		**End**	
	Mean	*(C.I.)*	*Mean*	*(C.I.)*	*Mean*	*(C.I.)*
Left Elbow Flexion ($deg \cdot s^{-1}$)	-76.55	(-91.39 , -61.71)	-87.24	(-107.63 , -66.55)	-83.37	(-102.47 , -64.28)
Left Shoulder Elevation ($deg \cdot s^{-1}$)	-46.35	(-58.52 , -34.18)	-55.49	(-69.89 , -41.09)	-58.51	(-72.36 , -44.66)
Left Shoulder Plane of Elevation ($deg \cdot s^{-1}$)	-138.97	(-164.20 , -113.733)	-166.85	(-202.55 , -131.15)	-165.32	(-194.94 , -135.70)

Vertical Displacement

Maximum Vertical Displacement

Data for the VD_{max} are shown in Table 29. Mauchly's test of sphericity was not significant for VD_{max} ($p=0.273$). Univariate RM ANOVA did reveal significant time-dependent changes for VD_{max} ($p=0.776$, observed power = 0.085).

Table 29 - Maximum Vertical Displacement Height

Descriptive Data						
Vertical Displacement - Maximum Height						
	Start		**Middle**		**End**	
	Mean	*(C.I.)*	*Mean*	*(C.I.)*	*Mean*	*(C.I.)*
Vertical Displacement (m)	1.0154	(0.992 , 1.039)	1.0143	(0.991 , 1.038)	1.0146	(0.992 , 1.038)

Minimum Vertical Displacement

Data for the VD_{min} are shown in Table 30. Mauchly's test of sphericity was not significant for VD_{min} ($p=0.610$). Univariate RM ANOVA revealed significant time-dependent changes for VD_{min} ($p=0.013$, observed power = 0.786). Minimum VD showed significant changes between t_{start} vs. t_{mid} ($p=0.034$) and t_{start} vs. t_{end} ($p=0.030$), but not for t_{mid} vs. t_{end} ($p=1.000$).

Table 30 - Minimum Vertical Displacement Height

Descriptive Data						
Vertical Displacement - Minimum Height						
	Start		**Middle**		**End**	
	Mean	*(C.I.)*	*Mean*	*(C.I.)*	*Mean*	*(C.I.)*
Vertical Displacement (m)	0.9908	(0.969 , 1.013)	0.9877	(0.966 , 1.010)	0.9875	(0.966 , 1.009)

Maximum Vertical Displacement Velocity

Data for the vVD_{max} are shown in Table 31. Mauchly's test of sphericity was significant for vVD_{max} ($p=0.037$). Univariate RM ANOVA revealed a non-significant trend for time-dependent changes for vVD_{max} ($p=0.084$, observed power = 0.454).

Table 31 - Maximum Vertical Displacement Height Velocity

Descriptive Data						
Vertical Displacement - Maximal Height Velocity						
	Start		**Middle**		**End**	
	Mean	*(C.I.)*	*Mean*	*(C.I.)*	*Mean*	*(C.I.)*
Vertical Displacement Velocity ($m \cdot s^{-1}$)	0.1653	(0.142 , 0.188)	0.1801	(0.160 , 0.200)	0.1837	(0.162 , 0.206)

Minimum Vertical Displacement Velocity

Data for the vVD_{min} are shown in Table 32. Mauchly's test of sphericity was significant for vVD_{min} ($p=0.009$). Univariate RM ANOVA reveal a non-significant trend for time-dependent changes for vVD_{min} ($p=0.072$, observed power = 0.473).

Table 32 - Minimum Vertical Displacement Height Velocity

Descriptive Data						
Vertical Displacement - Minimal Height Velocity						
	Start		**Middle**		**End**	
	Mean	*(C.I.)*	*Mean*	*(C.I.)*	*Mean*	*(C.I.)*
Vertical Displacement Velocity ($m \cdot s^{-1}$)	-0.1661	(-0.188 , -0.144)	-0.1786	(-0.199 , -0.159)	-0.1848	(-0.205 , -0.164)

Stride Parameter Data

Stride duration was recorded using the accelerometer and data from each minute of the exhaustive run were entered into a quadratic model. The quadratic modeling results (Table 33) showed a significant positive linear coefficient, indicating stride duration increased over the exhaustive run. The graphical representation of the mathematical model is presented in Figure 27.

Table 33 – Quadratic Model of Stride Duration

Stride Duration Model

Parameter	Intercept	SE	p-value	Linear Coefficient	SE	p-value	Quadratic Coefficient	SE	p-value
Stride Duration	0.0105	0.0040	0.021 *	0.0195	0.0080	0.016 *	-0.0051	0.0256	0.844

* indicates statistical significance

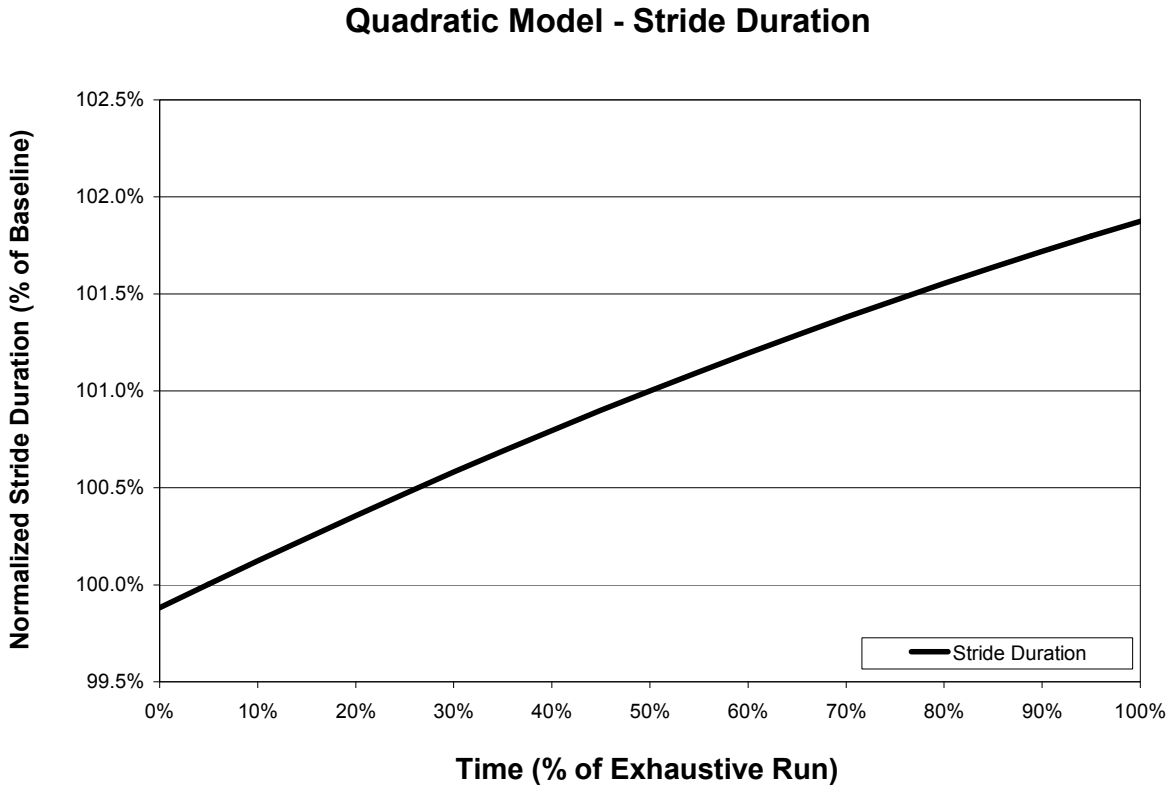

Figure 27 – Graph of Quadratic Model of Stride Duration

4. Relationship Between EMG and Kinematic Variables

Legs

Knee Flexion

Correlations between changes in EMG parameters and changes in KF variables are presented in Table 34. No correlations were statistically significant.

Table 34 - Correlation Between Knee Flexion Data and EMG Parameters

Correlations - Knee Flexion

		Knee Flexion			
Integrated EMG		Maximum	Minimum	Maximum Velocity	Minimum Velocity
Vastus Lateralis	r-value	0.369	0.163	0.002	0.113
	p-value	0.369	0.727	0.996	0.790
Semimembranosus	r-value	0.442	-0.009	0.010	0.420
	p-value	0.272	0.984	0.981	0.301
Rectus Femoris	r-value	-0.109	0.212	-0.325	-0.253
	p-value	0.817	0.686	0.478	0.584
Median Power Frequency		Maximum	Minimum	Maximum Velocity	Minimum Velocity
Vastus Lateralis	r-value	-0.079	-0.524 †	0.385	0.308
	p-value	0.852	0.228	0.347	0.458
Semimembranosus	r-value	0.055	-0.140	-0.077	0.470
	p-value	0.897	0.764	0.856	0.240
Rectus Femoris	r-value	-0.253	0.578 †	-0.579 †	-0.205
	p-value	0.546	0.174	0.132	0.626

† = Moderate correlation with non-significant p-value

Hip Flexion

Correlations between changes in EMG parameters and changes in HF variables are presented in Table 35. Changes in iEMG of the semimembranosus shared statistically significant ($p<0.01$) strong relationships with ΔHF_{min} (hip extension, $r=0.871$) and ΔvHF_{min} ($r=0.873$).

Table 35 - Correlation Between Hip Flexion Data and EMG Parameters

Correlations - Hip Flexion

		Hip Flexion			
Integrated EMG		Maximum	Minimum	Maximum Velocity	Minimum Velocity
Semimembranosus	r-value	0.341	0.871 *	0.257	0.873 *
	p-value	0.409	0.005	0.539	0.005
Gluteus Maximus	r-value	0.661 †	0.525 †	0.226	0.664 †
	p-value	0.075	0.181	0.590	0.073
Rectus Femoris	r-value	0.118	-0.082	0.145	0.378
	p-value	0.802	0.862	0.756	0.403
Median Power Frequency		Maximum	Minimum	Maximum Velocity	Minimum Velocity
Semimembranosus	r-value	-0.302	0.364	-0.139	0.073
	p-value	0.467	0.376	0.743	0.863
Gluteus Maximus	r-value	-0.262	0.199	-0.143	-0.098
	p-value	0.531	0.637	0.735	0.818
Rectus Femoris	r-value	-0.146	-0.184	-0.512 †	-0.408
	p-value	0.731	0.663	0.195	0.315

* = Correlation with statistical significance at $p<0.05$

† = Moderate correlation with non-significant p-value

Pelvis Axial Rotation

Correlations between changes in EMG parameters and changes in PAR kinematic variables are presented in Table 36.

Table 36 - Correlation Between Pelvis Axial Rotation Data and EMG Parameters

Correlations - Pelvis Axial Rotation

		Pelvis Axial Rotation			
Integrated EMG		Maximum	Minimum	Maximum Velocity	Minimum Velocity
Erector Spinae	r-value	0.498	-0.361	0.188	-0.267
	p-value	0.172	0.340	0.629	0.487
External Oblique	r-value	-0.246	0.306	-0.205	0.333
	p-value	0.494	0.390	0.570	0.347
Median Power Frequency		Maximum	Minimum	Maximum Velocity	Minimum Velocity
Erector Spinae	r-value	-0.264	0.521 †	0.211	0.430
	p-value	0.432	0.100	0.533	0.187
External Oblique	r-value	0.385	-0.493	-0.172	-0.477
	p-value	0.243	0.123	0.613	0.138

† = Moderate correlation with non-significant p-value

Torso

Upper Torso Axial Rotation

Correlations between changes in EMG parameters and changes in UTAR kinematic variables are presented in Table 37.

Table 37 - Correlation Between Upper Torso Axial Rotation Data and EMG Parameters

Correlations - Upper Torso Axial Rotation

		Upper Torso Axial Rotation			
Integrated EMG		Maximum	Minimum	Maximum Velocity	Minimum Velocity
Erector Spinae	r-value	-0.083	0.159	-0.323	-0.593 †
	p-value	0.807	0.641	0.333	0.071
External Oblique	r-value	-0.143	-0.234	-0.061	-0.038
	p-value	0.657	0.465	0.851	0.912
Median Power Frequency		Maximum	Minimum	Maximum Velocity	Minimum Velocity
Erector Spinae	r-value	0.310	-0.319	0.190	0.129
	p-value	0.281	0.267	0.516	0.676
External Oblique	r-value	0.076	0.327	0.143	0.160
	p-value	0.795	0.255	0.627	0.601

† = Moderate correlation with non-significant p-value

Torso Flexion

Correlations between changes in EMG parameters and changes in TF kinematic variables are presented in Table 38. A statistically significant (p=0.034) moderate relationship (r=0.640) between change in erector spinae iEMG and ΔTF_{max} was observed. A significant (p=0.001) strong relationship (p=-0.813) between rectus abdominus MdPF and ΔTF_{min} (torso extension) was also observed.

Table 38 - Correlation Between Torso Flexion Data and EMG Parameters

Correlations - Torso Flexion

		Torso Flexion			
Integrated EMG		Maximum	Minimum	Maximum Velocity	Minimum Velocity
Erector Spinae	r-value	0.640 *	0.222	-0.245	0.369
	p-value	0.034	0.512	0.559	0.329
Rectus Abdominus	r-value	-0.137	0.223	-0.147	0.330
	p-value	0.672	0.486	0.706	0.352

Median Power Frequency		Maximum	Minimum	Maximum Velocity	Minimum Velocity
Erector Spinae	r-value	-0.110	-0.396	-0.521 †	-0.023
	p-value	0.721	0.180	0.122	0.947
Rectus Abdominus	r-value	-0.106	-0.813 *	0.403	-0.110
	p-value	0.730	0.001	0.248	0.748

* = Correlation with statistical significance at p<0.05
† = Moderate correlation with non-significant p-value

Arms

Elbow Flexion

Correlations between EMG parameters and elbow flexion kinematic variables are presented in Table 39. No significant relationships were observed.

Table 39 - Correlation Between Elbow Flexion Data and EMG Parameters

Correlations - Elbow Flexion Angle

		Elbow Flexion Angle			
Integrated EMG		Maximum	Minimum	Maximum Velocity	Minimum Velocity
Brachioradialis	r-value	0.027	0.096	-0.070	0.292
	p-value	0.941	0.793	0.829	0.357
Median Power Frequency		Maximum	Minimum	Maximum Velocity	Minimum Velocity
Brachioradialis	r-value	0.231	0.365	-0.079	-0.241
	p-value	0.470	0.243	0.787	0.406

Shoulder Elevation

Correlations between EMG parameters and shoulder elevation kinematic variables are presented in Table 40. Latissimus dorsi iEMG exhibited a statistically significant (p=0.016) moderate relationship (r=0.731) with ΔvSE_{min}. Anterior deltoid iEMG exhibited a statistically significant (p=0.024) moderate relationship (r=0.701) with ΔSE_{max}.

Table 40 - Correlation Between Shoulder Elevation Data and EMG Parameters

Correlations - Shoulder Elevation

		Shoulder Elevation			
Integrated EMG		Maximum	Minimum	Maximum Velocity	Minimum Velocity
Latissimus Dorsi	r-value	0.118	-0.028	0.511 †	0.731 *
	p-value	0.730	0.934	0.108	0.016
Anterior Deltoid	r-value	0.701 *	0.533 †	-0.327	-0.175
	p-value	0.024	0.112	0.326	0.606
Middle Deltoid	r-value	-0.106	-0.201	0.104	0.419
	p-value	0.771	0.577	0.760	0.199
Posterior Deltoid	r-value	-0.132	0.023	-0.184	-0.039
	p-value	0.699	0.946	0.567	0.905
Trapezius	r-value	0.225	0.155	-0.093	0.053
	p-value	0.628	0.740	0.843	0.909
Median Power Frequency		Maximum	Minimum	Maximum Velocity	Minimum Velocity
Latissimus Dorsi	r-value	-0.328	-0.072	-0.155	-0.382
	p-value	0.324	0.834	0.631	0.220
Anterior Deltoid	r-value	-0.231	0.197	-0.214	0.042
	p-value	0.494	0.561	0.505	0.897
Middle Deltoid	r-value	0.541 †	-0.434	0.065	0.007
	p-value	0.086	0.183	0.842	0.982
Posterior Deltoid	r-value	0.087	-0.083	0.260	0.419
	p-value	0.799	0.808	0.414	0.175
Trapezius	r-value	-0.059	-0.373	0.055	0.317
	p-value	0.863	0.258	0.865	0.315

* = Correlation with statisticalsignificance at p<0.05
† = Moderate correlation with non-significant p-value

Shoulder Plane of Elevation

Correlations between EMG parameters and shoulder plane of elevation kinematic variables are presented in Table 41. There was a statistically significant ($p<0.001$) strong relationship ($r=0.863$) between iEMG of the latissimus dorsi and ΔSPE_{max}, and a statistically significant ($p=0.037$) moderate relationship ($r=0.662$) between latissimus dorsi iEMG and

ΔSPE_{maxV}. There was a statistically significant (p=0.028) moderate relationship (r=-0.632) between anterior deltoid iEMG and $\Delta vSPE_{min.}$. Median power frequency of the latissmus dorsi had a statistically significant (p=0.016) moderate relationship (r=-0.674) with ΔSPE_{max}.

Table 41 - Correlation Between Shoulder Plane of Elevation Data and EMG Parameters

Correlations - Shoulder Plane of Elevation

		Shoulder Plane of Elevation			
Integrated EMG		Maximum	Minimum	Maximum Velocity	Minimum Velocity
Latissimus Dorsi	r-value	0.863 *	0.072	0.662 *	-0.042
	p-value	<0.001	0.825	0.037	0.903
Anterior Deltoid	r-value	-0.007	0.186	-0.548 †	-0.632 *
	p-value	0.984	0.584	0.081	0.028
Middle Deltoid	r-value	0.583 †	-0.220	-0.053	-0.384
	p-value	0.060	0.516	0.878	0.218
Posterior Deltoid	r-value	-0.070	-0.254	-0.212	-0.187
	p-value	0.829	0.425	0.508	0.542
Trapezius	r-value	-0.297	-0.235	-0.254	-0.649 †
	p-value	0.518	0.613	0.583	0.115
Median Power Frequency		Maximum	Minimum	Maximum Velocity	Minimum Velocity
Latissimus Dorsi	r-value	-0.674 *	0.073	0.256	-0.035
	p-value	0.016	0.821	0.422	0.909
Anterior Deltoid	r-value	-0.111	-0.006	0.006	-0.146
	p-value	0.732	0.985	0.984	0.633
Middle Deltoid	r-value	-0.300	-0.320	-0.002	-0.090
	p-value	0.343	0.311	0.996	0.769
Posterior Deltoid	r-value	0.311	0.152	0.374	0.307
	p-value	0.326	0.636	0.231	0.307
Trapezius	r-value	-0.229	0.377	0.043	0.151
	p-value	0.475	0.228	0.895	0.623

* = Correlation with statistical significance at p<0.05
† = Moderate correlation with non-significant p-value

Whole Body Kinematic Variables

Correlations between iEMG parameters and whole body kinematic variables are presented in Table 42. There was a non-significant (p=0.065) moderate relationship (r=0.548) between change in iEMG of vastus lateralis and ΔVD_{max}. There was a statistically significant (p=0.028) strong relationship (r=0.860) between change in trapezius iEMG and ΔVD_{min}.

Table 42 - Correlation Between iEMG and Whole Body Variables

Correlations - Whole Body Variables

		Vertical Displacment				Stride
Integrated EMG		Maximum	Minimum	Maximum Velocity	Minimum Velocity	Duration
Vastus Lateralis	r-value	0.548 †	0.074	0.400	0.173	0.183
	p-value	0.065	0.818	0.176	0.572	0.531
Semimembranosus	r-value	0.311	-0.031	0.258	0.116	0.122
	p-value	0.325	0.923	0.395	0.707	0.677
Gluteus Maximus	r-value	0.440	0.081	0.190	-0.072	0.126
	p-value	0.152	0.802	0.534	0.814	0.668
Rectus Femoris	r-value	0.370	0.303	-0.031	-0.098	-0.152
	p-value	0.263	0.366	0.925	0.762	0.620
Erector Spinae	r-value	-0.068	-0.192	0.191	0.128	-0.330
	p-value	0.852	0.595	0.597	0.725	0.322
Latissimus Dorsi	r-value	-0.276	-0.001	-0.220	-0.474	0.362
	p-value	0.412	0.998	0.515	0.141	0.247
Rectus Abdominus	r-value	0.170	0.478	0.021	0.085	-0.080
	p-value	0.618	0.137	0.948	0.792	0.804
External Oblique	r-value	-0.178	0.036	-0.246	-0.426	0.506 †
	p-value	0.600	0.916	0.467	0.192	0.093
Anterior Deltoid	r-value	-0.291	0.210	-0.188	-0.178	-0.074
	p-value	0.385	0.535	0.560	0.581	0.820
Middle Deltoid	r-value	0.456	0.347	0.101	-0.135	0.001
	p-value	0.159	0.296	0.755	0.675	0.996
Posterior Deltoid	r-value	0.558 †	0.527 †	0.183	0.031	0.050
	p-value	0.060	0.078	0.550	0.920	0.866
Trapezius	r-value	0.398	0.860 *	-0.036	0.020	0.133
	p-value	0.434	0.028	0.946	0.970	0.776
Brachioradialis	r-value	0.000	0.397	-0.039	-0.114	0.120
	p-value	1.000	0.257	0.910	0.738	0.726

* = Correlation with statistical significance at p<0.05
† = Moderate correlation with non-significant p-value

Correlations between MdPF parameters and whole body kinematic variables are presented in Table 43. There were statistically significant ($p=0.006$, $p<0.001$) moderate and strong relationships ($r=0.713$, $r=0.868$) between changes in MdPF of latissimus dorsi and ΔvVD_{min} and ΔvVD_{min}, respectively. There was a statistically significant ($p=0.024$) moderate relationship ($r=0.644$) between change in brachioradialis MdPF and ΔVD_{min}.

Table 43 - Correlation Between MdPF and Whole Body Variables

Correlations - Whole Body Variables

		Vertical Displacment				Stride
Median Power Frequency		Maximum	Minimum	Maximum Velocity	Minimum Velocity	Duration
Vastus Lateralis	r-value	-0.325	0.096	-0.403	-0.239	-0.026
	p-value	0.302	0.767	0.173	0.432	0.929
Semimembranosus	r-value	0.005	0.294	-0.124	-0.225	0.204
	p-value	0.987	0.354	0.687	0.459	0.485
Gluteus Maximus	r-value	0.329	0.405	0.262	0.264	0.417
	p-value	0.296	0.192	0.387	0.383	0.138
Rectus Femoris	r-value	-0.131	-0.396	0.021	-0.008	-0.142
	p-value	0.684	0.203	0.946	0.979	0.628
Erector Spinae	r-value	0.292	0.265	-0.165	-0.230	0.453
	p-value	0.356	0.405	0.590	0.450	0.104
Latissimus Dorsi	r-value	0.310	0.096	0.713 *	0.868 *	0.436
	p-value	0.327	0.767	0.006	<0.001	0.119
Rectus Abdominus	r-value	0.523 †	0.314	0.081	-0.127	0.119
	p-value	0.081	0.320	0.792	0.680	0.685
External Oblique	r-value	0.341	0.000	0.491	0.416	0.237
	p-value	0.278	0.999	0.088	0.158	0.415
Anterior Deltoid	r-value	0.038	0.419	-0.236	-0.207	-0.404
	p-value	0.907	0.175	0.438	0.497	0.152
Middle Deltoid	r-value	0.472	0.215	0.386	0.256	0.453
	p-value	0.121	0.502	0.192	0.399	0.103
Posterior Deltoid	r-value	-0.181	-0.270	-0.148	-0.139	0.111
	p-value	0.574	0.397	0.629	0.652	0.704
Trapezius	r-value	0.004	-0.023	-0.264	-0.169	-0.150
	p-value	0.991	0.944	0.384	0.582	0.608
Brachioradialis	r-value	0.451	0.644 *	0.005	-0.067	0.001
	p-value	0.141	0.024	0.988	0.828	0.998

* = Correlation with statistical significance at $p<0.05$

† = Moderate correlation with non-significant p-value

V. DISCUSSION

The purpose of this study was to describe the fatigue-related kinematic and electromyographic changes during high intensity treadmill running, as well as the relationship between these two types of variables. This project used a within-subject repeated measures design, in which time was the independent variable. The kinematic dependent variables were the maximum and minimum joint angle and angular velocities for nine different joints. The electromyographic dependent variables were change in iEMG and MdPF in thirteen muscles. Additional dependent variables which represented whole body kinematics included stride rate, stride length, and the maximum and minimum vertical displacements and displacement velocities. It was hypothesized that muscles and joints of the upper body would exhibit fatigue-related changes and that muscles and joints of the legs would exhibit compensatory changes. The results of this data may be used by researchers, coaches, and athletes to further understand fatigue-related changes during running and develop scientifically-based fatigue-resistance programs which improve running performance and decrease the risk for injury.

A. DEMOGRAPHIC DATA

All subjects were recruited from intercollegiate teams and running clubs. There was considerable variation in the size of individuals, and this reflects the diversity within the

competitive running population of this age group. Because all subjects were injury-free and performing their normal training routines, it is reasonable to believe that these data reflect that of a greater population of healthy, competitive runners.

B. BODY COMPOSITION DATA

Body composition data were used solely for descriptive purposes and therefore will not be discussed in detail. Body composition data are similar to those previously reported in long distance runners[119, 191]. This consistency in body composition supports the idea that this group of runners is typical to that of other groups of distance runners studied. This is an important consideration, because excessive body fat may influence metabolic factors during running[59].

C. MAXIMAL OXYGEN UPTAKE DATA

Maximal oxygen uptake data from this study are consistent with previous reports describing the physiologic profile of highly trained runners[27, 29, 43, 168, 234]. These data indicate this group of runners was highly trained, and therefore capable of running at a high intensity for an extended period of time. Further discussion of VO_{2max} in relation to running performance and the variables studied is beyond the scope of this project.

D. EXHAUSTIVE RUN DATA

1. Duration of Run

The mean duration time of the exhaustive run was 16.1 minutes. The mean 5K personal best of the subjects was 932 seconds, approximately 15.5 minutes. Assuming subjects ran at maximal voluntary effort during a 5K race and that subjects ran until volitional exhaustion on the treadmill, these data suggest this group of subjects performed the exhaustive run at an effort similar to that of a 5K race. This intensity is approximately 90 to 95% of VO_{2max}[28].

2. Heart Rate

Data collection began when subjects reached a heart rate consistent with one corresponding to 90% to 95% of their VO_{2max}. Heart rate increased progressively throughout the exhaustive run, which is consistent with previously reported exhaustive running protocols[4]. Maximal heart rate values during the exhaustive run (186.1 ± 11.1 beats·min^{-1}) were similar to those achieved during the VO_{2max} test (188.2 ± 10.8 beats·min^{-1}), indicating the intensity was similar between the two protocols. In addition to motor unit activation associate with the VO_2 slow component[29, 99, 201], increased heat production and thermoregulatory control during the run may account for some of the HR increase[4]. Increases in skin blood flow are used to help cool the body, and this mandates a greater cardiac output, thus heart rate[4].

3. Blood Lactate

Resting blood lactate values were similar to those values taken before the VO_{2max} test. Blood lactate values recorded immediately after the exhaustive run (14.7 ± 4.9 mmol/L) were also similar to the maximal values attained during the VO_{2max} test (13.8 ± 4.9 mmol/L). The large increase in blood lactate concentration following the exhaustive run confirms subjects ran at a very high intensity, and these values are similar to those reported in the literature[100, 162, 175]. These increases are likely reflective of fast-twitch motor unit recruitment, as the type II muscle fibers produce considerable lactate[240].

4. Electromyography

Methodology

Pilot data revealed electrocardiographic and motion artifact in the EMG data. This noise is primarily in the 30Hz and below range, and therefore a bandpass filter with a lower cutoff frequency of 30Hz and upper cutoff frequency of 500Hz was used prior to any EMG analysis[206]. Previous studies examining EMG during running have utilized cutoff frequencies in 30Hz[4] and above[214] to remove movement artifact. Spectral power frequency changes during running are often expressed as a percentage of a certain time point during the run [29] and this normalization was used in this study. The recommendation to use distance normalization for EMG analysis[111] is relatively recent (2005), and therefore few studies have used stride length to normalize iEMG data. Integrated EMG reflects the overall muscle activity over an arbitrary time frame, usually dictated by the duration of one stride cycle[241]. It is not entirely appropriate to use one stride cycle for normalization, as stride rate and stride length change over the course of exhaustive treadmill running[111]. Consequently, changes in stride length, regardless of mechanism, may

result in changes in iEMG as measured during one stride cycle and mask the effects of fatigue[111]. By computing the iEMG to travel a specific distance, one can obtain a better measurement of the level of muscle activation required to perform a unit of work[111]. In this study, the distance used for normalization was one meter. Polynomial modeling has been used previously in exploring fatigue-related changes in EMG parameter[29, 202] and this technique was in this study, as well.

General Interpretation of Results

Prior to evaluating EMG results, it is important to briefly review the factors which affect EMG parameters during running. As stated in the Review of Literature, median power frequency may increase as a result of increased MFCV. This may increase through increased fast twitch motor unit activation[29], increases in muscle temperature[199], increases in torque (activating more of the superficial fast twitch motor units and dampening the low-pass filtering effect of tissue)[31], or shortening of the M-wave. Median power frequency may decrease as a result of greater slow twitch motor unit activation, metabolic by-product accumulation[31] (or other changes within the cell which affect excitation-contraction coupling[178, 201]), or lengthening of the M-wave (which may be independent of MFCV). Although motor unit synchronization and muscle wisdom have been suggested to decrease SPF[201], these do not appear to occur commonly[70, 150] or be applicable to dynamic contractions, such as those during running[255]. Integrated EMG increases with increases in muscle temperature and progressive motor unit activation[88, 252] and would therefore decrease with decreases in muscle temperature or motor unit activation.

Legs

Vastus Lateralis

The vastus lateralis did not have a significant quadratic or linear coefficient in the MdPF model. However, the p-value (0.095) for the linear coefficient indicated a trend towards a negative coefficient, and therefore a trend towards a net linear decrease in MdPF. The model-predicted end MdPF was 92.0% of the start of run. In other words, MdPF values decreased 8.0% from starting values. The iEMG model of this muscle showed a very strong, though non-significant (p=0.055) trend towards a positive linear coefficient. The model-predicted change in iEMG was 143.2% of starting value, or a rise of 43.2%.

It was hypothesized that MdPF of the vastus lateralis would significantly increase in the subjects in this study, due to their high level of training. Though muscle fiber type was not measured, it would be expected that the vastus lateralis of these subjects would contain a high percentage of type I muscle fibers and aerobic enzymes which would minimize metabolic stress at the cellular level, thus minimize decreases in MdPF[55]. However, certain individuals did have an increase in MdPF of the vastus lateralis, despite the overall trend was towards a decrease. The previous research which suggested that trained muscles show increases in MdPF with fatigue was performed on an isokinetic dynamometer[94]. The highly dynamic activity of running, which includes eccentric and concentric muscle contractions, may account for the difference in results. The increase in iEMG is consistent with the hypotheses, and is likely attributable to progressive motor unit recruitment.

Semimembranosus

The positive value to the quadratic coefficient of MdPF in the semimembranosus indicates MdPF decreased initially, and this was followed by an increase at the inflection point of 0.72, as shown in Figure 25 (page 97). Though it was not statistically significant (p=0.057), the linear coefficient was negative, indicating a trend towards net decrease in MdPF. The increase in MdPF following the inflection point suggests fast twitch motor unit activation may have substantially increased around this time. Together, these data suggest that accumulation of metabolic by-products in the semimembranosus exceeded factors which increase MdPF, such as fast twitch motor unit recruitment, for the first 72% of the run. For the last 28% of the run, fast twitch motor unit recruitment (which increases MdPF) had a greater effect on MdPF than local metabolic changes. The net model-predicted was 88% of initial MdPF.

Increased motor unit recruitment is supported by the statistically significant positive linear coefficient of iEMG throughout the duration of the run combined with the net result of the model-predicted iEMG change was 156.2% of starting values. Indeed, high frequency fast twitch motor units may be recruited the entire time, while metabolic byproducts are accumulating simultaneously. The alterations in MdPF simply reflect the balance between these factors. It is unlikely the increase in iEMG could be attributed to additional slow twitch motor unit recruitment, due to the order of recruitment described in Henneman's principle[72, 117, 231, 252]. To attain the running speeds used in this study, it is likely that all slow twitch fibers were already recruited, and further recruitment would come from fast twitch oxidative motor units, followed by fast twitch glycolytic motor units[157, 231]. Increased temperature may also potentially account for this late upward shift in MdPF. However, this is not likely the case, since this quadratic pattern was only seen in the semimembranosus.

While differences between protocols prohibit direct comparison between the incremental speed running data of Taylor[240] and the constant speed running of this study, the results are consistent with one another. Both studies are based on the notion that intramuscular changes occur at high intensities. Taylor found iEMG of the vastest lateralis to increase while MnPF decreased[240].

Rectus Femoris

The rectus femoris was the only hip flexor studied in this investigation. Though it is one of the key hip flexor muscles[183], it may not be representative of all hip flexor muscles, since it serves as a knee extensor as well and demonstrates a biphasic EMG pattern[8, 111, 170, 183]. The linear coefficient of median power frequency of the rectus femoris was significant, negative in magnitude. The model-predicted change in MdPF was 90.5% of original value, this suggests metabolic by-product accumulation outweighed factors which increase MdPF. Furthermore, the linear and quadratic coefficients for the iEMG model did not show significance, and the model-predicted end value was 120.9% of original. This suggests further motor unit recruitment in this muscle was limited compared to the other leg muscles, all of which had net changes greater than 140%. The rectus femoris has previously been demonstrated to be among the first muscles to show electromyographic signs of fatigue during running[111]. The biphasic activation of this muscle may accelerate fatigue, as this is energetically costly at the cellular level[75]. Fatigue and limited recruitment may also be due to its relatively large percentage of type II muscle fibers[82]. If a considerable number fast twitch motor units are active from the start of exercise (by the very nature of this muscle's fiber type composition), there are less muscle fibers to progressively recruit throughout duration of the run.

Gluteus Maximus

The gluteus maximus did not have significant linear or quadratic coefficients for the MdPF model, and the net model-predicted MdPF was 97% of starting values. This muscle did have a statistically significant positive linear coefficient for iEMG and a model-predicted end value of 168.3% of starting value. Together, these changes in the gluteus maximus suggest increased motor unit recruitment in these muscles in the absence of substantial metabolic by-product accumulation. Though there is no published research to describe how the gluteus maximus responds to fatiguing conditions, there is considerable data to show it is very active during running[163, 183, 194]. The gluteus maximus had the smallest net decrease in MdPF and the greatest net increase in iEMG of the leg muscles studied (Table 13, page 102). This suggests this muscle is relatively fatigue resistant and is likely an important contributor in running performance under fatiguing conditions.

Torso

Latissimus Dorsi

The latissimus dorsi had a statistically significant negative linear coefficient for MdPF and statistically significant positive linear coefficient in iEMG. The model-predicted change in MdPF was the greatest of all the muscles studied in this project, showing a 17% decrease from initial values. The iEMG increase to 155.8% of initial values was of similar magnitude to those reported for the leg muscles. Together, the significant coefficients and the large changes in EMG parameters indicate this muscle is highly active during running and may experience fatigue at a similar, or greater, level as the legs. This suggests increased muscle recruitment, and increased metabolic by-product accumulation consistently occurring within the population

studied. It should be noted that the latissimus dorsi was considered a torso muscle in this study, due to its anatomical location. Functionally, this muscle could actually be considered in the arm group, since its primary function is shoulder extension.

Erector Spinae

The linear coefficient of the erector spinae MdPF was not statistically significant, but displayed a trend towards significance ($p=0.074$), indicating a decrease in MdPF. The model predicted values for MdPF was 87.1% and this value is among the greatest decreases for the muscles studied. The lack of significance of the linear coefficient combined with a dramatic decrease in model-predicted value suggests there was considerable variation in the degree to which MdPF changed during the run, with the overall trend was a substantial decrease. This agrees with Nagamachi's[190] findings. However, Nagamachi's subjects showed a considerably greater decrease in MnPF. The difference may be due to differences in exhaustive running protocols (with Nagamachi's methodology including changes in speed and incline, rather than a constant speed), the training levels of subjects, and the treadmill used during the test.

The linear coefficient for iEMG was statistically significant and positive in magnitude. The model predicted value was 168.9%, which was greater than any of the leg muscles and only exceeded by the values of the abdominal muscles. This degree of recruitment emphasizes the high level of activity of these muscles during high intensity running[244].This combination of increased iEMG and a trend for decreased MdPF suggests increased motor unit recruitment in these muscles with concurrent metabolic changes, similar to that of the latissimus dorsi.

Rectus Abdominus and External Oblique

The combination of unchanged linear coefficients in MdPF and statistically significant positive linear coefficients in iEMG for the rectus abdominus and external oblique suggests

increased motor unit recruitment in these muscles in the absence of metabolic byproduct accumulation. The rectus abdominus had a model-predicted MdPF of 98.1% of starting value, and that of the external oblique was 94.8%. The lack of change in MdPF model coefficients and minimal model-predicted changes suggest that neuromuscular fatigue does not occur in these muscles uniformly. Compared to other muscles, the change in MdPF was little, and this is logical as these muscles should be very fatigue resistant due to their very nature[96]. Furthermore, alterations in MdPF of the abdominal muscles may be difficult to observe during running. While the primary mover muscles display a predictable activation pattern with each stride, the respiratory activity of the abdominal muscles combined with their biomechanical functions may result in differing activation patters from stride to stride[2]. Additionally, the abdominal muscles are used to stabilize the vertebral column[57, 98, 127], and this fine movement was not studied in this project.

The model-predicted change in iEMG was the highest among any muscles studied, 276.9% for the rectus abdominus and the 179.2% for the external oblique. The positive linear coefficients and large net change in iEMG of the abdominal muscles is likely related to progressively increased respiration, as the rectus abdominus and external oblique contribute significantly to respiration during high intensity exercise[2, 230]. While respiratory variables were not measured during the exhaustive run, the nature of the exercise demanded a gradual increase in ventilatory equivalent throughout the run[214]. This is consistent with increases in heart rate and blood lactate concentration over the time span of the run. It is noteworthy that the two abdominal muscles studied are not the only muscles involved in respiration during intense exercise. Deeper abdominal muscles, such as the internal oblique and transversus abdominus are highly active during running[214].

Arms

Trapezius

The trapezius did not show significant quadratic or linear coefficients for MdPF or iEMG models. The model predicted value for MdPF was 98.8%, suggesting this muscle experienced very little metabolic change over the course of the run. Interestingly, the trapezius was only one of two muscles studied (the other being the middle deltoid) to show a decrease in iEMG, showing a net change of 97.8% of initial values. These data do not suggest the upper trapezius is not important during running, as the muscle shows distinct bursts of activity throughout the running cycle. The regular EMG bursts observed may likely be associated with scapular retraction (when the humerus is being pulled into extension), or upward rotation (when the humerus is elevating). However, measurement of these kinematics were beyond the scope of this project. However, these data do suggest the recruitment patterns in the trapzieus do not change considerably during exhaustive running.

It was expected that this muscle would display changes in EMG parameters due to its function as an accessory respiratory muscle[50]. During intense exercise, the trapezius functions to lift the shoulder girdle, thereby increasing thoracic volume to aid in inspiration. While the rectus abdominus and external oblique exhibited significant increases in iEMG, which are very likely related to respiration[230], the trapezius failed to demonstrate this. While this study did not assess the degree to which the trapezius contributes to respiration, it does indicate this muscle does not progressively get recruited for this, or progressively recruited for any purpose. It should be noted that this project examined the EMG of the upper trapezius, which would likely be the most important for lifting the shoulder girdle. Electromyographic analysis of the middle or lower trapezius may or may not yield different results.

Anterior, Middle, and Posterior Deltoids

The three deltoid muscles did not show statistically significant quadratic or linear coefficients for MdPF or iEMG models. The anterior and middle deltoid did not have substantial changes in model-predicted MdPF (95.3% and 99.7%, respectively). Conversely, the posterior deltoid did show a noteworthy decrease (86.9%). The only muscle showing a greater drop was the latissimus dorsi muscle. It is interesting that both of these muscles are used (in different ways) to move the humerus posteriorly. However, the latissimus dorsi showed more consistent changes within this population of runners, evidenced by its statistically significant linear coefficient for changes in MdPF and iEMG.

The anterior and posterior deltoid showed similar increases in model-predicted iEMG (115.5% and 123.2%, respectively). The middle deltoid showed a considerable drop in model-predicted iEMG (89.5%). The nearly unchanged MdPF data suggests that this muscle did not experience significant metabolic changes during the exhaustive run, and therefore it seems unlikely that local muscular fatigue is associated with the substantial decrease in iEMG in the middle deltoid. Again, it must be emphasized that caution be used in interpreting results for these muscles, as the quadratic and linear coefficients were not signficiant.

Brachioradialis

The brachioradialis was the only arm muscle showing a statistically significant change in an EMG parameter coefficient, specifically an increase in the linear coefficient for iEMG. The lack of significant linear coefficient for MdPF combined with the relatively small model-predicted change in MdPF suggests metabolic changes in this muscle were minimal. The model-predicted change in iEMG was the greatest of the arm muscles, at 134.0% of starting values.

This is actually greater than one of the leg muscles (rectus femoris, 120.9%). This indicates the brachioradialis did have a notable increase in motor unit recruitment during the exhaustive run.

EMG Summary

Fatigue-related changes during high-intensity distance running are likely related to peripheral fatigue, associated with metabolic byproduct accumulation and changes within the sacrolemma altering excitation-contraction coupling[225]. The concurrent decrease in MdPF and increase in iEMG is similar to that seen in Bouissou's results[31]. However, the latter research was conducted using a cycling protocol which lasted an average of 82.6 seconds. During a submaximal endurance test following a marathon, the iEMG was higher and the MnPF for the vastus lateralis was lower compared to baseline values[192]. In other words, greater muscle recruitment was needed to achieve the same level of torque (increased iEMG), and the balance of factors favored decreases in MnPF, consistent with alterations in excitation-contraction coupling. Such changes are consistent with those found in this study, although it may not be totally appropriate to compare 5K intensity running to marathon running,

Maximum MnPF has previously been found to occur before the ventilatory threshold during incremental speed treadmill running[240]. At intensities above lactate threshold, MnPF of the vastus lateralis was found to decrease[240]. This study was conducted at an intensity above the ventilatory and lactate thresholds, and this may explain why MdPF never increased and therefore account for the progressive decrease in MdPF. However, Borrani did not find this to be the case[29]. Borrani's protocol[29] is the most similar to that of this study, as the exhaustive run was performed at 95% of VO2max and regionally competitive runners were used. Borrani found a similar pattern of initial decrease in MnPF during the primary component of VO2 kinetics, followed by an increase during the slow component[29]. A direct comparison between the EMG

results of this investigation and Borrani's cannot be performed, as the latter were normalized to the SC, rather than the start of the run, and only graphical results were provided (no quantitative values).

The lack of change in the linear coefficients for change in MdPF for most of the muscles is somewhat surprising, considering the universal trend for most of the model-predicted values to decrease. This is attributable to wide variation in MdPF kinetics between individuals, as indicated by large standard errors. In some cases, it was evident that some subjects experienced a significant decrease in MdPF in a specific muscle, whereas other subjects experienced a significant increase in MdPF in that muscle. Furthermore, there was variation within the degree to which the magnitude of MdPF changed, regardless of direction. This inter-subject variation in MdPF kinetics, with specific subjects showing data opposite the trend, has been described previously in running studies[4]. Indeed, inter-subject variation in running mechanics are likely related to difference in muscle activation patterns during running[41]. It has also been suggested that some of the fatigue-related changes in SPF may be masked by other factors. During dynamic exercise, water content of the active muscles increases[224], which may increase muscle fiber thickness. This could increase MFCV and therefore increase MdPF[31]. All of these factors may account for this variability.

It is important to note that these data reflect the population studied as a whole. One reason for lack of significant findings is considerable variability between subjects. For example, in examining the data of the individual data from the anterior deltoid, 5 of 15 subjects displayed a significant ($p<0.05$) estimate. Of these 5 subjects, two of them had increases in iEMG, and three has decreases in iEMG. While it is clear that certain individuals show signs of neuromuscular fatigue in specific muscles, the wide variation between subjects does not allow

for applications to be made to an entire population of distance runners. Previous research indicates the inter-session reliability of MdPF during running is good, and it is unlikely that day-to-day variability accounts for the wide variety of results[190]. It should also be noted that the one muscle measured from a functional group (ie, the semimembranosus of the three-muscle hamstring group) does not necessarily reflect the activity of all muscles within the group. Changes in muscle recruitment by other muscles in the group may compensate for fatigue-related effects in any given muscle[255].

5. Kinematic Changes

Kinematic data were analyzed using multivariate RM ANOVA. This procedure examined groups of variables, classified by their anatomic locations. Theoretically, running is a whole body activity in which each movement at each joint has the ability to affect kinematics elsewhere, and therefore all kinematic variables are somehow related. However, a multivariate analysis using all variables at once would not be appropriate for this analysis, as it would likely require data from hundreds of subjects. When multivariate RM ANOVA revealed statistical significance, further stastical analyses were performed to determine the nature of changes within a single variable.

Correlation analyses were performed to determine the relationship between changes in EMG parameters with changes in kinematic parameters. It must be emphasized that correlation analysis does not infer a cause-and-effect relationship, but rather a general association between the variables. Pearson product moment correlations greater than 0.50 were considered to indicate moderate relationships, and values greater than 0.80 were indicative of strong relationships. As thresholds for correlation interpretations are subjective[52], the author used

points which have been previously utilized in exercise-related research[51, 187]. All relationships which met these criteria and were statistically significant are discussed below. It should be noted that a large number of correlations were performed and statistical significance was interpreted as correlations with $p \leq 0.05$. By definition, this means that five percent of significant correlations may be due to chance alone, and this must be considered when interpreting these correlations. As described below, most correlations which reached statistical significance demonstrated a seemingly logical relationship between kinematic data and EMG data, which suggests chance played a minimal role in these results.

It should be noted that there were some instances of non-significant relationships with $r \geq 0.50$ suggest a trend was present, but limited by inter-subject variability. When n=15, any $r>0.514$ should be statistically significant using a two-tailed test with statistical significance set at $p \leq 0.05$[104]. However, data were occasionally lost, due to EMG electrodes or retroreflective markers falling off subjects, and therefore some correlations do not represent n=15. It is possible that some of these relationships would be found to be statistically significant with greater subject numbers, but with greater numbers some of these may have also fallen below 0.50. Lastly, it should be noted that by definition the correlations examine the relationship between two variables within each subject. This differs from quadratic modeling techniques which only consider data from the individual muscle. Therefore, relationships between two variables may exist, whether or not significant time-dependent changes were observed in the individual variables themselves. For example, there may have been considerable inter-subject variability in an individual EMG variable, with some subjects showing an increase and some a decrease, causing an overall group result of no significant changes. The same may hold true for an associated kinematic variable with the end result being no statistically significant changes in the

group. However, it is possible, that all subjects who experienced an increase in the EMG variable also experienced a similar increase in the kinematic variable, and likewise for those with decreases. In such a situation, correlation analysis would identify a relationship, even though the individual variables themselves did not show statistical significance.

Correlations may yield a positive or negative correlation coefficient, and the sign of the r-value determines the nature of the relationship. For this study, relationships between EMG and kinematics were interpreted on the context of a change in EMG consistent with the model-predicted data. For example, polynomial modeling predicted an increase in iEMG and decrease in MdPF of the latissimus dorsi. Thus, for iEMG, r-values were interpreted such that "an *increase* in iEMG was associated with…" Conversely, for MdPF, r-values were interpreted such that "a *decrease* in MdPF was associated with…" Standardizing the nomenclature in this manner allows a more consistent interpretation of correlation analyses.

Legs

Knee Flexion

Univariate RM ANOVA revealed a statistically significant ΔKF_{max} during the exhaustive run, though the paired comparisons tests did not show significance when the three time points were compared. There was a non-significant trend ($p=0.097$) for KF_{max} to increase between t_{start} (109.43 ± 11.85^{o}) and t_{end} (111.83 ± 11.97^{o}) of run. The time-dependent trend in KF_{max} is consistent with previously published findings[193, 264]. Maximal knee flexion angle occurs during the forward swing component of the running cycle (Figure 29). Increased KF during forward swing may reduce the distance from the hip joint to center of mass of the leg segment as whole, thereby reducing moment of inertia and requiring less work for the hip flexors to swing the thigh anteriorly[223]. Thus, this may be thought of as a method to increase mechanical efficiency.

However, greater KF during forward swing may also require greater metabolic energy, as the knee extensors must concentrically contract to extend the knee joint in preparation for landing. If the knee joint is not optimally extended upon impact, this may decrease leg stiffness, thus decreasing mechanical efficiency[116]. The methodology of this study allowed the investigators to determine if these KF parameters changed, and also if the activity of the associated muscles changed. However, it was beyond the scope of the project to determine if the potential advantages of increasing KF_{max} (increased mechanical efficiency) outweighed the potential disadvantages (decreasing metabolic efficiency).

The vastus lateralis, rectus femoris, and semimembranosus muscles all cross the knee joint and therefore can directly control knee flexion and extension[230]. Fatigue of the knee extensors muscles may reduce the eccentric contraction which decelerate the shank, thereby allowing increases in KF[183]. Alternatively, increases in KF_{max} may result from greater activation of the hamstring muscle group during follow through. However, correlation analysis did not reveal any noteworthy relationships between EMG data and ΔKF_{max}. It is possible that muscles not studied in this project, such as the biceps femoris, may be responsible for this change. Indeed, the biceps femoris has previously been shown to fatigue during high-intensity running[111].

There were no trends in KF_{min}, nor statistically significant correlations of this variable to any EMG variables. It was expected that such a relationship be found, considering the vastus lateralis demonstrated trends towards linear changes in iEMG and MdPF. The only time the vastus lateralis exhibits a burst in EMG during running is during is before and during stance, at which time it supports the body's weight[183]. Fatigue in this vastus lateralis could theoretically decrease the force it generates to support the body's weight during stance, resulting in greater

KF. Increases in KF during stance may result in increased KF angle at follow-through, at which time this angle is at its minimum (Figure 29).

In this study, vKF_{max} showed a trend to decrease with running duration, though this was not formally explored due to the lack of multivariate statistical significance. This is opposite that of the findings of Gazeau, who used a similar demographic of subjects[101]. However, it should be noted that the run duration in Gazeau's study was 301 ± 82.7s, which is considerably shorter than that of this study. No EMG parameters were found to be related to vKF_{max} at a level of statistical significance. Likewise, minimum vKF was not formally explored due to lack of significance in the multivariate test. There was a trend for the magnitude of to vKF_{min} decrease in a time-dependent manner, though there was considerable variability in this variable. This trend seems logical, as fatigue in the knee extensors would likely decrease knee extension velocity.

The relative lack of relationships between kinematic and EMG variables emphasizes the complex control over the knee joint. A number of biarticular muscles cross this joint and these may interact in a complex manner to regulate knee joint angles. Additionally changes in landing velocity, which are dependent on vertical displacement, may also contribute to KF variables during the stance phase.

Hip Flexion

Values for HF_{max} and HF_{min} are similar to those reported for Schache[216] during treadmill running at a slightly slower speed. Maximum HF showed statistically significant changes between the t_{start} and t_{mid}, and t_{start} and t_{end}. This trend is consistent with published findings[193, 264]. If all other factors are held equal, increase in HF_{max} should increase stride length, as the runner theoretically has more time to travel forwards in the air before impact. During treadmill running, this should concurrently decrease stride rate, as more absolute time is spent in the air, provided

all other factors remain unchanged. As discussed previously, stride duration increased (therefore, stride rate decreased) during the exhaustive run. To maintain speed, subjects must have concurrently increased stride length. It is not known whether a primary decrease in stride rate required subjects to adopt a compensatory increase in stride length, or if a primary increase in stride length forced subjects to reduce stride rate to continue running on the treadmill.

The semimembranosus, gluteus maximus, and rectus femoris all cross the hip joint and therefore may influence hip flexion parameters[163, 230]. Based on the EMG data, it is very surprising that maximum hip flexion angle increased during the run, considering the drastic model-predicted decrease in MdPF of the rectus femoris. Although this muscle is respsonible for hip flexion, there were no correlations between ΔHF_{max} and EMG parameters of the rectus femoris. Other hip flexors not studied in this investigation, such as the iliopsoas and tensor fascia lata, may be responsible for the increase in hip flexion angle[8, 170, 183]. Despite the previously described changes in semimembranosus EMG parameters, they were not correlated to ΔHF_{max}.

Maximum vHF_{max} showed a trend to increase during the run, though there was considerable variability in this variable. It is possible that that other muscles mentioned previously in regard to HF_{max} may be responsible for the increase in vHF_{max}[8, 170, 183]. Additionally, decreased eccentric braking by the hip extensors may have also contributed to increased vHF_{max}.

Though a formal statistical examination of minimum joint angles in the legs was not appropriate (based on the findings of the multivariate test, where $p=0.097$), there appeared to be a trend for the magnitude of HF_{min} angle to increase. In other words, maximum hip extension angle may increase in a time-dependent manner, though this was not statistically significant. The

magnitude of vHF_{min} (hip extension velocity) also showed a tendency to increase during the run, though this was not formally examined due to lack of significance in multivariate tests. Greater hip extension velocity is associated with decreased energetic cost of running[263]. Additionally, iincreases in hip extension velocity are related to increases in time to exhaustion during high intensity treadmill running[101]. With this considered, it is possible that those runners who experienced an increase in vHF_{min} actually adapted their stride mechanics to fatigue to increase their efficiency.

Potentially, increased hip extension could be a result of greater propulsion during stance, achieved through greater power output of the hip extensor muscles groups. This is supported by the statistically significant correlations between ΔiEMG of the semimembranosus with ΔHF_{min} (hip extension) and ΔvHF_{min} (hip extension velocity), which showed a strong relationship between these variables. Thus, as iEMG of this muscles increased, maximum hip extension angle increased, as well as maximum hip extension velocity. This is logical, as the semimembranosus contracts during the stance phase to move the body over the foot[157, 183].

Pelvis Axial Rotation

Pelvis rotation is a key element of running and helps to increase stride length by allowing the entire leg to reach further in front of the body[124]. The univariate RM ANOVA for ΔPAR_{max} resulted in p=0.066. While this did not meet the *a priori* significance level, this suggested a trend towards significance that may have been achieved with greater subject numbers. Though further analysis was not conducted, it appears the trend was for PAR_{max} to increase, meaning the pelvis rotated more (in a counter-clockwise direction). Conversely, the univariate RM ANOVA for ΔPAR_{min} did not show any trend for significance. There were no trends for vPARmax or $vPAR_{min}$ to change.

The lack of trend of PAR_{min} is surprising from a methodological standpoint, as the magnitude of PAR_{max} and PAR_{min} should be similar, as maximum angle represents counter-clockwise rotation about the z-axis of the pelvis, and minimum angle represents clockwise rotation about this axis (Figure 30). However, the magnitudes for these variables were quite different, with the mean of PAR_{max} 11.75^{o} and PAR_{min} -5.33^{o} at t_{start}. This yields a total of approximately 17 ^{o} total range of motion in PAR.

The discrepancy between PAR_{max} and PAR_{min} data may be explained by two potential sources of error. First, a static calibration was taken prior to the exhaustive run, with subjects facing forwards on the treadmill, so that the long side of the treadmill belt and the anterior side of the subject's body parallel were to the positive X-axis of the GCS. This was the reference angle used, and this static angle was subtracted from all PAR data. While the purpose of the static calibration is to set the initial angle to zero, it is possible that subjects may have stood slightly off-parallel to the X-axis of the system. This may have resulted in all PAR data being shifted by a small margin, resulting in the described mathematical asymmetry. If the discrepancy between PAR_{max} and PAR_{min} is attributable to mathematic errors and PAR is assumed to be bilaterally equal, this means PAR was approximately 8.5 ^{o} on each side. This is similar in magnitude to the PAR values reported by Schache[216] (Left: 7.2 ± 2.7 ^{o}, Right: 7.8 ± 2.3 ^{o}) whose subjects performed treadmill running at a slower speed (3.98 ± 0.47 $m \cdot s^{-1}$).

The second source of error may have been rooted in the equipment interfering with movement at the pelvis. All electrodes were placed on the right side of the body, and leads were plugged into the telemetric unit placed on the right side of the treadmill near the level of the pelvis. While subjects were instructed to run as naturally as possible in spite of the equipment, the wires in this area may have affected movement patterns around the pelvis and given the

subjects a sense of movment restriction. Because the equipment was concentrated near the pelvis, it is likely that this source of error would occur here moreso than any other areas of the body. This is may be further supported by the apparent bilateral differences between $vPAR_{max}$ (101.84 $deg \cdot s^{-1}$ at t_{start}) and $vPAR_{min}$ (-120.93 $deg \cdot s^{-1}$ at t_{start}). If the error were purely related to camera placement, the magnitude of these velocities would be expected to be more similar.

The muscles of the erector spinae group and external obliques insert on the pelvis and therefore can contribute to pelvis axial rotation[230]. However, the way these and other axial rotation muscles influence torso rotation, hence pelvis rotation, are quite complicated, and dependent upon the degree of rotation, the effort of movement, and many other factors, which makes interpretation of the muscle activity during dynamic movements difficult[7]. Although pelvis movement is theoretically bilaterally symmetric during running, only EMG of the right erector spinae was studied, and this muscle group would be expect to have different functions with direction of axial rotation. Therefore, similar r-values between EMG parameters and PAR_{max} and PAR_{min} would not necessarily be expected in correlation analysis. Nonetheless, PAR data may have error within it (as described in the preceding paragraphs), and therefore correlations between iEMG variables and PAR parameters from this study must be treated with caution.

Minimum PAR (the most clockwise rotation, Figure 30) occurs approximately when the right leg starts its follow-through stage, which is the float stage of the stride cycle, during which the entire system is an open kinetic chain. To axially rotate the pelvis counterclockwise for the next stride, an external force must be applied to the pelvis. This may come from a combination of the momentum of the upper torso[124] and muscular contraction. It was presumed that with fatigue in the erector spinae group, the muscular contraction to axially rotate the pelvis may be

generated at a slower rate, which would allow the lower body's momentum to continue rotating the pelvis clockwise for longer, thereby increasing the magnitude of PAR_{min} (more clockwise rotation). However, none of these EMG parameters were correlated to PAR_{min} at a statistically significant level. This emphasizes the importance of momentum and possibly other axial muscles controlling pelvic rotation.

Torso

Upper Torso Axial Rotation

Upper torso axial rotation helps the pelvis to rotate and move the legs through the stride cycle[124]. Like PAR, UTAR is a variable in which the maximum and minimum values are synonymous with counterclockwise and clockwise rotations about a central axis, respectively (Figure 31). Therefore, it was expected that the magnitude of the values and their statistical properties would be similar for maximum and minimum. This was the case to some degree, with $UTAR_{max}$ 20.40^{o} and $UTAR_{min}$ -16.33^{o} at t_{start}. Compared to PAR, these bilateral measurements are closer on a relative and absolute scale. Similar to the pelvis, it is likely that variation in marker placement resulted in bilateral asymmetry in UTAR in this study. Because the differences between $UTAR_{max}$ and $UTAR_{min}$ were not as drastic as those of PAR, it is presumed that there was not as much error with this measurement. This lends further support to equipment interference causing the unexpected asymmetry in PAR.

Maximum UTAR increased significantly from the t_{start} to t_{mid}, and from t_{start} to t_{end}. The magnitude of $UTAR_{min}$ increased significantly from the t_{mid} to t_{end}. Interestingly, this was the only kinematic variable examined which displayed a statistically significant increase between the t_{mid} and t_{end}. Taken together, these findings show that UTAR range of motion increases throughout the exhaustive run. However, it is not possible to determine if the benefits of

increases in UTAR (increasing use of elastic energy to rotate the pelvis) outweigh the potential disadvantages (possibly more metabolic energy to control rotation). Correlation analysis did not reveal any notable relationships between EMG parameters and $UTAR_{max}$ or $UTAR_{min}$.

Maximum velocities of the torso did not show any statistically significant time-dependent changes in the multivariate tests and were not explored further. The lack of significance in multivariate testing for the maximal angular velocities, which precluded further analysis, may have resulted from excessive inter-individual variation in vUTAR, as well as the other variable in the group, vTF. However it should be noted that $vUTAR_{max}$ showed a trend to increase from 203.6 $deg \cdot s^{-1}$ at t_{start} to 216.4 $deg \cdot s^{-1}$ at t_{end}. These numbers are similar to those of $vUTAR_{min}$, which increased significantly increased in magnitude from t_{start} (-200.8 $deg \cdot s^{-1}$) to t_{end} (-219.5 $deg \cdot s^{-1}$). It was expected that the magnitude of these numbers would be similar, as the movement should theoretically be symmetrical.

The greatest UTAR clockwise velocity occurs after the point of maximal hip extension of the left side, in synch with or just preceding contact on the right side. The axial momentum occurring at this time point transfers momentum to rotate the pelvis clockwise for the next stride cycle. At the time of right side contact, the lower body can be considered part of a closed kinetic chain, while the upper body an open kinetic chain. Therefore, it would be expected that contraction of the erector spinae would rotate the upper torso in relation to the pelvis at this time point. However, no statistically significant correlations between UTAR and kinematic variables were observed. Muscles of the erector spinae muscle group and external obliques originate along the vertebral column and therefore can contribute to upper torso axial rotation[230]. Other spinal muscles not examined in this study, such as the multifidus, may also play a large part in UTAR[7, 155]. Tissue properties, including elastic recoil, also contribute to this movement[155].

Additionally, momentum of the upper body, which is dependent on the arms, also contributes to this movement[124].

Although the external oblique muscles are involved in UTAR, there were no correlations between EMG parameters of this muscle and rotational kinematics. In part, this may be due to the respiratory functions of this muscle, which makes it extremely difficult to determine how these muscles affect the torso and pelvis during running. The oblique muscles have been shown to simultaneously control respiration and movement, whereas the erector spinae are only involved with movement[214]. With increases in treadmill speed, the oblique muscles appear to contribute greater activity to movement than respiration[214]. However, this study involved constant-speed running. With this considered, it is possible that increase in iEMG found in this study may be attributable to both, movement control and respiration. Even if relationships between EMG parameters of abdominal muscles and kinematic were observed, it would not be possible to determine if these relationships were purely coincidental.

Torso Flexion

Flexion and extension of the torso during running help stabilize the body and create smooth movement[125]. Torso flexion did not show any time-dependent statistically significant changes over the course of the exhaustive run. However, like all other variables, it is important to note that this describes the findings from the population studied as a whole, with some subjects displaying remarkable ΔTF_{max} (Subject 14: 5.3^{o} at t_{start}, 8.0^{o} at t_{mid}, 14.2^{o} at t_{end}) and others not (Subject 6: -3.5^{o} at t_{start}, -3.4^{o} at t_{mid}, -3.8^{o} at t_{end}).

Muscles of the erector spinae group and the rectus abdominus attach to the pelvis and therefore can control torso flexion[57, 230]. Correlation analysis revealed a statistically significant moderate relationship between ΔiEMG and ΔTF_{max}. As iEMG increased, TF_{max} increased. This

is initially somewhat counterintuitive, as the erector spinae group serve as torso extensors. One possible explanation is that muscle of the erector spinae group eccentrically contract to limit TF_{max}. Therefore, increases in TF angle may necessitate greater erector spinae motor unit activation, hence increased iEMG of this muscle. While the abdominal muscles studied do attach to the pelvis, no noteworthy correlations between EMG parameters of these muscles and TF variables were observed. The lack of relationship between EMG parameters of the rectus abdominus and kinematics is likely attributable to the respiratory activity of this muscle[2, 230].

Arms

Elbow Flexion

Elbow flexion angle is nearly synchronized with HF, so that EF_{max} (elbow extension) occurs with ipsilateral HF_{max}, and EF_{min} (elbow flexion) occurs with ipsilateral HF_{min} (Figure 33). Maximum EF increased significantly over the exhaustive run (more extension), with significant differences between t_{start} and t_{mid}, and t_{start} and t_{end}. Increased elbow extension shifts the center of mass of the arm segment distally, which allows the arms to contribute greater momentum to the whole body and this potentially aids the legs[124, 125]. However, moving the more distally located arm center of mass of the arm segment may potentially require greater muscular activation to move the segment, and therefore greater metabolic energy.

While the magnitude of vEF_{max} showed a visual trend to increase during the run, statistical analysis did not reveal any trends Theoretically, increases in vEF_{max} could generate greater vertical ground reaction forces and therefore increase the arms' contributions to vertical lift[125] and also explain increases in EF_{max} due to increases in momentum of the distal arm segment. Increases in elbow extension angle could result from activation of the elbow flexors, greater activation of the elbow extensors, or a combination of the two. Only one muscle from

these groups was studied, and this was the brachioradialis, which serves as an elbow flexor[230]. Correlation analysis did not reveal any noteworthy relationships between changes in EMG parameters of this muscle and change in EF parameters. While the increase in iEMG of the brachioradialis muscle does suggest this muscle is very active during high intensity running, it apparently is not the only muscle responsible for changes in EF. Other muscles which may account for these kinematic changes include the biceps brachii, brachialis, and triceps brachii[230].

Shoulder Elevation

The univariate RM ANOVA showed a statistically significant trend for SE_{min} to change in a time-dependent manner, and paired comparisons showed a non-significant trend ($p=0.073$) for SE_{min} to decrease between the t_{mid} and t_{end} of the run. This may be explained in part by changes in momentum of the whole arm segment. The magnitude of vSE_{max} and vSE_{min} both increased significantly between the t_{start} and t_{mid}, and t_{start} and t_{end}. Though, momentum of the arm segment was not calculated in this study, increases SE velocities would increase the momentum of the arm segment. This is important, considering vertical momentum of the arms contributes to vertical lift of the entire body[125].

The latissimus dorsi, deltoid muscles, and trapezius all have an attachment to the humerus and therefore can control shoulder elevation[230]. Changes in anterior deltoid iEMG had a significant moderate relationship with ΔSE_{max}. The relationship with SE_{max} was likely due to concentric contraction of the anterior deltoid raising the distal humerus while it is traveling in an anterior direction. No further statistically significantly correlations were observed between SE and EMG parameters.

Shoulder Plane of Elevation

Though univariate RM ANOVA did not reveal a time-dependent changes for SPE_{max} and SPE_{min}, there was a non-significant trend for the magnitude of the former variable to increase ($p=0.090$). This may be due to increased muscular force pulling the humerus anteriorly, or decreased posterior muscular force to eccentrically brake the humerus while it travels anteriorly. The latissimus dorsi, deltoid muscles, and trapezius all have an attachment to the humerus and therefore can control shoulder plane of elevation[230]. Changes in iEMG of the latissimus dorsi had a statistically significant strong relationship to ΔSPE_{max}. This is logical, considering the latissimus dorsi pulls the humerus posteriorly. Change in latissimus dorsi MdPF had a statistically significant moderate relationship to ΔSPE_{max}, negative in sign. Thus as MdPF decreased, SPE_{max} increased. It is surprising that decreases in MdPF are associated with increases in posterior humeral movement. It would be expected that muscle force would decrease with fatigue, and therefore SPE_{max} would decrease. Considering iEMG increased and MdPF both decreased significantly, it appears that the increased muscular activation played a greater role in kinematic changes than the decrease in MdPF.

Maximum vSPE significantly decreased between the t_{start} and t_{mid} of the run, but changes were not significant ($p=0.075$) between the t_{start} and t_{end}. In other words, there was no clear trend for changes in $vSPE_{max}$. Changes in iEMG of the latissimus dorsi had a statistically significant moderate relationship with $\Delta vSPE_{max}$, positive in sign. Therefore, as iEMG of the latissimus dorsi increased, $vSPE_{max}$ increased. Again, increased activitation of the latissmus dorsi likely results in greater posterior pull on the humerus, thereby increasing $vSPE_{max}$. Change in iEMG of the anterior deltoid and a statistically significant moderate relationship with $\Delta vSPE_{min}$, negative in sign. Therefore, as iEMG of the anterior deltoid increased, the magnitude of $vSPE_{min}$

increased. This is logical, as increased muscle activation of this muscle would draw the humerus anteriorly in the transverse plane.

Vertical Displacement

Maximum VD did not change significantly during the run, however VD_{min} did show a significant decrease between t_{start} and t_{mid}, and t_{start} and t_{end}. Thus total VD (as defined by the VD_{max} - VD_{min}) increased during the run. The difference in group means between t_{start} and t_{end} of the run was about 0.002m. While this may seem minute, Williams[263] found differences in vertical oscillation of this magnitude between runners with low and medium submaximal oxygen consumption, with the more economical group having lower total vertical movement. An increase in total VD requires greater external work, since the mass of the body is moving through an increased range[257]. However, the shock absorbing characteristic of the treadmill may have limited the accuracy of this measurement and may explain the large discrepancy between these results and those obtained from overground running. Indeed, VD during treadmill running has been demonstrated to be lower than that of overground running[257]. Alterations in VD are likely related to whole leg stiffness or knee stiffness. Previous research has shown a change in leg and knee stiffness to be associated with decreases in stride rate during constant velocity exhaustive treadmill running[78], which is consistent with the results of this study.

Maximum vVD showed a non-significant ($p=0.084$) trend to increase during the run. The trend for greater vVD_{max} suggests subjects lifted themselves off the treadmill quicker. This is consistent with the non-significant trend for increased maximum hip flexion velocity, and the significant trend for vSE_{max}, as these variables likely contribute to vertical lift. Likewise, the magnitude of vVD_{min} showed a non-significant ($p=0.072$) trend to increase during the run. This occurs just prior to contact. Because VD_{max} was unchanged, and theoretically the body has equal

time to be accelerated by gravity, it is not completely clear why vVD_{min} shows this trend. It may be possible that the biphasic nature of VD may explain account for this. With each complete stride cycle, vVD shows two positive peaks and two negative peaks. This is a result of the occurrence of a right and left side impact with each stride. This analysis only examined maximum and minimum VD's, which only account for one of the positive and one of the negative peaks occurring with each stride cycle.

The relationship between change in EMG parameters and changes in variables reflecting whole body kinematics (vertical displacement and stride duration) revealed a few notable relationships. The only statistically significant correlation for ΔiEMG parameters was that of the trapezius in relation to ΔVD_{min}. Considering the iEMG of the trapezius changed very little during the run for the group as a whole, it is not clear how to interpret this finding. It is possible that subjects who experienced a substantial increase in their trapezius activation also increased shoulder vertical movement (through an optimal combination of changes to SE and SPE parameters). This is possible, considering the momentum of the arms do contribute significantly to vertical lift of the body[125].

Change in MdPF of the latissimus dorsi had statistically significant relationships with ΔvVD_{max} and ΔvVD_{min}. In other words, runners who maintained their latissmus dorsi MdPF had greater vVD_{max} and a smaller magnitude of vVD_{min}. Additionally, ΔMdPF of the brachioradialis shares a statistically significant moderate relationship with ΔVD_{min}. In other words, subjects whose MdPF remained higher (less fatigue) managed to maintain greater VD_{min} height during the run. This is likely attributable to these muscles contributing to arm kinematics which produce greater whole body vertical lift.

Taken together, these findings suggest a very complex pattern in regulating vertical displacement during intense running. Increasing minimum vertical displacement while maintaining maximum vertical displacement would minimize total range of vertical displacement, and this is one factor associated with optimal running economy[263]. Therefore, there may be an optimal combination of muscle activation patterns to maintain VD during exhaustive running.

Stride Duration

To the author's knowledge, this is the first study to evaluate changes in stride parameters during a run using multiple measurements to create a polynomial model. Stride cycle duration showed a significant positive linear coefficient. The quadratic coefficient was not significant (Table 33, page 115). Thus, stride duration generally increased in a linear fashion for the duration of the run in this group of subjects. Because the exhaustive run protocol was performed on a treadmill with a constant speed, all stride parameters (stride cycle duration, stride rate, stride length) are all mathematically interdependent and therefore do not need to be examined separately. Therefore, an increase in stride cycle duration (equivalent to a decrease in stride rate), mandated a concurrent increase in stride length for the subject to stay on the treadmill. This would not necessarily be the case during overground running, as runners could potentially increase their stride cycle duration (decrease stride rate) without any change in stride length, and therefore decrease their running speed.

The time-dependent increase in stride cycle duration and stride length found in this study is consistent with some previous studies[71, 101, 102]. However, these results also contradict other previously reported findings in stride parameters, whereby exhaustive running was reported to decrease stride cycle duration, increased stride rate, and/or decrease stride length[83, 84]. These

conflicts may be related to differences in the methodology. For example, this study specifically aimed to examine a running intensity equivalent to 5K race pace, and the stride parameter findings may not necessarily be extrapolated to other race distances. Furthermore, differences between subject populations may be responsible for the contradiction. In this study, the majority of subjects experienced an increase in stride cycle duration, however a few subjects experienced the opposite. Differences in training background and treadmill experience may account for these discrepancies.

While stride parameters are the end-product of the coorindated muscle movements of running, no noteworthy correlations between EMG variables and stride duration were observed. The lack of findings between EMG and stride parameters emphasize the highly integrated nature of running, such that no one single muscle is responsible for changes in whole body kinematics, but rather the contributions of all muscles in the entire system.

Summary of Kinematic Changes

A number of significant relationships were found in comparing time-dependent changes in electromyographic and kinematic variables. The relationships found within the legs were very logical when the motor patterns of the stride cycle are considered[183]. Many of the relationships found within the torso and arms were also logical. However, the relationship between electromyographic and kinematic variables in the torso and arms have not been fully described in the literature, as it has been for the legs. Therefore, some of the results of this study cannot be interpreted in relation to normative data.

Equally important to the relationships found are the relationships that were not found. Kinematic changes should have an underlying change in motor activation pattern. In some cases, these relationships were not found. For example, the brachioradialis is used in elbow flexion, but

no relationship was found between changes in EMG parameters in this muscle and changes in kinematics. This emphasizes the fact that some of the muscles studied could be responsible for some of the kinematic changes, but not all the kinematic changes which occurred during the exhaustive run could be accounted for by these muscles alone. Indeed, running kinematics are not solely related to muscle activity at a given joint, but rather the net result of muscle contraction, momentum transferred from other body segments, and tissue properties[244].

While a considerable number of time-dependent kinematic changes were observed, many of these occurred between the t_{start} and t_{mid}, with no significant changes between the t_{mid} and t_{end}. This suggests that time-dependent kinematic changes during treadmill running approximating 5K race intensity primarily occur during the first half of the run. Though these changes appear to progress throughout the entire run, they do not manifest themselves to the same degree in the second half, which may prevente statistical significance. This suggests that the majority of kinematic changes during the exhaustive run protocol were not necessarily related to fatigue near the end of the run, but rather changes in the beginning of the run.

It is unlikely kinematic changes merely result from adjustments to the treadmill itself, as subjects were acclimated to the treadmill and given a warm-up period. Additionally, treadmill speed was gradually increased to test speed, and all data recording were taken at the same speed. Other studies involving high-intensity fatiguing running have also found some variables to change from t_{start} to t_{mid}, but not t_{mid} to t_{end}[101]. Instead, these changes may be reflective of adaptations to maximize efficiency of high-intensity running. In other words, kinematics during the beginning of the run may not be ideal for metabolic or mechanical efficiency. As the run continues, the neuromuscular system adapts to optimize efficiency. This may supported by the increase in KF_{max} and $vHF_{max,}$ both of which are presumably associated with greater running

economy[101, 223]. However, changes in other variables, such as VDmax are associated with decreased running economy[257, 263]. Therefore, it is not clear if these findings represent optimization or fatigue.

Most muscles showing changes in iEMG parameters displayed a linear change, indicating a progressive mechanism of change in the muscles. Furthermore, stride rate showed a progressive linear change. It is well-established that running at a stride rate different than freely chosen results in poorer running economy. However, changes in stride rate here are freely chosen, but different to the starting stride rate. Oxygen consumption increases during constant intensity running, thereby decreasing running economy[29, 152, 201]. While this was not measured in this study, a progressive increase in heart rate was noted. Together, these factors suggest runners become progressively less economical during high-intensity running. However, the degree to which kinematics influence this cannot be determined from this study, as changes in kinematics did not consistently progress in a linear manner

Again, it should be emphasized that this study was designed to examine fatigue in running approximating 5K race intensity and therefore is not necessarily applicable to other race intensities. The importance of protocol-specificity can be seen when examining results of varied protocols, especially when the same subjects were used[4, 5, 11]. Ament found a decrease in MdPF in the gastrocnemius and soleus while runners ran to exhaustion at 5kph at 33% incline[5], whereas no changes were found in the same subjects when they performed the protocol at 20%[4]. Lastly, it must be emphasized again that considerable variation existed between individuals and the results reported here reflect that of the whole group.

6. Study Limitations

Muscle Selection

Electromyographic data were collected for selected muscles crossing the each joint during the exhaustive run, and this is one limitation. While the rectus femoris represents a hip flexor muscle, and the gluteus maximus and semimembranosus represent hip extensor muscles, there are many other muscles crossing these joints and the net action of these muscles is responsible for movement at the joint[183]. Further, some of these muscles are biarticular and therefore serve multiple functions during the running cycle[8, 183]. Therefore these findings cannot necessarily be extrapolated to other muscles with similar joint actions. It is not entirely appropriate to say a particular muscle group (ie, the "hip flexors" or "hip extensors") fatigues. For example, it is therefore possible that a single measured hip flexor muscle may fatigue, but hip flexion angle may not change as other muscles may compensate. Conversely, it is possible that the muscle studied may not show signs of neuromuscular fatigue, though all unmeasured muscles of that group do fatigue, unbeknownst to the investigator. However, equipment and methological limitations prohibit studying many more muscles than already studied. The muscles chosen for this study served to provide a broad overview of muscles crossing many of the major joints of the body. Additionally, all of these muscles had the ability to control movement at the joints of interest.

Equipment Considerations

It has been suggested that differences between overground and treadmill running may stem from systematic and individual sources of error[193]. The treadmill used in this study was capable of reaching high enough speeds to fatigue highly trained runners. However, all treadmill

studies have a limitation in the sense that there are slight differences between treadmill and overground running[193]. One of these differences stems from the fact that most treadmills, including the one used in this study are specifically built to absorb shock and thereby reduce the risk of injury. However, this characteristic may prevent researchers from obtaining accurate measurements in some key variables, such as knee flexion angle upon impact, and vertical displacement height.

However, similar electromyographic patterns of leg muscles have been observed to be very similar when overground and treadmill running were observed[219]. Differences between overground and treadmill running may also be dependent on previous treadmill running experience[85], which was not controlled for in this study. It has also been suggested that treadmill speeds greater than 5 $m \cdot s^{-1}$ increase[262] and decrease[193] the kinematic differences between overground and treadmill running. Therefore, it is not possible to predict what differences, if any, would be observed between treadmill running and overground running in this specific population of subjects. Based on this, the applicability to actual competitive performance from this study, or any study utilizing treadmill running, are open to the interpretation of the individual reader.

The combination of surface electrodes and adhesive tape secured to the skin, and bundles of EMG leads hanging from the subject may have made runners uncomfortable and altered running mechanics. This may have resulted in altered neuromuscular activation patterns. To reduce this, the electrode leads were grouped together and secured to the treadmill to limit movement. Subjects were given time to acclimate to the equipment during the warm-up period. Leads which interfered with running movements were rearranged until subjects felt comfortable while running.

Treadmill Speed and Volitional Exhaustion

Subjects were asked to run to volitional exhaustion. To account for individual variation in ability level, subjects did not run at the same absolute speed, but rather a specific physiologic intensity. Potentially differences in speed could have introduced an extra source of error into the data. However, running kinematics have been shown to be reliable across a wide range of running speeds[147, 203].

Different levels of personal motivation may have allowed individual subjects to reach varying degrees of their maximal physiological capacity. Differences in blood lactate measurements before and after the exhaustive run strongly suggest that subjects ran at a very high intensity level. Furthermore, these measurements were similar to values recorded from the VO_{2max} test. The VO_{2max} test also requires volitional exhaustion and a very strong effort was verified by observing a RER > 1.10 or heart rate exceeding 95% of age predicted maximum. These measurements taken together strongly suggests subjects ran to volitional exhaustion, and if not exhaustion, to a highly fatigued state.

Muscle Temperature

Muscle temperature is known to be associated with changes in EMG parameters. While muscle temperature was not measured in this study, it was assumed that temperature did not significantly increase over the course of the exhaustive run. To minimize temperature fluctuations, the subjects were provided a 10 minute warm-up period prior to the exhaustive run to help them achieve a steady themoregulatory state. Previous research has shown that following the initial increase in temperature at the onset of exercise, muscle temperature remains constant during constant power exercise and therefore cannot explain the continuous change in EMG

parameters[29]. Furthermore, wavelet analysis of four leg muscles during 30 minutes of overground running revealed that temperature did not significantly affect frequency patterns[255].

The data from this study also suggest that temperature alone was not responsible for changes in EMG parameters. For instance, increases in temperature are associated with increases in MdPF, and these data demonstrate decreases in MdPF. If temperature did significantly rise during the exhaustive run, it is possible that thermally-derived increased in MdPF could mask physiologic decreases in MdPF. Also, there does not appear to be any clear relationship between iEMG and MdPF changes. For instance, the model-predicted change in iEMG values of gluteus maximus and latissimus dorsi were very similar (168.3% and 168.9% of starting values, respectively). However the model-predicted change in MdPF for these muscles were very different (97.0% and 81.1%, respectively).

Soft Tissue Filtering

Because type II muscle fibers are closer to the muscle surface than type I fibers, fast twitch motor unit recruitment decreases the low-pass filtering effect of tissue on the EMG signal. Therefore, as fast twitch fibers are recruited, their contribution to the power spectrum is magnified. This may mask decreases in MdPF and therefore limit the interpretation of EMG findings. However, model-predicted decreases in MdPF were observed in all muscles in this study, and significant decreases have been observed in previous studies[182, 190]. If all of the muscles in this study showed a net increase in MdPF, rather than the net decrease observed, this filtering issue would have been further considered as a source of error.

Unilateral Data Analysis

The treadmill and equipment setup limited the view of the right side of the body at some points during the running cycle. This prevented fully accurate kinematic analysis of the right side of the body for parts of the running cycle. The left side had a clear view the throughout the stride cycle, and therefore this side of the body was analyzed. Combining the right-side EMG analysis with the left-side kinematic analysis may not be totally appropriate. That said, running kinematics have been shown to be bilaterally symmetric[147] and reliable[203] during treadmill running at a variety of speeds. However, linear and angular displacement data are more reliable than angular velocity data, namely when using data from a single stride[147]. To account for this, seven complete strides were collected for each subject, and the mean value of these strides were used. This reduces much of the variability in kinematic data[147]. Differences in marker placement could also potentially account for bilateral differences[147], but a static calibration was used to minimize this source of error. Lastly, Borrani found no bilateral differences between the MnPF during exhaustive running using a similar protocol with similar subjects[29]. Together, these points suggest that unilateral data analysis using the methods employed is an acceptable methodology.

Inter-subject Variation, Sample Size and Statistical Analysis

While a power analysis was performed on pilot data and the correct statistical tests were chosen and performed appropriately for this project, results for some variables may still have been limited by sample size. This may be due to some key variables exhibiting relatively large and consistent fatigue-related changes, while others demonstrate much more subtle or inconsistent changes. Though a power analysis was performed prior to data collection, this analysis assumed univariate statistical methodology. This project was based upon the fact that

running is a whole body activity, in which every movement at one joint may affect movement at another joint. Therefore, it was not appropriate to assume all kinematic dependent variables were independent of one another. To limit this interdependence, multivariate tests were performed by body group (legs, torso, and arms), as the correlation between variables was expected to be highest within a given body region.

The observed powers indicate that for many results, sufficient power was available to determine if a statistically significant result was truly meaningful and if non-significant trends could potentially become significant with increased sample size. For instance, HF_{max} demonstrated an observed power of 0.989, suggesting the statistically significant p-values for this data analysis are legitimate and related findings should be considered seriously. Considering adequate power was achieved for many variables using 15 subjects, it may be interpreted that these were the variables which show the greatest and most consistent fatigue-related changes, and therefore these are the most important to focus on when dealing with a population of runners.

Some variables which had results approaching statistical significance and results may have been limited by observed power. For these particular variables, greater subject numbers may or may not have produced statistical significance. Such is the case for PAR_{max}, which had a p-value of 0.066 with an observed power of 0.532. However, some other variables, such as TF_{min}, showed very lower power, suggesting a valid interpretation of this variable would require a tremendous sample size. This is likely attributable to changes in this variable being very small or inconsistent, and therefore it is not appropriate to make definitive conclusions with regard to results for these data. While it can be argued that more subjects could be included to attain adequate power and possibly attain statistical significance, the demonstrated variability suggests

these variables may differ too much between runners for the information to be applicable to a general population of runners. This is especially evident, given many other variables demonstrated sufficient power. Therefore, it is somewhat unjustified to further study such variables in a group setting using a considerably larger sample size, as the goal of this project was to describe the major fatigue-related changes most competitive runners of this demographic experience during high-intensity running.

The existing variability also emphasizes the point that most runners may follow a pattern of time-dependent changes, while others may show a completely different pattern of time-dependent changes. This should be considered when making applications using the results of this study. For example, coaches may want to emphasize fatigue-resistance training programs targeting the limiting factors found in this study to their whole team, but may need to make adjustments for certain individuals who differ from the general group.

7. Summary of Findings

Specific Aim 1

The iEMG most, but not all, muscles studied increased during the exhaustive run. Because the quadratic components of these parameters were not significant, there does not appear to be any specific breakpoint or threshold at which the rate of iEMG increase drastically changes, as previously reported in different exhaustive run protocols[240]. However, the muscles which showed a significant change in iEMG polynomial model coefficients all showed positive trends. Those muscles which did not have a significant model coefficient also showed increases in model-predicted iEMG, though this data needs to be treated with caution.

The semimembranosus and gluteus maximus had significant linear coefficients in iEMG, and the vastus lateralis had a strong trend in linear coefficient. The rectus femoris did not show a trend in linear coefficient, and also had the lowest model-predicted change in iEMG. The muscles of the torso group all experience significant time-dependent changes, emphasizing their importance during running. The latissimus dorsi and erector spinae showed changes on the same level as the leg muscles. The abdominal muscles studied here show increases in iEMG beyond those of the leg muscles, and this is likely attributable to their role in respiration. The brachioradialis was the only arm muscle which had a significant linear coefficient. Though three arm muscles had a model-predicted increase in iEMG, these increases were among the least of the muscles studied. The middle deltoid and trapezius were the only two muscles studied which had a decrease in model-predicted iEMG.

Together, these data indicate that iEMG generally increases (relative to baseline) in most of the muscles studied during treadmill running at an intensity approximating 95% VO_{2max}. Previous investigations have shown the leg muscles to be very responsive to fatiguing conditions, and this was the first investigation to show that muscles of the torso respond similarly. Additionally, this investigation revealed that EMG of some arm muscles change during fatiguing conditions, though not to the same degree of the legs and torso.

Specific Aim 2

The model-predicted change in MdPF was that of a decrease (relative to baseline) for all muscles studied during treadmill running at an intensity approximating 95% VO_{2max}. The semimembranosus displayed a significant quadratic effect and a strong linear trend, which together resulted in a net decrease in MdPF. The rectus femoris showed a linear decrease in MdPF, while the vastus lateralis did not showed a non-significant trend for a linear decrease in

MdPF. The latissimus dorsi was the only torso muscle which had a significant MdPF model coefficient, and this was for a decrease. The erector spinae showed a non-significant trend for decrease in MdPF. None of the arm muscles showed trends for change in MdPF. The results of this study suggest MdPF follows a consistent time-dependent pattern of change in select muscles during high intensity running, though MdPF kinetics vary widely between individuals. With the exception of one previous publication examining fatigue-related changes of the erector spinae[190], this was the first study to determine MdPF kinetics of torso and arm muscles during running.

Specific Aim 3

This was the first investigation to describe changes in three-dimensional kinematics of the upper and lower body during exhaustive running. A variety of significant findings were observed in running kinematics, including statistically significantly changes in HF_{max}, $UTAR_{max}$, $UTAR_{min}$, $vUTAR_{min}$, EF_{max}, SE_{min}, vSE_{max}, $vSPE_{max}$, and vSE_{min}. Additionally, non-significant trends were observed in a number of variables. While most investigations of fatigue during running have focused on the legs, the results of this study indicate the torso and upper body exhibit time-dependent kinematic changes.

For some variables, changes in EMG appeared to be highly related to changes in kinematics, and in other cases unrelated. Together, this data suggests that quantifiable neuromuscular factors influence running kinematics and how they change with fatigue. However, changes in EMG did not account for all kinematic changes. This likely is due to only a selected group of muscles being studied. Additionally, it may be due to the complex interactions which occur between the body segments, such that no two body segments are truly independent of one another.

Significant changes in VD_{max} and stride duration suggest that the end result of the electromyographic and kinematic changes alter whole body running kinematics. Changes in some EMG parameters were related to these whole body kinematics, but many were not. This emphasizes the complexity of running and the need to study all regions of the body, rather than the legs alone.

8. Future Directions

The results of this project provided a greater understanding of how different muscles respond to high intensity running, what kinematic changes occur with fatigue, and how the time-dependent electromyographic and kinematic changes are related to one another. Each one of these areas should be further examined to better determine the underlying mechanisms of fatigue-related changes during running. Through continued research, this information may eventually be used to develop optimized injury prevention and performance enhancement training programs for distance runners.

It is suspected that muscles which show the greatest decreases in MdPF limit distance running performance. Future investigations may be performed to determine if changes in MdPF are associated with performance level. If this is the case, it will be necessary to further explore what factors account for these differences in MdPF kinetics. While some muscles demonstrated consistent changes in EMG parameters, as indicated by statistically significant model coefficients, other muscles showed wide variation. Gamet[94] attributed these changes to training background, but there are likely more underlying factors, such as differences in muscle fiber type and muscle activation patterns, which may influence EMG parameters during dynamic contractions. If modifiable factors are found to be related to MdPF kinetics, intervention

programs, such as resistance training, may be developed and tested to determine if they change MdPF kinetics and enhance distance running performance.

Future research projects may also focus on specific joints to get a more detailed idea of which muscles contribute most to time-dependent kinematic changes. For instance, only one elbow flexor muscle was studied, and changes in its EMG were unrelated to kinematic changes. A thorough analysis of multiple agonist and antagonist muscles would provide more insight to the degree which neuromuscular changes related to EMG. By understanding which muscles have the greatest influence on a given joint during running, future investigations of EMG during high intensity running can focus on the most important muscle groups at each joint. Additionally, this information may be further explored to determinine how intervention programs affects changes in iEMG, and if these changes kinematics and performance.

The results of this study may be applicable to highly trained young male runners who race at distances of approximately 5km. Further investigation is needed to determine if different EMG and kinematic changes occur in females. Additionally, older runners and runners of different performance levels may display different time-dependent changes in these variables. Lastly, different mechanisms of fatigue occur at different aerobic intensity levels, and therefore it is expected that EMG and kinematic changes will differ with different running durations. Taken together, these considerations show the need to perform similar studies using different demographic groups over a variety of race distances.

9. Summary

In summary, this investigation was the first to describe time-dependent changes in EMG parameters and kinematic changes of multiple regions of the body and attempt to relate these

changes to one another. A number of novel observations were described, some of which were consistent with the original hypotheses. Many of these findings confirm the coaching anecdote that the upper body contributes to running performance. The results of this study provide a base for future research to further investigate how these findings relate to running performance of different race distances, what account for inter-individual variation in these factors, and how specific training programs alter these factors in multiple demographic groups of runners.

APPENDIX A – GLOSSARY OF ABBREVIATED TERMS

A number of abbreviations are used throughout this manuscript. To improve readability, all abbreviations are briefly defined in this appendix.

ΔEF	Change in elbow flexion angle
ΔEF_{max}	Change in maximum elbow flexion angle
ΔEF_{min}	Change in minimum elbow flexion angle
ΔHF	Change in hip flexion angle
ΔHF_{max}	Change in maximum hip flexion angle
ΔHF_{min}	Change in minimum hip flexion angle
ΔKF	Change in knee flexion angle
ΔKF_{max}	Change in maximum knee flexion angle
ΔKF_{min}	Change in minimum knee flexion angle
ΔPAR	Change in pelvic axial rotation angle
ΔPAR_{max}	Change in maximum pelvic axial rotation angle
ΔPAR_{min}	Change in minimum pelvic axial rotation angle
ΔSE	Change in shoulder elevation angle
ΔSE_{max}	Change in maximum shoulder elevation angle
ΔSE_{min}	Change in minimum shoulder elevation angle
ΔSPE	Change in shoulder plane of elevation angle
ΔSPE_{max}	Change in maximum shoulder plane of elevation angle
ΔSPE_{min}	Change in minimum shoulder plane of elevation angle
ΔTF	Change in torso flexion angle
ΔTF_{max}	Change in maximum torso flexion angle
ΔTF_{min}	Change in minimum torso flexion angle

ΔUTAR	Change in upper torso axial rotation angle
$\Delta UTAR_{max}$	Change in maximum upper torso axial rotation angle
$\Delta UTAR_{min}$	Change in minimum upper torso axial rotation angle
ΔVD	Change in vertical displacement
ΔVD_{max}	Change in maximum vertical displacement
ΔVD_{min}	Change in minimum vertical displacement angle
ΔvEF	Change in elbow flexion angular velocity
ΔvEF_{max}	Change in maximum elbow flexion angular velocity
ΔvEF_{min}	Change in minimum elbow flexion angular velocity
ΔvHF	Change in hip flexion angular velocity
ΔvHF_{max}	Change in maximum hip flexion angular velocity
ΔvHF_{min}	Change in minimum hip flexion angular velocity
ΔvKF	Change in knee flexion angular velocity
ΔvKF_{max}	Change in maximum knee flexion angular velocity
ΔvKF_{min}	Change in minimum knee flexion angular velocity
ΔvPAR	Change in pelvic axial rotation angular velocity
$\Delta vPAR_{max}$	Change in maximum pelvic axial rotation angular velocity
$\Delta vPAR_{min}$	Change in minimum pelvic axial rotation angular velocity
ΔvSE	Change in shoulder elevation angular velocity
ΔvSE_{max}	Change in maximum shoulder elevation angular velocity
ΔvSE_{min}	Change in minimum shoulder elevation angular velocity
ΔvSPE	Change in shoulder plane of elevation angular velocity
$\Delta vSPE_{max}$	Change in maximum shoulder plane of elevation angular velocity
$\Delta vSPE_{min}$	Change in minimum shoulder plane of elevation angular velocity
ΔvTF	Change in torso flexion angular velocity
ΔvTF_{max}	Change in maximum torso flexion angular velocity
ΔvTF_{min}	Change in minimum torso flexion angular velocity
ΔvUTAR	Change in upper torso axial rotation angular velocity
$\Delta vUTAR_{max}$	Change in maximum upper torso axial rotation angular velocity
$\Delta vUTAR_{min}$	Change in minimum upper torso axial rotation angular velocity
ΔvVD	Change in vertical displacement velocity

ΔvVD_{max}	Change in maximum vertical displacement velocity
ΔvVD_{min}	Change in minimum vertical displacement velocity
5K	Five kilometers
ADP	Adenosine diphosphate
ANOVA	Analysis of variance
ATP	Adenosine tri-phosphate
BLa	Blood lactate
CNS	Central nervous system
CO	Cardiac output
COG	Center of gravity
COM	Center of mass
EF	Elbow flexion angle
EF_{max}	Maximum elbow flexion angle
EF_{min}	Minimum elbow flexion angle
EMG	Electromyography
H+	Hydrogen ion
HF	Hip flexion angle
HF_{max}	Maximum hip flexion angle
HF_{min}	Minimum hip flexion angle
HR	Heart rate
HR $VO_{2\text{-}95}$	Heart rate at 95% of maximal oxygen consumption
HRR	Heart rate reserve
ICC	Intraclass correlation coefficient
iEMG	Integrated EMG
ISB	International society of biomechanics
KF	Knee flexion angle
KF_{max}	Maximum knee flexion angle
KF_{min}	Minimum knee flexion angle
LCS	Local coordinate system
LDH	Lactate dehydrogenase
MdPF	Median power frequency

MFCV	Mean fiber conduction velocity
MnPF	Mean power frequency
MRI	Magnetic resonance imaging
MUAP	Motor unit action potential
MVC	Maximal voluntary contraction
NAD	Nicotinamide adenine dinucleotide
PAR	Pelvic axial rotation angle
PAR_{max}	Maximum pelvic axial rotation angle
PAR_{min}	Minimum pelvic axial rotation angle
P_i	Inorganic phosphate
RER	Respiratory equivalent ratio
RM	Repeated measures
RMS	Root mean squared
SC	Slow component
SD	Standard deviation
SDH	Sorbitol dehydrogenase
SE	Shoulder elevation angle
SE (statistical)	Standard error
SE_{max}	Maximum shoulder elevation angle
SE_{min}	Minimum shoulder elevation angle
SPE	Shoulder plane of elevation angle
SPE_{max}	Maximum shoulder plane of elevation angle
SPE_{min}	Minimum shoulder plane of elevation angle
SPF	Spectral power frequency
tEnd	End of exhaustive run
TF	Torso flexion angle
TF_{max}	Maximum torso flexion angle
TF_{min}	Minimum torso flexion angle
tMid	Mid-point of exhaustive run
tStart	Start of exhaustive run
UTAR	Upper torso axial rotation angle

$UTAR_{max}$	Maximum upper torso axial rotation angle
$UTAR_{min}$	Minimum upper torso axial rotation angle
VD	Vertical displacement
VD_{max}	Maximum vertical displacement
VD_{min}	Minimum vertical displacement
vEF	Elbow flexion angular velocity
vEF_{max}	Maximum elbow flexion angular velocity
vEF_{min}	Minimum elbow flexion angular velocity
vHF	Hip flexion angular velocity
vHF_{max}	Maximum hip flexion angular velocity
vHF_{min}	Minimum hip flexion angular velocity
vKF	Knee flexion angular velocity
vKF_{max}	Maximum knee flexion angular velocity
vKF_{min}	Minimum knee flexion angular velocity
VO_2	Volume of oxygen consumption
VO_{2max}	Maximum volume of oxygen consumption
VO_{2res}	Oxygen consumption reserve
vPAR	Pelvic axial rotation angular velocity
$vPAR_{max}$	Maximum pelvic axial rotation angular velocity
$vPAR_{min}$	Minimum pelvic axial rotation angular velocity
vSE	Shoulder elevation angular velocity
vSE_{max}	Maximum shoulder elevation angular velocity
vSE_{min}	Minimum shoulder elevation angular velocity
vSPE	Shoulder plane of elevation angular velocity
$vSPE_{max}$	Maximum shoulder plane of elevation angular velocity
$vSPE_{min}$	Minimum shoulder plane of elevation angular velocity
vTF	Torso flexion angular velocity
vTF_{max}	Maximum torso flexion angular velocity
vTF_{min}	Minimum torso flexion angular velocity
vUTAR	Upper torso axial rotation angular velocity
$vUTAR_{max}$	Maximum upper torso axial rotation angular velocity

$vUTAR_{min}$	Minimum upper torso axial rotation angular velocity
vVD	Vertical displacement velocity
vVD_{max}	Maximum vertical displacement velocity
vVD_{min}	Minimum vertical displacement angular velocity

APPENDIX B – SAS CODE FOR PROCESSING IEMG DATA

```
data iemgset;
input id mgroup1 mgroup2 muscle time timepercent centered iemgratio;
logratio=log(iemgratio);
cards;
```

Data was pasted here using this format:

A				B	C	D	E
2	1	1	1	1	0.08	-0.45	1.00
2	1	1	1	2	0.17	-0.36	1.18
2	1	1	1	3	0.25	-0.28	0.98
2	1	1	1	4	0.33	-0.20	.
2	1	1	1	5	0.42	-0.11	0.80

… (continued to end)

18	1	1	1	11	0.79	0.25	0.83
18	1	1	1	12	0.86	0.33	0.62
18	1	1	1	13	0.93	0.40	0.80
18	1	1	1	14	1.00	0.47	0.88

A = Subject number

B = Time Point (minute)

C = Time Pont (percent of max)

D = Time Point (center measured)

E = iEMG (as a percentage of initial value)

```
;
proc mixed data=iemgset;
  class id muscle time;
  model logratio = timepercent timepercent*timepercent/solution outp=pred2r
outpm=pred2f ;
  repeated / subject=id type=ar(1);
run;
proc sort data=pred2f;
  by timepercent;
```

```
run;
goptions reset=all;
symbol1 c=blue v=star h=.8 i=j ;
axis1 order=(0 to 1 by 0.1) label=(a=90 'Predicted Log(iEMG ratio)');
proc gplot data=pred2f;
  plot pred*timepercent      /vaxis=axis1 ;
run;
quit;
proc mixed data=iemgset;
  class id muscle time;
  model   logratio   =   centered   centered*centered/solution   outp=pred2r
outpm=pred2f ;
  repeated / subject=id type=ar(1);
run;
proc sort data=pred2f;
  by centered;
run;
goptions reset=all;
symbol1 c=blue v=star h=.8 i=j ;
axis1 order=(0 to 1 by 0.1) label=(a=90 'Predicted Log(iEMG ratio)');
proc gplot data=pred2f;
  plot pred*centered      /vaxis=axis1 ;
run;
quit;
proc mixed data=iemgset;
  class id muscle time;
  model  logratio  =  timepercent  timepercent*timepercent/solution  outp=pred2r
outpm=pred2f;
  repeated / subject=id type=ar(1);
random   int   timepercent   timepercent*timepercent/   subject=id   type=un(1)
solution;
run;
proc sort data=pred2f;
  by timepercent;
run;
goptions reset=all;
symbol1 c=blue v=star h=.8 i=j ;
axis1 order=(0 to 1 by 0.1) label=(a=90 'Predicted Log(iEMG ratio)');
```

```
proc gplot data=pred2f;
  plot pred*timepercent      /vaxis=axis1 ;
run;
quit;
proc mixed data=iemgset;
  class id muscle time;
  model    logratio    =    centered    centered*centered/solution    outp=pred2r
outpm=pred2f;
  repeated / subject=id type=ar(1);
random int centered centered*centered/ subject=id type=un(1) solution;
run;
proc sort data=pred2f;
  by centered;
run;
goptions reset=all;
symbol1 c=blue v=star h=.8 i=j ;
axis1 order=(0 to 1 by 0.1) label=(a=90 'Predicted Log(iEMG ratio)');
proc gplot data=pred2f;
  plot pred*centered      /vaxis=axis1 ;
run;
quit;
```

APPENDIX C – SAS CODE FOR PROCESSING MDPF DATA

```
data iemgset;
input id mgroup1 mgroup2 muscle time timepercent centered iemgratio;
logratio=log(iemgratio);
cards;
```

Data was pasted here using this format:

A				B	C	D	E
2	1	1	1	1	0.083	-0.447	1.000
2	1	1	1	2	0.167	-0.364	0.939
2	1	1	1	3	0.250	-0.281	1.161
2	1	1	1	4	0.333	-0.197	.
2	1	1	1	5	0.417	-0.114	1.047

… (continued to end)

18	1	1	1	11	0.786	0.255	1.031
18	1	1	1	12	0.857	0.326	1.075
18	1	1	1	13	0.929	0.398	1.038
18	1	1	1	14	1.000	0.469	1.089

A = Subject number

B = Time Point (minute)

C = Time Pont (percent of max)

D = Time Point (center measured)

E = MdPF (as a percentage of initial value)

```
;
proc mixed data=iemgset;
  class id muscle time;
  model logratio = timepercent timepercent*timepercent/solution outp=pred2r
outpm=pred2f ;
  repeated / subject=id type=ar(1);
run;
```

```
proc sort data=pred2f;
  by timepercent;
run;
goptions reset=all;
symbol1 c=blue v=star h=.8 i=j ;
axis1 order=(-1 to 0 by 0.1) label=(a=90 'Predicted Log(MdPF ratio)');
proc gplot data=pred2f;
  plot pred*timepercent      /vaxis=axis1 ;
run;
quit;
proc mixed data=iemgset;
  class id muscle time;
  model    logratio    =    centered    centered*centered/solution    outp=pred2r
outpm=pred2f ;
  repeated / subject=id type=ar(1);
run;
proc sort data=pred2f;
  by centered;
run;
goptions reset=all;
symbol1 c=blue v=star h=.8 i=j ;
axis1 order=(-1 to 0 by 0.1) label=(a=90 'Predicted Log(MdPF ratio)');
proc gplot data=pred2f;
  plot pred*centered      /vaxis=axis1 ;
run;
quit;
proc mixed data=iemgset;
  class id muscle time;
  model  logratio  =  timepercent  timepercent*timepercent/solution  outp=pred2r
outpm=pred2f;
  repeated / subject=id type=ar(1);
random   int   timepercent   timepercent*timepercent/   subject=id   type=un(1)
solution;
run;
proc sort data=pred2f;
  by timepercent;
run;
goptions reset=all;
```

```
symbol1 c=blue v=star h=.8 i=j ;
axis1 order=(-1 to 0 by 0.1) label=(a=90 'Predicted Log(MdPF ratio)');
proc gplot data=pred2f;
  plot pred*timepercent      /vaxis=axis1 ;
run;
quit;
proc mixed data=iemgset;
  class id muscle time;
  model    logratio    =    centered    centered*centered/solution    outp=pred2r
outpm=pred2f;
  repeated / subject=id type=ar(1);
random int centered centered*centered/ subject=id type=un(1) solution;
run;
proc sort data=pred2f;
  by centered;
run;
goptions reset=all;
symbol1 c=blue v=star h=.8 i=j ;
axis1 order=(-1 to 0 by 0.1) label=(a=90 'Predicted Log(MdPF ratio)');
proc gplot data=pred2f;
  plot pred*centered      /vaxis=axis1 ;
run;
quit;
```

APPENDIX D – NORMATIVE EMG DATA

This appendix includes EMG data from a typical subject which is generally representative of the EMG data from most subjects in the study. This subject ran for 22 minutes before volitional exhaustion. Therefore, data from Minute 1 (start of data collection), Minute 11 (mid-point of data collection), and Minute 22 (end of data collection) are represented here.

The top graph under each minute represents the filtered EMG signal. The x-axis is time. Each black vertical line along the x-axis represents one foot impact on the right side. The y-axis is amplitude of the EMG signal. Because the amplitude can vary from person-to-person and from test-to-test, and the amplitude was normalized to the first minute of data collection, these graphs remain unitless for the y-axis.

The bottom graph under each minute represents the power frequency spectrum. The x-axis represents frequency in Hertz. For visual purposes, x-axis was stopped at 300Hz. While there is some data beyond this point, it is not easily visualized on the graph and therefore not included. The y-axis represents amplitude. For purposes already described above, amplitude shall remain unitless for these graphs.

Vastus Lateralis

Minute 1

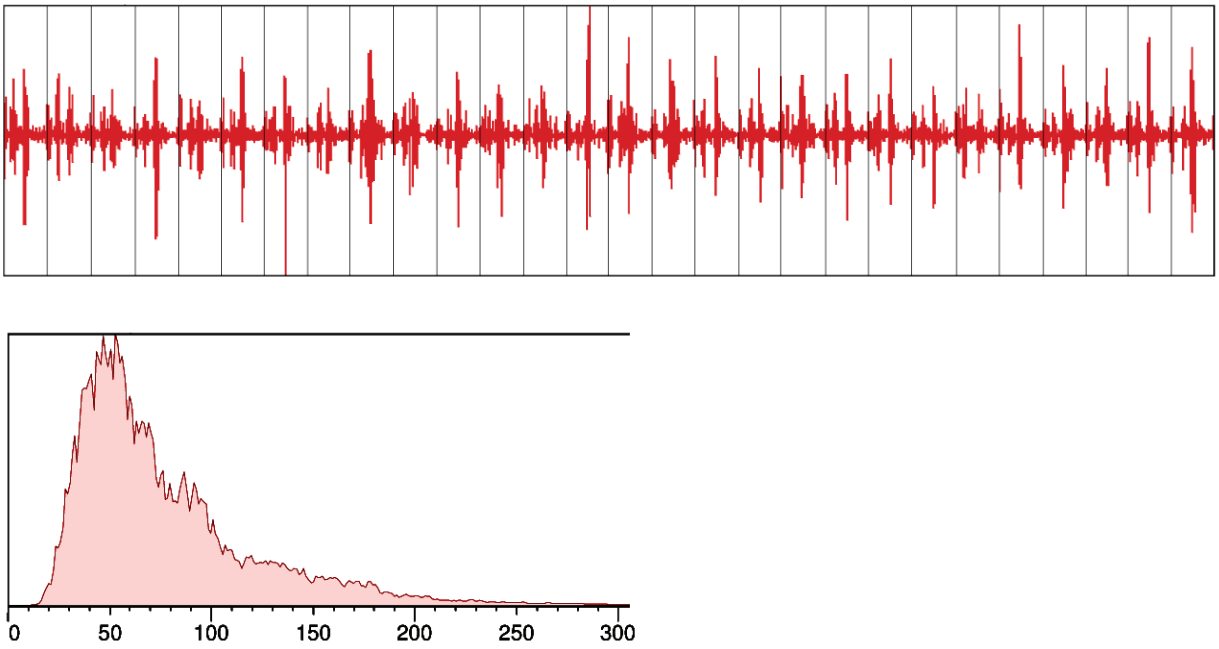

Minute 11

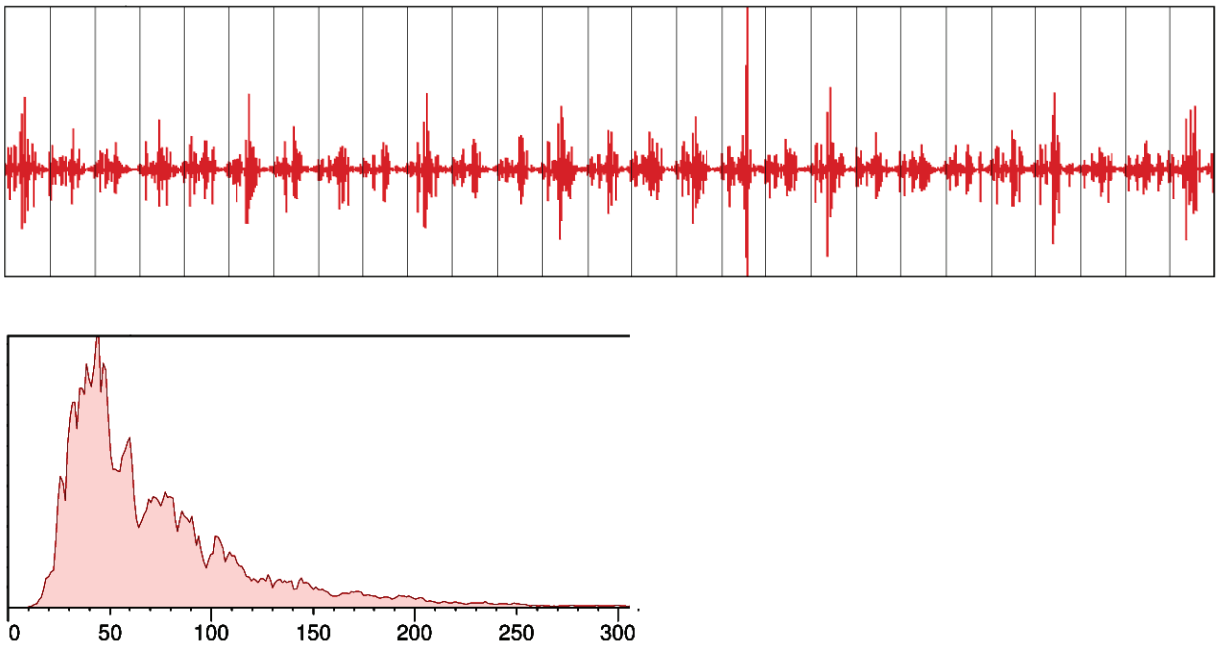

Minute 22

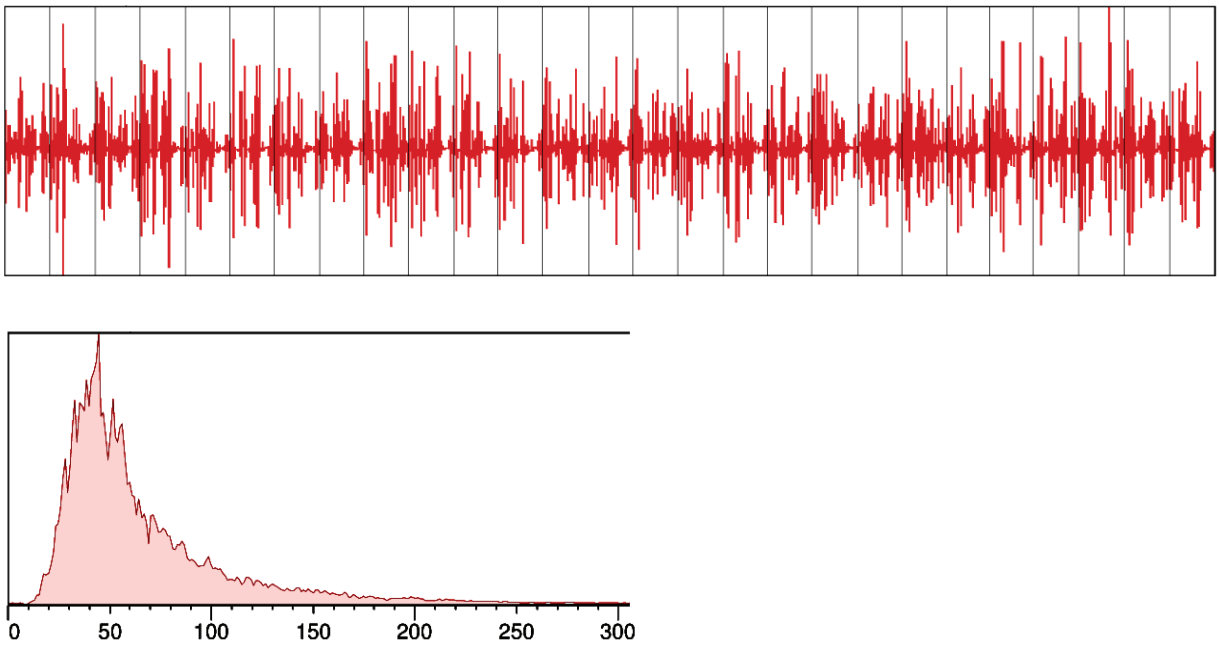

Semimembranosus

Minute 1

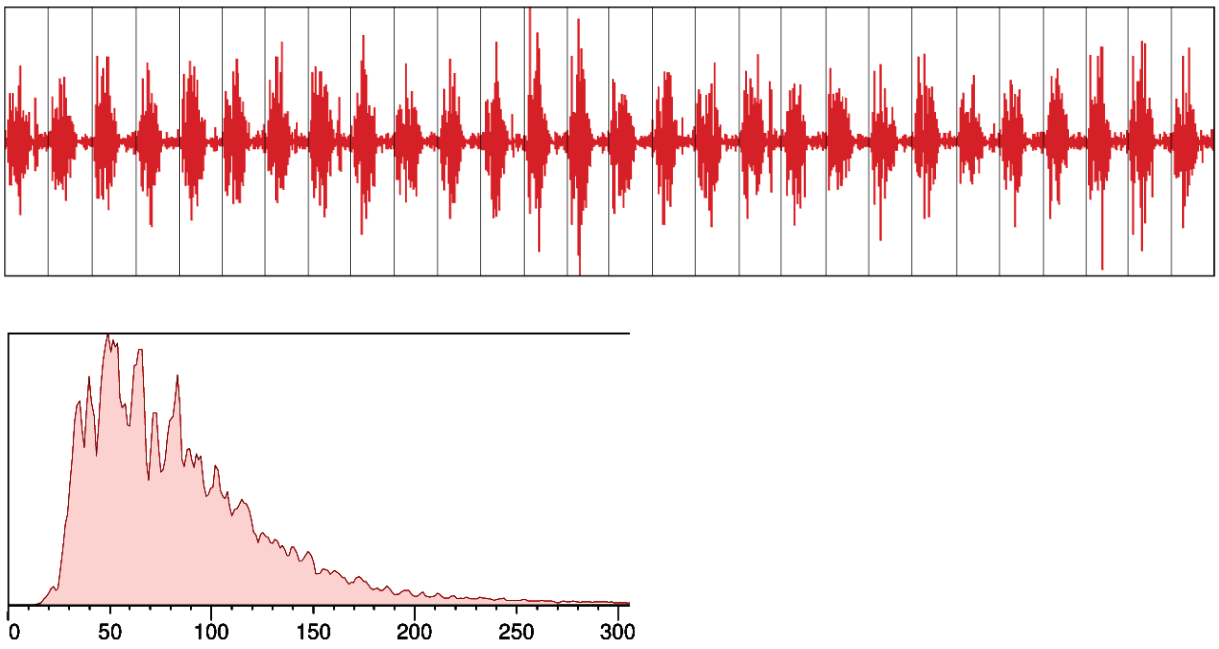

Minute 11

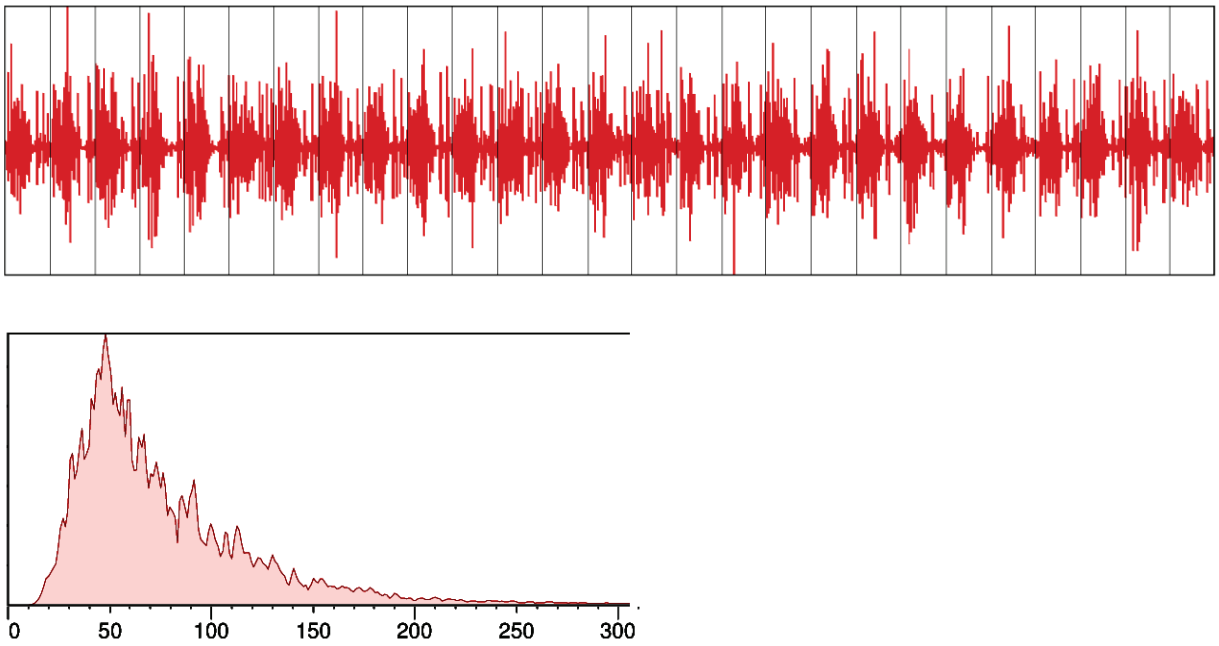

Minute 22

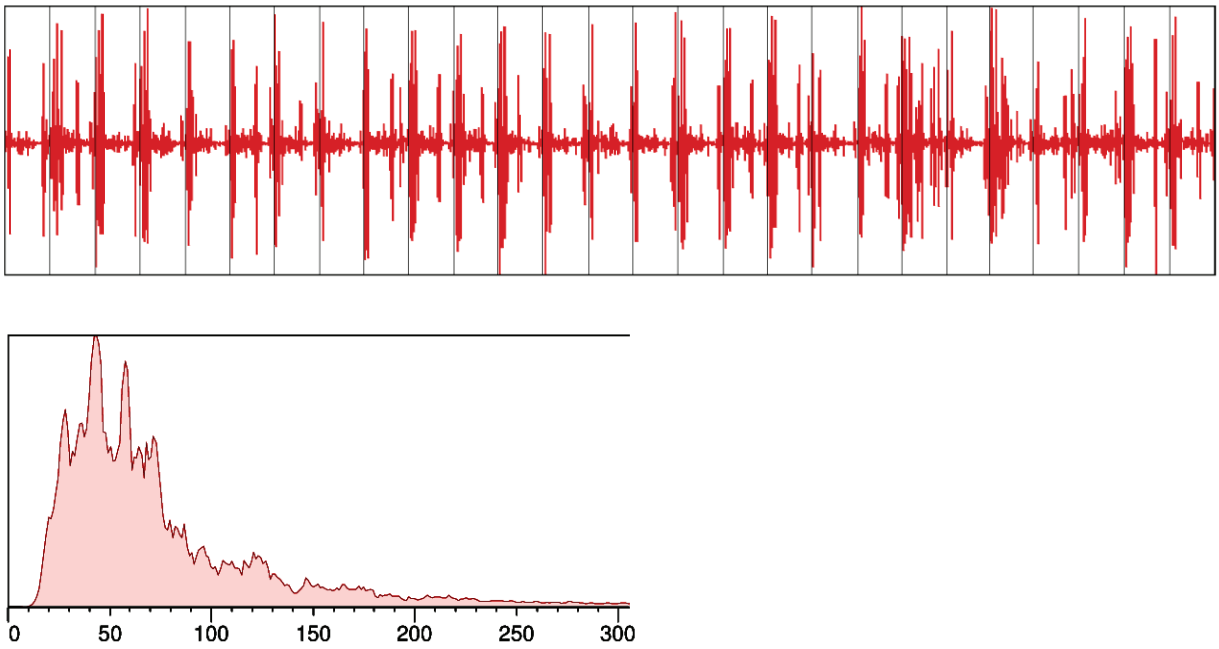

Gluteus Maximus

Minute 1

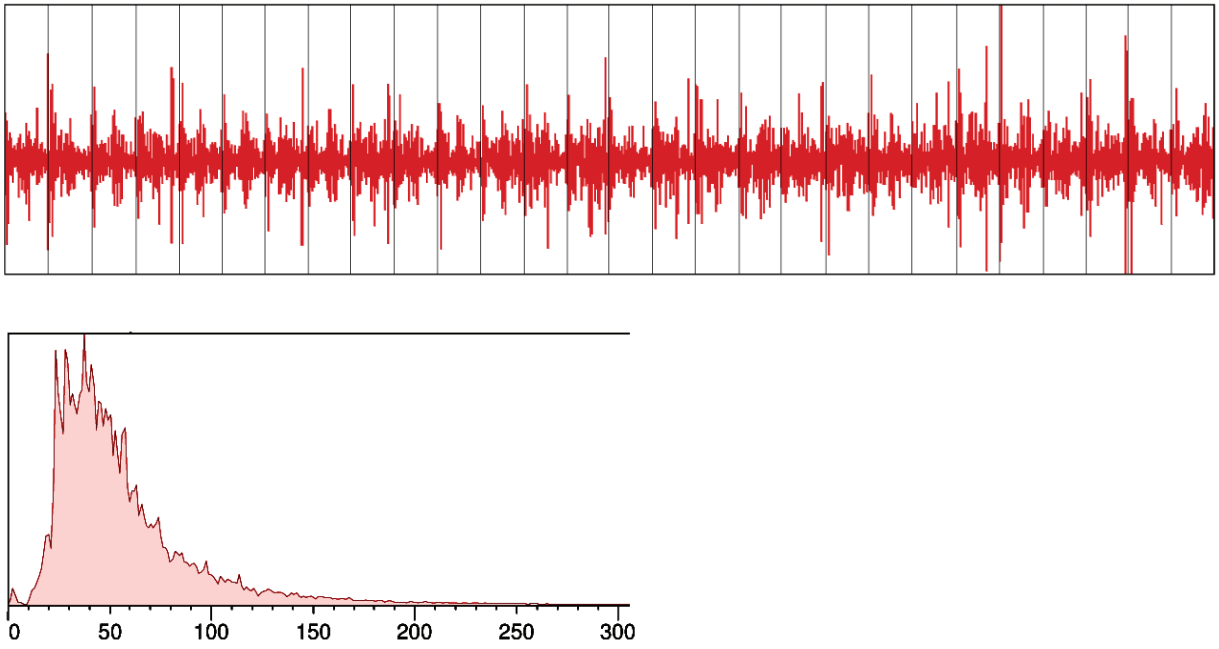

Minute 11

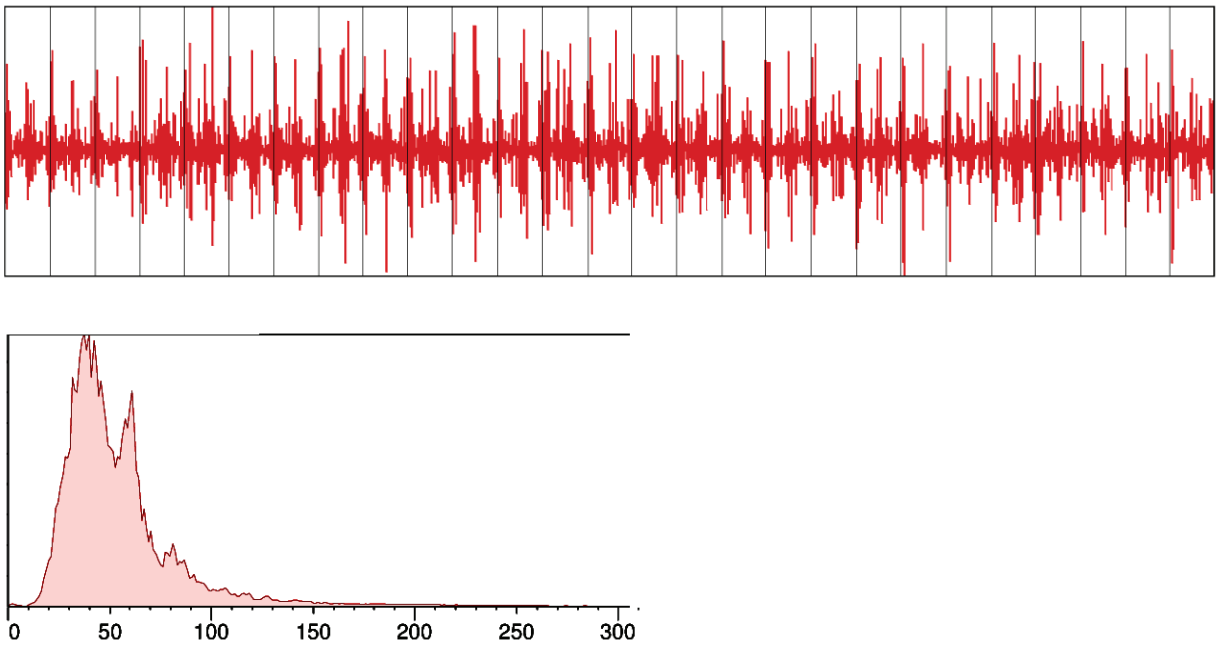

Minute 22

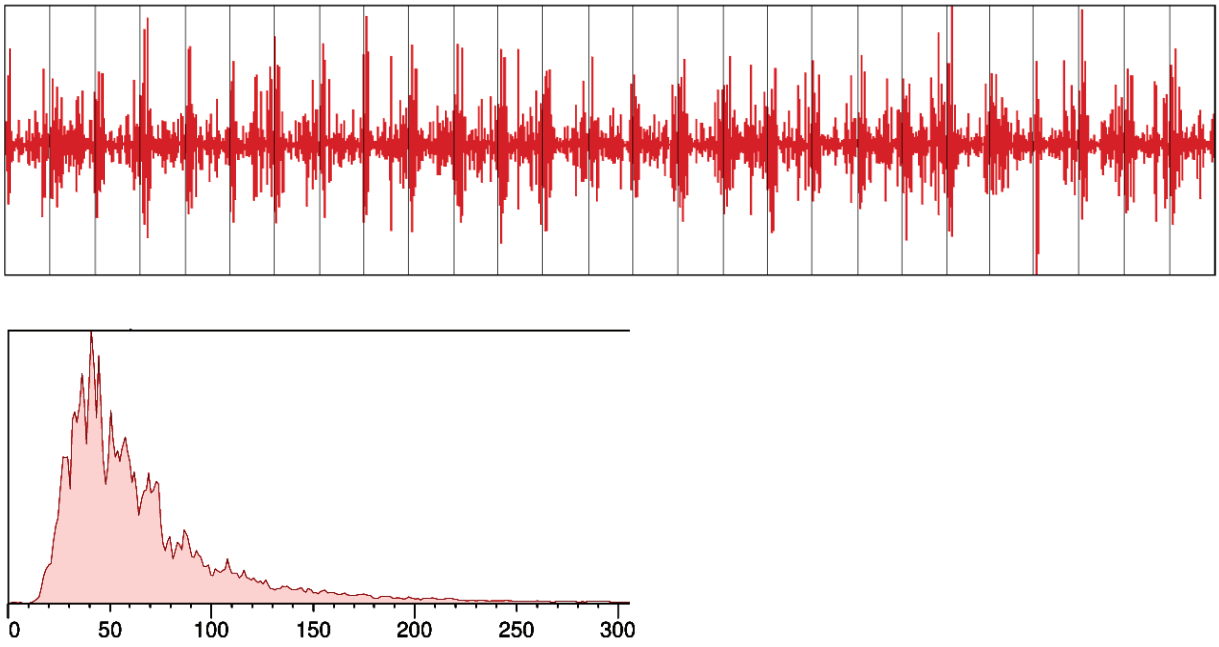

Rectus Femoris

Minute 1

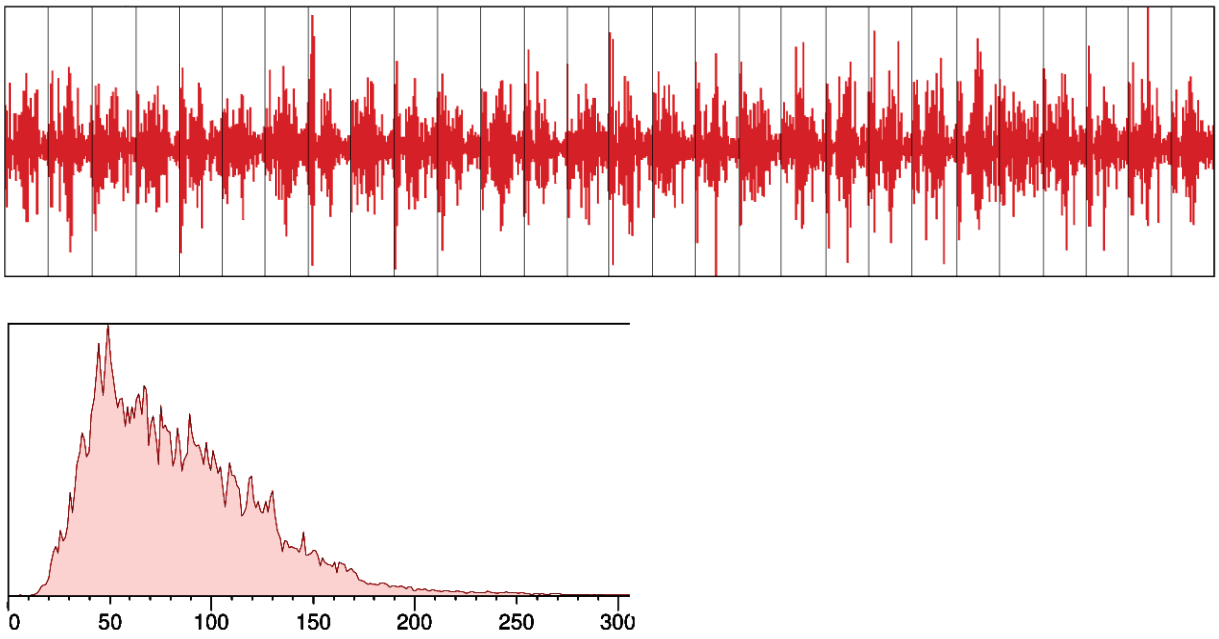

Minute 11

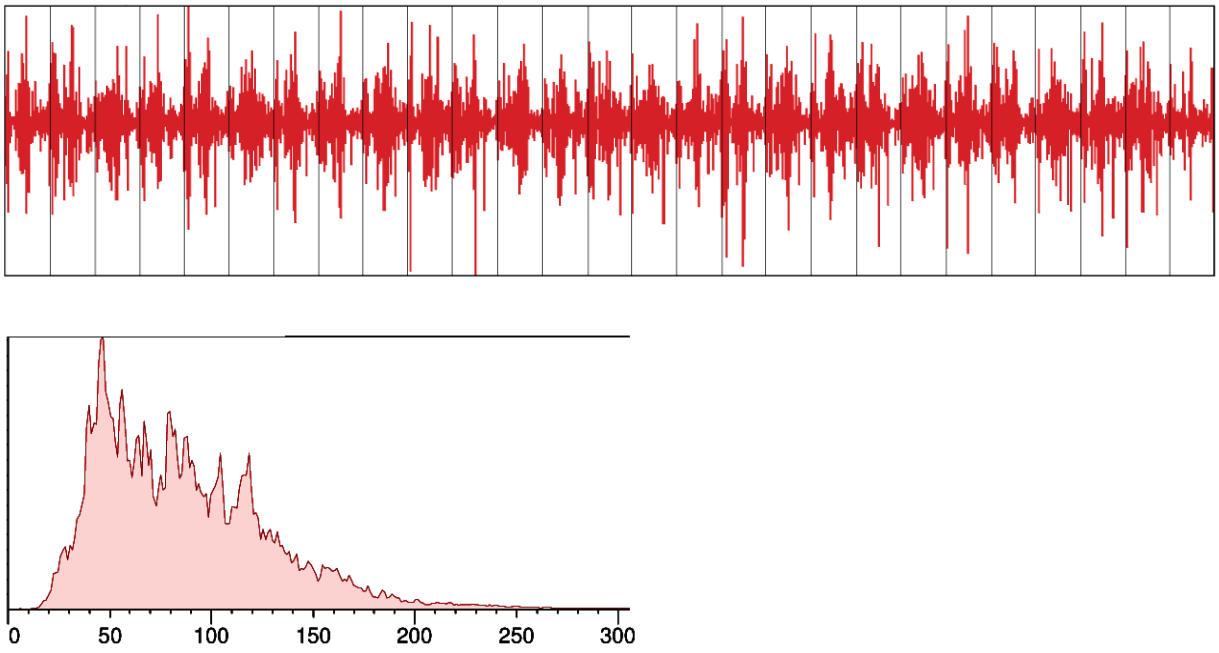

Minute 22

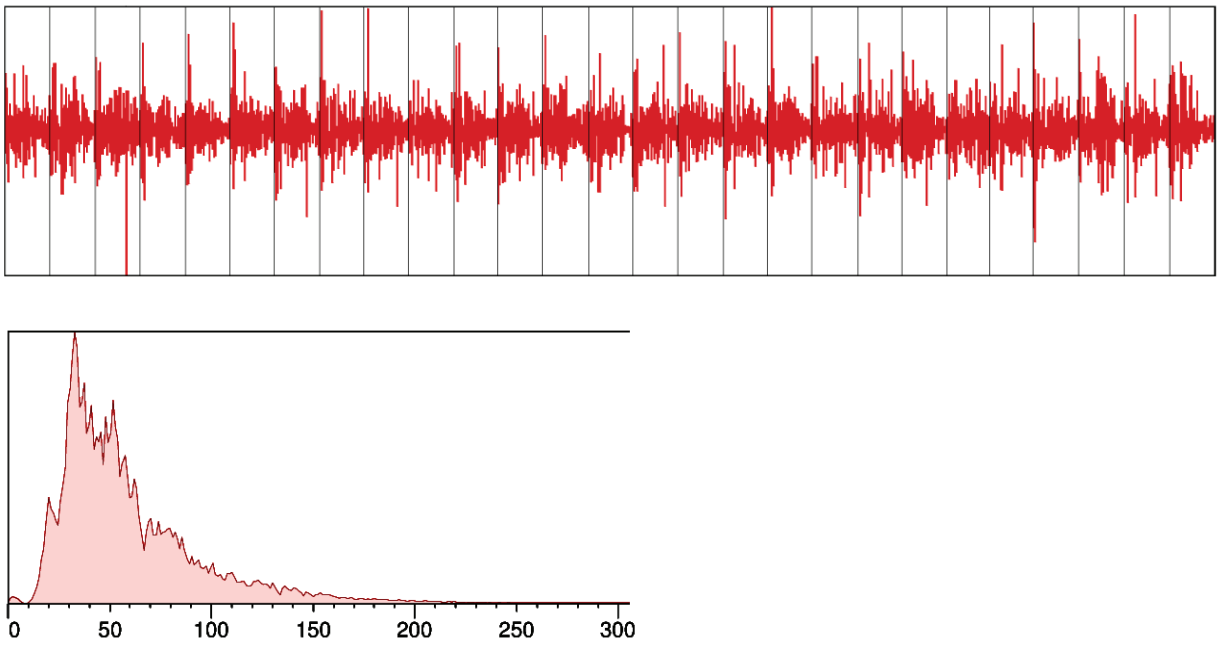

Erector Spinae

Minute 1

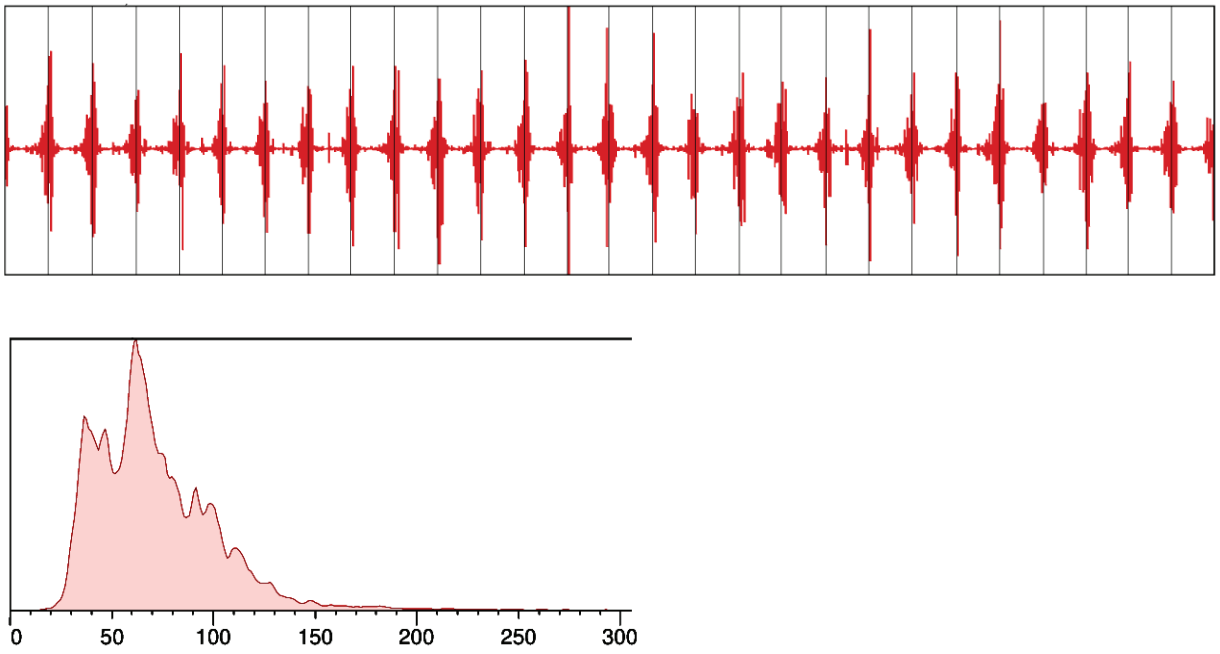

Minute 11

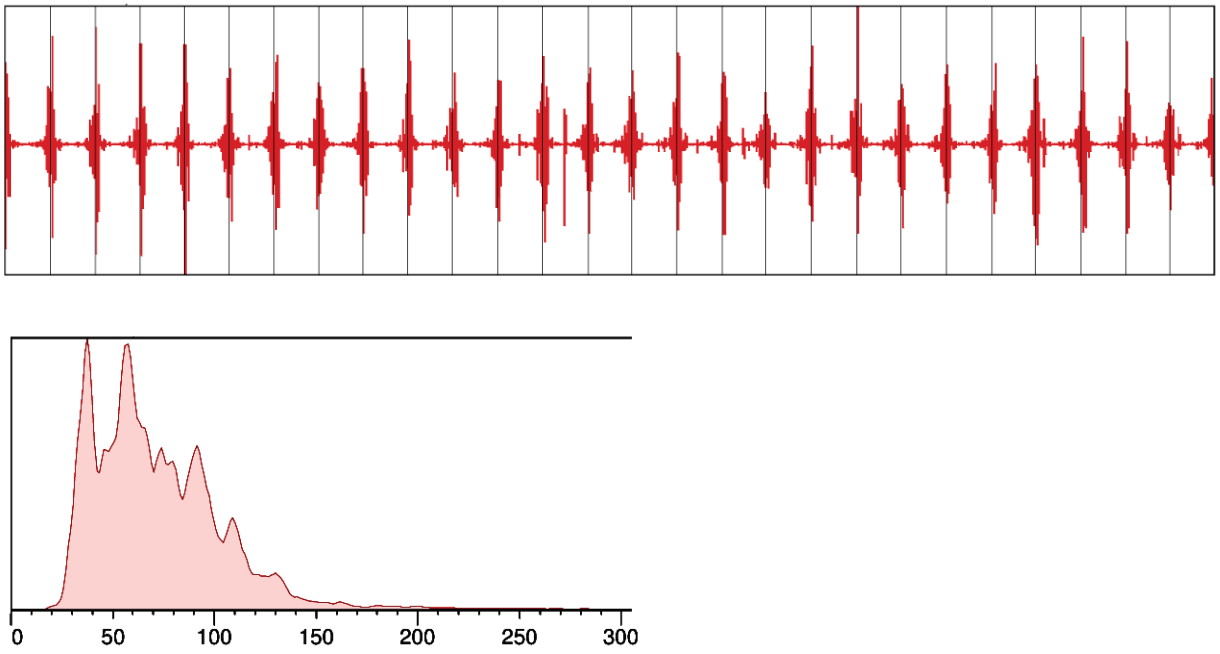

Minute 22

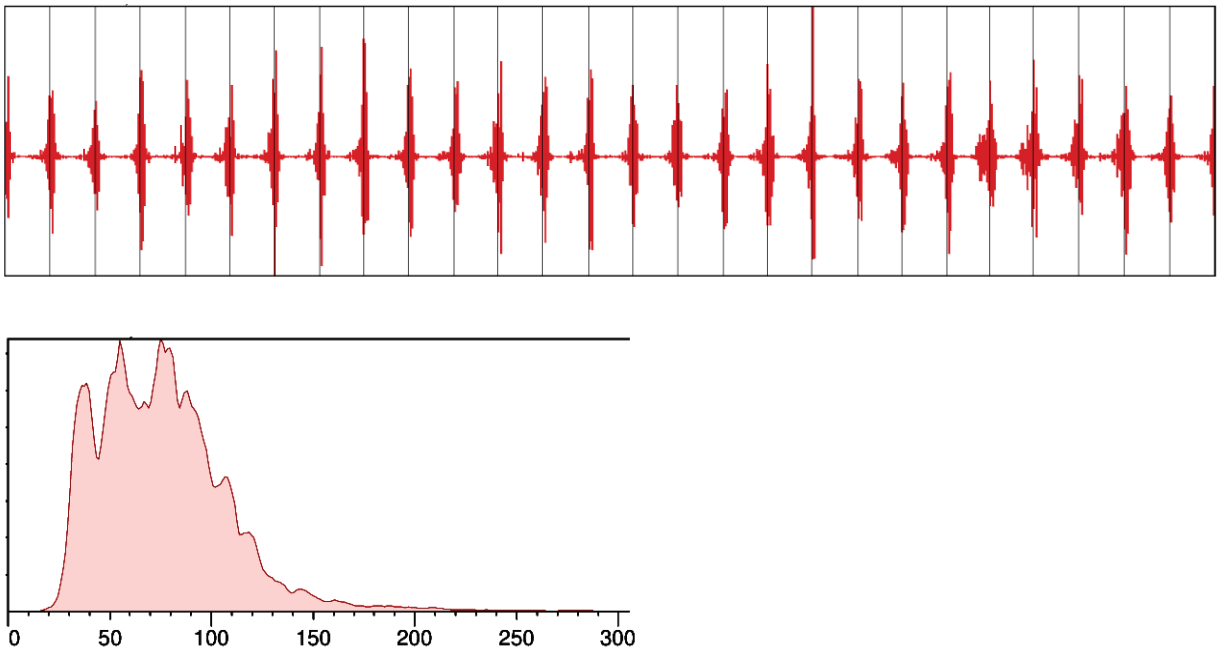

Latissimus Dorsi

Minute 1

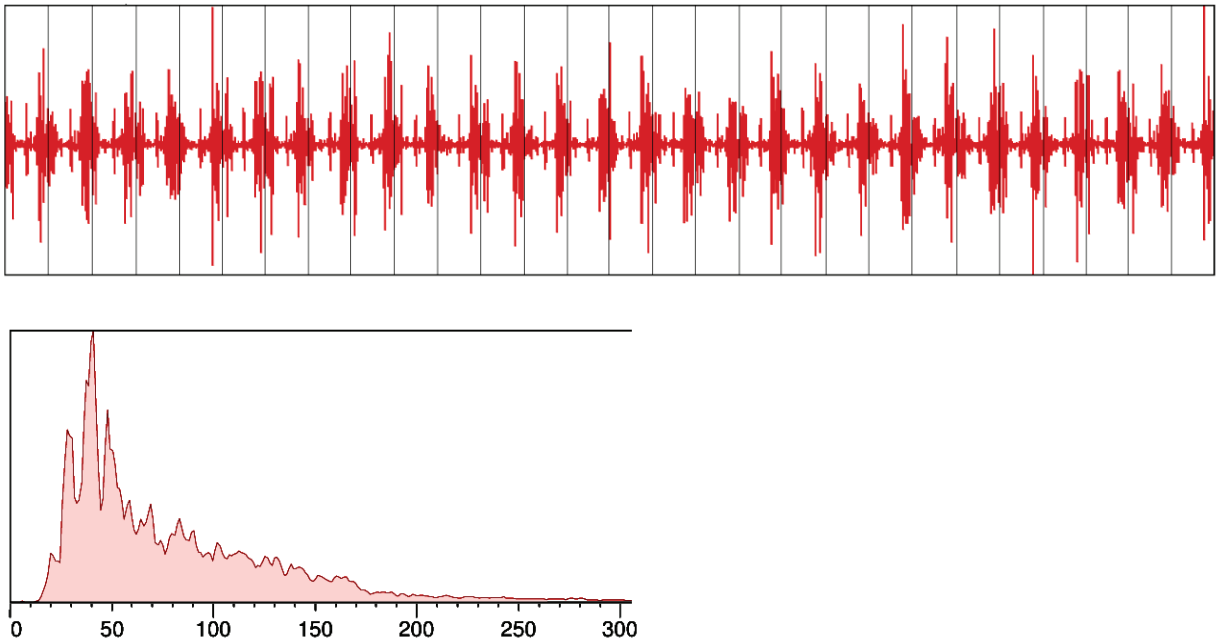

Minute 11

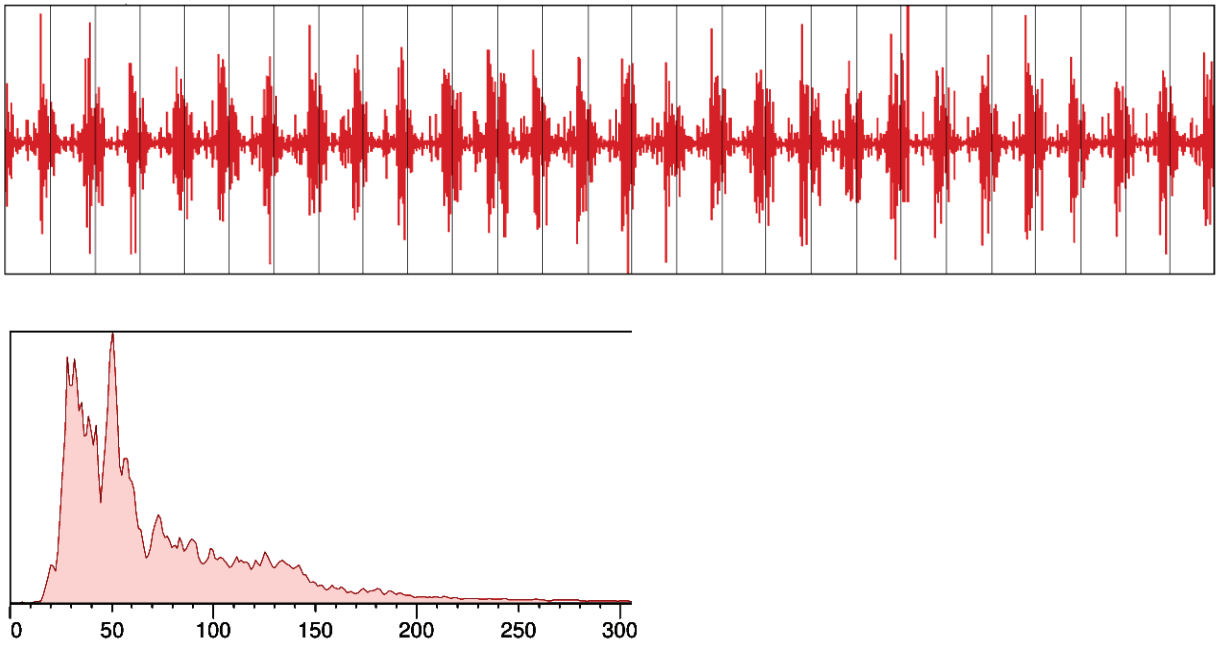

Minute 22

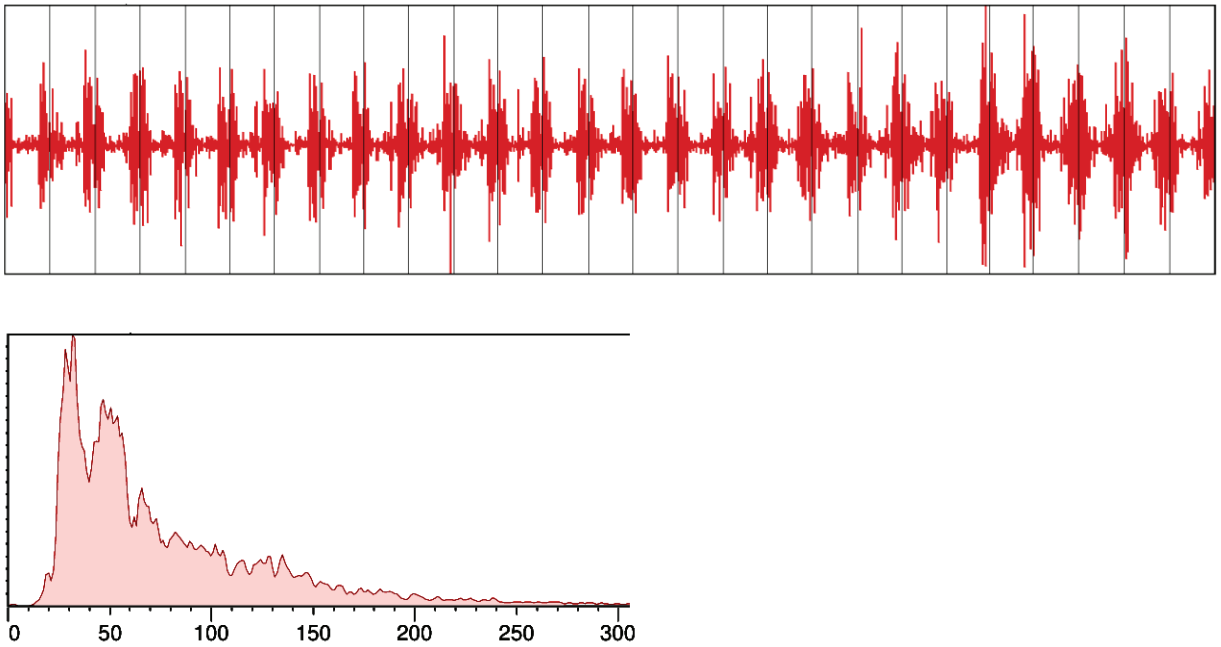

Rectus Abdominus

Minute 1

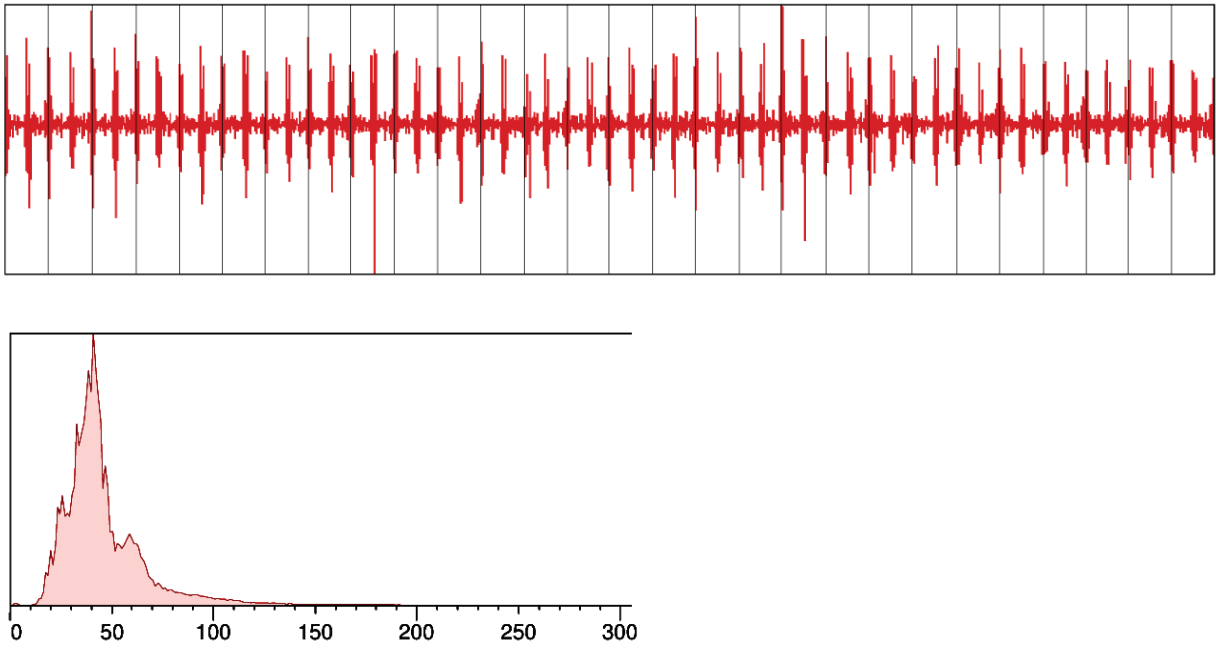

Minute 11

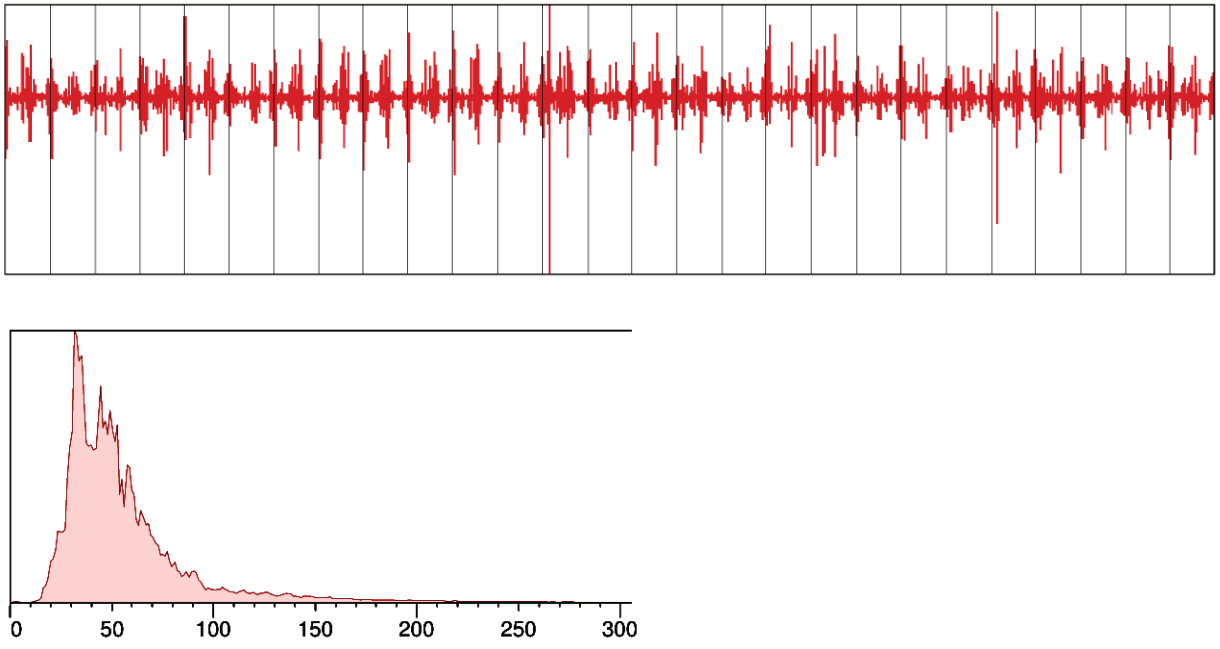

Minute 22

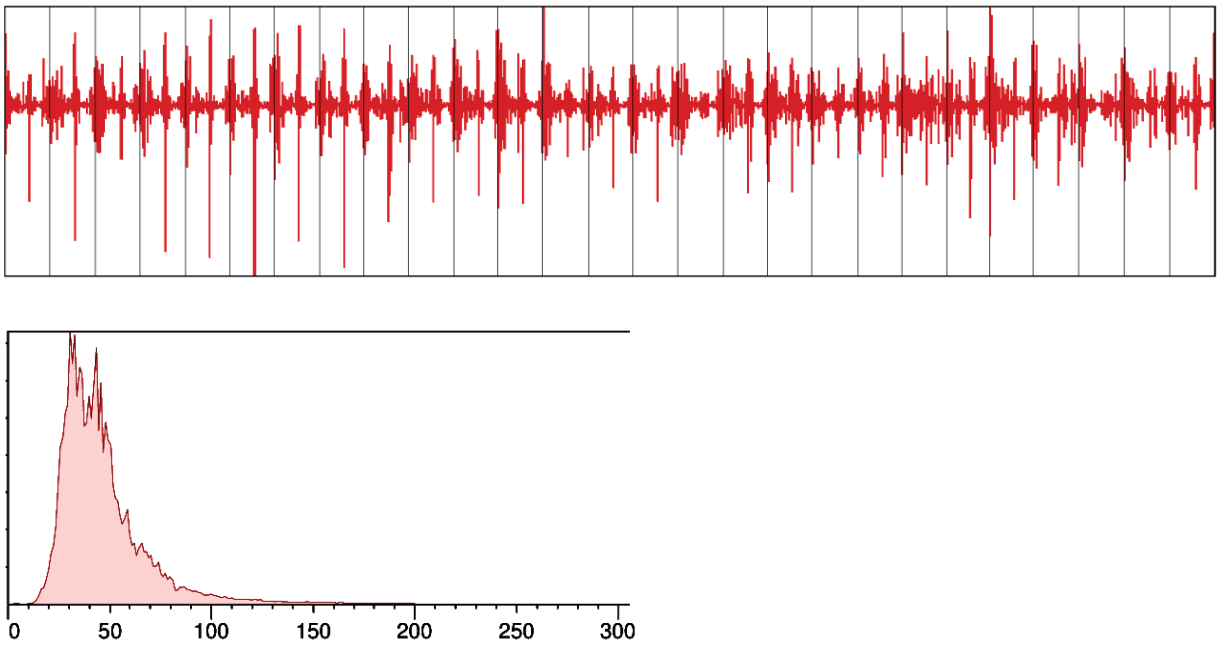

External Oblique

Minute 1

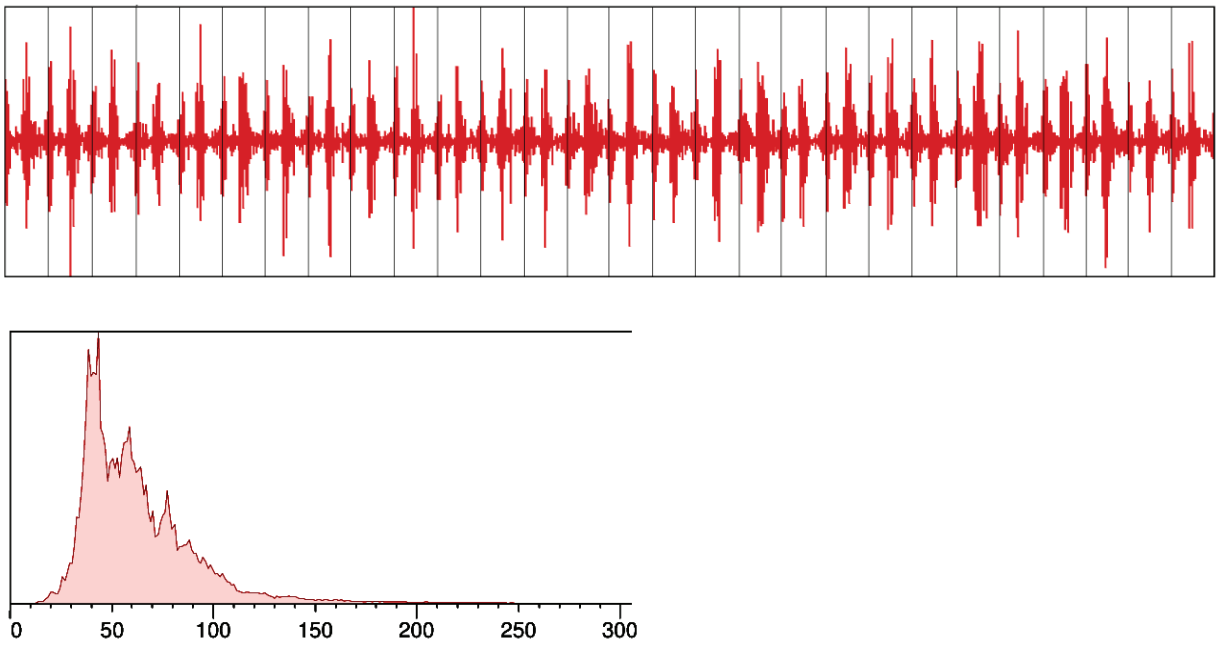

Minute 11

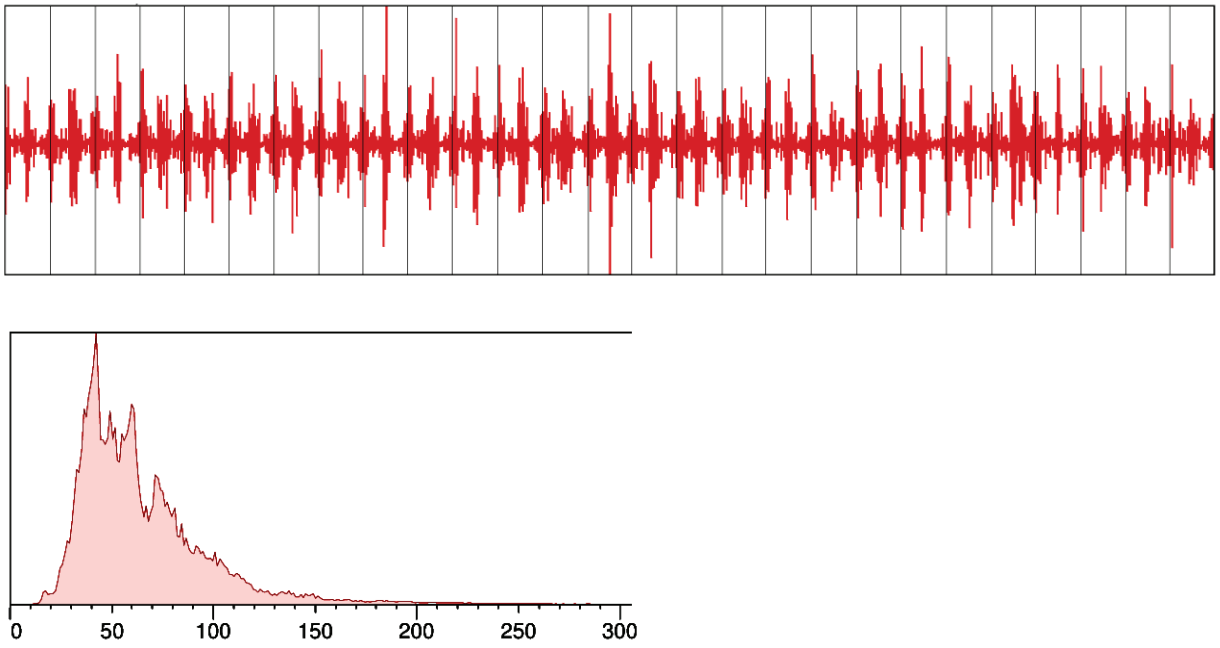

Minute 22

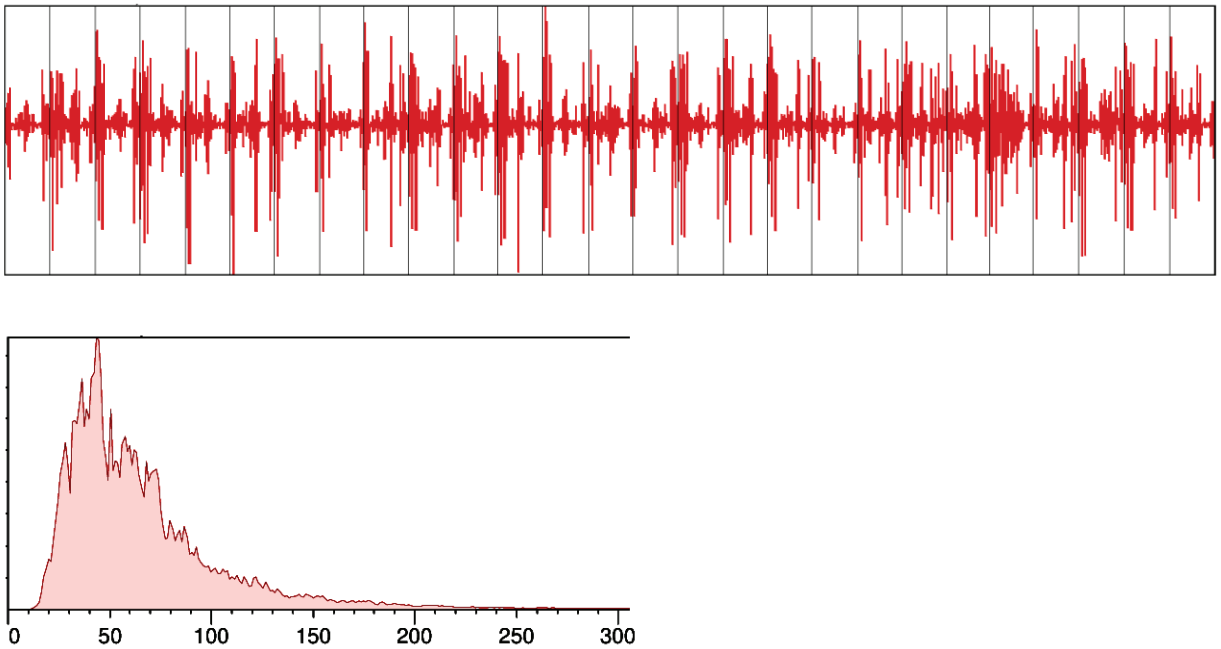

Anterior Deltoid

Minute 1

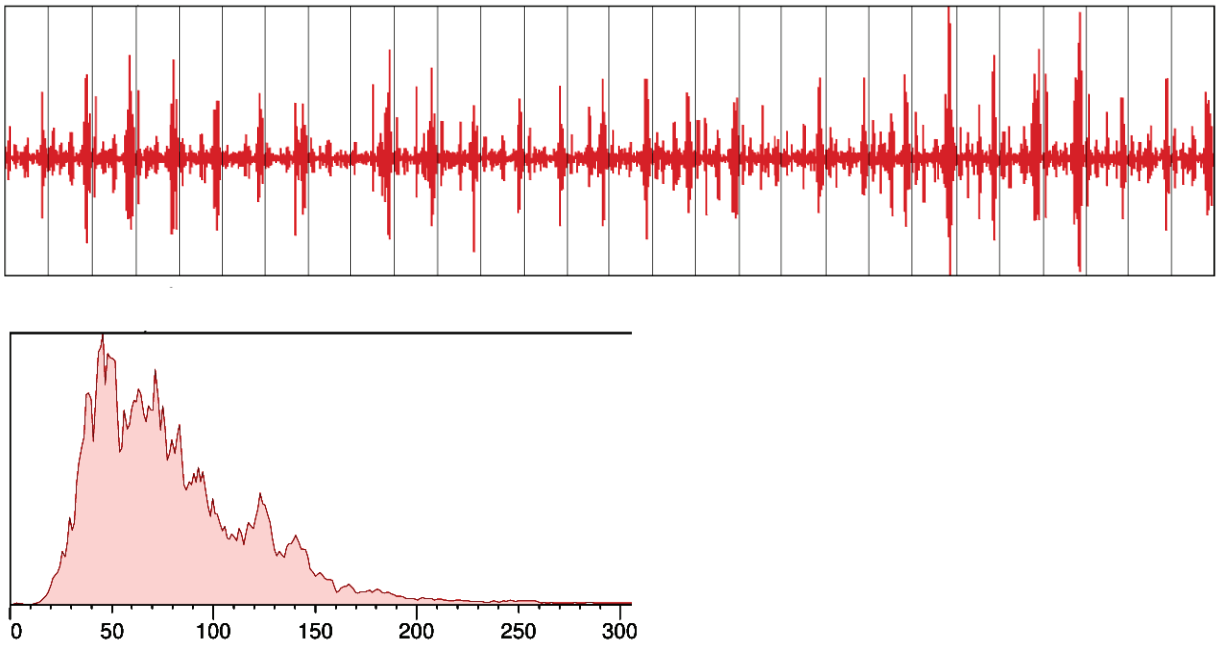

Minute 11

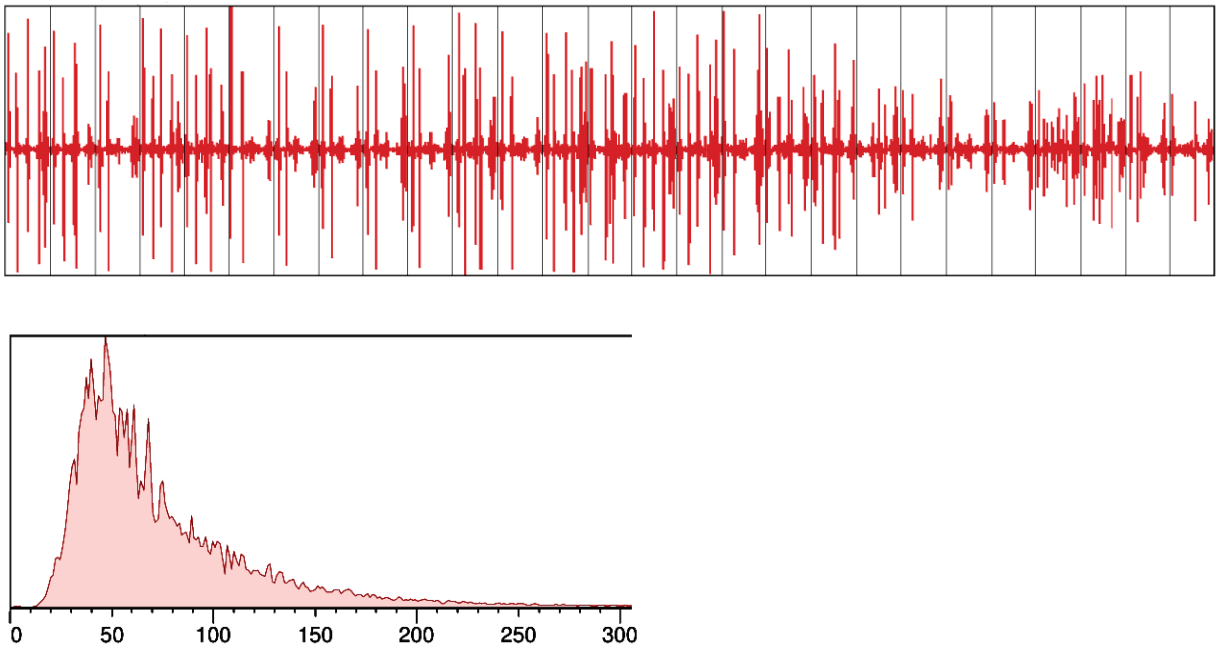

Minute 22

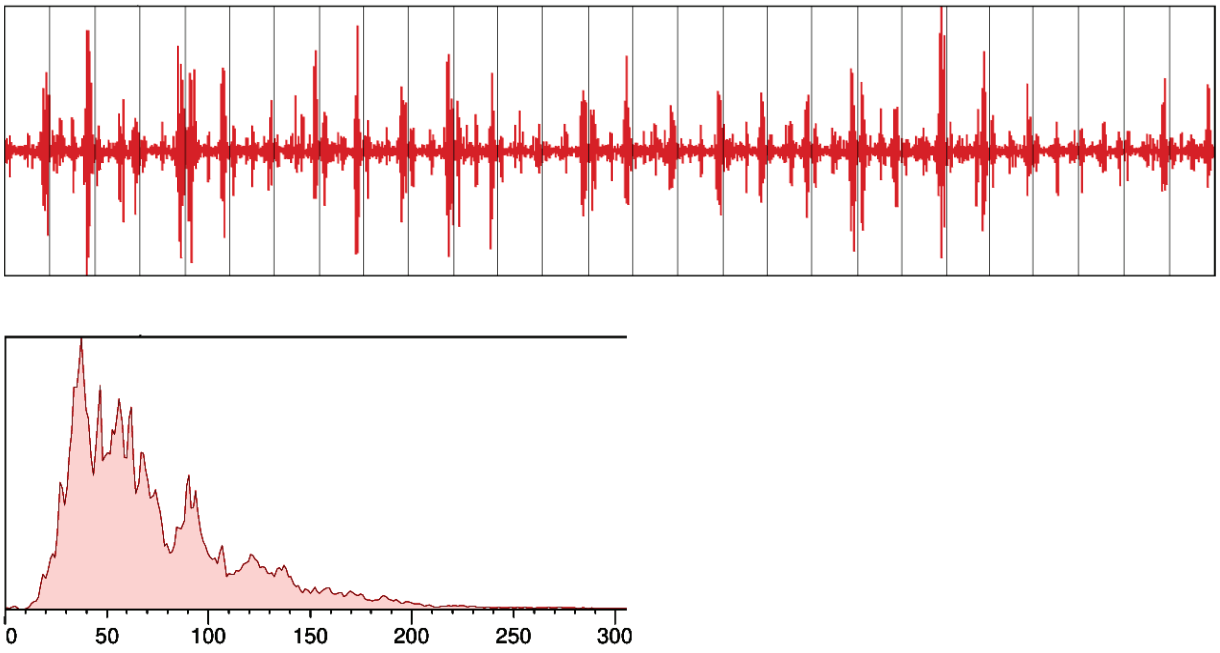

Middle Deltoid

Minute 1

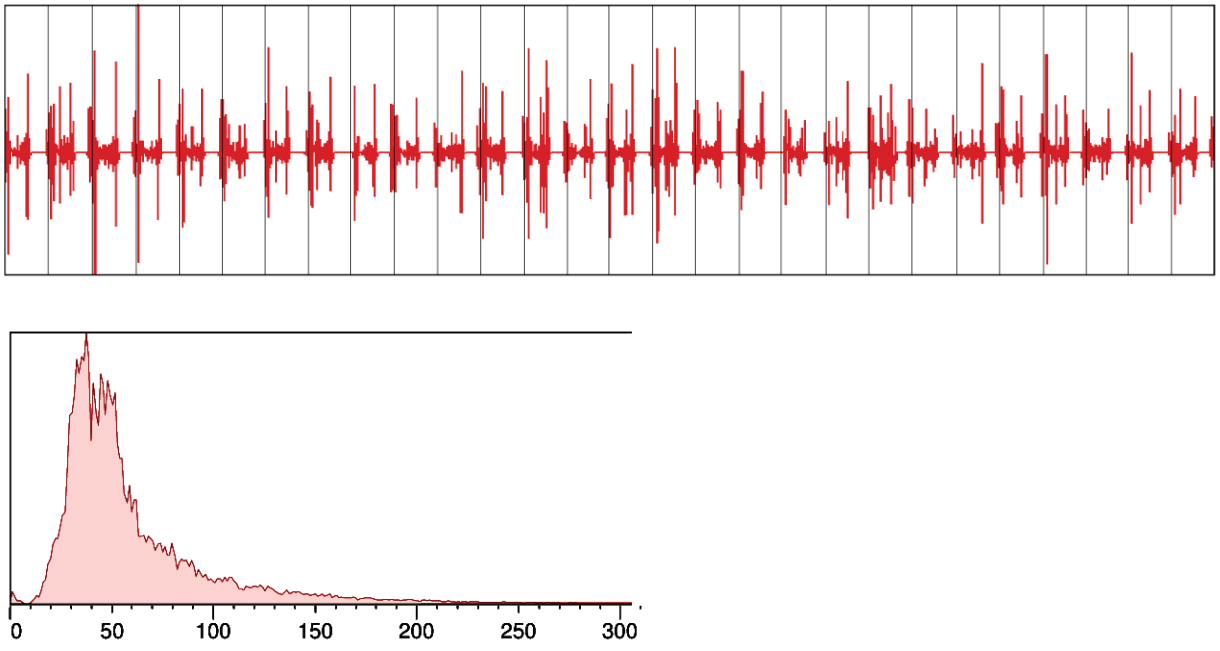

Minute 11

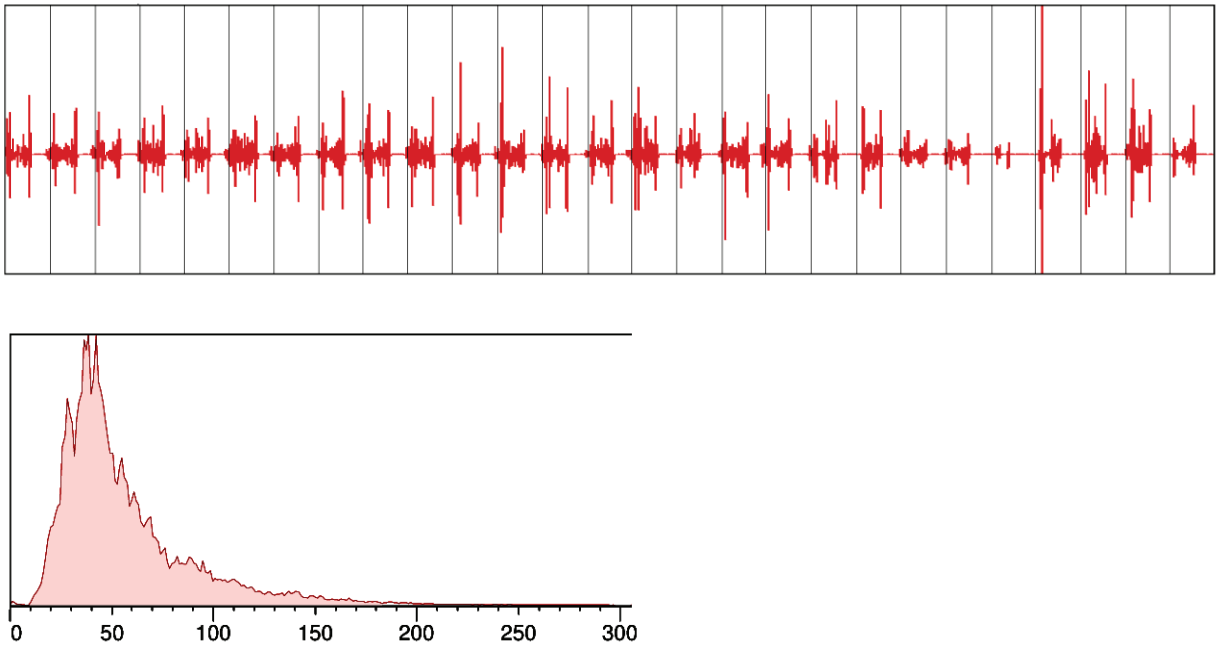

Minute 22

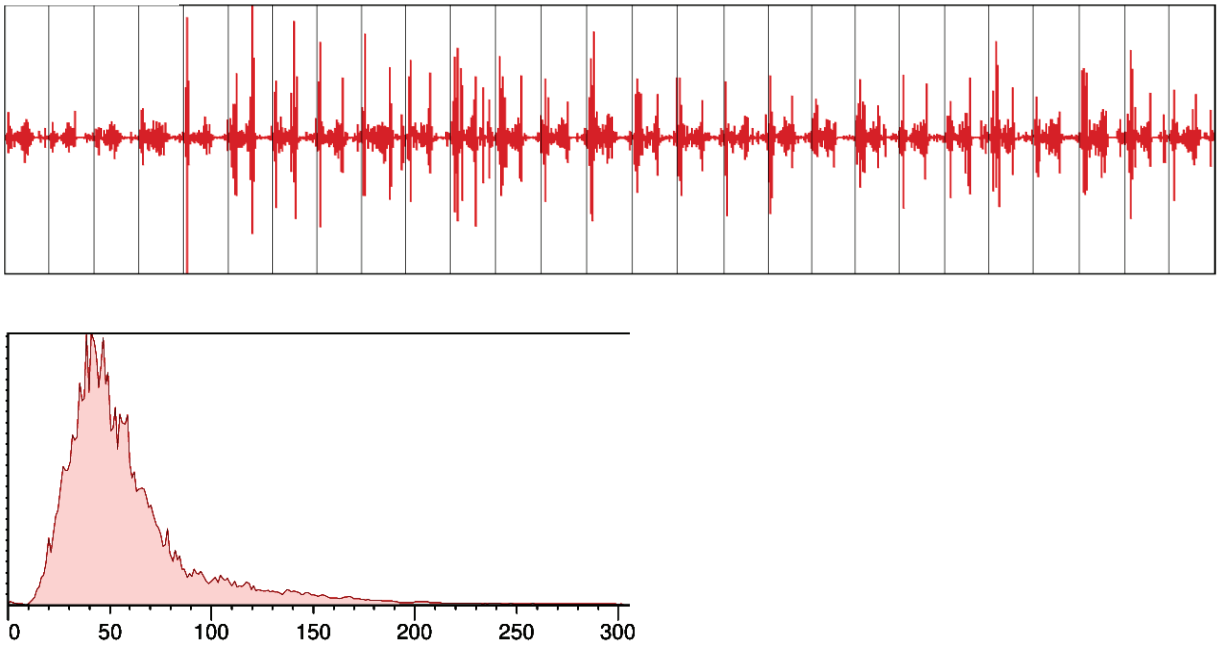

Posterior Deltoid

Minute 1

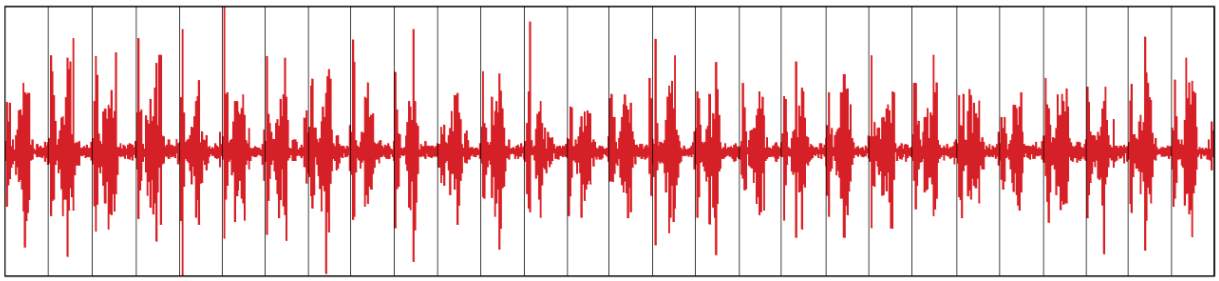

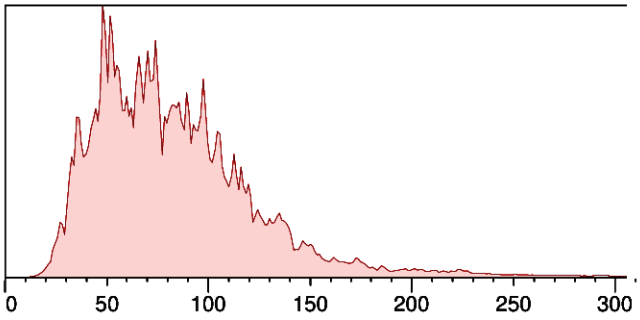

Minute 11

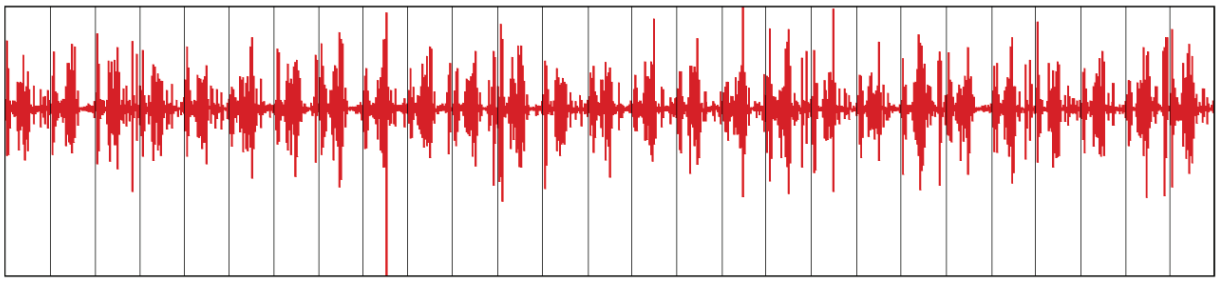

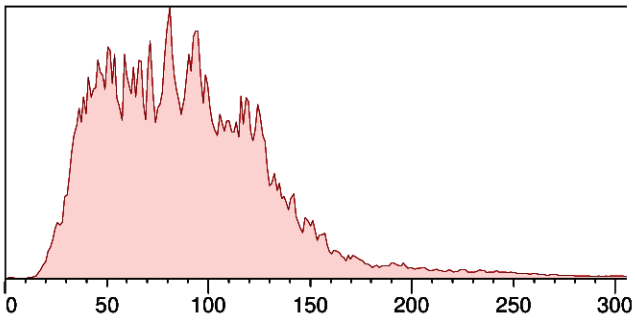

Minute 22

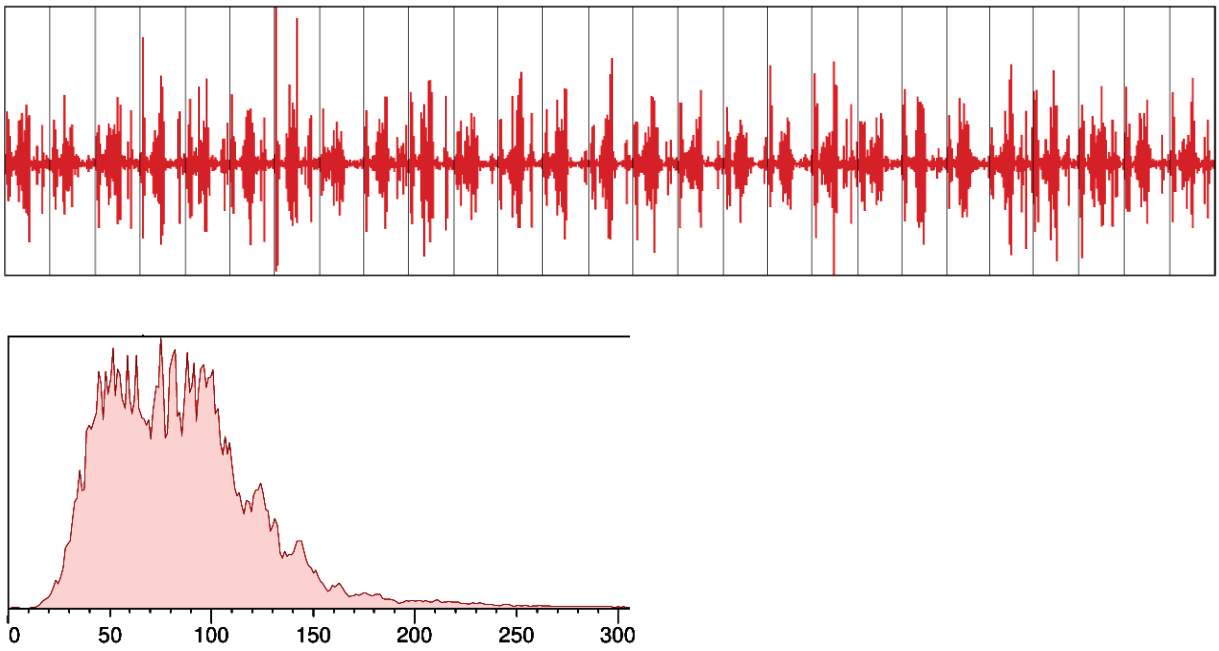

Trapezius

Minute 1

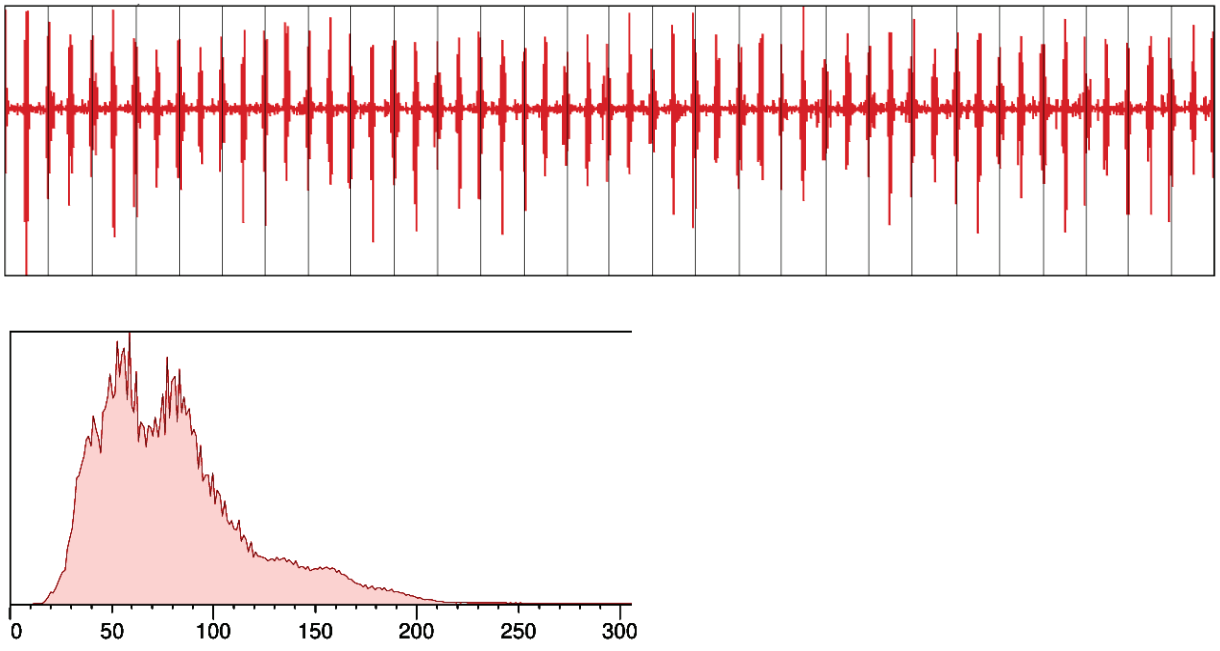

Minute 11

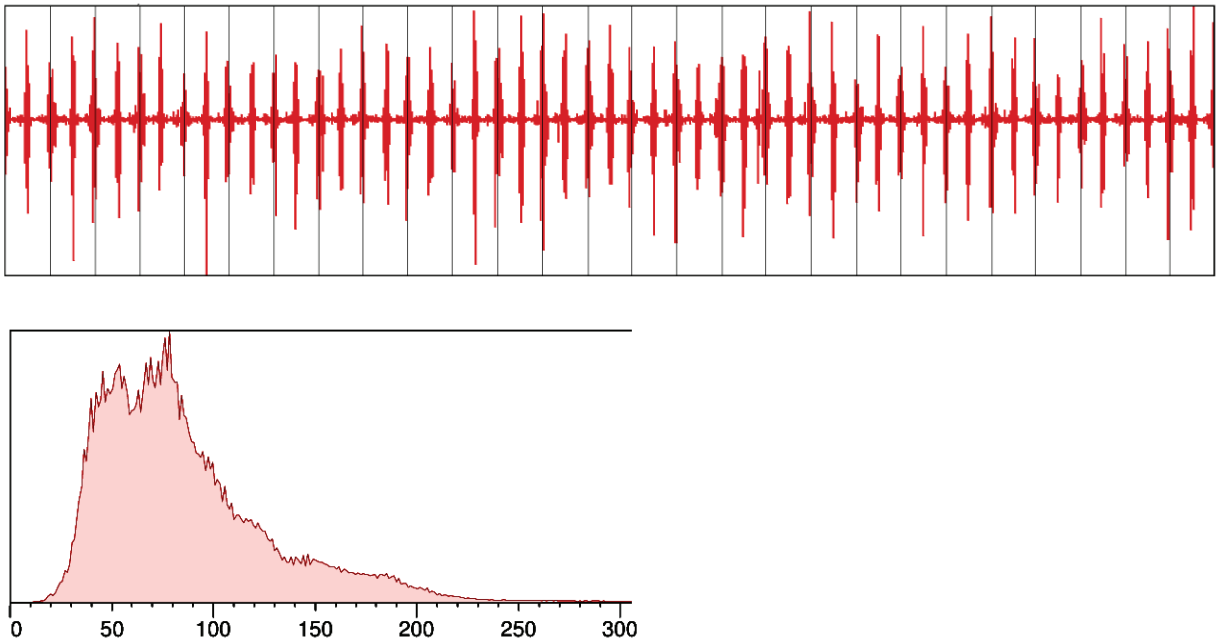

Minute 22

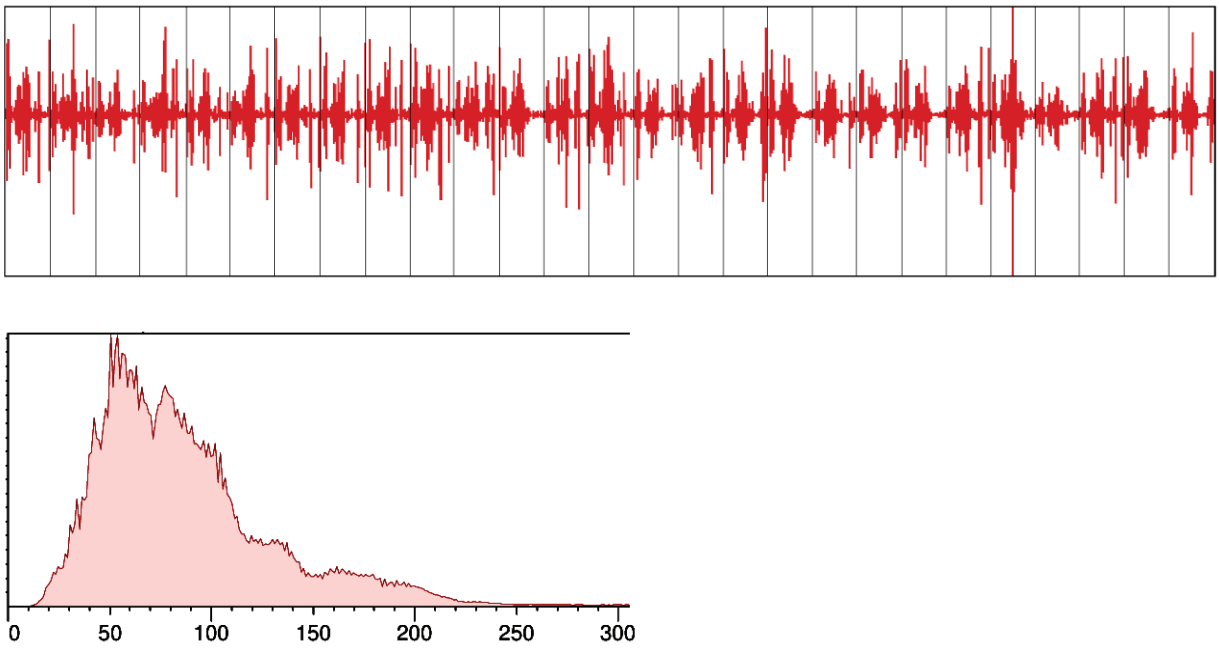

Brachioradialis

Minute 1

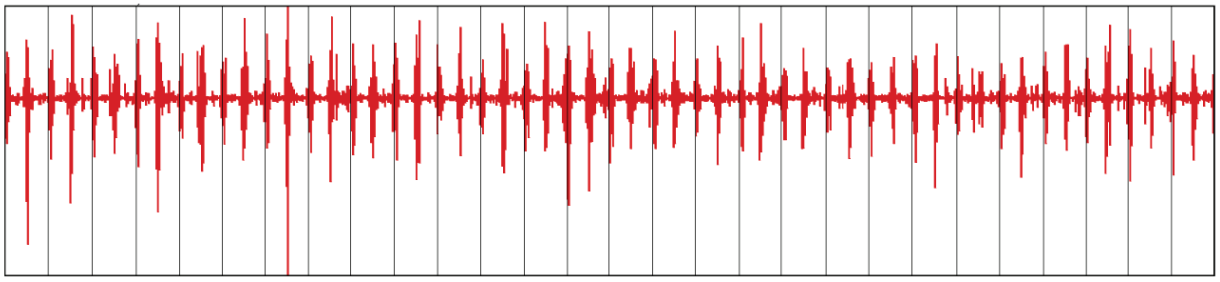

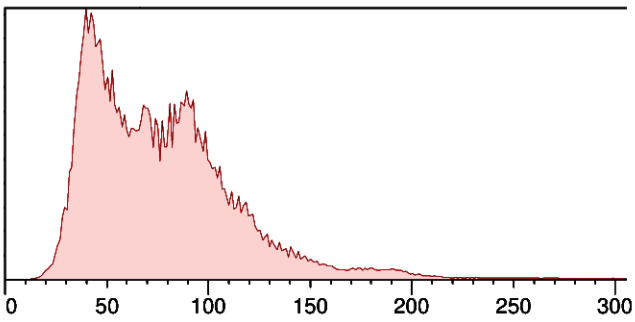

Minute 11

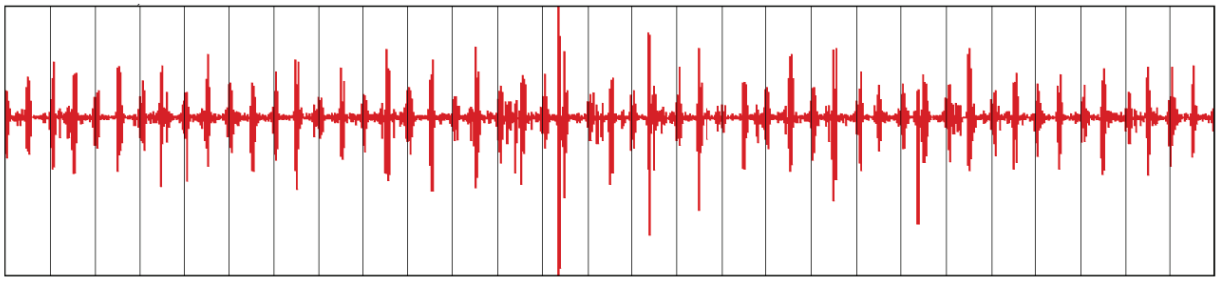

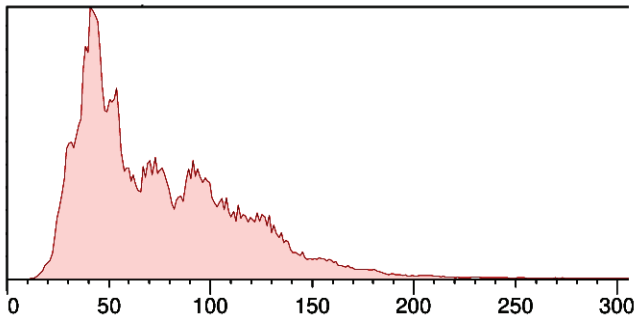

Minute 22

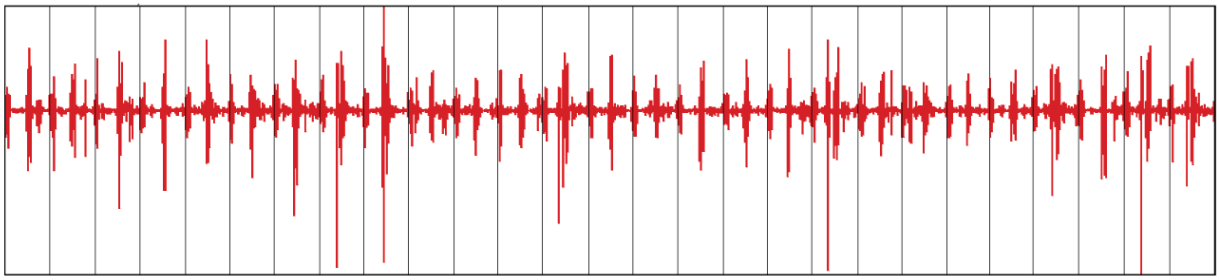

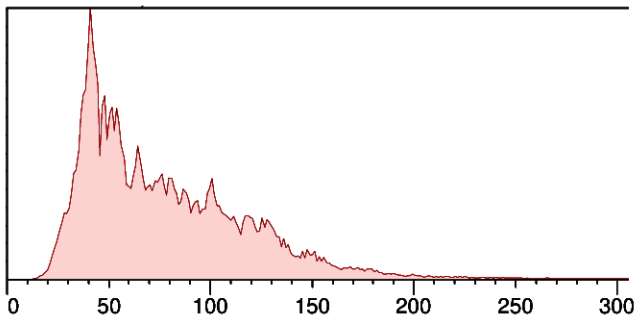

APPENDIX E – NORMATIVE KINEMATIC DATA

An understanding of the temporal patterns of kinematic variables aids in interpreting the kinematic data. Therefore typical data for each kinematic variable are graphically presented for this purpose. The time of contact was determined using accelerometer data. The start of forward swing was defined as the time point of maximum hip extension angle (minimum hip flexion angle)[227]. The start of foot descent was determined as the time point of maximum hip flexion angle[227]. This study was only concerned with maximum and minimum joint angles, and not specific time points, such as the time of impact. Therefore, the exact support period of each stride cycle was estimated, rather than calculated.

The time points of the stride cycle are represented in Figure 28. In this graph, and all graphs, the x-axis represents time as a percentage of total stride cycle duration. The time of contact is represented with red arrows (right foot strike) and blue arrows (left foot strike). The phases of the stride cycle are color coded. Continuous joint angle data are graphed on the y-axis. Positive values represent hip flexion, and negative values represent hip extension, as indicated by the black arrows on the left side of the graph. It should be noted that Left Forward Swing (light yellow) does not begin at 0% of the stride cycle, but rather is a continuation from the previous stride cycle, beginning after the 90% mark.

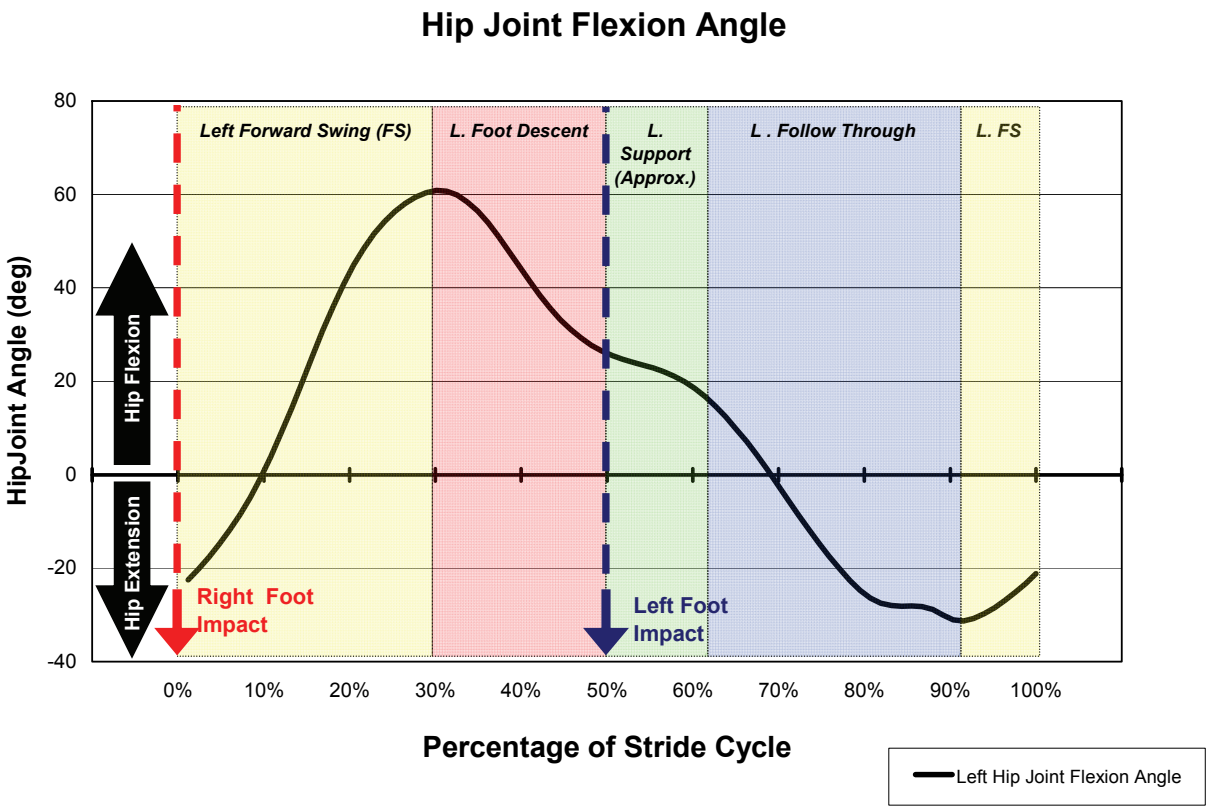

Figure 28 - Typical Hip Flexion Joint Angle Data

Graphs for all other joint angles are presented throughout the rest of this appendix, using a similar format to Figure 28. The joint angle of interest is plotted in a thick continuous black line with values along the primary y-axis. The reference hip flexion angle is plotted on all graphs with a thin dashed line, with values along the secondary y-axis.

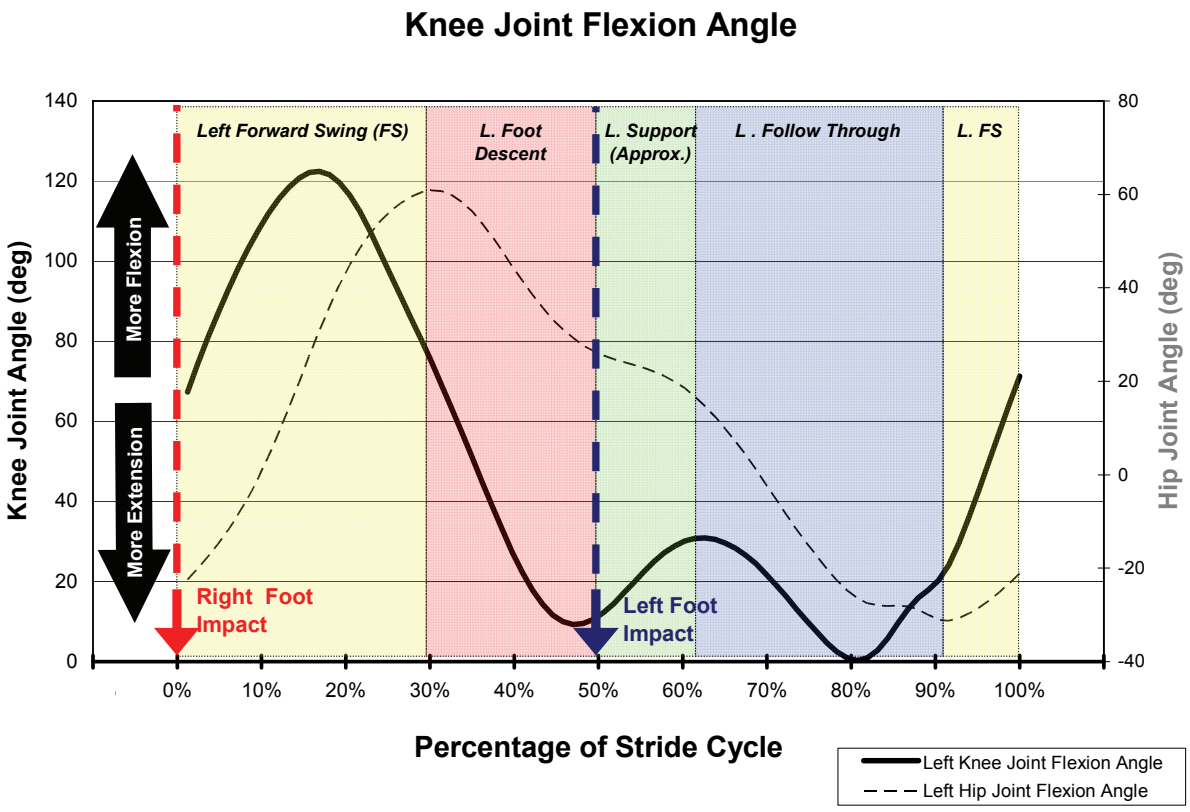

Figure 29 - Typical Knee Flexion Joint Angle

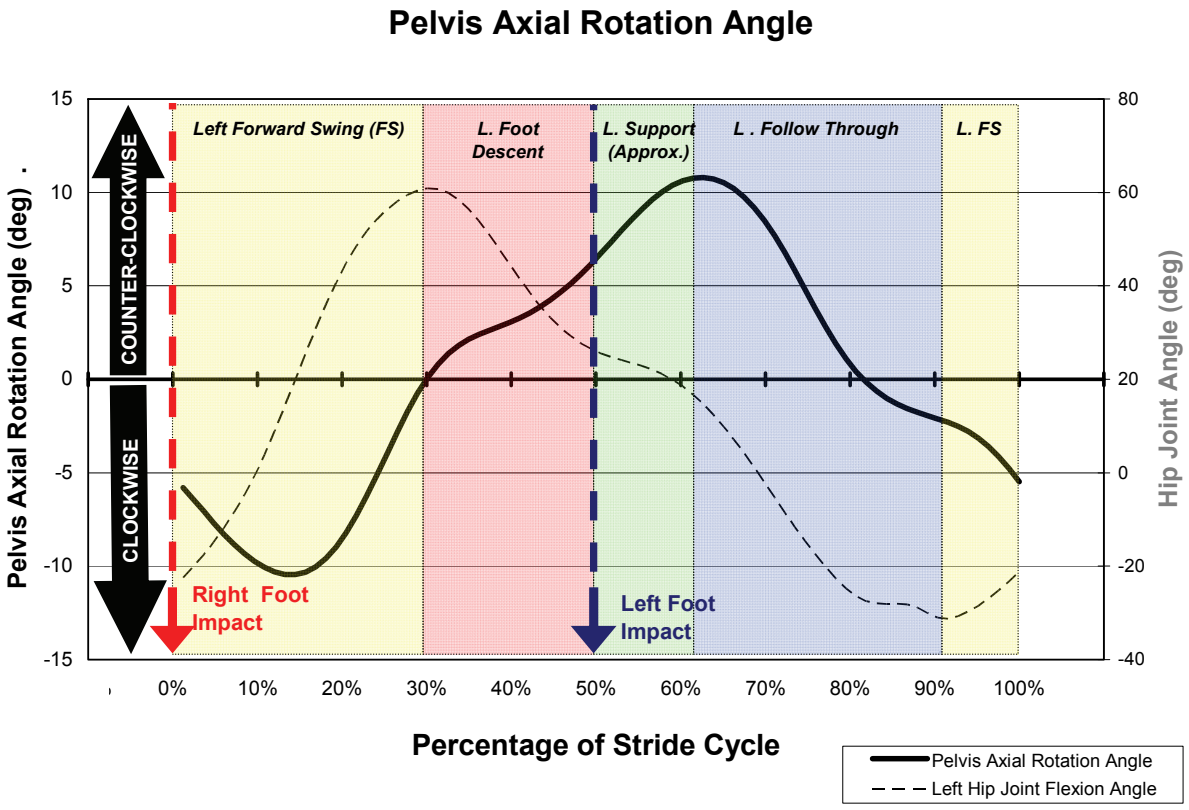

Figure 30 - Typical Pelvis Axial Rotation Data

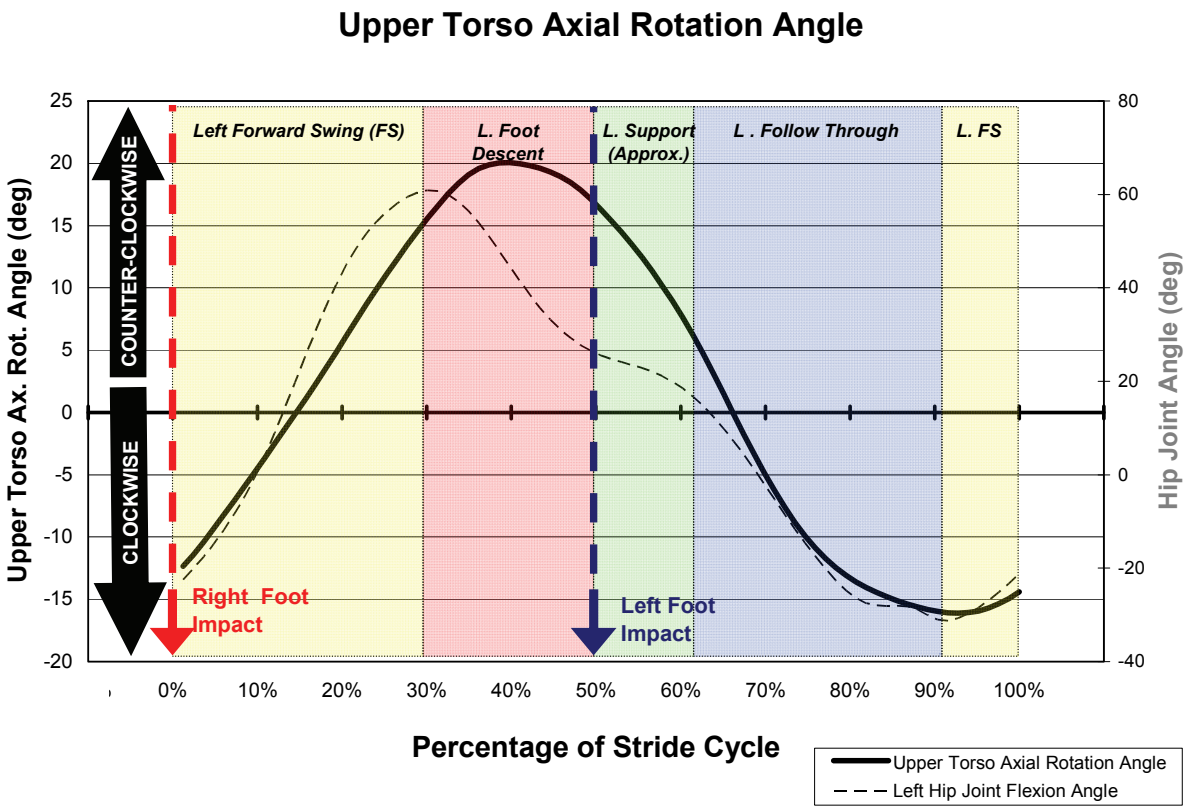

Figure 31 - Typical Upper Torso Axial Rotation Data

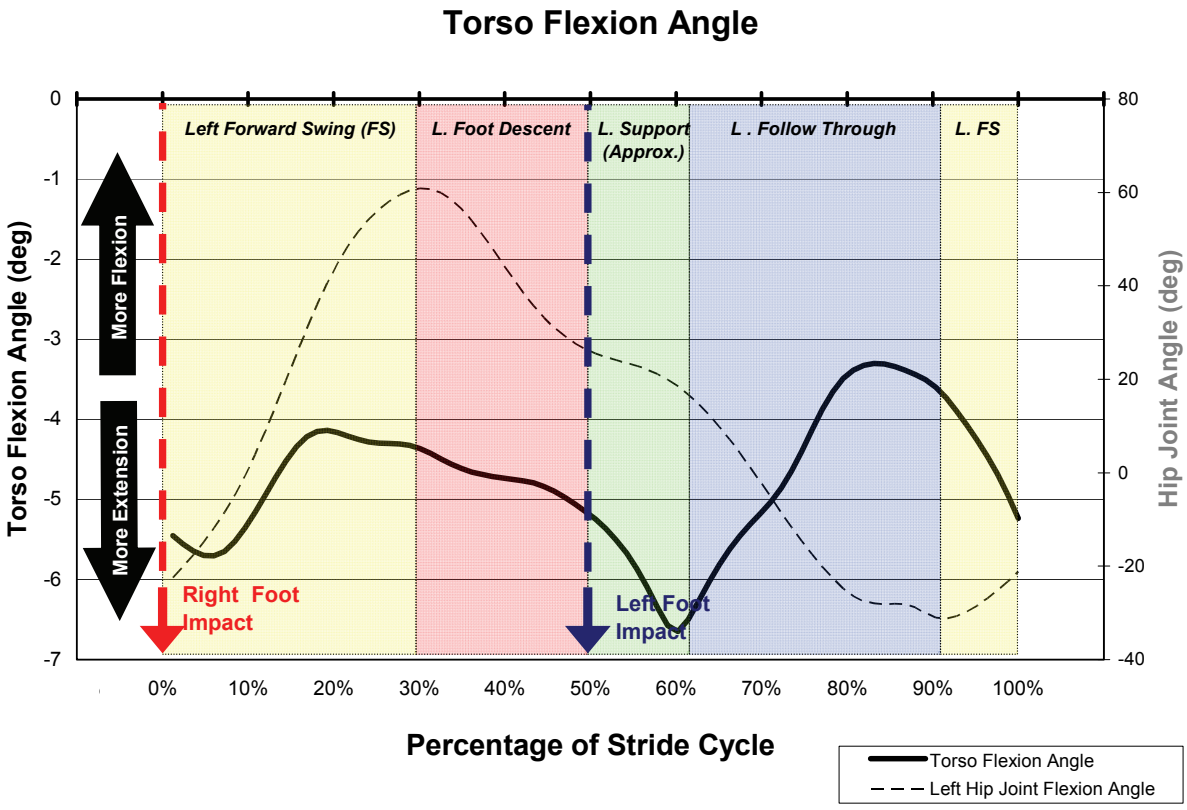

Figure 32 - Typical Torso Flexion Data

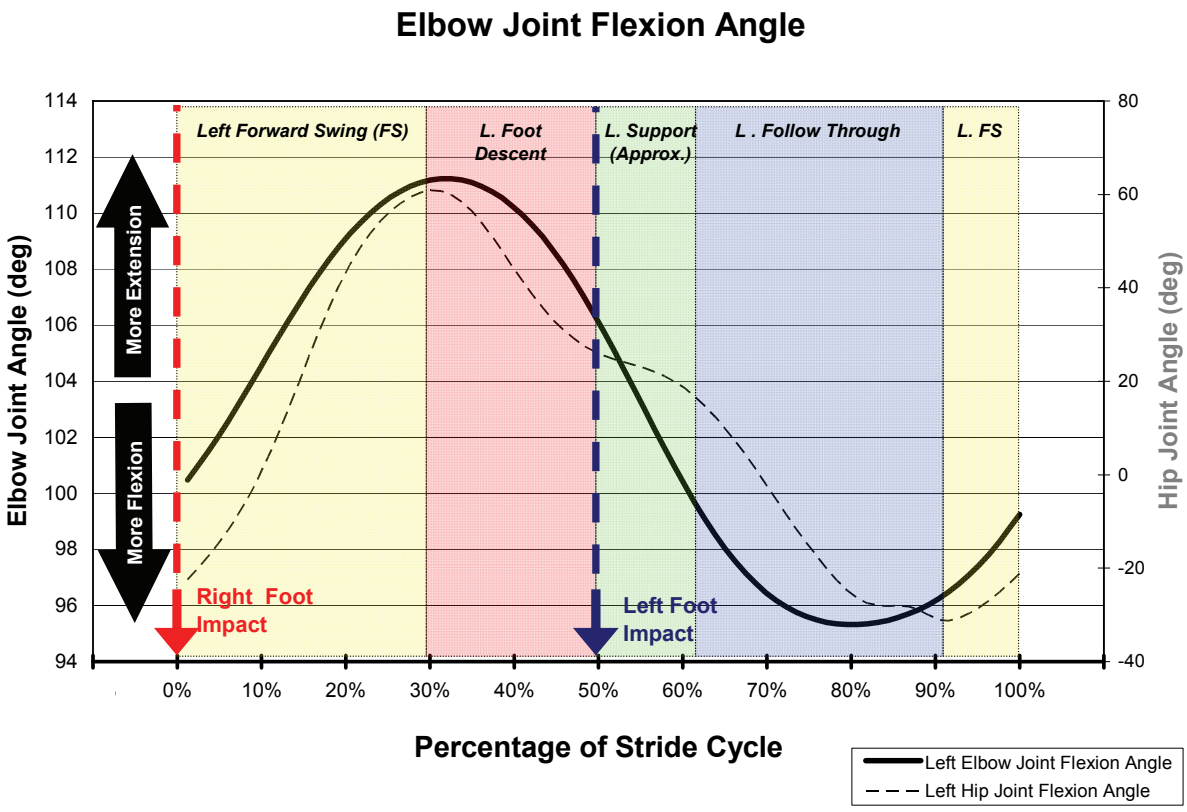

Figure 33 - Typical Elbow Joint Flexion Data

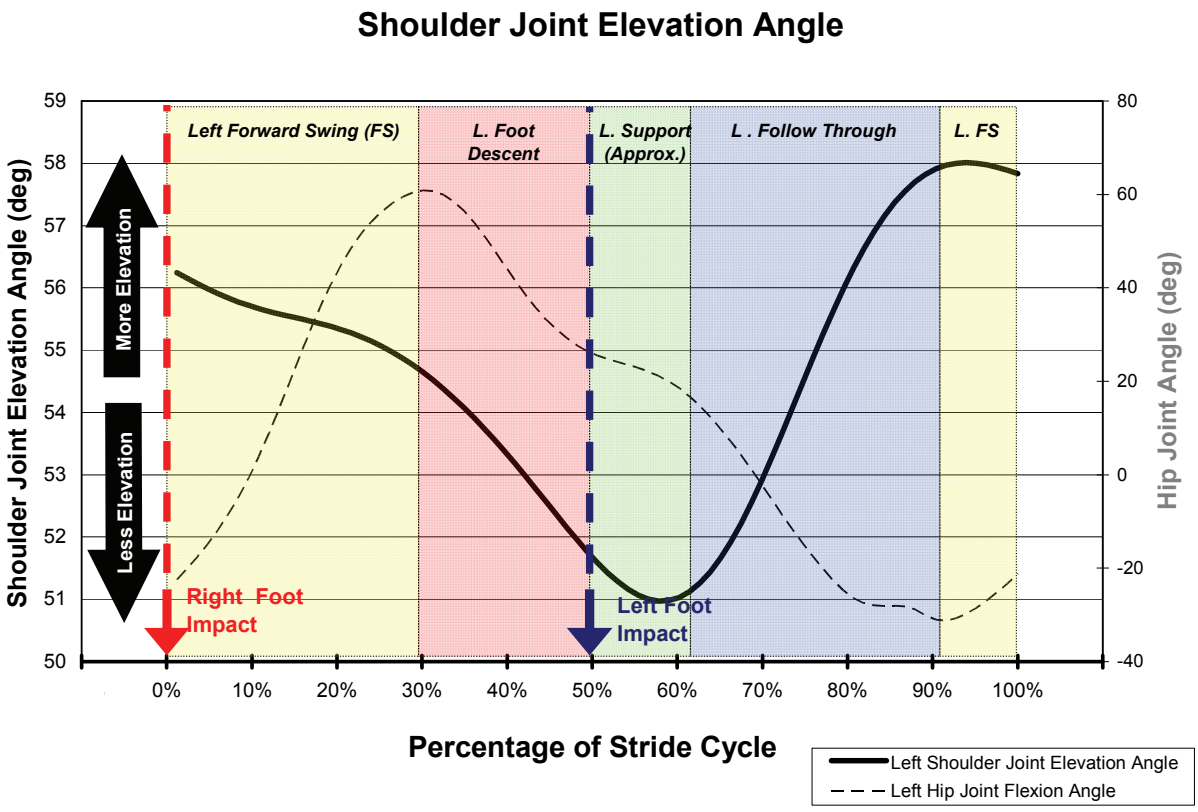

Figure 34 - Typical Shoulder Joint Elevation Angle Data

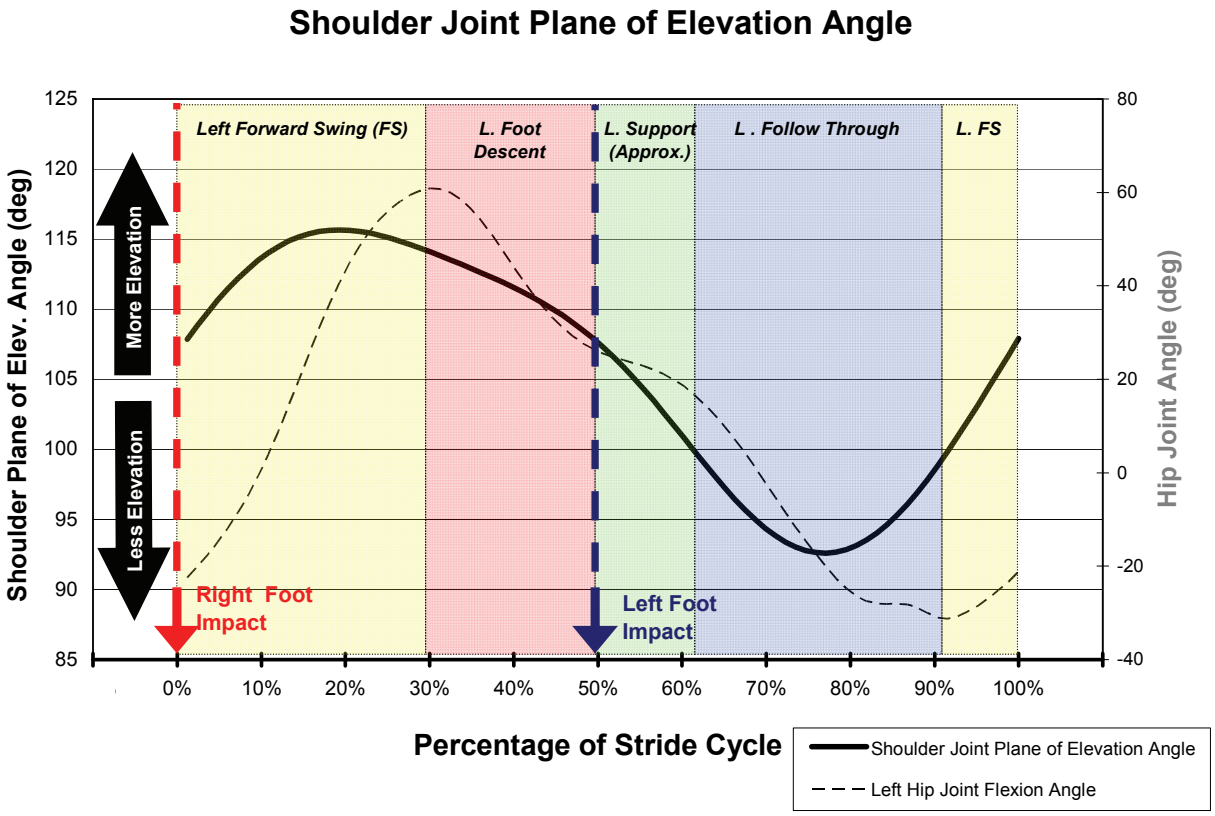

Figure 35 - Typical Shoulder Plane of Elevation Angle Data

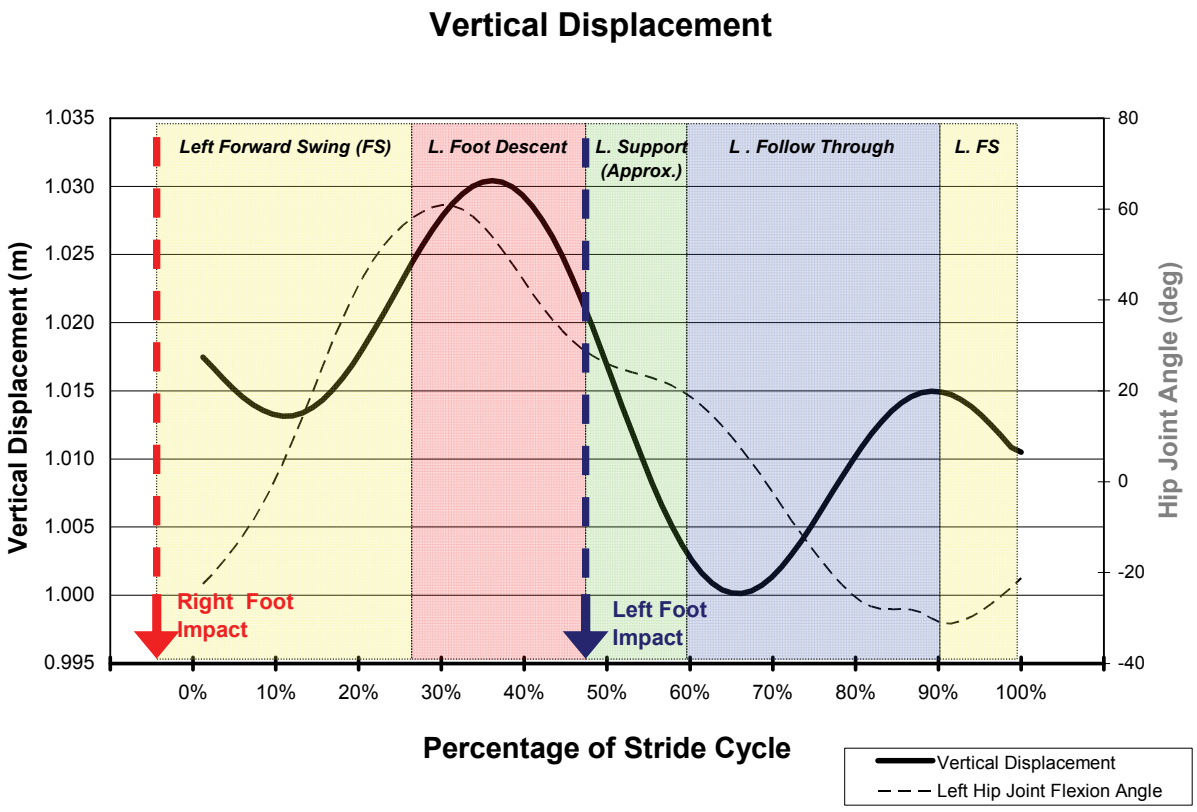

Figure 36 - Typical Vertical Displacement Data

BIBLIOGRAPHY

1. Run stronger, run faster. *Runners World*:50-56, 1997.

2. Abraham, K. A., H. Feingold, D. D. Fuller, M. Jenkins, and J. H. Mateika. Respiratory-related activation of human abdominal muscles during exercise. *Journal of Physiology*. 541:653-663, 2002.

3. Adrian, M. and E. Kreighbaum. Mechanics of distance-running during competition. In *3rd International Seminar on Biomechanics*. Rome: Karger, Basel, pp. 354-358, 1971.

4. Ament, W., G. J. J. Bonga, A. L. Hof, and G. J. Verkerke. Electromyogram median power frequency in dynamic exercise at medium exercise intensities. *European Journal of Applied Physiology*. 74:180-186, 1996.

5. Ament, W., G. J. J. Bonga, A. L. Hof, and G. J. Verkerke. EMG median power frequency in an exhausting exercise. *Journal of Electromyography and Kinesiology*. 3:214-220, 1993.

6. Anderson, T. Biomechanics and running economy. *Sports Medicine*. 22:76-89, 1996.

7. Andersson, E. A., H. Grundstrom, and A. Thorstensson. Diverging intramuscular activity patterns in back and abdominal muscles during trunk rotation. *Spine*. 27:E152-E160, 2002.

8. Andersson, E. A., J. Nilsson, and A. Thorstensson. Intramuscular EMG from the hip flexor muscles during human locomotion. *Acta Physiologica Scandinavica*. 161:361-370, 1997.

9. Andreassen, S. and L. Arendt-Nielsen. Muscle fiber conduction velocity in motor units of human anterior tibial muscle: a new size principle parameter. *Journal of Physiology*. 1:561-571, 1987.

10. Arendt-Nielsen, L. and K. Mills. The relationship between mean power frequency of the EMG spectrum and muscle fiber conduction velocity. *Electroencephalography and Clinical Neurophysiology*. 60:130-134, 1985.

11. Arendt-Nielsen, L. and T. H. Sinkjaer. Quantification of human dynamic muscle fatigue by electromyograph and kinematic profiles. *Journal of Electromyography and Kinesiology*. 1:1-8, 1991.

12. Aristotle. Progression of Animals Cambridge, MA: Harvard University Press, 1961.

13. Armstrong, L. E. and G. Gehlsen. Running mechanics of national class distance runners during a marathon. *Track and Field Quarterly Review*, 1988.

14. Arnaud, S., M. C. Zattara-Hartmann, C. Tomei, and Y. Jammes. Correlation between muscle metabolism and changes in M-wave surface electromyogram: dynamic constant load leg exercise in untrained subjects. *Muscle and Nerve*. 20:1197-1199, 1997.

15. Avogadro, P., A. Dolenec, and A. Belli. Changes in mechanical work during severe exhausting running. *European Journal of Applied Physiology*. 90:165-170, 2003.

16. Avogadro, P., H. Kyrolainen, and A. Belli. Influence of mechanical and metabolic strain on the oxygen consumption slow component during forward pulled running. *European Journal of Applied Physiology*. 93:203-209, 2004.

17. Barnard, J. R., V. R. Edgerton, T. Furukawa, and J. B. Peter. Histochemical, biochemical, and contractile properties of red, white, and intermediate fibers. *American Journal of Physiology*. 220:410-414, 1971.

18. Basmajian, J. V. and C. J. De Luca. *Muscles Alive: Their Functions Revealed by Electromyography*. 5th edition ed. Baltimore: Williams and Wilkins, 1985, 561.

19. Basset, D. R. and E. T. Howley. Limiting factors for maximum oxygen uptake and determinants of endurance performance. *Medicine & Science in Sports & Exercise*. 32:70-80, 2000.

20. Basset, D. R. and E. T. Howley. Maximal oxygen uptake: "classical" versus "contemporary" viewpoints. *Medicine & Science in Sports & Exercise*. 29:591-603, 1997.

21. Bearden, S. E. and R. J. Moffatt. Leg electromyography and the VO2-power relationship during bicycle ergometry. *Medicine & Science in Sports & Exercise*. 33:1241-1245, 2001.

22. Belli, A., H. Kyrolainen, and P. V. Komi. Moment and power of lower limb joints in running. *International Journal of Sports Medicine*. 23:136-141, 2002.

23. Bendahan, D., B. Giannesini, and P. J. Cozzone. Functional investigations of exercising muscle: a noninvasive magnetic resonance spectroscopy-magnetic resonance imaging approach. *Cellular and Molecular Life Sciences*. 61:1001-1015, 2004.

24. Benson, R. Improving your biomechanics. In: *The Running Times Guide to Breakthrough Running*. G. Bakoulis and C. Karu (Eds.) Champagne, IL: Human Kinetics, 2000, pp. 15-23.

25. Bigland-Ritchie, B., E. F. Donovan, and C. S. Roussos. Conduction velocity and EMG power spectrum changes in fatigue of sustained maximal efforts. *Journal of Applied Physiology*. 51:1300-1305, 1981.

26. Bigland-Ritchie, B. and J. J. Wood. Integrated EMG and oxygen uptake during dynamic contractions of human muscles. *Journal of Applied Physiology*. 36:475-479, 1974.

27. Billat, V., P. M. Lepretre, A. M. Heugas, M. H. Laurence, D. Salim, and J. P. Koralsztein. Training and bioenergetic characteristics in elite male and female Kenyan runners. *Medicine & Science in Sports & Exercise*. 35:297-304; discussion 305-296, 2003.

28. Billat, V. L. Interval training for performance: a scientific and empirical practice. Special recommendations for middle- and long-distance running. Part I: Aerobic interval training. *Sports Medicine*. 31:13-31, 2001.

29. Borrani, F., R. Candau, G. Y. Millet, S. Perrey, J. Fuchslocher, and J. D. Rouillon. Is the VO2 slow component dependent on progressive recruitment of fast-twitch fibers in trained runners? *Journal of Applied Physiology*. 90:2212-2220, 2001.

30. Bottinelli, R., M. Canepari, M. A. Pellegrino, and C. Reggiani. Force-velocity properties of human skeletal muscle fibres: myosin heavy chain isoform and temperature dependence. *Journal of Physiology*. 495:573-586, 1996.

31. Bouissou, P., P. Y. Estrade, F. Goubel, C. Y. Guezennec, and B. Serrurier. Surface EMG power spectrum and intramuscular pH in human vastus lateralis muscle during dynamic exercise. *Journal of Applied Physiology*. 67:1245-1249, 1989.

32. Bourdin, M. A., A. Belli, L. M. Arsac, C. Bosco, and J. R. Lacour. Effect of vertical loading on energy cost and kinematics of running in trained male subjects. *Journal of Applied Physiology*. 79:2078-2085, 1995.

33. Brody, L. R., M. T. Pollock, S. H. Roy, C. J. De Luca, and B. Celli. pH-induced effects of median frequency and conduction velocity of the myoelectric signal. *Journal of Applied Physiology*. 71:1878-1885, 1991.

34. Brown, D. A. Muscle: The ultimate force generator in the body. In: *Kinesiology of the Musculoskeletal System: Foundations to Physical Rehabilitation*. D. A. Neumann (Ed.) St. Louis, MO: Mosby, Inc., 2002.

35. Brozek, J., E. Grande, J. T. Anderson, and A. Keys. Densitometric analysis of body composition: revision of some quantitative assumptions. *Annals of the New York Academy of Science*. 110:113-140, 1963.

36. Buckalew, D. P., D. A. Barlow, J. W. Fischer, and J. G. Richards. Biomechanical profile of elite women marathoners.330-340.

37. Burke, R. E., D. N. Levine, F. E. Zajac, P. Tsairis, and W. K. Engel. Mammalian motor units: physiological-histochemical correlation in three types in cat gastrocnemius. *Science*. 174:709-712, 1971.

38. Cairns, S. P., A. J. Knicker, M. W. Thompson, and G. Sjogaard. Evaluation of models used to study neuromuscular fatigue. *Exercise and Sports Science Reviews*. 33:9-16, 2005.

39. Campbell, A. Build a better body. *Runners World*:74-79, 2005.

40. Candau, R., A. Belli, G. Y. Millet, D. Georges, B. Barbier, and J. D. Rouillon. Energy cost and running mechanics during a treadmill run to voluntary exhaustion in humans. *European Journal of Applied Physiology*. 77:479-485, 1998.

41. Cappellini, G., Y. P. Ivanenko, R. E. Poppele, and F. Lacquaniti. Motor patterns in human walking and running. *Journal of Neurophysiology*. 95:3426-3437, 2006.

42. Cappozzo, A. Force actions in the human trunk during running. *Journal of Sports Medicine*. 23:14-22, 1983.

43. Caputo, F. and B. S. Denadai. Effects of aerobic endurance training status and specificity on oxygen uptake kinetics during maximal exercise. *European Journal of Applied Physiology*. 93:87-95, 2004.

44. Cavagna, G. A. Force platforms as ergometers. *Journal of Applied Physiology*. 39:174-179, 1975.

45. Cavagna, G. A. and M. Kaneko. Mechanical work and efficiency in level walking and running. *Journal of Physiology*. 268:467-481, 1977.

46. Cavanagh, P. R. and R. Kram. The efficiency of human movement - a statement of the problem. *Medicine and science in sports and exercise*. 17:304-308, 1985.

47. Cavanagh, P. R. and R. Kram. Mechanical and muscular factors affecting the efficiency of human movement. *Medicine & Science in Sports & Exercise*. 17:326-331, 1985.

48. Chandler, R. F., C. E. Clauser, J. T. McConville, H. M. Reynolds, and J. W. Young. *Investigation of inertial properties of the human body (Aerospace Medical Research Laboratory Tech. Rep. No. 74-137)*. Dayton, OH: Wright-Patterson Air Force Base, AMRL, 1975.

49. Chao, E. Y. Justification of triaxial goniometer for the measurement of joint rotation. *Journal of Biomechanics*. 13:989-1006, 1980.

50. Charlton, C. G., B. Crowell, Jr., and R. Benson. Identification of motor neurons for accessory muscles of inspiration and expiration, pectoralis, trapezius and external oblique: comparison with non-respiratory skeletal muscle. *Synapse*. 2:219-224, 1988.

51. Cheng, C. P., R. J. Herfkens, and C. A. Taylor. Comparison of abdominal aortic hemodynamics between men and women at rest and during lower limb exercise. *Journal of Vascular Surgery*. 37:118-123, 2003.

52. Cohen, J., P. Cohen, S. G. West, and L. S. Aiken. *Applied multiple regression/correlation analysis for the behavioral sciences*. 3rd ed. Hillsdale, NJ: Lawrence Erlbaum Associates, 2003

53. Conley, D. L. and G. S. Krahenbuhl. Running economy and distance running performance of highly trained athletes. *Medicine & Science in Sports & Exercise*. 12:357-360, 1980.

54. Conley, K. E., W. F. Kemper, and G. J. Crowther. Limits to sustainable muscle performance: interaction between glycolysis and oxidative phosphorylation. *Journal of Experimental Biology*. 204:3189-3194, 2001.

55. Costill, D. L., J. Daniels, W. Evans, W. Fink, G. Krahenbuhl, and B. Saltin. Skeletal muscle enzymes and fiber composition in male and female track athletes. *Journal of Applied Physiology*. 40:149-154, 1976.

56. Costill, D. L., W. J. Fink, and M. L. Polock. Muscle fiber composition and enzyme activities of elite distance runners. *Medicine and Science in Sports*. 8:96-100, 1976.

57. Cromwell, R. L., T. K. Aadland-Monahan, A. T. Nelson, S. M. Stern-Sylvestre, and B. Seder. Sagittal plane analysis of head, neck, and trunk kinematics and electromyographic activity during locomotion. *Journal of Orthopaedic and Sports Physical Therapy*. 31:255-262, 2001.

58. Crouter, S., C. Foster, P. Esten, G. Brice, and J. P. Porcari. Comparison of incremental treadmill exercise and free range running. *Medicine & Science in Sports & Exercise*. 33:644-647, 2001.

59. Cureton, K. J. and P. B. Sparling. Distance running performance and metabolic responses to running in men and women with excess weight experimentally equated. *Medicine & Science in Sports & Exercise*. 12:288-294, 1980.

60. Daanen, H. A. M., M. Mazure, M. Holewijn, and E. A. Van Der Velde. Reproducibility of the mean power frequency of the surface electromyogram. *European Journal of Applied Physiology*. 61:274-277, 1990.

61. Dabaere, F., S. P. Swinnen, E. Beatse, S. Sunaert, P. Van Hecke, and J. Duysens. Brain areas involved in interlimb coordination: a distributed network. *NeuroImage*. 14:947-958, 2001.

62. Daniels, J. *Daniels' Running Formula*. Champaign, IL: Human Kinetics, 1998, 287.

63. Daniels, J. A physiologist's view of running economy. *Medicine & Science in Sports & Exercise*. 17:332-338, 1985.

64. Davis, J. A. and V. A. Convertino. A comparison of heart rate methods for predicting endurance training intensity. *Medicine and Science in Sports*. 7:295-298, 1975.

65. Davis, M. J. and S. P. Bailey. Possible mechanisms of central nervous fatigue during exercise. *Medicine & Science in Sports & Exercise*. 29:45-57, 1997.

66. de Leva, P. Joint center longitudinal positions computed from a select subset of Chandler's data. *Journal of Biomechanics*. 29:1231-1233, 1996.

67. De Luca, C. J. Myoelectrical manifestations of localized muscular fatigue in humans. *CRC Critival Reviews in Biomedical Engineering*. 11:251-279, 1985.

68. De Luca, C. J. The use of surface electromyography in biomechanics. *Journal of Applied Biomechanics*. 13:135-163, 1997.

69. De Luca, C. J., R. S. LeFever, M. P. McCue, and A. P. Xenakis. Behaviour of human motor units in different muscles during linearly varying contractions. *Journal of Physiology*. 329:113-128, 1982.

70. De Luca, C. J., A. M. Roy, and Z. Erim. Synchronization of motor firings in human muscles. *Journal of Neurophysiology*. 70:2010-2023, 1993.

71. Derrick, T. R., D. Dereu, and S. P. McLean. Impacts and kinematic adjustments during an exhaustive run. *Medicine & Science in Sports & Exercise*. 34:998-1002, 2002.

72. Desmedt, J. E. and E. Godaux. Ballistic contractions in man: characteristic recruitment pattern of single motor units of the tibialis anterior muscle. *Journal of Physiology*. 264:673-693, 1977.

73. Dietz, V., K. Fouad, and C. M. Bastiaanse. Neuronal coordination of arm and leg movements during human locomotion. *European Journal of Neuroscience*. 14:1906-1914, 2001.

74. Diss, C. E. The reliability of kinetic and kinematic variables used to analyse normal running gait. *Gait & Posture*. 14:98-103, 2001.

75. Duchateau, J. and K. Hainaut. Electrical and mechanical failures during sustained and intermittent contractions in humans. *Journal of Applied Physiology*. 58:942-947, 1985.

76. Duffield, R., B. Dawson, and C. Goodman. Energy system contribution to 1500- and 3000-metre track running. *Journal of Sports Sciences*. 23:993-1002, 2005.

77. Duffield, R., B. Dawson, H. C. Pinnington, and P. Wong. Accuracy and reliability of a Cosmed K4b2 portable gas analysis system. *Journal of Science and Medicine in Sport*. 7:11-22, 2004.

78. Dutto, D. J. and G. A. Smith. Changes in spring-mass characteristics during treadmill running to exhaustion. *Medicine & Science in Sports & Exercise*. 34:1324-1331, 2002.

79. Eberstein, A. and R. Beattie. Simultaneous measurement of muscle conduction velocity and EMG power spectrum changes during fatigue. *Muscle and Nerve*. 8:768-773, 1985.

80. Egbuono, M. E., P. R. Cavangah, and T. A. Miller. Degradation of running economy through changes in running mechanics. *Medicine & Science in Sports & Exercise*. 22:S17, 1990.

81. Eisenmann, J. C., N. Brisko, D. Shadrick, and S. Welsh. Comparative analysis of the Cosmed Quart b2 and K4b2 gas analysis during submaximal exercise. *Journal of Sports Medicine and Physical Fitness*. 43:150-155, 2003.

82. Eldgerton, V., J. Smith, and D. Simpson. Muscle fiber type populations of human leg muscles. *Histochemical Journal*. 7:259-266, 1975.

83. Elliot, B. and T. Ackland. Biomechanical effects of fatigue on 10,000 meter running technique. *Research Quarterly for Exercise and Sport*. 52:160-166, 1981.

84. Elliot, B. C. and A. D. Roberts. A biomechanical evaluation of the role of fatigue in middle-distance running. *Canadian Journal of Applied Sports Science*. 5:203-207, 1980.

85. Elliott, B. C. and B. A. Blanksby. A cinematographic analysis of overground and treadmill running by males and females. *Medicine and Science in Sports*. 8:84-87, 1976.

86. Elliott, B. C. and B. A. Blanksby. The synchronization of muscle activity and body segment movements during a running cycle. *Medicine and Science in Sports*. 11:322-327, 1979.

87. Enoka, R. M. *Neuromechanics of Human Movement*. 3rd Edition ed. Champaign, IL: Human Kinetics, 2002.

88. Enoka, R. M., G. A. Robinson, and A. R. Kossev. Task and fatigue effects on low-threshold motor units in human hand muscle. *Journal of Neurophysiology*. 62:1344-1359, 1989.

89. Enoka, R. M. and D. G. Stuart. Neurobiology of muscle fatigue. *Journal of Applied Physiology*. 72:1631-1648, 1992.

90. Fenn, W. O. Work against gravity and work due to velocity changes in running: movements of the center of gravity within the body and foot pressure on the ground. *American Journal of Physiology*. 93:433-462, 1930.

91. Finni, T., H. Kyrolainen, J. Avela, and P. V. Komi. Maximal but not submaximal performance is reduced by constant-speed 10-km run. *Journal of Sports Medicine and Physical Fitness*. 43:411-417, 2003.

92. Fitts, R. H. Cellular mechanisms of muscle fatigue. *Physiological Reviews*. 74:49-94, 1994.

93. Fitts, R. H. and J. O. Holloszy. Lactate and contractile force in frog muscle during development of fatigue. *American Journal of Physiology*. 231:430-433, 1976.

94. Gamet, D., J. Duchene, C. Garapon-bar, and F. Goubel. Surface electromyogram power spectrum in human quadriceps muscle during incremental exercise. *Journal of Applied Physiology*. 74:2704-2710, 1993.

95. Gamet, D., J. Duchene, and F. Goubel. Reproducibility of kinetics of electromyogram spectrum parameters during dyanmic exercise. *European Journal of Applied Physiology*. 74:504-510, 1996.

96. Gandevia, S. C., D. K. McKenzie, and I. R. Neering. Endurance properties of respiratory and limb muscles. *Respiration Physiology*. 53:47-61, 1983.

97. Gantchev, N., A. Kossev, A. Gydikov, and Y. Gerasimenko. Relation between the motor units recruitment threshold and their potentials propagation velocity at isometric activity. *Electromyography and Clinical Neurophysiology*. 32:221-228, 1992.

98. Gardner-Morse, M. G. and I. A. F. Stokes. The effects of abdominal muscle coactivation on lumbar spine stability. *Spine*. 23:86-91, 1998.

99. Garland, S. W., D. J. Newham, and D. L. Turner. The amplitude of the slow component of oxygen uptake is related to muscle contractile properties. *European Journal of Applied Physiology*. 91:192-198, 2004.

100. Gass, G. C., S. Rogers, and R. Mitchell. Blood lactate concentration following maximum exercise in trained subjects. *British Journal of Sports Medicine*. 15:172-176, 1981.

101. Gazeau, F., J. P. Koralsztein, and V. Billat. Biomechanical events in the time to exhaustion at maximal aerobic speed. *Archives of Physiology and Biochemistry*. 105:583-590, 1997.

102. Gerlach, K. E., S. C. White, H. W. Burton, J. M. Dorn, J. J. Leddy, and P. J. Horvath. Kinetic changes with fatigue and relationship to injury in female runners. *Medicine & Science in Sports & Exercise*. 37:657-663, 2005.

103. Giannesini, B., P. J. Cozzone, and D. Bendahan. Non-invasive investigations of muscular fatigue: metabolic and electromyographic components. *Biochimie*. 85:873-883, 2003.

104. Glass, G. V. and K. D. Hopkins. *Statistical Methods in Education and Psychology*. 3rd ed. Boston: Allyn and Bacon, 1995.

105. Gollnick, P. D., R. B. Armstrong, C. W. Saubert, K. Piehl, and B. Saltin. Enzyme activity and fiber composition in skeletal muscle of untrained and trained men. *Journal of Applied Physiology*. 33:312-319, 1972.

106. Gomez, A. L., R. J. Radzwich, C. R. Denegar, J. S. Volek, M. R. Rubin, J. A. Bush, B. K. Doan, R. B. Wickham, S. A. Mazzetti, R. U. Newton, D. N. French, K. Hakkinen, N. A. Ratamess, and W. J. Kraemer. The effects of a 10-kilometer run on muscle strength and power. *Journal of Strength and Conditioning Research*. 16:184-191, 2002.

107. Green, H. J. and A. E. Patla. Maximal aerobic power: neuromuscular and metabolic considerations. *Medicine & Science in Sports & Exercise*. 24:38-46, 1992.

108. Grood, E. S. and W. J. Suntay. A joint coordinate system for the clinical description of three-dimensional motions: application to the knee. *J Biomech Eng*. 105:136-144, 1983.

109. Hagberg, M. and B. E. Ericson. Myoelectric power spectrum dependence on muscular contraction level of elbow flexors. *European Journal of Applied Physiology and Occupational Physiology*. 48:147-156, 1982.

110. Hanon, C., C. Thepaut-Mathieu, C. Hausswirth, and J. M. LeChevlaier. Electromyogram as an indicator of neuromuscular fatigue during incremental exercise. *European Journal of Applied Physiology*. 78:315-323, 1998.

111. Hanon, C., C. Thepaut-Mathieu, and H. Van De Walle. Determination of muscular fatigue in elite runners. *European Journal of Applied Physiology*. 94:118-125, 2005.

112. Haridas, C. and E. P. Zehr. Coordinated interlimb compensatory responses to electrical stimulation of cutaneous nerves in the hand and foot during walking. *Journal of Neurophysiology*. 90:2850-2861, 2003.

113. Hausswirth, C., A. X. Bigard, and C. Y. Guezennec. Relationships between running mechanics and energy cost of running at the end of a triathlon and a marathon. *International Journal of Sports Medicine*. 18:330-339, 1997.

114. Hausswirth, C., J. Brisswalter, J. M. Vallier, D. Smith, and R. Lepers. Evolution of electromyographic signal, running economy, and perceived exertion during different prolonged exercises. *International Journal of Sports Medicine*. 21:429-436, 2000.

115. Hayes, P. R., S. J. Bowen, and E. J. Davies. The relationships between local muscular endurance and kinematic changes during a run to exhaustion at vVO2max. *Journal of Strength and Conditioning Research*. 18:898-903, 2004.

116. Heise, G. and P. E. Martin. "Leg spring" characteristics and the aerobic demand of running. *Medicine & Science in Sports & Exercise*. 30:750-754, 1998.

117. Henneman, E., G. Somjen, and D. O. Carpenter. Excitability and inhibility of motoneurones of different sizes. *Journal of Neurophysiology*. 28:599-620, 1965.

118. Henneman, E., G. Somjen, and D. O. Carpenter. Functional significance of cell size on spinal motoneurons. *Journal of Neurophysiology*. 28:560-580, 1965.

119. Hickner, R. C., P. M. Mehta, D. Dyck, P. DeVita, J. A. Houmard, T. Koves, and P. Byrd. Relationship between fat-to-fat-free mass ratio and decrements in leg strength after downhill running. *Journal of Applied Physiology*. 90:1334-1341, 2001.

120. Hickson, R. C., M. A. Rosenkoetter, and M. M. Brown. Strength training effects on aerobic power and short-term endurance. *Medicine & Science in Sports & Exercise*. 12:336-339, 1980.

121. Hill, A. V., C. N. H. Long, and H. Lupton. Muscular exercise, lactic acid, and the supply and utilization of oxygen. Part I-III. *Proceedings of the Royal Society B*. 96:438, 1924.

122. Hinrichs, R. N. Case studies of asymmetrical arm action in running. *International Journal of Sport Biomechanics*. 8:129-144, 1992.

123. Hinrichs, R. N. Upper extremity function in distance running. In: *Biomechanics of Distance Running*. P. R. Cavanagh (Ed.) Champaign, IL: Human Kinetics Books, 1990, pp. 107-133.

124. Hinrichs, R. N. Upper extremity function in running. II: Angular momentum considerations. *International Journal of Sport Biomechanics*. 3:242-263, 1987.

125. Hinrichs, R. N., P. R. Cavanagh, and K. R. Williams. Upper extremity function in running. I: Center of mass and propulsion considerations. *International Journal of Sport Biomechanics*. 3:222-241., 1987.

126. Hochachka, P. W. and C. L. Beatty. Patterns of control of maximum metabolic rate in humans. *Compartive Biochemistry and Physiology Part A*. 136:215-225, 2003.

127. Hodges, P. Preparatory trunk motion accompanies rapid upper limb movement. *Experimental Brain Research*. 124:69-79, 1999.

128. Holloszy, J. O. and E. F. Coyle. Adaptations of skeletal muscle to endurance exercise and their metabolic consequences. *Journal of Applied Physiology*. 56:831-838, 1984.

129. Honig, C. R., R. J. Connett, and T. E. J. Gayeski. O2 transport and its interaction with metabolism; a systems view of aerobic capacity. *Medicine & Science in Sports & Exercise*. 24:47-53, 1992.

130. Horita, T. and T. Ishiko. Relationships between muscle lactate accumulation and surface EMG activities during isokinetic contractions in man. *European Journal of Applied Physiology and Occupational Physiology*. 56:18-23, 1987.

131. Houtman, C. J., D. F. Stegeman, J. P. Van Dijk, and M. J. Zwarts. Changes in muscle fiber conduction velocity indicate recruitment of distinct motor unit populations. *Journal of Applied Physiology*. 95:1045-1054, 2003.

132. Huang, H. J. and D. P. Ferris. Neural coupling between upper and lower limbs during recumbent stepping. *Journal of Applied Physiology*. 97:1299-1308, 2004.

133. Hug, F., P. Decherchi, T. Marqueste, and Y. Jammes. EMG versus oxygen uptake during cycling exercise in trained and untrained subjects. *Journal of Electromyography and Kinesiology*. 14:187-195, 2004.

134. Hug, F., M. Faucher, N. Kipson, and Y. Jammes. EMG signs of neuromuscular fatigue related to the ventilatory threshold during cycling exercise. *Clinical Physiology and Functional Imaging*. 23:208-214, 2003.

135. Jackson, K. M., J. Joseph, and S. J. Wyard. A mathematical model of arm swing during human locomotion. *Journal of Biomechanics*. 11:277-289, 1978.

136. James, S. L. and C. E. Brubaker. Running mechanics. *Journal of the American Medical Association*. 221:1014-1016, 1972.

137. Jammes, Y., F. Caquelard, and M. Badier. Correlation between surface electromyogram, oxygen uptake, and blood lactate concentration during dynamic leg exercises. *Respiration Physiology*. 112:167-174, 1998.

138. Jammes, Y., M. C. Zattara-Hartmann, F. Caquelard, S. Arnaud, and C. Tomei. Electromyographic changes in vastus lateralis during dynamic exercise. *Muscle and Nerve*. 20:247-249, 1997.

139. Jang, J., E. C. Chaloupka, M. A. Mastrangelo, G. B. Biren, and R. J. Robertson. Physiological comparisons among three maximal treadmill exercise protocols in trained and untrained individuals. *European Journal of Applied Physiology*. 84:291-295, 2001.

140. Jansen, R., W. Ament, G. J. Verkerke, and A. L. Hof. Median power frequency of the surface electromyogram and blood lactate concentration in incremental cycle ergometry. *European Journal of Applied Physiology*. 75:102-108, 1997.

141. Johnston, R. E., T. J. Quiin, R. Kertzer, and N. B. Vroman. Improving running economy through strength training. *Strength and Conditioning*. 17:7-12, 1995.

142. Jones, A. M. and J. H. Doust. A 1% treadmill grade most accurately reflects the energetic cost of outdoor running. *Journal of Sports Sciences*. 14:321-327, 1996.

143. Juel, C. Potassium and sodium shifts during in vitro isometric muscle recovery. *European Journal of Physiology*. 406:458-463, 1986.

144. Kadaba, M. P., H. K. Ramakrishnan, M. E. Wootten, J. Gainey, G. Gorton, and G. V. B. Cochran. Repeatability of kinematic, kinetic, and electromyographic data in normal adult gait. *Journal of Orthopaedic Research*. 7:849-860, 1989.

145. Kang, J., E. C. Chaloupka, M. A. Mastrangelo, G. B. Biren, and R. J. Robertson. Physiological comparisons among three maximal treadmill exercise protocols in trained and untrained individuals. *European Journal of Applied Physiology*. 84:291-295, 2001.

146. Kanosue, K., M. Yoshida, K. Akazawa, and K. Fujii. The number of active motor units and their firing rates in voluntary contractions of the human brachialis muscle. *Japanese Journal of Physiology*. 29:427-443, 1979.

147. Karamanidis, K., A. Arampatzis, and G.-P. Bruggemann. Symmetry and reproducibility of kinematic parameters during various running techniques. *Medicine & Science in Sports & Exercise*. 35:1009-1016, 2003.

148. Kayser, B. Exercise starts and ends in the brain. *European Journal of Applied Physiology*. 90:411-419, 2003.

149. Kirkendall, D. T. Mechanisms of peripheral fatigue. *Medicine & Science in Sports & Exercise*. 22:444-449, 1990.

150. Kranz, H., A. M. Williams, J. Cassell, D. J. Caddy, and R. B. Silberstein. Factors determining the frequency content of the electromyogram. *Journal of Applied Physiology*. 55:392-399, 1983.

151. Krustrup, P., J. Gonzalez-Alonso, B. Quistorff, and J. Bangsbo. Muscle heat production and anaerobic energy turnover during repeated intense dynamic exercise in humans. *Journal of Physiology*. 536:947-956, 2001.

152. Krustrup, P., K. Soderlund, M. Mohr, and J. Bangsbo. The slow component of oxygen uptake during intense, sub-maximal exercise in man is associated with additional fibre recruitment. *Pflugers Archives - European Journal of Physiology*. 447:855-866, 2004.

153. Kuipers, H., G. Rietjens, F. Verstappen, H. Schoenmakers, and G. Hofman. Effects of stage duration in incremental running tests on physiological variables. *International Journal of Sports Medicine*. 24:486-491, 2003.

154. Kukulka, C. G. and H. P. Clamann. Comparison of the recruitment and discharge properties of motor units in human brachial biceps and adductor pollicis during isometric contractions. *Brain Research*. 219:45-55, 1981.

155. Kumar, S., Y. Narayan, and M. Zedka. An electromyographic study of unresisted trunk rotation with normal velocity among healthy subjects. *Spine*. 21:1500-1512, 1996.

156. Kushmerick, M. J., R. A. Meyer, and T. R. Brown. Regulation of oxygen consumption in fast- and slow-twitch muscle. *American Journal of Physiology: Cell Physiology*. 32:C598-C606, 1992.

157. Kyrolainen, H., J. Avela, and P. V. Komi. Changes in muscle activity with increasing running speed. *Journal of Sports Sciences*. 23:1101-1109, 2005.

158. Kyrolainen, H., R. Kivela, S. Koskinen, J. McBride, J. L. Andersen, T. Takala, S. Sipila, and P. V. Komi. Interrelationships between muscle structure, muscle strength, and running economy. *Medicine & Science in Sports & Exercise*. 35:45-49, 2003.

159. Kyrolainen, H., T. Pullinen, R. Candau, J. Avela, P. Huttunen, and P. V. Komi. Effects of marathon running on running economy and kinematics. *European Journal of Applied Physiology*. 82:297-304, 2000.

160. Lambert, E. V., A. St.ClairGibson, and T. D. Noakes. Complex systems model of fatigue: intergrative homoeostatic control of peripheral physiological systems during exercise in humans. *British Journal of Sports Medicine*. 39:52-62, 2005.

161. Larsson, B., B. Mansson, C. Karlberg, P. Syvertsson, J. Elert, and B. Gerdle. Reproducibility of surface EMG variables and peak torque during three sets of ten dynamic contractions. *Journal of Electromyography and Kinesiology*. 9:351-357, 1999.

162. Legaz Arrese, A., D. Munguia Izquierdo, and J. R. Serveto Galindo. Physiological measures associated with marathon running performance in high-level male and female homogeneous groups. *International Journal of Sports Medicine*. 27:289-295, 2006.

163. Lieberman, D. E., D. A. Rachlen, H. Pontzer, D. M. Bramble, and E. Cutright-Smith. The human gluteus maximus and its role in running. *Journal of Experimental Biology*. 209:2143-2155, 2006.

164. Lindstrom, L., R. Kadefors, and I. Petersen. An electromyographic index for localized muscle fatigue. *Journal of Applied Physiology*. 43:750-754, 1977.

165. Lindstrom, L., R. Magnusson, and I. Petersen. Muscular fatigue and action potential conduction velocity changes studied with frequency analysis of EMG signals. *Electroencephalography and Clinical Neurophysiology*. 10:341-356, 1970.

166. Luchtenberg, D. Specific strength training for running - Part I. *National Strength and Conditioning Association Journal*. 11:62-65, 1989.

167. Luchtenberg, D. Specific strength training for running - Part II. *National Strength and Conditioning Association Journal*. 11:43-51, 1989.

168. Lucia, A., J. Esteve-Lanao, J. Olivan, F. Gomez-Gallego, A. F. San Juan, C. Santiago, M. Perez, C. Chamorro-Vina, and C. Foster. Physiological characteristics of the best Eritrean runners-exceptional running economy. *Applied Physiology, Nutrition, & Metabolism = Physiologie Appliquee, Nutrition et Metabolisme*. 31:530-540, 2006.

169. Mackey, A. H., S. E. Walt, G. A. Lobb, and N. S. Stott. Reliability of upper and lower limb three-dimensional kinematics in children with hemiplegia. *Gait and Posture*. 22:1-9, 2005.

170. Mann, R. A., G. T. Moran, and S. E. Dougherty. Comparative electromyography of the lower extremity in jogging, running, and sprinting. *American Journal of Sports Medicine*. 14:501-510, 1986.

171. Martin, D. E. and P. N. Coe. *Better training for distance runners*. Champaign, IL: Human Kinetics, 1997.

172. Martin, P. E. and D. W. Morgan. Biomechanical considerations for economical walking and running. *Medicine & Science in Sports & Exercise*. 24:467-474, 1992.

173. Mateika, J. H. and J. Duffin. Coincidental changes in ventilation and electromyographic activity during consecutive incremental exercise tests. *European Journal of Applied Physiology*. 68:54-61, 1994.

174. Meyer, T., J. P. Welter, J. Scharhag, and W. Kindermann. Maximal oxygen uptake during field running does not exceed that measured during treadmill exercise. *European Journal of Applied Physiology*. 88:387-389, 2003.

175. Midgley, A. W., L. R. McNaughton, and S. Carroll. Physiological determinants of time to exhaustion during intermittent treadmill running at vVO2max. *International Journal of Sports Medicine*. 28:273-280, 2007.

176. Midgley, A. W., L. R. McNaughton, and M. Wilkinson. The relationship between lactate turnpoint and the time at VO2max during a constant velocity run to exhaustion. *International Journal of Sports Medicine*, In Press.

177. Millet, G. Y. and R. Lepers. Alterations of neuromuscular function after prolonged running, cycling and skiing exercises. *Sports Medicine*. 34:105-116, 2004.

178. Mills, K. R. and R. H. Edwards. Muscle fatigue in myophosphorylase deficiency: power spectral analysis of the electromyogram. *Electroencephalography and Clinical Neurophysiology*. 57:330-335, 1984.

179. Milner-Brown, H. S., R. B. Stein, and R. Yemm. The orderly recruitment of motor units during voluntary isometric contractions. *Journal of Physiology*. 230:359-370, 1973.

180. Misiaszek, J. E. and E. M. Krauss. Restricting arm use enhances compensatory reactions of leg muscles during walking. *Experimental Brain Research*. 161:474-485, 2005.

181. Miura, H., H. Araki, H. Matoba, and K. Kitagawa. Relationship among oxygenation, myoelectric activity, and lactic acid accumulation in vastus lateralis muscle during exercise with constant work rate. 21:180-184, 2000.

182. Mizarhi, J., O. Verbitsky, and E. Isakov. Fatigue-related loading imbalance on the shank in running: a possible factor in stress fractures. *Annals of biomedical engineers*. 28:463-469, 2000.

183. Montgomery-III, W. H., M. Pink, and J. Perry. Electromyographic analysis of hip and knee musculature during running. *American Journal of Sports Medicine*. 22:272-278, 1994.

184. Morin, J. B., T. Jeannin, B. Chevallier, and A. Belli. Spring-mass model characteristics during spring running: correlation with performance and fatigue-induced changes. *International Journal of Sports Medicine*. 27:158-165, 2006.

185. Mortimer, J. T., R. Magnusson, and I. Petersen. Conduction velocity in ischemic muscle: effect on EMG frequency spectrum. *American Journal of Physiology*. 219:1324-1329, 1970.

186. Myburgh, K. H. What makes an endurance athlete world class? Not simply a physiological conundrum. *Compartive Biochemistry and Physiology Part A*. 136:171-190, 2003.

187. Myers, J. B., S. M. Lephart, Y. Tsai, T. C. Sell, J. T. Jolly, and J. M. Smoliga. Relationship between upper torso and pelvis rotation and driving performance in the golf drive. *Journal of Sports Sciences*, In Press.

188. Myers, M. J. and K. Steudel. Effect of limb mass and its distribution on the energetic cost of running. *Journal of Experimental Biology*. 116:363-373, 1985.

189. Naeije, M. and H. Zorn. Relation between EMG power spectrum shifts and muscle fiber action potential conduction velocity changes during local muscular fatigue in man. *European Journal of Applied Physiology*. 50:23-33, 1982.

190. Nagamachi, A., T. Ikata, S. Katoh, and T. Morita. Spectral analysis of erector spinae muscle surface electromyography as an index of exercise performance in maximal treadmill running. *Journal of Medical Investigation*. 47:29-35, 2000.

191. Nevill, A. M., D. Brown, R. Godfrey, P. Johnson, L. Romer, A. D. Stewart, and E. M. Winter. Modeling maximum oxygen uptake of elite endurance athletes. *Medicine & Science in Sports & Exercise*. 35:488-494, 2003.

192. Nicol, C., P. V. Komi, and P. Marconnet. Fatigue effects of marathon running on neuromuscular performan II. Changes in force, integrated electromyographic activity and endurance capacity. *Scandinavian Journal of Medicine and Science in Sports*. 1:18-24, 1991.

193. Nigg, B. M., R. W. De Boer, and V. Fischer. A kinematic comparison of overground and treadmill running. *Medicine & Science in Sports & Exercise*. 27:98-105, 1995.

194. Nilsson, J., A. Thorstensson, and J. Halbertsma. Changes in leg movements and muscle activity with speed of locomotion and mode of progression in humans. *Acta Physiologica Scandinavica*. 123:457-475, 1985.

195. Noakes, T. D. Physiological models to understand exercise fatigue and the adaptations that predict or enhance athletic performance. *Scandinavian Journal of Medicine and Science in Sports*. 10:123-145, 2000.

196. Paavolainen, L., K. Hakkinen, I. Hamalainen, A. Nummela, and H. Rusko. Explosive-strength training improves 5-km running time by improving running economy and muscle power. *Journal of Applied Physiology*. 86:1527-1533, 1999.

197. Paavolainen, L., A. Nummela, H. Rusko, and K. Hakkinen. Neuromuscular characteristics and fatigue during 10km running. *International Journal of Sports Medicine*. 20:516-521, 1999.

198. Petrofsky, J. S. Frequency and amplitude analysis of the EMG during exercise on the bicycle ergometer. *European Journal of Applied Physiology*. 41:1-15, 1979.

199. Petrofsky, J. S. and A. R. Lind. The influence of temperature on the amplitude and frequency components of the EMG during brief and sustained isometric contractions. *European Journal of Applied Physiology*. 44:189-200, 1980.

200. Place, N., R. Lepers, G. Deley, and G. Y. Millet. Time course of neuromuscular alterations during a prolonged running exercise. *Medicine & Science in Sports & Exercise*. 36:1347-1356, 2004.

201. Poole, D. C., W. Schaffartzik, D. R. Knight, T. Derion, B. Kennedy, H. J. Guy, R. Prediletto, and P. D. Wagner. Contribution of exercising legs to the slow component of oxygen uptake in humans. *Journal of Applied Physiology*. 71:1245-1253, 1991.

202. Potvin, J. R. Effects of muscle kinematics on surface EMG amplitude and frequency during fatiguing dynamic contractions. *Journal of Applied Physiology*. 82:144-151, 1997.

203. Queen, R. M., M. T. Gross, and H. Y. Liu. Repeatability of lower extremity kinetics and kinematics for standardized and self-selected running speeds. *Gait & Posture*. 23:282-287, 2006.

204. Rau, G., E. Schulte, and C. Disselhorst-Klug. From cell to movement: to what answers does EMG really contribute? *Journal of Electromyography and Kinesiology*. 14:611-617, 2004.

205. Reber, L., J. Perry, and M. Pink. Muscular control of the ankle in running. *American Journal of Sports Medicine*. 21:805-810; discussion 810, 1993.

206. Redfern, M. S., R. E. Hughes, and D. B. Chaffin. High pass filtering of electromyographic signals to remove ECG interference. *Clinical Biomechanics*. 8:44-48, 1993.

207. Reinschmidt, C., A. J. Van Den Bogert, B. M. Nigg, A. Lundberg, and N. Murphy. Effect of skin movement on the analysis of skeletal knee joint motion during running. *Journal of Biomechanics*. 30:729-732, 1997.

208. Robergs, R. A., F. Ghiasvand, and D. Parker. Biochemistry of exercise-induced metabolic acidosis. *American Journal of Physiology - Regulatory, Integrative, and Comparative Physiology*. 287:R502-R516, 2004.

209. Rotstein, A. and Y. Meckel. Estimation of %VO2 reserve from heart rate during arm exercise and running. *European Journal of Applied Physiology*. 83:545-550, 2000.

210. Rowland, T. W. The circulatory response to exercise: role of the peripheral pump. *International Journal of Sports Medicine*. 22:558-565, 2001.

211. Saltin, B., A. P. Gagge, and J. A. J. Stolwijk. Muscle temperature during submaximal exercise in man. *Journal of Applied Physiology*. 25:679-688, 1968.

212. Saltin, B. and S. Strange. Maximal oxygen uptake: "old" and "new" arguments for a cardiovascular limitation. *Medicine & Science in Sports & Exercise*. 24:30-37, 1992.

213. Saunders, M. J., E. M. Evans, S. A. Arngrimsson, J. D. Allison, G. L. Warren, and K. J. Cureton. Muscle activation and the slow component rise in oxygen uptake during cycling. *Medicine & Science in Sports & Exercise*. 32:2040-2045, 2000.

214. Saunders, S. W., D. Rath, and P. W. Hodges. Postural and respiratory activation of the trunk muscles changes with mode and speed of locomotion. *Gait & Posture*. 20:280-290, 2004.

215. Schache, A. G., P. Blanch, D. Rath, T. Wrigley, and K. Bennell. Three-dimensional angular kinematics of the lumbar spine and pelvis during running. *Human Movement Science*. 21:273-293, 2002.

216. Schache, A. G., P. D. Blanch, D. A. Rath, T. V. Wrigley, R. Starr, and K. L. Bennell. A comparison of overground and treadmill running for measuring three-dimensional kinematics of the lumbo-pelvic-hip complex. *Clinical Biomechanics*. 16:667-680, 2001.

217. Schache, A. G., P. D. Blanch, D. A. Rath, T. V. Wrigley, R. Starr, and K. L. Bennell. Intra-subject repeatability of the three dimensional angular kinematics within the lumbo-pelvic-hip complex during running. *Gait and Posture*. 15:136-145, 2002.

218. Scheuermann, B. W., J. H. T. McConnell, and T. J. Barstow. EMG and oxygen uptake responses during slow and fast ramp exercise in human. *Experimental Physiology*. 87:91-100, 2002.

219. Schwab, G. H., D. R. Moynes, F. W. Jobe, and J. Perry. Lower extremity electromyographic analysis of running gait. *Clinical Orthopaedics*. 176:166-170, 1983.

220. Scott, W. and J. S. S. A. Binder-Macleod. Human skeletal muscle fiber type classifications. *Physical Therapy*. 81:1810-1816, 2001.

221. Seburn, K. L., D. J. Sanderson, A. N. Belcastro, and D. C. McKenzie. Effect of manipulation of plasma lactate on integrated EMG during cycling. *Medicine & Science in Sports & Exercise*. 24:911-916, 1992.

222. Shankar, S., R. E. Gander, and B. R. Brandell. Changes in myoelectric signal (MES) power spectra during dynamic contractions. *Electroencephalography and Clinical Neurophysiology*. 73:142-150, 1989.

223. Shim, J., E. O. Acevedo, R. R. Kraemer, R. W. Haltom, and J. L. Tryniecki. Kinematic changes at intensities proximal to onset of lactate accumulation. *Journal of Sports Medicine and Physical Fitness*. 43:274-278, 2003.

224. Sjogaard, G. and B. Saltin. Extra- and intracellular water spaces in muscles of man at rest and with dynamic exercise. *American Journal of Physiology - Regulatory, Integrative, and Comparative Physiology*. 12:R271-280, 1982.

225. Skof, B. and V. Strojnik. Neuromuscular fatigue and recovery dynamics following prolonged continuous run at anaerobic threshold. *British Journal of Sports Medicine*. 40:219-222, 2006.

226. Slawinski, J. S. and V. L. Billat. Difference in mechanical and energy cost between highly, well, and nontrained runners. *Medicine & Science in Sports & Exercise*. 36:1440-1446, 2004.

227. Slocum, D. B. and S. L. James. Biomechanics of running. *Journal of the American Medical Association*. 205:97-104, 1968.

228. Sloniger, M. A., K. J. Cureton, B. M. Prior, and E. M. Evans. Anaerobic capacity and muscle activation during horizontal and uphill running. *Journal of Applied Physiology*. 83:262-269, 1997.

229. Sloniger, M. A., K. J. Cureton, B. M. Prior, and E. M. Evans. Lower extremity muscle activation during horizontal and uphill running. *Journal of Applied Physiology*. 83:2973-2079, 1997.

230. Smith, L. K., E. L. Weiss, and L. D. Lekmkuhl. *Brumstrom's Clinical Kinesiology*. Philadelphia, PA: F.A. Davis Company, 1996.

231. Solomonow, M., C. Baten, J. Smit, R. Baratta, H. Hermens, R. D'Ambrosia, and H. Shoji. Electromyogram power spectra frequencies associated with motor unit recruitment strategies. *Journal of Applied Physiology*. 68:1177-1185, 1990.

232. Spreit, L. L., R. A. Howlett, and G. J. F. Heigenhauser. An enzymatic approach to lactate production in human skeletal muscle during exercise. *Medicine & Science in Sports & Exercise*. 32:756-763, 2000.

233. Spurrs, R. W., A. J. Murphy, and M. L. Watsford. The effect of plyometric training on distance running performance. *European Journal of Applied Physiology*. 89:1-7, 2003.

234. St. Clair-Gibson, A., M. I. Lambert, J. A. Hawley, S. A. Broomhead, and T. D. Noakes. Measurement of maximal oxygen uptake from two different laboratory protocols in runners and squash players. *Medicine & Science in Sports & Exercise*. 31:1226-1229, 1999.

235. St.Clair-Gibson, A., E. J. Schabort, and T. D. Noakes. Reduced neuromuscular activity and force generation during prolonged cycling. *American Journal of Physiology: Regulatory, Integrative, and Comparative Physiology*. 281:R187-196, 2001.

236. Stalberg, E. Propagation velocity in human muscle fibers in situ. *Acta Physiologica Scandinavica*. 70:3-112, 1966.

237. Swain, D. P., B. C. Leutholtz, M. E. King, L. A. Haas, and D. J. Branch. Relationship between %heart rate reserve and %VO2 reserve in treadmill exercise. *Medicine & Science in Sports & Exercise*. 30:318-321, 1998.

238. Swain, P. D. and B. C. Leutholtz. Heart rate reserve is equivalent to %VO2 reserve, not to %VO2max. *Medicine & Science in Sports & Exercise*. 29:410-414, 1997.

239. Szentesi, P., R. Zaremba, W. van Mechelen, and G. J. M. Steinen. ATP utilization for calcium uptake and force production in different types of human skeletal muscle fibers. *Journal of Physiology*. 531:393-403, 2001.

240. Taylor, A. D. and R. Bronks. Electromyographic correlates of the transition from aerobic to anaerobic metabolism in treadmill running. *European Journal of Applied Physiology*. 69:508-515, 1994.

241. Taylor, A. D. and R. Bronks. Reproducibility and validity of the quadriceps muscle integrated electromyogram threshold during incremental cycle ergometry. *European Journal of Applied Physiology*. 70:252-257, 1995.

242. Tesch, P. A. and J. Karlsson. Muscle fiber types and size in trained and untrained muscles of elite athletes. *Journal of Applied Physiology*. 59:1716-1720, 1985.

243. Tesch, P. A., P. V. Komi, I. Jacobs, I. Karlsson, and J. T. Viitasalo. Influence of lactate accumulation on EMG frequency spectrum during repeated concentric contractions. *Acta Physiologica Scandinavica*. 119:61-67, 1983.

244. Thorstensson, A., H. Carlson, M. R. Zomlefer, and J. Nilsson. Lumbar back muscle activity in relation to trunk movements during locomotion in man. *Acta Physiologica Scandinavica*. 116:13-20, 1982.

245. Tonkonogi, M. and K. Sahlin. Physical exercise and mitochondrial function in human skeletal muscle. *Exercise and Sports Science Reviews*. 30:129-137, 2002.

246. Troni, W., M. DeMattei, and V. Contegiacomo. The effect of temperature on conduction velocity in human muscle fibres. *Journal of Electromyography and Kinesiology*. 1:281-287, 1991.

247. van Ingen Schenau, G. J. Some fundamental aspects of the biomechanics of overground versus treadmill locomotion. *Medicine & Science in Sports & Exercise*. 12:257-261, 1980.

248. Vaughan, C. L. *Forces and moments at the hip, knee, and ankle joints.*: Oxford Orthopaedic Engineering Centre, 1983, pp. 10: 17-18.

249. Vaughan, C. L., B. L. Davis, and J. C. O'Connor. *Dynamics of human gait*. Champaign, Ill.: Human Kinetics Publishers, 1992, xii, 137 p.

250. Vollestad, N. K. Measurement of human muscle fatigue. *Journal of Neuroscience Methods*. 74:219-227, 1997.

251. Vollestad, N. K. and P. C. S. Blom. Effect of varying exercise intensity on glycogen depletion in human muscle fibers. *Acta Physiologica Scandinavica*. 125:395-405, 1985.

252. Vollestad, N. K., O. Vaage, and L. Hermansen. Muscle glycogen depletion patterns in type I and subgroups of type II fibers during prolonged severe exercise in man. *Acta Physiologica Scandinavica*. 122:433-441, 1984.

253. Wagner, P. D. Diffusive resistance to O2 transport in muscle. *Acta Physiologica Scandinavica*. 168:609-614, 2000.

254. Wagner, P. D. A theoretical analysis of factors determining VO2max at sea level and altitude. *Respiration Physiology*. 106:329-343, 1996.

255. Wakeling, J. M. Motor units are recruited in a task-dependent fashion during locomotion. *Journal of Experimental Biology*. 207:3883-3890, 2004.

256. Walsh, M. L. Whole body fatigue and critical power. *Sports Medicine*. 29:153-166, 2000.

257. Wank, V., U. Frick, and D. Schmidtbleicher. Kinematics and electromyography of lower limb muscles in overground and treadmill running. *International Journal of Sports Medicine*. 19:455-461, 1998.

258. Westerblad, H. and D. G. Allen. Recent advances in the understanding of skeletal muscle fatigue. *Current Opinion in Rheumatology*. 14:648-652, 2002.

259. Weyand, P., K. Cureton, D. Conley, and M. Sloniger. Percentage anaerobic energy utilized during track running events. *Medicine & Science in Sports & Exercise*. 25:S105, 1993.

260. Whipp, B. J. The slow component of O2 uptake kinetics during heavy exercise. *Medicine & Science in Sports & Exercise*. 26:1391-1326, 1994.

261. Whittle, M. W. and D. Levine. Three-dimensional relationships between the movements of the pelvis and lumbar spine during normal gait. *Human Movement Science*. 18:681-692, 1999.

262. Williams, K. R. Biomechanics of running. *Exercise and Sports Science Reviews*. 13:389-441, 1985.

263. Williams, K. R. and P. R. Cavanagh. Relationship between distance running mechanics, running economy, and performance. *Journal of Applied Physiology*. 63:1236-1245, 1987.

264. Williams, K. R., R. Snow, and C. Agruss. Changes in distance running kinematics with fatigue. *International Journal of Sport Biomechanics*. 7:138-162, 1991.

265. Willis, W. T. and M. R. Jackman. Mitochondrial function during heavy exercise. *Medicine & Science in Sports & Exercise*. 26:1347-1354, 1994.

266. Willson, J. D. and T. W. Kernozek. Plantar loading and cadence alterations with fatigue. *Medicine & Science in Sports & Exercise*. 31:1828-1833, 1999.

267. Winter, D. A. *Biomechanics and Motor Control of Human Movement*. New York: John Wiley and Sons, Inc., 1990

268. Winter, D. A. A new definition of mechanical work done in human movement. *Journal of Applied Physiology*. 46:79-83, 1979.

269. Wolosker, H. and L. de Meis. pH-dependent inhibitory effects of Ca2+, Mg2+, and K+ on Ca2+ efflux by sarcoplasmic reticulum ATPase. *American Journal of Physiology: Cell Physiology*. 266:C1376-C1381, 1994.

270. Wu, G., S. Siegler, P. Allard, C. Kirtley, A. Leardini, D. Rosenbaum, M. Whittle, D. D. L'Lima, L. Cristofolini, H. Witte, O. Schmid, and I. Stokes. ISB recommendation on definitions of joint coordinate systems of various joints for the reporting of human joint motion - part I: ankle, hip, and spine. *Journal of Biomechanics*. 35:543-548, 2002.

271. Wu, G., F. C. T. van der Helm, H. E. J. D. Veeger, M. Makhsous, P. V. Roy, C. Anglin, J. Nagels, A. R. Karduna, K. McQuade, X. Wang, F. W. Werner, and B. Buchholz. ISB recommendation on definitions of joint coordinate systems of various joints for the reporting of human joint motion - Part II: shoulder, elbow, wrist, and hand. *Journal of Biomechanics*. 38:981-992, 2005.

272. Zipp, P. Recommendation for the standardization of lead positions in surface electromyography. *European Journal of Applied Physiology*. 50:41-54, 1982.

273. Zwarts, M. J. and D. F. Stegeman. Multichannel surface EMG: basic aspects and clinical utility. *Muscle and Nerve*. 28:1-17, 2003.

274. Zwarts, M. J., T. W. Van Weerden, and T. M. Haenen. Relationship between average muscle fiber conduction velocity and EMG power spectra during isometric contraction, recovery and applied ischemia. *European Journal of Applied Physiology and Occupational Physiology*. 56:212-216, 1987.